

SETTLEMENT ANALYSIS OF ANNULAR FOOTINGS

**A Thesis Submitted
In Partial Fulfilment of the Requirements
for the Degree of
DOCTOR OF PHILOSOPHY**

**by
R. S. KARMARKAR**

**to the
DEPARTMENT OF CIVIL ENGINEERING
INDIAN INSTITUTE OF TECHNOLOGY, KANPUR
AUGUST, 1982**

SETTLEMENT ANALYSIS OF ANNULAR FOOTINGS

A Thesis Submitted
In Partial Fulfilment of the Requirements
for the Degree of
DOCTOR OF PHILOSOPHY

1982

by

R. S. KARMARKAR

to the

**DEPARTMENT OF CIVIL ENGINEERING
INDIAN INSTITUTE OF TECHNOLOGY, KANPUR
AUGUST, 1982**

4 JUN 1984

CE-1982-D-KAR-SET

CENTRAL LIBRARY
Kanpur

Acc. No. A.....82702

CERTIFICATE

This is to certify that the thesis 'Settlement Analysis of Annular Footings' submitted by Shri R.S. Karmarkar in partial fulfilment of the requirements for the Degree of Doctor of Philosophy at the Indian Institute of Technology, Kanpur is a record of bonafide research work carried out under my supervision and guidance. The work embodied in this thesis has not been submitted elsewhere for the award of a degree.



(MADHIRA R. MADHAV)

Professor

Department of Civil Engineering,
Indian Institute of Technology Kanpur

August, 1982

I certify that the thesis entitled "Settlement Analysis of Annular Footings" submitted in partial fulfillment of the requirements for the award of Doctor of Philosophy at the Indian Institute of Technology Kanpur is a record of bonafide research work carried out under my supervision and guidance. The work embodied in this thesis has not been submitted elsewhere for the award of a degree.
Date: 15/3/83



ACKNOWLEDGEMENT

The author is highly indebted to his thesis supervisor Dr. M.R. Madhav, for suggesting the problems of this thesis and for the valuable guidance and encouragement given at all the stages of the work undertaken for this thesis.

The author is thankful to Dr. N.S.V. Kameswara Rao, Dr. Yudhbir and Dr. Umesh Dayal for their encouragement.

The author wishes to express his thanks to Sri S.L. Narasimhan and Sri N.B.S. Rao for the useful discussions he had with them.

The author is grateful to Dr. Y.R. Waghmare for his kindness in helping the author during the author's stay at I.I.T. Kanpur.

The author is thankful to the Government of Goa, Daman and Diu and to the authorities of the College of Engineering, Farmagudi, Goa, for sponsoring him for undertaking the research work.

The author wishes to express his appreciation for the assistance given by Sri J.C. Verma, Sri G.S. Trivedi, and Sri R.S. Dwivedi in the tracing , typing and duplicating work for this thesis.

TABLE OF CONTENTS

	Page
CERTIFICATE	i
ACKNOWLEDGEMENT	ii
LIST OF TABLES	viii
LIST OF FIGURES	x
NOTATIONS AND SYMBOLS	xiv
SYNOPSIS	xviii
 CHAPTER- 1 : INTRODUCTION	 1
1.1 : General	1
1.2 : Annular or Ring Footings as Foundations	2
1.3 : Elasto-plastic Analysis	2
1.4 : The Choice of Method of Numerical Analysis	4
1.5 : Organisation of the Thesis	5
 CHAPTER- 2 : LITERATURE REVIEW	 11
2.1 : General	11
2.2 : Analytical Work Connected with Settlement of Circular or Annular Footings in Contact with Homogeneous Isotropic Mass of Soil-With no Consideration of Time Effects	13
2.2.1: Linear Elastic Solutions	13
2.2.2: Non-linearity as a consequence of Loss of Contact	18
2.2.3: Non-Linearity in Load Settlement Response Under Increasing load	20
2.3 : Analytical Work in Connection with Piled Annular Footings	27
2.4 : Consolidation Settlement of Circular Footings	27
2.4.1: Flexible Circular Footings	27
2.4.2: Rigid Circular Footings	28
2.4.3: Rafts of Finite Rigidity	28
2.5 : Miscellaneous Studies	29
2.6 : Concluding Remarks	30

	Page
CHAPTER- 3 : ELASTO-PLASTIC SETTLEMENT ANALYSIS OF CENTRALLY LOADED RIGID ANNULAR FOOTINGS	
3.1 : Introduction	32
3.2 : Assumptions and Statement of the Problem	35
3.2.1: Assumptions	35
3.2.2: Important Implications of the General Assumptions	36
3.3 : Analysis	37
3.3.1: Footing Discretization	38
3.3.2: Elastic Case	38
3.3.3: Elasto-plastic Case	40
3.4 : Results and Discussion	45
3.4.1: Discretization	45
3.4.2: Computational Economy	46
3.4.3: Footing Resting on the Surface of Semi-infinite Soil Mass	47
3.4.4: Embedded Footing	54
3.4.5: Surface Footing on Finite Layer of Soil	59
3.5 : Conclusions	65
CHAPTER- 4 : ELASTO-PLASTIC SETTLEMENT ANALYSIS OF CENTRALLY LOADED ANNULAR FOOTINGS OF FINITE RIGIDITY	
4.1 : Introduction	85
4.2 : Assumptions and Statement of the Problem	87
4.2.1: Assumptions	87
4.2.2: Statement of the Problem	88
4.3 : Analysis	89
4.3.1: The Soil Flexibility Matrix	89
4.3.2: Footing Rigidity Matrix	90
4.3.3: Coupling of Soil and Plate Responses:Elastic Case	93
4.3.4: Coupling of Soil and Plate: Elasto-plastic Case	94
4.3.5: Separation or Tension Cut-off	95
4.3.6: Bending Moments and Shear in the Footing	96
4.4 : Results and Discussion	98
4.4.1: General	98
4.4.2: Footings of Finite Rigidity Resting on Semi-infinite Soil	99

	Page
4.4.2.1: Effect of plastic yielding of soil on bending moments and shear forces	99
4.4.2.2: Elasto-plastic settlement: Effect of relative rigidity	108
4.4.2.3: Effect of radius ratio n	108
4.4.3 : Footing Resting on a Soil Layer of Finite Depth Underlain by Rough Rigid Base	111
4.5 : Conclusions	120
CHAPTER- 5 : ELASTO-PLASTIC ANALYSIS OF CENTRALLY LOADED PILED RIGID ANNULAR FOOTINGS	145
5.1 : Introduction	145
5.2 : Assumptions and Statement of the Problem	148
5.2.1: Assumptions	148
5.2.2: Statement of the Problem	149
5.3 : Analysis	149
5.3.1: General	149
5.3.2: Influence Coefficients	150
5.3.3: Final Form of Equations to be Solved	156
5.3.4: Elastic Case	156
5.3.5: Elasto-plastic Case	156
5.4 : Results and Discussion	158
5.4.1: General	158
5.4.2: Single Floating Pile in Semi-infinite Soil	159
5.4.3: Effect of Radius Ratio n on Settlement Response of Pile Ring Footing System	161
5.4.4: Effect of Positioning of Pile-Ring	163
5.4.5: Combined Effect of Length and Number of Piles in Nearly Equivalent Systems	164
5.4.6: Ring Footing with Two or More Pile Rows (Rings)	165
5.5 : Conclusions	167
CHAPTER- 6 : ELASTO-PLASTIC ANALYSIS OF SETTLEMENT OF ECCENTRICALLY LOADED RIGID ANNULAR FOOTINGS	176
6.1 : Introduction	176
6.2 : Assumptions and Statement of the Problem	177
6.2.1: Assumptions	177
6.2.2: Statement of the Problem	178

6.3 :	Analysis	178
6.3.1:	General	178
6.3.2:	Elastic Case	178
6.3.3:	Elastic Case with Tension Cut-off	180
6.3.4:	Elasto-plastic Case Without Tension Cut-off	181
6.3.5:	Elasto-plastic Case with Tension Cut-off	182
6.4 :	Results and Discussion	183
6.4.1:	Minimisation of Computational Effort	183
6.4.2:	Footing Resting on the Surface of Semi-infinite Soil	185
6.4.2.1:	General	185
6.4.2.2:	Effect of radius ratio n	188
6.4.2.3:	Effect of eccentricity	190
6.4.2.4:	Marching of yielded and tension cut-off zones	192
6.4.3:	Effect of Embedment of Footing	194
6.4.4:	Footing Resting on Soil Layer of Finite Depth Underlain by Rough Rigid Base	197
6.4.4.1:	General	197
6.4.4.2:	Settlement and rotation response for Poisson's ratio=.5	198
6.4.4.3:	Effect of and Correction for Poisson's ratio	199
6.5 :	Conclusions	200
CHAPTER- 7 :	CONSOLIDATION SETTLEMENT OF ANNULAR FOOTINGS	221
7.1 :	Introduction	221
7.1.1:	General	221
7.1.2:	Consolidation Under Flexible Annular Footings	222
7.1.3:	Consolidation Under Completely Rigid Annular Footings	224
7.2 :	Consolidation Settlement of Flexible Annular Footing	227
7.2.1:	Assumptions and Statement of the Problem	227
7.2.1.1:	Assumptions	227
7.2.1.2:	Statement of the problem	227
7.2.2:	Analysis	228
7.2.3:	Solution Procedure	231
7.2.4:	Results and Discussion	233
7.2.4.1:	General	233
7.2.4.2:	Effect of drainage boundary conditions	234

	Page
7.2.4.3: Effect of radius ratio n	235
7.2.4.4: Effect of period of construction T_c	236
7.2.4.5: Effect of depth of consolidating layer	238
7.2.4.6: Effect of anisotropy	239
7.3: Consolidation Settlement of Rigid Annular Footing	240
7.3.1: Assumptions and Statement of the Problem	240
7.3.1.1: Assumptions	240
7.3.1.2: Statement of the problem	240
7.3.2: Analysis	241
7.3.3: Solution Procedure	241
7.3.4: Results and Discussion	246
7.3.4.1: General	246
7.3.4.2: Changes in contact pressure distribution	247
7.3.4.3: Effect of infinite rigidity in comparison to infinite flexibility on time rate of settlement	250
7.3.4.4: Effect of radius ratio n	252
7.3.4.5: Dependence of peak contact pressure on construction time T_c	252
7.3.4.6: Effect of anisotropy with respect to permeability	253
7.4: Conclusions	254
CHAPTER- 8 : SUMMARY AND CONCLUSIONS	276
8.1: Summary	276
8.2: Conclusions	280
8.3: Suggestions for Further Study	285
REFERENCES	287

LIST OF TABLES

Table No.		Page
3.1	Values of $w(n)$ for Rigid Ring (Elastic Case)	53
3.2	Settlement Correction Factor C_c for Depth of Embedment	55
3.3	Settlement Correction Factors C_n and C_v for Radius Ratio (n) and Poisson's Ratio (ν)	56
3.4	Values of C for Typical Cases	61
3.5	Approximate Corrections to q_y for Depth of Layer of Soil	64
4.1	Design Moment and Shear Values Based on Elasto-Plastic Analysis Expressed as Percentage of Values Based on Elastic Theory	103
4.2	Typical Design Moment and Shear Values for a Ring Footing With $n=.8$ Expressed as Percentage of Corresponding Values for Circular Footing, Under Equal Area and Total Load Conditions	113
5.1	Load Sharing by Pile Rings	167
6.1	Equivalent Central Settlement and Rotation Coefficients	189
6.2	Typical Values of Maximum and Minimum Coefficient of Settlement and Distance of Point of Rotation	192
6.3	Rotation Correction Factors R_n and R for Radius Ratio (n) and Poisson's Ratio (ν)	196

Table No.	Page
7.1 Effect of τ_{oct} on Consolidation Under Flexible Strip Footing	230
7.2 Degree of Consolidation Achieved at the End of Construction	237

LIST OF FIGURES

Figure/s	Page/s
2.1 The Unknown Elasto-plastic Load Settlement Curve	31
2.2 Typical Constitutive Law Models	31
3.1 Rigid Annular Footing on Semi-infinite Continuum	67
3.2 Problem Type Definition Sketch	67
3.3 Yielded and Elastic Portions of Soil Pressures	68
3.4 Typical Load Settlement Curves	69
3.5 Equivalent Circular and Annular Footings	69
3.6 Design Chart for Settlement of Centrally Loaded Rigid Annular Surface Footing	70
3.7 Typical Contact Pressures Beneath Rigid Footings Resting on or Embedded in Semi-infinite Soil	71
3.8 Contact Pressure Beneath Rigid Ring on Semi-infinite Soil	72
3.9a Embedded Footing- Comparison of Load Settlement Response with Surface Footing	73
3.9b Embedded Footing-Comparison of Elastic Settlements of Circular Footing	73
3.10 Finite Depth Settlement Factors	74-83
3.11 Typical Contact Pressures Beneath Ring Footing on Finite Layer	84
4.1 Types of Loading Configuration on Footing of Finite Rigidity	123
4.2 Plate Discretization	124
4.3 Comparison with Available Elastic Solutions	125-127

Figure/s	Page/s
4.4 Maximum (Critical) Bending Moment and Shear at Various Load Levels in a Uniformly Loaded Footing	128
4.5 Dependence of Critical B.M./S.F. on Load Level	129
4.6 Dimensionless Design Moment for Uniformly Loaded Ring Footings	130
4.7 Dimensionless Design Shear for Uniformly Loaded Ring Footings	131
4.8 Comparison of Typical Maximum Values of Radial and Tangential Bending Moments	132
4.9a Effect of Width of Uniformly Loaded Area (Innermost Portion) on Maximum Shear and Moment	133
4.9b Effect of Position of Single Loaded Annular Ring	134
4.10 Maximum Moment and Shear Variation With Load Level for Innermost One Nineth Width Loaded	135
4.11 Method of Calculating Design Shear for Ring Footing Loaded at Inner Edge	135
4.12 Design Charts for Settlement Influence Factor and Differential Deflection Factor for Uniformly Loaded Ring Footing	136-138
4.13 & 4.14 Maximum Settlement Factor and Differential Deflection Factor for Various Loadings on Footing on Semi-infinite Soil	139-140
4.15 & 4.16 Settlement Curves for Footing Resting on Soil of Finite Depth	141-142
4.17 Settlement of Embedded Circular Uniformly Loaded Footing Relative to Centre of Footing	143
4.18 Variation of Design Moment and Shear with Depth of Embedment for Uniformly Loaded Footing	144

Figure/s	Page/s
5.1 Definition Sketch of Piled Rigid Ring Footing	169
5.2 Application of Mindlin's Solution	170
5.3 Load Settlement Response for Single Floating Pile	171
5.4 Settlement Factor and Percentage Pile Load for Equivalent Pile Raft Systems	172
5.5 Effect of Positioning of Pile Ring on Settlement and Pile Load Share	173
5.6 Comparison of Nearly Equivalent Systems of Piled Ring Footings	174
5.7 Effect of Positioning of Pile Rings	175
6.1 Eccentrically Loaded Rigid Annular Footing: Definition Sketch	202
6.2 Contact Stresses	202
6.3 Typical Load Settlement Curves	203
6.4 to 6.7 Rotation/Settlement Eccentricity Curves	204-211
6.8 Marching of Tension Cut-off and Yielded Zones	212
6.9 Typical Contact Pressures Under Rigid Circular Footing Under Eccentric Load for $c/a=0$ and $c/a=5$	213
6.10 Load Eccentricity Relation at Tension Cut-off Condition	213
6.11 to 6.16 Finite Depth Settlement and Rotation Factors	214-219
6.17 Effect of Poisson's Ratio on Settlement Factor for Eccentrically Loaded Rigid Annular Footing on Finite Depth of Soil	220
7.1a Flexible Ring Footing on a Consolidating Finite Layer and Finite Difference Grid	256

Figure/s		Page/s
7.1b	Variation of Construction Load	256
7.2	Comparison of Typical Results for Consolidation Under Circular Footing	257
7.3	Flexible Footing-Effect of Drianaage Boundary Conditions	257
7.4	Flexible Footing-Effect of Radius Ratio	258
7.5	Consolidation of Flexible Ring Footing Under Construction Loading	259-262
7.6	Flexible Footing Degree of Consolidation at the End of Construction	263
7.7	Effect of Depth of Consolidation Layer	264
7.8	Flexible Footing-Effect of Anisotropy	265
7.9	Discretized Rigid Ring Footing on Finite Layer with Finite Difference Grid	266
7.10	Operational Flow Chart	267
7.11	Typical Changes in Contact Pressure During Consolidation Under a Rigid Ring and a Rigid Circular Footing	268
7.12	Effect of Layer Depth and Drianaage on Peaks	269
7.13	Contact Pressure Variation Near Centre and Half Radius of a Rigid Circular Footing	270
7.14	Effect of Radius Ratio of Peaking	270
7.15	Comparison of Variation of Edge Pressure Under Rigid Strip Footing	271
7.16	Comparison of Time Rate Settlement of Rigid and Flexible Footings	272
7.17	Effect of Construction Time on Peak Pressures	273
7.18	Comparison of Effect of Anisotropy on Consolidation Under Flexible and Rigid Footings	274
7.19	Effect of Anisotropy on Peak Pressures	275

NOTATIONS AND SYMBOLS

A Area

a Outer radius of footing

B A quantity related to pore pressures

b Width of element; outer radius of equivalent ring; coefficient of pore pressure generation

C Correction factor; a ratio of settlements; a quantity related to pore pressures

c Depth of embedment; a constant; coefficient of consolidation

c_v Coefficient of consolidation

D Flexural rigidity of footing; differential deflection

d Horizontal distance between elements; diameter of pile

E Modulus of elasticity

e Eccentricity

F Shear force per unit width

f A coefficient depending on soil compressibility

g Clear distance between strip loads; coefficient of numerical integration

h	Thickness (depth) of finite layer of soil
I	Settlement influence factor/coefficient; influence coefficient matrix
K	Relative rigidity; a constant
k	Coefficient of permeability; a number of elements; vertical displacement of centre of footing
L	Length of pile
l	Length of element; number of annular elements
M	Bending moment per unit width
m	Ratio of length to width of element; number of annular elements; number of piles; anisotropy ratio
n	Radius ratio i.e. ratio of inner radius to outer radius of annular footing
P	Plate (footing) rigidity matrix; point load; load on a pile
p	Contact pressure; percentage pile load
Q	Total vertical load on footing
q	Intensity of loading
R	Ring-circle equivalence factor; rotation correction factor; a distance
r	Radial (horizontal) distance
s	Ratio of distance of a row (ring) of piles from inner edge to width of footing; number of nodes on vertical line
T	Nondimensional time
t	Time; a geometric quantity in case of embedded footing; thickness of plate (footing)
U	Degree of consolidation of settlement; unity (as vector); a quantity related to sum of pore pressures on a vertical time

u	Excess pore pressure
w	External load
w	Deflection of plate (footing); a settlement coefficient as a function of radius ratio
x	Width of (embedded) element; distance from centre of footing in the direction of eccentricity
y	Ratio of elemental radial distance to radial distance; length of (embedded) element
Z	Soil flexibility matrix
z	Depth below surface
α	Ratio of depth of embedment to half length of element; weightage coefficient (consolidation); an angle; rotation of footing about centre; correction factor for Poisson's ratio
β	Ratio of length to width of embedded element; a dimensionless quantity in consolidation; an angle
δ	Dimensionless settlement influence factor; small quantities
ν	Poisson's ratio
θ	Bulk stress
ϕ	Rotation influence factor
ρ	Settlement
σ	Stress
τ	Shear stress
[]	Matrix in matrix expressions
{ }	Vector in matrix expressions
L 1	Row matrix
-	(Bar): Dimensionless quantities; distances to centre of areas
'	(Dash); Modified/derived quantities

Subscripts and their Indications

av	Average
b	Base of pile
c	Critical (absolute maximum); construction; circular; embedded
d	Design
e	Elastic
eq	Equivalent
f	Finite rigidity; failure; footing
h	Finite depth of layer of soil
i	A position
j	A position
k	An elemental ring
o	Centre; constant; average; surface
oct	Octahedral
p	Plate (footing); pile; pore pressure
r	Ring
s	Soil; semi-infinite; shaft of pile; settlement
T	Tangential (moment)
t	Time
u	Ultimate; undrained
y	Yield/ultimate
z	Depth
v	For Poisson's ratio = ν

SYNOPSIS

R.S. Karmarkar

Ph.D. Thesis

Department of Civil Engineering
Indian Institute of Technology, Kanpur, India
(July 1982)

SETTLEMENT ANALYSIS OF ANNULAR FOOTINGS

Footings in the form of an annular ring, with or without piles, are highly economical and well suited for tall isolated structures such as overhead water tanks, towers, chimney stacks etc. Such structures are usually centrally loaded. However forces such as those due to wind load may cause eccentric loading on the footing. Solutions available to-date for analysis of settlement of such footings are limited to those based on Elastic theory alone. Solutions for consolidation settlement of ring footings are not available and need to be developed.

Except under a fully flexible footing, the contact pressures near the outer and the inner edges of a ring footing are very high even under small loads and are always likely to be beyond the yield capacity of the soil. Therefore, even under working load conditions, the soil in contact below the footing will be in plastic state over some zone. The case of centrally loaded rigid ring footing

resting on a semi-infinite mass of soil is taken up first. Using the method of numerical integration of available solutions from elasticity theory and the concept of limiting yield stress, an elasto-plastic analysis has been carried out to obtain an entire load-deformation response to failure. The available results from some experimental and Finite Element investigations have been compared with those of the present work and good agreement has been found to exist. The validity of the proposed elasto-plastic analysis is thus established. The deformation is found to be nonlinear throughout and tends to infinity under high loads.

The method has been extended to study the effect of embedment of a centrally loaded rigid ring footing on settlement response. Correction factors are given for different values of ratios of depth of embedment to outer radius, and inner radius to outer radius and for different values of Poisson's ratio.

The settlement response of a centrally loaded rigid ring footing resting at the surface of a compressible soil layer of finite depth is also studied.

The case of axisymmetrically loaded ring footing of finite rigidity, defined in terms of dimensions of the footing and the relative elastic properties of the soil and the footing, has been investigated. The effect of finite rigidity on settlement and bending moments in the footing is studied under elasto-plastic soil conditions. The footing has been idealised as a plate and an integrated foundation-soil interaction analysis has been carried out. The plastic yielding of the soil is found to have significant effect on the bending moments in the footing. A study of shear stresses in the footing has also been made. The effects of embedment of the footing and the finite layer of the soil are also studied. The positioning of the applied load on the footing is another significant parameter studied in this analysis.

To restrict the settlement, it is advantageous to provide a few short piles below a ring footing. In the present work, the axisymmetric case of centrally loaded rigid ring footing with one or more concentric rows of incompressible piles has been investigated under elasto-plastic conditions of the soil. The technique of numerical integration of available elastic solutions is again used coupled with plastic yield of soil in contact with the piles and the footing. For the footing and the piles,

the load sharing and the extent of plastic yielding of soil in contact, depends on a number of parameters including the imposed total load. Therefore, an integrated elasto-plastic analysis of the entire pile-raft system has been carried out.

Eccentric loading on a ring footing, whether permanent or occasional, increases the possibility and extent of plastic yielding of soil especially under the edges. The present work includes elasto-plastic analysis of eccentrically loaded rigid ring footings either placed on or in semi-infinite or on finite soil. Under all loads, the settlement as well as rotation of the footing is found to vary nonlinearly with load. Under higher eccentricity and/or load, the settlement/rotation values are found to tend to infinity. Just as under all loads, it is necessary to consider the plastic yielding of the soil, it is found necessary to consider separation which occurs under some conditions, and which accentuates rotation. This aspect is also studied coupled with elasto-plastic conditions of soil.

In addition to the final settlements, it is necessary to study the time rate of settlement of ring footings. The extreme cases of fully flexible and fully rigid ring footings undergoing axisymmetric consolidation

have been investigated. Except for the Mandel-Cryer effect in the initial stages of consolidation, the Terzaghi-Rendulic theory predicts the overall consolidation response in a computationally economical manner with sufficient accuracy. Therefore, it has been adopted in the present study. The effects of various drainage boundary conditions, the radii ratio, the depth ratio, construction time and anisotropy with respect to permeability have been studied. In case of rigid footing, although the main aim was to study the consolidation settlements, a study of changes in contact pressures with time has also been included.

During the course of the investigations on annular footings in this work, it has been observed that from the point of view of settlement at all load levels, annular or ring footings are advantageous over circular footings and that it is essential to consider the plastic yielding of the soil at all load levels, and separation of footing from the soil wherever it occurs.

CHAPTER 1

INTRODUCTION

1.1 GENERAL

A structure is only as good as its foundation. A proper choice of type of foundation suitable for the structure as well as for the foundation soil and a proper design of foundation are of utmost importance. A good design embodies a judicious combination of requirements of safety and economy for which, an accurate geotechnical prediction of performance of the structure under all loads and at all times is essentially required.

In general, the aspects of design of a foundation are:

- 1) The stability of the structure with reference to its ultimate load bearing capacity(strength problem).
- 2) The settlement (Deformation behaviour)
 - (a) Maximum settlement
 - (b) Differential settlement.
- 3) Foundation-soil interaction.

The research work done in regard to the first aspect mentioned above has now reached a limiting stage where the methods of predicting the ultimate capacity are already well established. The second aspect in regard to deformation

behaviour is however still a challenging research activity. A need for prediction of the entire load settlement response to failure has briskly activated the research in this field since late sixties of this century. (Davis, 1969, Roscoe, 1970). The third aspect, although of a relatively recent origin, has brought in radical changes in the outlook on foundation design recognising the fact that the geotechnical and structural aspects of foundation design should not be uncoupled.

The research work in regard to annular footings foundations is however, surprisingly though, quite scanty.

1.2 ANNULAR OR RING FOOTINGS AS FOUNDATIONS

For any isolated tall and heavy civil engineering as structure, a circular shape in plan is ideally suited structurally, functionally and aesthetically. Presently, all types of storage tanks, chimney stacks, silos and towers for several purposes such as aviation control, observatory, transmission, television etc. are the structures for which circular or annular footings are being or could be advantageously used. Annular footings are also suited where the columns or 'legs' of a structure lie on a circle in plan.

1.3 ELASTO-PLASTIC ANALYSIS

The importance of existence of very high stresses in soil near the edges of rigid footings has been recognized since

late thirties (Borowicka, 1936, 1939). Analytical and numerical solutions based on the theory of elasticity have shown that except for very flexible footings, the contact pressures near the edges of a footing are extremely high (theoretically, of infinite magnitude). (Brown, 1968). Therefore, even under small loads, a portion of the soil is bound to yield plastically. This fact has been recognised and some values of limiting edge pressure are suggested by various researchers, for example , Schultze (1961), Zeevaert(1972). The existance of yielding and the consequent limiting of edge contact stress and the dependence of pressure distribution on load level has been confirmed experimentally also, e.g. Selvadurai and Kempthorne (1980). However, incorporation of these facts in the entire load-settlement analysis of annular footings has not been found in the present literature. The technique of using limiting stress concept has been used (e.g. Hain, 1975) but it has been reported to be not valid when large portions of soil yield under the footing. At lower load levels, this approach does not give results far from elastic analysis.

The major portion of work at present is based on elastic theory alone and that too pertaining to circular footings (and not annular footings). Even though elasto-plastic analysis is likely to give results close to those of

elastic analysis in the lower range of load levels, it is necessary to find the extent of agreement quantitatively. Further, elasto-plastic analysis becomes necessary and important at working loads and in the nearby range of loading in which the actual conditions may exist. The load-settlement behaviour, if predicted sufficiently accurately, in the range of loading between working load and failure, is of utmost importance, to visualise and predict the risk involved. All such studies are possible only if an elasto-plastic analysis is employed. It ought to be mentioned here that in the present age of competitive designs, and low factors of safety, the prediction of the entire load settlement response, including situations of existence of yielding of soil over considerable area of the footing, is all the more necessary. In several situations the allowable bearing pressure is to be read off against allowable settlement for which the entire load-settlement curve should be predicted realistically. It is therefore appropriate to use a reasonably accurate simplified elasto-plastic analysis than relying on rigorous elastic analysis by itself.

1.4 THE CHOICE OF METHOD OF NUMERICAL ANALYSIS

For elasto-plastic analysis of the type of problems tackled in the present work, the suitable methods are

approximate numerical techniques, viz., (a) the Finite Element Method (FEM) and (b) the method of numerical integration of elastic solutions with the simplified concept of limiting the stress to yield stress value of soil. The Boundary Element Method (BEM) is not considered here because of the complexity involved through iterative procedure and the requirement of availability of elastic solution involving body forces.

Assuming that appropriate stress-strain relation and elasto-plastic model are available and that sufficient data of fixed or variable soil parameters, stress paths etc. is properly incorporated, a FEM elasto-plastic solution of a three dimensional problem is computationally very costly. If a parameteric study or design data is the aim, FEM may turn out to be computationally prohibitive. At the same time, FEM is a powerful and perhaps the only tool to deal with a specific complex problem and should be used in such cases when the need arises.

There are several situations wherein elastic solutions are readily available. It is desirable to take full advantage of these and the method of numerical integration is the one which is based on this. This method avoids soil discretization, which is the main cause for using up computer memory and time to a great degree in

methods like FEM. Even in some nonhomogeneous conditions, elastic solutions based on some average or equivalent values are expected to give fairly good results.

As far as introducing plastic yield of soil is concerned, the method of first finding the stresses from elastic theory and then limiting the stresses to yield stress value of soil causing redistribution of stresses has been already in use. This method involves a computation effort which, in comparison to FEM employing even simplified elasto-plastic analysis, could be termed as negligible. However, as pointed out earlier, the present methods of this type do not cover the entire range of load-deformation response.

It may be added here that if FEM is to be used for axisymmetric problems involving solution upto collapse load, enormous computational cost will be involved since fifteen-noded elements would have to be used (Sloan and Randolph, 1982).

1.5 ORGANISATION OF THE THESIS

In the preceeding sections of this chapter, a brief introduction has been given regarding the importance of the problem taken up in this thesis and the need to employ an appropriate method of analysis and a method of solution with a wide parameteric coverage and yielding fairly

accurate results at reasonable computational costs.

In the following paragraphs, a brief description of the contents of the succeeding chapters is given.

Chapter 2 is devoted to a broad review of literature available in the field relevant to the present work.

Chapter 3 deals with the load settlement response of a smooth perfectly rigid annular centrally loaded footing. (Circular footing is dealt with throughout the thesis as a particular case of annular footing). Along with the general and particular assumptions, some remarks about the implied limitations are given. The analysis presented is based on the use, to start with, of available elastic solutions for settlements due to a point load. In general, the solutions are numerically integrated using appropriate discretization of the footing. The following types of problems are handled:

Problem type A - Footing resting on the surface of a semi-infinite soil.

Problem type B - Footing embedded in semi-infinite soil.

Problem type C - Footing resting on the surface of a soil layer of finite thickness, underlain by rough rigid base.

For dealing with elasto-plastic analysis, the concept of limiting stress has been used. This along with partitioning and modification of influence coefficient matrix have been employed to obtain the load settlement response in the entire range of loading upto failure.

Chapter 4 deals with the same cases as of Chapter 3 but taking into account the finite rigidity of the footing. All the studies are made in terms of the finite rigidity of the footing relative to soil. A broad study of bending moments and shear forces (maximum values in particular) induced in the footing has been included in this chapter. The footing is idealised as thin plate and the interaction analysis is carried out by combining the inverted soil flexibility matrix with the plate rigidity matrix. The configuration of loading on the footing plays an important role and its effects have been studied broadly in this chapter. In some cases, like a centrally loaded relatively flexible footing, separation occurs between some portion of the footing and the supporting soil. This has been taken into account in the analysis contained in this chapter.

The effect of supplementing a centrally loaded rigid ring footing resting on semi-infinite soil by piles has been studied in Chapter 5. The piles are assumed incompressible. Along with the footing, the piles are also

discretized and an integrated elasto-plastic analysis is carried out in this chapter. Some results for a single floating pile are included for the purpose of comparison with available solutions. The effects of length, number and positioning of piles are broadly studied and discussed in this chapter.

Chapter 6 deals with eccentrically loaded rigid ring footings. The three types of problems dealt with in Chapters 3 and 4 are included for study in this chapter also. The problem of separation or lift-off, which crops up due to high eccentricities along with plastic yielding of soil has been dealt with in this chapter. The method of analysis is similar to that of Chapter 3 or 4, but the method of solution has been modified slightly to achieve economy in computations.

Chapter 7 deals with the aspect of consolidation settlement under perfectly flexible and perfectly rigid annular footings resting on a finite layer of soil. The earlier portion of this chapter deals with flexible footings. Terzaghi-Rendulic theory has been used, on the lines of Madhav and Vitkar (1981) to solve this problem. In the latter portion of this chapter, the problem of consolidation of rigid footings is handled. The changes in contact pressure distribution, which are obtained as a by -product of the

solution, are also studied. The construction of footing does take sufficient time and this aspect has been included in this chapter assuming linear build-up of load. Several types of soil may have higher permeability in horizontal direction than in the vertical direction. The anisotropy on account of permeability has also been included in the study.

In all the above mentioned chapters, comparison has been included, with available solutions. Also charts have been presented in all the chapters which could be directly used for design.

The concluding chapter (Chapter 8) contains the summary of the work covered in this thesis, the conclusions drawn on the basis of the study taken up and some suggestions for further study.

CHAPTER 2

LITERATURE REVIEW

2.1 GENERAL

Literature in the field of integrated soil-foundation-superstructure analysis for an accurate prediction of behaviour with the inclusion of time effects also, is scanty, mainly because incorporation of details—especially of superstructure—amounts to loss of generality. Even in the field of soil-foundation interaction, the earlier work proceeded along one detail or the other making highly simplifying assumptions about the rest of the system. The 'gaps' created in the research work of this type—although there is a brisk research activity since late sixties to fill them up—still continue to exist to a certain extent. A brief discussion about these gaps in the field relevant to the present work is presented in the following few paragraphs.

An extract from the lectures by Davis (1969) on the analysis of the settlement of foundations is quoted below.

'The use of elastic theory for the prediction of settlement becomes inappropriate once the load to cause local yield within the soil mass has been passed. Further increase in load produces growth of plastic regions until

they are sufficiently extensive to permit continuous settlement, at which point the ultimate bearing capacity is reached. During the elasto-plastic phase between wholly elastic conditions and full plastic failure, the stress distribution departs increasingly from the elastic distribution. In the plastic regions, the strains at any point are no longer determined solely by the stresses at the point, so that even if the stress distribution can be approximately estimated in an elasto-plastic situation, the settlement can no longer be predicted by analytical or numerical integration of the stresses..... The dilemma is illustrated in figure (See Fig. 2.1).

The existence of a similar situation in the case of the basic stress-strain models for soil is expressed widely by Roscoe (1970) in the tenth Rankine lecture.

Another 'gap' manifested in spite of the tremendous research activity is , a means to obtain at nonprohibitive computational costs, a realistic end product in terms of stresses and deformation responses of foundations using the best available soil and mathematical models. For example, Das and Gangopadhyay (1978) have shown in a particular study that even though a bilinear elastic-plastic finite element analysis is adopted, it requires different sets of assumptions and computer runs to obtain realistic values of

stresses and deformations.

Yet another 'gap' is evident even to-date through the detached roles being played by the structural and geotechnical aspects of the design of foundations. The use of Winkler type of model of soil reaction found even to-date in literature is also indicative of this.

The separate facets of the relevant research work, with all the gaps, are still important in their own way. For example, elastic solutions are still the basis of ~~most of the~~ ^{considerable} research activity. Hence the various facets are included, atleast for the purpose of citing the examples, in the brief review which follows. The review is, in general, restricted to circular or annular footings.

2.2 ANALYTICAL WORK CONNECTED WITH SETTLEMENT OF CIRCULAR OR ANNULAR FOOTINGS IN CONTACT WITH HOMOGENEOUS ISOTROPIC MASS OF SOIL-WITH NO CONSIDERATION OF TIME EFFECTS

2.2.1 Linear Elastic Solutions

Under certain simplifying assumptions, a circular (or even annular) loading configuration is relatively easy for mathematical treatment, e.g. the work of Volterra (1953) on annular footing resting on Winkler type of foundation. Leaving aside the analyses based on Winkler type of soil model, there are several analytical elastic solutions for fully

flexible or fully rigid footings. The basis for most of these solutions is either Bonssinesq's (1885) or Mindlin's (1936) solution for point load. In this respect the tabulations by Ahivin and Ulery (1962) are useful. The solution for annular flexible footing resting on soil of finite thickness is given by Milovic (1973). The solution for flexible circular footing embedded in semi-infinite soil based on Mindlin's solution is given by Nishida (1966) and that for flexible annular footing on finite layer of soil is given by Zinovev (1979). Stress distribution under embedded circular footing using a combination of Westergaad-Mindlin solutions is studied by Babu Shankar (1977).

The case of axially loaded rigid circular raft in frictionless contact with a homogeneous isotropic elastic half-space has been considered by Sneddon (1946), Schiffman and Aggarwala (1961), Chan and Chaung (1979), and the corresponding case of adhesive contact has been studied by Mossakovski (1954), Keer (1967), Spence (1968), Popova (1972) and Egorov et al. (1973). The effect of embedment of rigid circular area in semi-infinite soil is investigated by Butterfield and Banerjee (1971) and that on the surface of a soil of finite thickness is studied by Egorov and Serebrjanyi (1963) and Poulos (1968). The effect of embedment of a rigid circular area in a soil of finite

thickness is investigated by Banerjee (1971).

Annular footings are considered by Egorov (1965) for smooth contact and by Shibuya et al. (1974, 1975) for smooth as well as adhesive contact. Annular footings are also studied by Valov (1968) and Dhaliwal and Singh (1977). The effect of finite depth is empirically studied by Egorov et al. (1979). A modified version of approximation suggested by Poulos and Davis (1975) is used by Madhav (1980) to extend the Milovic's solution for flexible rings to smooth rigid rings resting on a finite layer of soil.

The flexure of a thick circular raft resting on elastic medium is studied by Selvadurai (1980). A method of settlement calculation considering statically and kinematically admissible solutions for uniformly loaded circular area or vertically loaded rigid circular footing is suggested by Denvar (1981).

Moment loading on smooth rigid circular footing is studied by Borowicka (1943) and Sneddon (1946), for semi-infinite soil. Approximate solution for the corresponding case for circular footing resting on a soil layer of finite thickness is given by Egorov and Nichiporovich (1961). The case of eccentric loading on smooth rigid annular footings is investigated by Hara et al. (1975) and by Egorov et al. (1979, 1980). Eccentric loading of embedded rigid circular footing

is considered by Selvadurai (1980) and a study of stress and strain state of a subgrade under eccentric loading is done by Egorov et al. (1980). Wilson (1965) has suggested a novel method of converting asymmetric problems into axisymmetric problems by expressing the loading as a Fourier series.

The above mentioned work, although it pertains to fully flexible or fully rigid footings, is good enough to predict the overall elastic settlements. However, the differential settlements and bending moments and shear forces in a footing are highly sensitive to the relative rigidity (or flexibility) of the footing and to the loading configuration. Some significant works connected with circular footings of finite rigidity are mentioned below.

A significant work in this field (circular footings of finite rigidity) goes back to as early as 1939. Borowicka (1939) gave solutions for uniformly loaded and centrally point loaded circular footings. Except for a few works e.g. Ishkova (1951), the work in this field appears to have taken impetus only from late sixties. Analytical solutions are given by Brown (1969) to the problem of uniformly loaded circular footing resting on semi-infinite soil or a finite layer of soil. Analytical solutions are also advanced by Hooper (1976) for parabolic adhesive loading and by

Selvadurai (1979) for uniform loading using variational approach. Some numerical solutions in connection with circular rafts are those given by Barden (1965), Smith(1970), Zbirohowski-Koscia and Gunasekera (1970), Hooper (1974) and Chakravorty and Ghosh (1975). Various types of numerical techniques were used such as finite difference (e.g. Chakravorty and Ghosh), finite element (e.g. Smith), iterative (e.g. Zbirohowski-Koscia and Gunasekara) etc. Wood (1977) has presented an approximate analysis. Chakravorty and Ghosh have considered asymmetrical loading also.

Lastly, some of the important elastic solutions, although not fully covered under the topic of this section (such as pertaining to non-homogeneity, anisotropy etc.) but pertaining to circular shapes or footings are cited as follows. England (1962), Gerrard and Harrison (1970), Desai and Reese (1970), Chen and Engle (1972), Gerrard and Wardle (1973), Carrier and Christian (1973), Hooper (1975), Boswell and Scott (1975), Buragohain and Shah (1977), Varma et al. (1977), Wardle (1977), Hanuska et al. (1978), Brown and Gibson (1979) and Gazetas (1981, 1982). Circular footings with loads which are transverse, torsional etc. are not included in the review.

Many important elastic solutions are recorded by Giroud (1972) and Poulos and Davis (1974). A detailed discussion about the analytical approaches and methods to solve the interaction problem of 'plate on continuum' is presented by Selvadurai (1979).

2.2.2 Non-linearity as a Consequence of Loss of Contact

There are certain situations in which an elastic analysis would indicate the presence of tensile contact stresses between the footing and the soil. Since real soil is known to be extremely weak in tension, the existence of such tensile stresses is unrealistic, and loss of contact or separation would occur. This can occur due to moment or eccentric loading or even due to a loading near the centre of a relatively flexible circular footing. The conventional assumption of linear variation of contact pressure can give a rough estimate of the cut-off area. Dave (1977) studied this aspect for annular footing on the assumption of linear variation of contact pressure and concluded that annular footings are better than circular ones.

Cheung and Nag (1968) developed a simple but effective procedure to deal with the problem of separation of contact surfaces. It is outlined below.

- (i) Obtain a linear elastic solution.

- (ii) If all the contact pressures are compressive the problem is solved. Otherwise proceed to next step.
- (iii) Find out the nodes which are associated with tensile contact pressures and make the corresponding rows and columns in the original flexibility matrix zero.
- (iv) Invert the new flexibility matrix for the foundation to obtain a new stiffness matrix.
- (v) Combine this with the plate (footing) stiffness matrix by assuming compatibility at the nodes that have compressive contact stresses and go to step (ii).

Svec (1979) also used a method which is basically the same as that of Cheung and Nag, except that it replaces inversion of the full new foundation flexibility matrix by inversion of a small matrix related to the region of loss of contact only through a procedure of partitioning.

Gladwell and Iyer (1974) considered the loss of contact between a centrally loaded circular plate and the elastic half-space. Solutions using finite difference are obtained by Banerjee and Jankov (1975) for asymmetrically loaded circular rafts, considering separation.

In FEM, tension cut-off has been dealt with on the basis of 'no-tension' analysis developed by Zienkiewicz et al. (1968), e.g. Germanis and Valliappan (1975).

2.2.3 Non-linearity in Load Settlement Response Under Increasing Load

Brown's (1968) discussion on the effect of local bearing failure on behaviour of rigid circular rafts is significant of the awareness towards the need to study stages inbetween the linear elastic settlements and ultimate bearing capacity. (It is now a recognized fact that the whole response is nonlinear). Roscoe's (1970) tenth Rankine lecture also highlighted the need to predict load deformation characteristics in the entire load range. The research work in this aspect can be deemed to have started around this period and also it was accelerated due to the employment of FEM.

Desai and Reese (1970) employed FEM along with non-linear representation of stress-strain relationship to obtain a very realistic non-linear load-settlement response of circular bearing plate. The literature related to general techniques and analyses incorporating non-linearity in FEM can be cited in the works of Oden (1972), Desai and Abel (1972), Zienkiewics (1977) and Desai and Christian (1977). A brief discussion under classified headings is given below in connection with non-linearity in general.

(a) Pseudo-Elastic Methods of Non-linearity

In these methods the non-linearity is introduced through changes in elastic parameters of the soil with no consideration of onset of plastic yield. The most straight-forward methods are based on the shape of stress-strain curve of the soil. Bilinear is the simplest form. An approach in which the second portion of the bilinear model (or the last one in multilinear model) represents a very small slope is quite popular since it gives elasto-plastic like response (Fig. 2.2). One such work is by Dunlop and Duncan (1970) in which the stresses are checked against shear strength and if they exceed the strength, the corresponding elements are assigned a reduced value of modulus. Hyperbolic law (Fig. 2.2) based on Kodner's (1963) work is one of the most popular mathematical forms which follow closely the usual stress-strain curves. The formulation for use in FEM is given by Duncan et al. (1970). Ramberg-Osgood (1943) presented a three-parameter mathematical function. Wong (1971) suggested a parabolic function. Desai (1972) developed an approach in which the stress-strain data is simulated using cubic and bicubic spline functions (Fig. 2.2).

There are numerous ways in which the elastic parameters can be varied, hence a large variety of solutions are also seen in the literature. Clough and Woodward (1967)

suggested, in the study of embankments, that the deformation modulus $M_d (=E/2(1+\nu))$ should be changed keeping the bulk modulus $M_b (=E/2(1+\nu)(1-2\nu))$ constant. Girijavallabhan and Reese (1968) selected the value of E depending on the state of strains. Huang (1969) assumed that E should be changed with the first and second invariants of stress for sand and clay respectively. Das and Gangopadhyay (1978) even suggested, for the solution of the same problem, two different methods of changing elastic parameters. They reported that in the bilinear elastic portion, E should be changed keeping ν constant to obtain stresses correctly, whereas both E and ν should be changed keeping bulk modulus constant to obtain deformations correctly.

A very simple and interesting approach has been adopted recently by Bobe and Pietsch (1981). They have suggested that based on a new strength theory by Szabo (1970/71), a variable modulus $V = E(1-q_m/q_f)$ should be used which directly depends on the load level q_m/q_f , where q_m is the mean applied pressure on the bearing plate or foundation and q_f is the ultimate bearing pressure (which depends on geometry of the footing). However this modulus is to be used to find out directly the settlement at any load level, and the contact pressures etc. are to be worked back. The method is suggested to be used for shallow

foundations only and expression for q_f for rectangular plate or footing is given by them.

The above method by Bobe and Pietsch yields the following results which are qualitatively realistic.

- (1) The load-settlement response is non-linear throughout.
- (2) The settlement tends to infinity as load approaches ultimate load.
- (3) The contact pressure distribution (worked out) shows no peaks of extremely high pressures near the edges as predicted by elastic theory.

They have claimed that their method gives results tallying with some experimental results of other investigators.

In their method, it is found that although non-linearity in settlement response is actually a consequence of and should depend on the contact pressures changing with the load and the subsequent changes in the nature and extent of the yield of soil under the footing, they (the contact pressures) are not implicitly involved in the settlement calculations but are only worked out.

(b) Rigorous Elasto-Plastic Analysis

Most of the work in non-linear analyses is found in literature to have been based on the spatial separation

of elastic and yielded zones and treating them separately. In the rigorous analysis, the appropriate flow rules are applied to the soil in the regions which satisfy the appropriate yield criterian. In the rigorous analysis a need arises for dealing with the complexities of volume change, work done / extracted, work hardening or softening, large strains, tension cut-off etc. and for choosing the appropriate associated or non-associated flow rule, not only to get good predictions but also to get them at reasonable computational cost. The latter is usually quite difficult especially for 3-D analysis and it is found from literature that simplified methods (pseudo-elastic, simplified elastic-plastic etc.) are sought for. A comprehensive discussion about rigorous elasto-plastic analysis is found in the works of Nayak and Zienkiewicz (1972), Zienkiewicz (1977) and Desai and Christian (1977) .

(c) Simplified Elasto-Plastic Analysis

The stress-strain behaviour of soil can be represented in a very easy and simplified way as perfectly elastic-perfectly plastic (Fig. 2.2). In methods like FEM, it is not possible to deal with zero modulus, so either a small value is assigned or incremental stress-strain relations are introduced at the end of elastic limit (as in one of the rigorous elasto-plastic methods). But in the method using

numerical integrations, this can be achieved as described below in brief.

Hain (1975) suggested a method of 'limited contact stresses'. In this method the stresses only at the contact between the footing and the soil, which are the most significant ones from the points of view of local yielding and consequent settlement, are checked against strength of soil and if they exceed the strength value, they are held at that value. Further compatibility of displacements is not considered in this region which therefore does not violate the assumed simplified plasticity rule (large strains without increase in stress). Hain's method is outlined below in brief.

Initially a linear elastic analysis is performed. If the reaction at any point in the soil mass has exceeded the local ultimate bearing pressure it is held at that value and the stiffness matrix is modified effectively deleting the concerned nodes from the analysis. The excess load on the yielded elements is transferred to the non-yielded areas, causing redistribution. The iterative procedure is repeated until no further points yield during a cycle.

In this type of analysis, the contact pressure distribution is obtained at each stage of loading along with settlements.

A similar analysis is also performed by Poulos and Davis (1980) for piles.

Hain has reported however that an analysis of this sort is not expected to predict correctly the deflection of the plate when yielding has occurred over a large area of the plate.

Study of centrally loaded annular footings using FEM with hyperbolic stress-strain law and Mohr-Coulomb yield criterian has been presented by Patankar (1982) for some particular sizes of footings resting on the surface of sand . For the cases considered it has been concluded that lesser total and differential settlements are obtained with increasing values of ratio of inner to outer radius of the footing for the same intensity of loading. It has also been concluded that proximity of rigid layer improves the load settlement characteristics.

(d) Non-linearity Through Stress-path Method

In this method the stress-strain relations are governed by stress-path. For example a solution for circular footing on sand using stress-path method is given by Varadarajan and Arora (1982).

(e) Non-linear or Higher Order Elastic Theories

This approach has not been usually adopted as seen from the literature, probably because these theories involve

more number of soil parameters which are difficult and cumbersome to obtain. A ~~hyperelastic~~ formulation given by Trusdell is included in the work of Eringen (1962).

2.3 ANALYTICAL WORK IN CONNECTION WITH PILED ANNULAR FOOTINGS

There is no work found in the literature, directly dealing with piled annular footings. Poulos (1968) and Poulos and Davis (1980) have done elastic analysis of single and twin pile-rigid circular cap units, have extended it to pile-raft systems using interaction factors and have also suggested an approximate method to account for failure of piles. Such an extension from FEM results for a single unit, using non-linear interaction factor method is also suggested by Narasimhan (1982).

The Finite element method or the Boundary element method for the three dimensional problem has not been employed in many cases probably because of very high computational cost involved.

2.4 CONSOLIDATION SETTLEMENT OF CIRCULAR FOOTINGS

2.4.1 Flexible Circular Footings

Most of the available analytical solutions of the governing differential equations defining the phenomenon of time rate of settlement are for loading on homogeneous elastic half space. The solutions by Gibson and Lumb (1953), Davis and Poulos (1972) can be cited as those based on simple

diffusion theory. Solutions based on rigorous Biot's theory are given by De Jong (1957), Mandel (1957, 1961), Paria (1957), McNamee and Gibson (1960) and Gibson et al. (1970). The diffusion theory, (called as pseudo-consolidation theory) is reported to give results of settlement in between those from Biot's theory for $\nu = 0$ and $\nu = 0.5$ (Davis and Poulos, 1972).

2.4.2 Rigid Circular Footings

Analytical solutions for circular footings on semi-infinite soil are given by Agbezuge and Deresiewicz (1975) and Chiarella and Booker (1975). Agbezuge and Deresiewicz used Hankel-Laplace transforms to give solutions for $\nu = 0$ case. Chiarella and Booker used integral transforms and gave an analytical solution. In both the cases it has been concluded that there is a decrease in contact pressure at the centre of the rigid footing, with time (accompanied by an increase in contact pressure near the edge of the footing). Yamaguchi and Murakami (1977) gave solution for strip and indicated an analytical method for the solution for a circular footing.

2.4.3 Rafts of Finite Rigidity

Consolidation problems for rafts of finite rigidity can be solved using finite difference or finite element

methods, along the lines indicated by Sandhu and Wilson (1969), Christian and Boehmer (1970), Hwang et al. (1971, 1972), Yokoo et al. (1971), Booker (1973), Ghaboussi and Wilson (1973), Valliappan and Lee (1975), Asproudas and Desai (1975), Smith and Hobbs (1976), and Sandhu (1977).

An interesting method, for consolidation under footings of buildings, is given by Komornik and Mazurik (1977) in which a step-by-step iterative procedure with small time steps is adopted to find out and correct the compatible settlements.

2.5 MISCELLANEOUS STUDIES

A very limited literature is found to exist on laboratory and /or field tests on circular/annular footings. The references of Desai and Reese (1970) and Das and Gangopadhyay (1978) can be cited. There are several post-failure studies of failure of tanks/towers, e.g. Bozozuk (1972) for an annular footing, Bell and Iwakiri (1980) for a tank. Failure of circular structures like oil storage tanks could be very costly. For example, it has been reported by Bell and Iwakiri (1980) that the failure on 18th December 1974 of a hot oil tank 52.3 m. diameter at Mizurhima, Japan amounted to a loss of 150,000,000 dollars.

A study of effects of period of construction and anisotropy with respect to permeability on the consolidation

settlement under a fully flexible circular footing is conducted by Madhav and Vitkar (1981).

2.6 CONCLUDING REMARKS

It is observed from the literature that a solution for the entire load-settlement response of piled or unpiled annular footings with generalized results for direct use in the design is not available. The effect of finite rigidity of annular footings is a research area which also has remained unattended to. The consolidation under annular footings-rigid or flexible-taking construction time and anisotropy with respect to permeability into account has not been studied. A quantitative investigation of the unattended aspects mentioned so far in connection with annular footings is essentially required, to obtain a better understanding of the behaviour and economical design of such footings which are going to be used as foundation for a large number of tower like structures to come up in future.

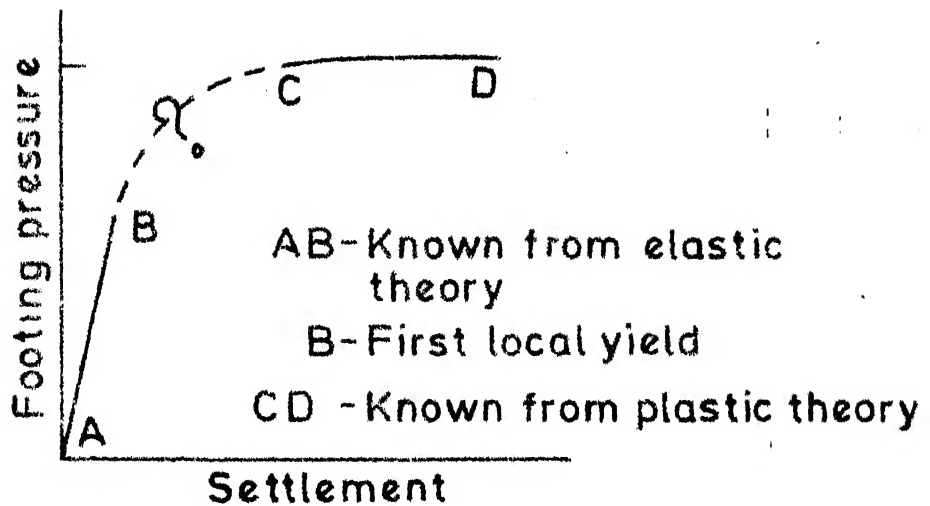


FIG.2.1 THE UNKNOWN ELASTO-PLASTIC LOAD SETTLEMENT CURVE

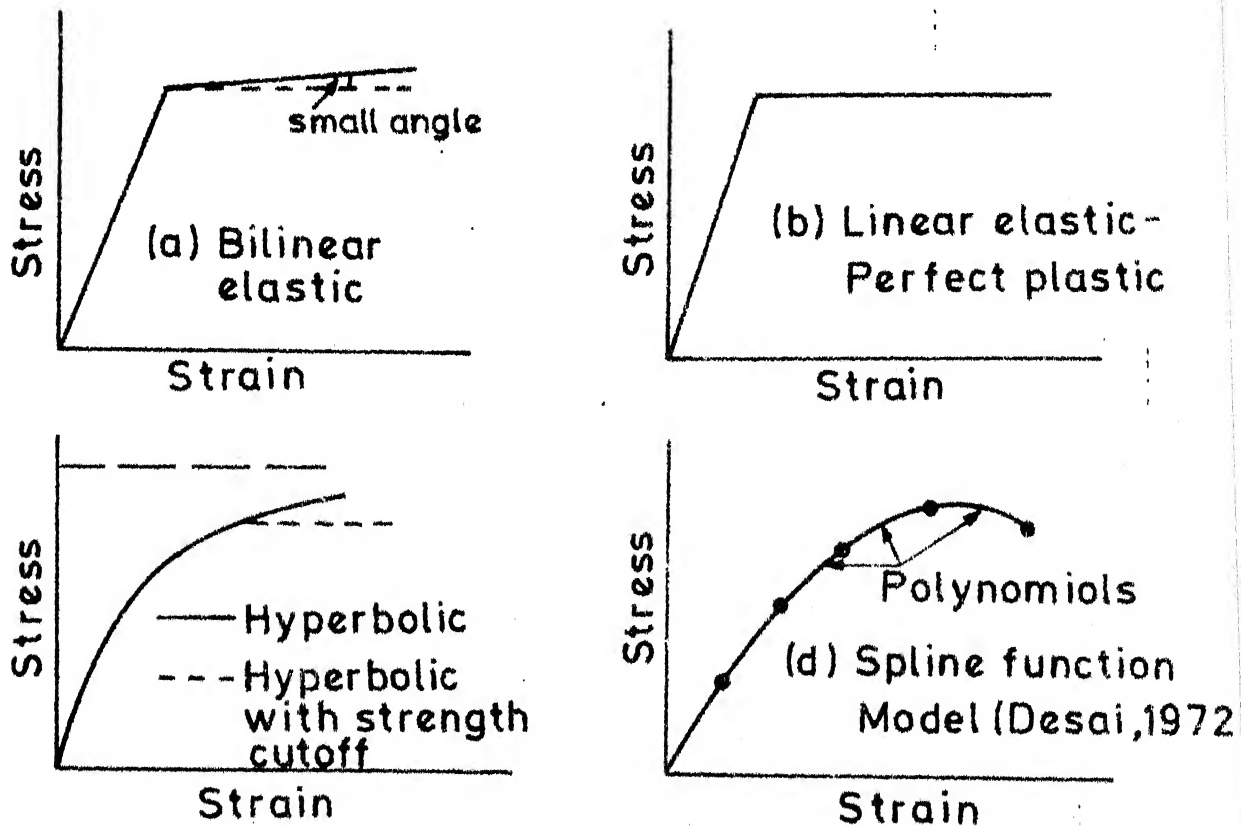


FIG.2.2 TYPICAL CONSTITUTIVE LAW MODELS

CHAPTER 3

ELASTO-PLASTIC SETTLEMENT ANALYSIS OF CENTRALLY LOADED RIGID ANNULAR FOOTINGS

3.1 INTRODUCTION

For isolated structures such as water tanks, cooling and other types of towers, silos, chimney stacks etc., footings in the form of an annular ring are well suited. Primarily such structures are centrally loaded and in several cases the footings can be classified as rigid relative to the soil on which they rest. A study of centrally loaded rigid ring footings (circular footing being a particular case) has been made in this Chapter for predicting the settlement response of the footings over the entire range of loading upto failure.

Since plastic yield of soil, as a consequence of high stresses introduced under a rigid footing, would always exist even under a small load on the footing, the elastic analysis alone is not strictly valid. An attempt is made herein to introduce a simplified elasto-plastic analysis in which the concept of limiting the stresses to yield stress of soil has been introduced. Advantage is taken of the available elastic solutions covering the entire soil mass. For the reasons mentioned in Chapter 1,

the method of numerical integration of the available solutions is used and a technique of partial inversion of modified influence coefficient matrix has been adopted. The results from the present analysis, in the very low range of loading represent elastic behaviour to a sufficiently high accuracy. Such results when compared to available elastic solutions which are exact in some cases and approximate in some other cases, show a good agreement. In a few cases, experimental data and results from FEM are available and the results of the present analysis when compared to these show good agreement.

Solutions for settlement analysis of rigid annular footings which cover an entire range of loading and take elasto-plastic conditions of soil into consideration are not available presently. The conventional settlement analysis is still based on the application of theory of elasticity assuming a linear stress-strain response of soil.

Relevant elastic solutions compiled by Poulos and Davis (1974) consists of the works of Borowicka (1939), Schiffman and Aggarwala (1961), Egorov and Serebryani (1963), Egorov (1965), Poulos (1968), Brown (1969) and Butterfield and Banerjee (1971). A judicious extension of Milovic's (1973) solution for flexible annular loadings for predicting approximately the elastic settlement under rigid annular

footings is done by Madhav (1980). Egorov et al. (1979) have given correction factors, for depth of layer, to be applied to the elastic solution for semi-infinite soil. These correction factors correlated to field data appear to indirectly include the effect of elasto-plastic nature of the soil in field. A study of circular footings under simplified elasto-plastic conditions is contained in Hain's (1975) work. However Hain has reported that the solution is not valid when large portion of soil yields under the footing. A non-linear load settlement response under all loads, a highly non-linear and rapidly increasing settlement under higher loads, and a tendency of infinite settlement as failure is approached are not obtained through Hain's solution. The concept of limiting stress which Hain adopted has been used in the present work also.

For simple soil conditions (homogeneous, isotropic) and the usual positions of foundation i.e. either on or inside a soil mass of considerable depth (treated as semi-infinite) or at the surface of a layer of finite depth, elastic solutions are readily available either in the form of expressions or tables (e.g. Poulos and Davis (1974)). These situations are taken up for study in this Chapter. For the central loading as considered in this Chapter, the footing discretization is limited only to the number of annular rings

and hence the size of the problem in terms of the size of the matrix is relatively extremely small, which is further reduced as yielding progresses. An overall study of a realistic load-settlement response with a significant improvement over elastic solutions has been achieved at a considerably low computational cost.

3.2 ASSUMPTIONS AND STATEMENT OF THE PROBLEM

3.2.1 Assumptions

(A) The general assumptions applicable throughout this thesis, except for the case of consolidation settlement (Chapter 7) are:

- (a) (i) The soil is homogeneous, isotropic and linearly elastic upto yielding.
- (ii) The footing has smooth contact with soil.
- (b) For the onset of yield and for the yielded soil, the following assumptions are made on the lines of Hain (1975), and Poulos and Davis (1980):
 - (i) The soil yields plastically when the contact stress reaches a yield pressure q_y and the stress is held at that value.
 - (ii) Although at the points of contact, compatibility of foundation and soil displacements at a yielded element is no longer possible, displacements anywhere in the soil caused by the limiting stress q_y are still given by

elastic theory.

(B) For the purpose of the study in this Chapter, the following assumptions are also applicable:

- (i) The footing is in the form of an annular ring (a circle being a particular case) and is perfectly rigid.
- (ii) The footing is loaded vertically and centrally (giving rise to an axisymmetric situation).

3.2.2 Important Implications of the General Assumptions

The general assumptions contained in 3.2.1(A) (a) and (b) above imply that the soil basically obeys linear elastic stress-strain relations and has a unique value of yield stress, for a given soil, irrespective of the geometry of the problem. The analysis based on these assumptions, although a significant improvement over purely linear elastic analysis, would amount to a simplified elasto-plastic analysis which is appropriate for clays, especially over-consolidated clays.

The assumption regarding smooth contact between the footing and the soil would amount to a slight overprediction of settlement, which would be less than 3 percent for rigid circular footings and even lesser for ring footings (Shibuya et al., 1975). The tangential forces due to adhesion are

more for lower values of Poisson's ratio and relative rigidity of the footing (Santos and Quera, 1981). Still, since they are small and self-balancing, the effect on settlement is likely to be less in all the usual cases.

Except for loading at the outer edge, the assumption of smooth contact leads to slight overprediction of bending moments in the footing, but is on the safer side. It can be said that this assumption is likely to give results, on the safer side in most of the cases and within about 5 percent of those expected for an actual footing in the field.

3.2.3 Statement of the Problem

A smooth perfectly rigid annular footing of outer radius 'a' and inner radius 'na' carries a central vertical load Q . The 'radius ratio' n is given by

$$n = \frac{\text{Inner radius of footing}}{\text{Outer radius of footing}} \quad (3.1)$$

$n = 0$ refers to the particular case of circular footing.

The following types of problems are studied.

Problem type A : Footing resting on the surface of a semi-infinite mass of soil (Figs. 3.1 and 3.2).

Problem type B : Footing is embedded to a depth 'c' in a semi-infinite mass of soil (Fig. 3.2).

Problem type C: Footing resting on the surface of a soil layer of finite thickness 'h' underlain by a rough rigid base (Fig. 3.2).

3.3 ANALYSIS

3.3.1 Footing Discretization

Most of the basic solutions obtained from the theory of elasticity, for the analysis of settlement, are for a point load. To deal with the variation of contact stress over the footing, the footing is discretized into small elements (Fig. 3.1) and it is assumed that the stress q_j over a small element j is uniform and except when the effect of an element as itself is to be found out, it amounts to a point load acting at the centre of the element. By increasing the number of elements, the inaccuracy involved due to this assumption brought down into tolerable limits.

3.3.2 Elastic Case

For expressing the relationship between elemental stresses and settlements, the basic form of Boussinesq's equation is conveniently adopted. The Boussinesq's equation expresses the vertical surface settlement at a point at a distance r from a point load Q acting vertically at the

surface of a semi-infinite mass of soil as below (Poulos and Davis, 1974).

$$\rho_z = \frac{q(1-v^2)}{2\pi E r} \quad (3.2)$$

where E and v are the elastic constants of the soil.

Treating a uniform load q acting on a small area dA as point load, Eq. 3.2 can be written as

$$\rho_z = \frac{q(1-v^2)}{E} \cdot \frac{dA}{2\pi r} \quad (3.3)$$

In general, the settlement ρ_{ij} at the centre of an element i due to a stress q_j acting on element j (Fig. 3.1) is expressed on the lines of Eq. 3.3 as

$$\rho_{ij} = q_j \cdot a \cdot \frac{1-v^2}{E} I_{ij} \quad (3.4)$$

where I_{ij} is a dimensionless influence coefficient representing any available appropriate elastic solution and 'a', the outer radius of the footing is introduced for the purpose of non-dimensionalising.

Eq. 3.4 in matrix form, representing settlements of all the elements, after non-dimensionalising, reduces to

$$\{\bar{\rho}\} = (1-v^2) [I] \{\bar{q}\} \quad (3.5)$$

where $\{\bar{\rho}\} = \frac{1}{a} \{\rho\}$ is the non-dimensional settlement vector,

$\{\bar{q}\} = \frac{1}{E} \{q\}$ is the non-dimensional contact pressure vector.

and $[I]$ is the influence coefficient matrix.

For a centrally loaded axisymmetric rigid footing, the settlement has to be uniformly equal to, say, ρ_0 . Eq. 3.5 can therefore be written as

$$\{\bar{\rho}\} = \bar{\rho}_0 \{U\} = (1 - v^2) [I] \{\bar{q}\} \quad (3.6)$$

where $\bar{\rho}_0 = \frac{1}{a} \rho_0$ and $\{U\}$ is unit vector.

For overall equilibrium of forces, it is necessary that

$$Q = \sum q_j dA_j \quad (3.7)$$

where, Q is the total applied load and dA_j is the elemental area of the j^{th} element of the footing over which contact stress q_j is acting.

Combining and solving equations 3.4 through 3.7, the settlement of the footing, ρ_0 is obtained as

$$\rho_0 = \frac{Q}{a} \frac{(1 - v^2)}{E} \delta \quad (3.8)$$

where δ is a dimensionless factor given by

$$\delta = \frac{1}{\{U\}^T [I]^{-1} \{U\}} \quad (3.9)$$

3.3.3 Elasto-Plastic Case

Under any load, the contact pressures on some of the elements of the rigid footing would reach the value q_y ,

the yield stress for the soil under consideration, and it is assumed to be held at that value (Fig. 3.3).

Let subscripts 'e' and 'y' represent the elastic and the yielded or plastic components respectively. Eq. 3.6 can now be written in the partitioned form as

$$\left\{ \begin{array}{c} \bar{\rho}_e \\ \bar{\rho}_y \end{array} \right\} = (1 - v^2) [I] \left\{ \begin{array}{c} \bar{q}_e \\ \bar{q}_y \end{array} \right\} \quad (3.10)$$

Since compatibility of displacements is satisfied for elements in the elastic region only, Eq. 3.10 is written as

$$\left\{ \bar{\rho}_e \right\} = \left\{ \bar{\rho}_0 \right\} = (1 - v^2) [I'] \left\{ \begin{array}{c} \bar{q}_e \\ \bar{q}_y \end{array} \right\} \quad (3.11)$$

where $[I']$ is the modified influence coefficient matrix corresponding to the coefficients of the elastic elements i.e. the first, say k_e rows where k_e is the number of elastic elements. For the yielded elements the stress value is known ($= \bar{q}_y$).

The equilibrium equation 3.7 is now written in the form of sum of forces on elastic and yielded elements.

$$Q = Q_e + Q_y = \sum q_e dA_e + \sum q_y dA_y \quad (3.12)$$

Going through the same procedure as in section 3.3.2 above, the settlement of the footing once again can be expressed as

$$\rho_o = \frac{Q}{a} \cdot \frac{1-v^2}{E} \delta \quad (3.13)$$

where δ is the dimensionless factor, which unlike in elastic case, is now a function of not only influence matrix (Eq. 3.9), but also of the nature and extent of yielded region under the footing.

Yet another convenient form of Eq. 3.13 is

$$\rho_o = q_{av} a \frac{1-v^2}{E} I_s \quad (3.14)$$

where

$$q_{av} = \frac{Q}{\text{Area of footing}} = \frac{Q}{\pi a^2 (1-n^2)} \quad (3.15)$$

and I_s is the settlement influence factor.

3.3.4 Elastic Solutions for Various Problem Types

The influence coefficient matrix $[I]$ is generated by calculating the influence coefficients I_{ij} representing the effect of contact pressure on element j on settlement of the centre of element i . The values of I_{ij} for various types of problems under consideration are obtained as follows. The elements i and j are both at the footing level in all the cases,

(i) Problem type A : Footing on the surface of semi-infinite mass of soil.

Under the assumed soil conditions, the Boussinesq's solution for a point load is applicable. The load acting on

an element j of area dA_j can be treated as a point load $q_j \times dA_j$ acting at the centre of the area dA_j , and for its effect on element i ($i \neq j$), I_{ij} is obtained as

$$I_{ij} = \frac{dA_j}{\pi a d_{ij}} \quad (3.16)$$

where d_{ij} is the distance between the centres of the elements i and j .

For an element bounded by radial lines and concentric circles, of radii, r_1 and r_2 ($r_2 > r_1$), the distance of centre of area, \bar{r} , from the centre of the circle is obtained as

$$\bar{r} = \frac{r_1 + r_2}{2} + \frac{(r_2 - r_1)^2}{6(r_2 + r_1)}$$

Eq. 3.16 is not applicable for the effect of an element on itself ($i = j$). The element is taken sufficiently small and the Boussinesq's solution integrated over a rectangle (Poularikas and Davis, 1974) is used to get

$$I_{ij} = \frac{b}{\pi a} \left(\ln \frac{\sqrt{(1+m^2)} + m}{\sqrt{(1+m^2)} - m} + m \ln \frac{\sqrt{(1+m^2)} + 1}{\sqrt{(1+m^2)} - 1} \right) \text{ for } i=j \quad (3.17)$$

where b = width of element and $m b$ = length of element.

(ii) Problem type B : Embedded footing

In this case, Mindlin's (Poulos and Davis, 1974) solution is used in place of Boussinesq-solution, to get

$$I_{ij} = \frac{dA_j}{8\pi a (1-v^2)} \left\{ \frac{3-4v}{R_1} + \frac{8(1-v^2)-(3-4v)}{R_2} \right. \\ \left. + \frac{4(3-4v)c^2-2c^2}{R_2^3} + \frac{24c^4}{R_2^5} \right\} \text{ for } i \neq j \quad (3.18)$$

where $R_1 = d_{ij}$ = distance between centres of elements i and j ,

c = depth of embedment of footing and

$$R_2 = \sqrt{(4c^2+R_1^2)}.$$

For $i = j$, Eq. 3.18 is not applicable. For this case, the Mindlin's formula integrated over a rectangle (Poulos and Davis, 1974) is used to get

$$I_{ij} = \frac{2b}{a(1-v^2)} K_0 \left[K_1 \left\{ \beta \ln \frac{1+\sqrt{1+\beta^2}}{\beta} + \ln(\beta + \sqrt{1+\beta^2}) \right\} \right. \\ \left. + K_2 \left\{ \ln \frac{\beta+t}{\sqrt{1+4\alpha^2}\beta^2} + \beta \ln \frac{1+t}{\beta s} - 2\alpha\beta \tan^{-1} \frac{1}{2\alpha\beta} \right. \right. \\ \left. \left. + 4\alpha\beta \tan^{-1} \frac{(1-s)(\beta s-t)}{2\alpha} + 2\alpha\beta K_1 \tan^{-1} \frac{1}{2\alpha t} \right. \right. \\ \left. \left. + \frac{8\alpha^2\beta t}{s^2(1+4\alpha^2t^2)} \left(2 + \frac{1}{4\alpha^2} - \frac{1}{t^2} \right) \right] \text{ for } i = j \quad (3.19) \right]$$

where $K_0 = \frac{1+v}{8\pi(1-v)}$, $K_1 = 3-4v$,

$$K_2 = 5 - 12v + 8v^2, \quad \alpha = 2c/l, \quad \beta = l/b,$$

$s = \sqrt{1+4\alpha^2}$, $t = \sqrt{1+\beta^2(1+4\alpha^2)}$, l = length of longer side of rectangle and b = length of shorter side of rectangle.

(iii) Problem type G : Footing on the surface of a soil layer of finite depth h .

In this case the available elastic solution in the form of Tables (Poulos and Davis, 1974) has been used. The settlement due to loading q_j on element j is given as

$$= \frac{I_p q_j}{2\pi h E}$$

from which I_{ij} is obtained as

$$I_{ij} = \frac{I_p}{2\pi (1-\nu^2) ah} \quad \text{for } i \neq j \quad (3.20)$$

where I_p is the value of the influence coefficient obtained from the Table by using Lagrangian interpolation.

For $i = j$ and also for elements which are close to each other, the I_p values, extrapolated, become inaccurate. Therefore the sector curves, following the method given by Poulos and Davis (1974), are used.

3.4 RESULTS AND DISCUSSION

3.4.1 Discretization

The annular footing was divided, depending on the radius ratio n , into 8 to 16 rings and further into 10 to 20 sectors. It was found that since the influence coefficients are more or less proportional to the inverse of the distance

between the elements, it was not necessary to subdivide the elements farther away from the neighbouring and the next-to-the-neighbouring elements. The effect of subdividing a neighbouring element was found to be of the order of about 2 percent only but it was found necessary to subdivide the neighbouring elements since the cumulative effect of neighbouring elements (which increase in number as distance increases) was found to be significant. The neighbouring elements and even the next-to-these elements were therefore suitably subdivided to obtain the components of the influence coefficient matrix. For finding the influence of a subelement on itself, formulae for rectangular loads or sector curves were used. It was observed that the best results are obtained by maintaining consistent order of accuracy (and not by increasing the accuracy wherever possible) as far as influence coefficients are concerned.

3.4.2 Computational Economy

In the present Chapter the elements involved at the stage of solution of matrix equations is extremely low in number. Further, in the general computer program developed in this thesis, a provision is included such that yielded elements are successively removed from the matrix equations by substituting the known yield stress values.

Due to this and since soil below the footing is not discretized, the computation becomes highly economical and more so for the simplified elasto-plastic analysis used in the present work. For example, the entire set of results for annular footings on a semi-infinite mass were obtained with CPU time of the order of 2 minutes 40 seconds only on DEC 10 system. The time for the other two cases was more because of involvement of more parameters (depth and Poisson's ratio).

3.4.3 Footing Resting on the Surface of Semi-Infinite Soil Mass

The complete load settlement response of a circular footing ($n = 0$), as obtained by the present analysis is compared (Fig. 3.4) with the results given by Desai (1968). The agreement between the results of the present study with experimental results and those obtained by FEM is good, thus validating the use of the present method.

From Fig. 3.4 it can be seen that all the three curves for $n = 0$ are non-linear throughout. This behaviour is attributable to the fact that even under light loading the soil near the edge of the footing yields, giving rise to the onset of plastic yielding at a very low value of load itself. It is also seen that as the load approaches failure

load, the settlement increases rapidly with increasing load and tends to become infinite at failure load. Thus, in the present analysis, the entire load settlement response is realistically predicted.

In the same Figure (Fig. 3.4), load settlement curves obtained from the present analysis for typical values of radius ratio n ($n = 0.4, 0.6, 0.8, 0.9$) are also shown for comparison between circular and annular footings.

For direct comparison of behaviour, under the same total load, of a ring footing with that of a circular footing using settlement influence factor plotted against contact pressure, a correction factor to I_s is introduced as below.

Let ' b ' be the outer radius of a ring footing which, with a given n value, has the same area as a circular footing of radius ' a ' (Fig. 3.5). Then, for equal area,

$$\pi a^2 = \pi b^2 (1-n^2) \quad (3.21)$$

Also q_{av} can be written as $Q/\pi a^2$ and $Q/\pi b^2 (1-n^2)$ for circle and ring respectively, where Q is the (same) total load. Then using Eq. 3.14, settlement of circular footing under load Q is given by

$$\rho_{oc} = \frac{Q}{\pi a^2} a \frac{1-v^2}{E} I_{sc} \quad (3.22)$$

and, settlement of ring footing under the same load Q

$$\rho_{or} = \frac{Q}{\pi b^2 (1-n^2)} b \frac{1-v^2}{E} I_{sr} \quad (3.23)$$

where I_{sc} and I_{sr} are for the same average contact pressure, so that $I_{sc} = I_{sr} = I_s$.

Denoting the correction factor by R_{eq} and using Eq. 3.21 above,

$$R_{eq} = \frac{\rho_{or}}{\rho_{oc}} = \frac{b}{a} = \frac{1}{\sqrt{(1-n^2)}} \quad (3.24)$$

For comparison of the response of a ring footing with that of a circular footing under the same total load, the I_s values obtained from the charts should be multiplied by R_{eq} .

The values of R_{eq} work out to about 1, 1.02, 1.08, 1.25, 1.67 and 2.3 for $n = 0, 0.2, 0.4, 0.6, 0.8$ and 0.9 respectively. Applying R_{eq} to $n = 0.8$, the settlement of equivalent annular footing is shown in Fig. 3.4. It is seen that the settlement for the equivalent annular footing is also less than that of circular footing. This is true for other values of n also. The settlement at all load levels for annular footings is less than that for a circular

footing and more so for higher values of n .

Fig. 3.6 shows the values of dimensionless settlement influence factor I_s obtained from the present analysis. For the purely elastic case, the dimensionless factor δ is a function of the influence coefficient matrix (Eq. 3.9), which depends on the geometry of the problem only. However, for elasto-plastic case, it is found that, since settlement depends also on the nature and extent of yielded region under the footing, δ or I_s is a function of radius ratio n as well as of load level indicated by the ratio of average applied load to yield stress of soil.

$$\delta \text{ or } I_s = f(n, q_{av}/q_y) \quad (3.25)$$

Because of this, curves for I_s in Fig. 3.6 have been drawn against q_{av}/q_y values for various values of n . Fig. 3.6 which is a design chart for settlement, is to be used in conjunction with Eq. 3.14 namely,

$$p_o = q_{av} a \frac{1 - v^2}{E} I_s$$

From Fig. 3.4 and Fig. 3.5 it can be seen that the settlement curves are non-linear throughout, but they are less non-linear at lower load levels (lower q_{av}/q_y values) and also over a larger range of load level for higher values of n .

On studying the settlements in the range of q_y/q_{av} ratio (a form of Factor of Safety) of about 5 to 1.2, it can be seen that for $n = 0.4, 0.6$ and 0.8 , the settlements, after applying the correction R_{eq} , are roughly 80 percent, 75 percent and 50 percent respectively of settlement for circular footing ($n=0$) for the same total load (and the same area of footing). For $n = 0.9$, this percentage varies from about 50 percent to 37 percent as q_y/q_{av} varies from 5 to 1.2. This clearly shows the advantage of ring footings as far as settlement response is concerned. It must be mentioned that for narrow rings, the settlement, increases almost linearly at a slower pace until q_y/q_{av} ratio of about 1.1 is reached. Thereafter the settlement is likely to increase rapidly for q_y/q_{av} values less than 1.1. If at all a situation of loading very near to failure is likely, a circular footing will show up excessive settlements well before factor of safety of unity is reached, whereas a narrow ring footing will collapse suddenly when the factor of safety falls below about 1.1.

The design chart of Fig. 3.6 can be used in a number of ways. For example, for a known value of load and dimensions of footing, the ratios q_{av}/q_y and n can be worked out and the corresponding settlement influence factor I_s can be directly read and used in Eq. 3.14,to predict settlement.

The permissible loading or even the required radius ratio can be worked out if other relevant data is available.

During the course of solution by the present analysis, the contact pressures and the progress of yield zone also are obtained at various load levels. Fig.3.7 shows typical contact pressure distributions. For the sake of comparison they are drawn for various values of q_y/q_{av} . In case of a circular footing, the yield starts at the outer edge and proceeds inwards under increasing loads. In case of an annular footing, the yield starts at the outer as well as the inner edges but the progress is faster from the outer edge (Fig. 3.7).

The portion of the load settlement response obtained by the present analysis without considering yield represents elastic behaviour. The results in this range are compared with available solutions from theory of elasticity. The settlements and contact pressures obtained by Egorov (1965) are compared with the present analysis (Table 3.1 and Fig. 3.8) and good agreement is found to exist.

From Table 3.1, it can be inferred that at a sacrifice of 5 percent increase in settlement, a circular central portion of radius about two-thirds of the outer radius can be simply dispensed with amounting to 45 percent

saving in footing material.

TABLE 3.1 : VALUES OF $w(n)$ FOR RIGID RING (ELASTIC CASE)

n	0	.2	.4	.6	.8	.9	
$w(n)$ Egorov (1965)	.50	.50	.51	.52	.57	.60	$\rho_0 = \frac{Q(1-v^2)}{Ea} w(n)$
$w(n)$ Present work (Elastic portion)	.50	.50	.51	.52	.55	.61	

This inference drawn on the basis of elastic theory alone could be misleading since yield conditions will always exist and they would increase settlement. Thus, under the same total load, q_{av} will increase in proportion to $(1-n^2)$ and $w(n)$ obtained from elasto-plastic analysis as done in the present work will change since it will be a function of q_{av}/q_y . For example, it has been worked out that, against 45 percent saving as predicted by elastic theory, only 16 percent and 11 percent saving is possible for q_{av}/q_y ratios of 0.5 and 0.67 respectively. It has to be however mentioned that due to plastic yielding of soil, redistribution of contact pressure takes place which would reduce the maximum bending moment in the footing slab and would lead

to a saving in reinforcement if the loading is uniformly distributed over the footing.

3.4.4 Embedded Footing

The results are obtained for this case exactly on the same lines as for the surface footing except that the additional parameters 'c' (depth of embedment) and ' ν ' (Poisson's ratio) come into picture. The embedment herein only means load transfer from footing to soil at depth c . However the load refers to net load at footing level and also q_y refers to the yield value at the depth c .

It has been found from the solutions obtained from the present study that the nature of the contact pressure distribution beneath an embedded footing is not noticeably different (Fig. 3.7) from that beneath a surface footing. It has been also found that the nature of the load-settlement response is also very similar for the embedded and surface footings (Fig. 3.9(a)). Hence it has been possible to express the settlement of embedded footing in terms of that of the surface footing with only the application of correction factors to account for the effects of depth of embedment c , the radius ratio n and the Poisson's ratio, ν .

The settlement of embedded footing is expressed as

$$s'_0 = q_{av} a \frac{1-\nu^2}{E} I'_s \cdot C_c C_n C_\nu \quad (3.26)$$

where I_s' is the settlement influence factor for surface footing corresponding to q_y at depth c and C_c , C_n and C_v are correction factors for c , n and v respectively. The values of these correction factors are presented in Tables 3.2 and 3.3.

I_s' is to be read from the design chart of Fig. 3.6 given for surface footing only, but against q_{av}/q_y value in which q_{av} should correspond to average net loading at the depth c and q_y should be the yield value at depth c which would be higher than that for the surface footing.

TABLE 3.2 : SETTLEMENT CORRECTION FACTOR C_c FOR DEPTH OF EMBEDMENT (Eq. 3.26)

c/a	0	.05	.1	.25	.5	.75	1	2	3	4	6	8	10	15 or more
C_c	1	.99	.98	.95	.91	.87	.83	.71	.65	.62	.58	.56	.55	.53

TABLE 3.3 : SETTLEMENT CORRECTION FACTORS C_n and C_v FOR RADIUS RATIO (n) AND POISSON'S RATIO (ν) (Eq. 3.26)

c/a	C_n						C_v					
	$n=0$	$n=.2$	$n=.4$	$n=.6$	$n=.8$	$n=.9$	$\nu=.05$	$\nu=.1$	$\nu=.2$	$\nu=.3$	$\nu=.4$	$\nu=.5$
0.00	1.0	1.0	1.00	1.00	1.00	1.00	1.0	1.00	1.00	1.00	1.00	1.00
0.05	1.0	1.0	1.00	1.00	0.99	0.97	1.0	0.99	0.99	0.98	0.98	0.97
0.10	1.0	1.0	1.00	0.99	0.98	0.95	1.0	0.99	0.98	0.96	0.96	0.95
0.25	1.0	1.0	1.00	0.99	0.95	0.91	1.0	0.98	0.95	0.93	0.91	0.89
0.50	1.0	1.0	0.99	0.98	0.93	0.89	1.0	0.97	0.93	0.90	0.87	0.84
0.75	1.0	1.0	0.99	0.98	0.93	0.89	1.0	0.96	0.92	0.88	0.84	0.81
1.00	1.0	1.0	0.99	0.98	0.94	0.90	1.0	0.96	0.91	0.86	0.82	0.79
2.00	1.0	1.0	1.00	0.99	0.96	0.94	1.0	0.96	0.90	0.85	0.80	0.76
3.00	1.0	1.0	1.00	0.99	0.97	0.96	1.0	0.96	0.90	0.85	0.80	0.75
6.00	1.0	1.0	1.00	1.00	0.99	0.97	1.0	0.96	0.90	0.85	0.80	0.75
10.00	1.0	1.0	1.00	1.00	0.99	0.99	1.0	0.96	0.90	0.85	0.80	0.75
15.00 or more	1.0	1.00	1.00	1.00	1.00	1.00	1.0	0.96	0.90	0.85	0.80	0.75

The available relations for ultimate bearing capacity q_{y_0} at depth = 0 and q_{yc} at depth = c can be used to get the ratio between these two and finally between q_{av} and q_y at depth c . One such relation, for example, based on empirical formulae for $\phi = 0$ soil is (Brinch Hansen, 1970):

$$\frac{q_{yc}}{q_{y_0}} = 1 + 0.4 \frac{c}{2a} , \frac{c}{2a} \leq 1 \quad (3.27)$$

$$\frac{q_{yc}}{q_{y_0}} = 1 + 0.4 \tan^{-1} \frac{c}{2a} , \frac{c}{2a} > 1$$

Since settlement of an embedded footing is related to that of surface footing (Eq. 3.26), most of the discussion given in Section 3.4.3 above holds good for this case also. The load settlement response is non-linear throughout, large settlements are predicted near total failure and ring footings are advantageous over circular ones.

The effect of embedment is particularly significant, firstly, as can be seen directly from Tables 3.2 and 3.3. Secondly, for higher values of depth of embedment, q_y is higher, q_{av}/q_y is lower and hence I_s , read against q_{av}/q_y from Fig. 3.6 is lower, which amounts to lower settlement obtained from the expression given in Eq. 3.26.

The effect of radius ratio as apparent from Table 3.3 is small, but it is actually quite significant due to its inclusion in the settlement influence coefficient itself.

The term $I_s' \cdot C_c C_n C_v$ in the expression for settlement (Eq. 3.26) is a function of not only c , n and v ; but also of q_{y_c}/q_{y_o} .

$$I_s' \cdot C_c C_n C_v = f(n, q_{av}/q_y, c, v, q_{y_c}/q_{y_o}) \quad (3.28)$$

Thus, the design chart of Fig. 3.6 for surface footings can be used in conjunction with Tables 3.2 and 3.3 and with an appropriate ratio of q_{y_c}/q_{y_o} , for prediction of settlement of embedded rigid ring footings.

The nature of contact pressure distribution, the changes in it at various load levels and the nature and extent of yielded zone under the footing are so similar to those for surface footing that the difference is not noticeable (Fig. 3.7).

It has been observed that (e.g. Fig. 3.9a) the settlement curves obtained by applying corrections to the $c/a = 0$ curves agree with the directly obtained curves within about 4 percent at all load levels.

As discussed in Section 3.4.3 for surface footings, a saving is possible by dispensing with some central portion of a circular footing and the saving is more for higher values of q_y/q_{av} . In case of embedded footing, since q_y is higher, the ratio q_y/q_{av} for the same load and footing will be higher

in comparison to surface footing. Therefore the saving in footing material will be more for embedded footing even when partial yield conditions exist.

Fig. 3.9(b) shows the comparison of results from the present analysis in the low range of q_{av}/q_y , representing elastic behaviour, with those of Butterfield and Banerjee (1971) for embedded circular footing. It is seen that there is a good agreement.

3.4.5 Surface Footing on Finite Layer of Soil

For this case, the available elastic solution in tabular form (Poulos and Davis, 1974) has been used. Unlike embedded footing, the load settlement response in this case is found to be dissimilar in nature to that of surface footing. The settlement is expressed, as

$$\rho_h = \frac{q_{av} a}{E} \cdot I_h \quad (3.29)$$

where I_h is the settlement influence factor, the subscript h denoting the case of soil of finite depth h.

In this case, I_h is a function of depth of layer, h, and Poisson's ratio also.

$$I_h = f(n, q_{av}/q_y, h, v) \quad (3.30)$$

Design charts are presented in Fig. 3.10 to readily obtain the value of I_h for the required data.

From Fig. 3.10, it can be seen that as in the earlier two cases, the settlement response is nonlinear throughout, there are large settlements near total failure and annular footings are advantageous over circular footing.

The depth of compressible layer has a significant effect on settlement. The settlement influence coefficients from the present work, as q_{av}/q_y tends to zero, correspond to elastic behaviour and agree fairly well with those given for circular footing by Poulos (1968) being 2 to 3 percent on higher side and agree within 1 to 2 percent with those for annular footings given by Madhav (1980). However the effect of depth of layer under all values of q_{av}/q_y is of particular interest in the present study. These effects can be directly taken into account if the design charts in Fig. 3.10 are used. Not enough data is available for comparison other than the results in the elastic range. Egorov et al. (1979) have suggested some correction factors, to account for finite depth, to be applied in the expression for elastic settlement of rigid annular footing resting on semi-infinite soil. These factors are reported to yield results close to those obtained from field data. Since field conditions would always involve plastic yield, these factors can be looked upon to include the effect of plastic yield or load level indirectly. For comparing their values with other solutions a factor G is introduced as below which

reflects the effect of depth of layer.

$$C = \frac{\rho_e}{\rho_h} \quad (3.25)$$

where ρ_h is the settlement for footing resting on soil of finite depth and ρ_e is the elastic settlement for semi-infinite soil under the same footing and loading. Some of the values of C which are taken directly from the Tables given by Egorov et al. (1979) are quoted in Table 3.4 along with worked out values based on elastic solutions by Poulos (1968) and those obtained from the present work using elasto-plastic analysis.

TABLE 3.4 : VALUES OF C (Eq. 3.25) FOR TYPICAL CASES

n	h/a	C							
		Poulos(1968)		Egorov et al. (1979)		Present		Work	
		Elastic	$\nu = .5$	$\nu = 0$	$\frac{q_y}{q_{av}} = 2$	$\frac{q_y}{q_{av}} = 1.5$	$\frac{q_y}{q_{av}} = 2$	$\frac{q_y}{q_{av}} = 1.5$	
v					v = .5	v = .5	v = 0	v = 0	
1	2	3	4	5	6	7	8	9	
0	2	1.90	1.43	1.3	1.35	0.87	1.16	0.79	
	1	3.46	2.07	1.9	3.14	2.35	1.74	1.43	
.4	2	-	-	1.3	1.52	1.16	1.39	1.15	
	1	-	-	1.7	2.83	2.20	2.03	1.76	
.8	2	-	-	1.2	1.12	1.05	1.12	0.85	
	1	-	-	1.5	1.68	1.40	1.40	1.12	

The corrections given by Egorov et al. are lower than in the elastic case. C worked out from the present work depends on Poisson's ratio and q_y/q_{av} ratio and the value in any case is lower than that in elastic case. The lower values of C indicating higher settlements; can be attributed to elasto-plastic settlement which occurs in field or which is predicted from the present analysis. Since it is more convenient to use directly the charts of Fig. 3.10, factor C has not been used to express the effect of depth of layer except for the comparison discussed above.

From the design charts of Fig. 3.10, it can be seen that the effect of h/a is more pronounced for lower values of n , for lower values of q_{av}/q_y and higher values of Poisson's ratio. For example, considering $h/a = 0$ and 4, the values of I_s/I_h (indicating ratio of settlement for semi-infinite soil to that for finite depth) for Poisson's ratio = .5 and $q_{av}/q_y = .3$ are about 1.38 and 1.25 for $n = 0$ and $n=.8$ respectively; the value of I_s/I_h for $n=0$, Poisson's ratio = .5 and $q_{av}/q_y = .6$ is 1.34 and for $n=0$, $q_{av}/q_y = .3$ and Poisson's ratio = 0, it is 1.21. For higher values of n , the effect of depth of layer although less pronounced, amounts to overall less settlements. Hence an annular footing resting on a finite depth of soil will show very small settlements.

From the design charts (Fig. 3.10) it can also be observed that as far as overall load-settlement response is concerned, the effect of having less depth of layer is similar to the effect due to increasing n . In both the cases, the settlements are less, the load-settlement curves are nearly linear except in the higher ranges of load level and a somewhat sudden failure occurs as load approaches failure load. This behaviour for lower values of h/a is explained as follows.

The contact pressures tend to be like uniform as h/a decreases. Initially, under increasing load, the yield zone progresses slowly. At the same time the contact pressures in the elastic zone increase and become more uniform. A stage comes when the contact pressures in the elastic region becomes almost uniform and only slightly less than the yield stress. A small increase in load at this stage is enough to cause a rapid advance of yield zone and a consequent high settlement.

Fig. 3.11 shows the progress of yield zone from some typical cases.

The value of q_y for footings resting on finite depth of soil may be taken as the same for footing on semi-infinite soil for $h/a \geq 1.42$. For lower values of h/a , q_y appropriate

for the required value of h/a is to be used. An approximate correction to q_y for depth of layer can be obtained by using Mandel and Salecon's (1969) values of N'_c . These values are for strip footings on clay, but their mutual proportions may be assumed to be same for annular footings. With this assumption, the correction factors, based on Mandel and Salecon's values are shown in Table 3.5.

TABLE 3.5 : APPROXIMATE CORRECTIONS TO q_y FOR DEPTH OF LAYER OF SOIL

h/a	≥ 1.42	1	.667	.5	.4	.333	.25	.2
Correction Factor	1	1.02	1.11	1.21	1.30	1.40	1.59	1.78

The only change, due to the correction for depth mentioned above, in the use of design charts (Fig. 3.10) will be because of the corrected value of q_y . The revised value of q_{av}/q_y is to be used. Due to this correction, the settlement at any load will work out less in comparison to that obtained without correction except for $h/a \geq 1.42$.

3.5 CONCLUSIONS

A simple elasto-plastic analysis using available elastic solutions and a modified procedure has been developed to obtain the entire load-settlement response of centrally loaded smooth rigid ring footings resting on or embedded in a semi-infinite soil mass or resting on a finite depth of compressible layer of soil underlain by a rough rigid base. It is seen that the results when compared with available solutions show good agreement with experimental as well as FEM results. Computational economy is achieved mainly due to the absence of soil mass discretization and due to condensation of flexibility matrix as plastic yielding progresses.

The following are the conclusions, drawn from the present study.

- (1) Due to the absence of purely elastic conditions at any level of loading, the load-settlement response is nonlinear throughout.
- (2) The settlement is implicitly related to the level of loading with respect to the ultimate load.
- (3) For the same load annular footings show lesser settlement in comparison to a circular footing.
- (4) The plastic yield starts near the edge/edges and proceeds towards centre under increasing load,

causing redistribution of contact pressure. Under increasing loads, the contact pressure tends to become uniform and this is likely to limit the induced bending moments in the footing loaded uniformly.

- (5) The response of an embedded footing in a semi-infinite soil is qualitatively very similar to that of surface footing resting on semi-infinite soil. It has been therefore possible to provide simple correction factors.
- (6) The load-settlement response tends to become less non-linear for narrower rings and/or shallower depth of soil layer. Also in these cases the settlement increases with load level at a slow rate but it increases suddenly near to the ultimate load. This needs attention from a practical point of view.

A design procedure has been outlined for predicting settlements in all the three cases considered.

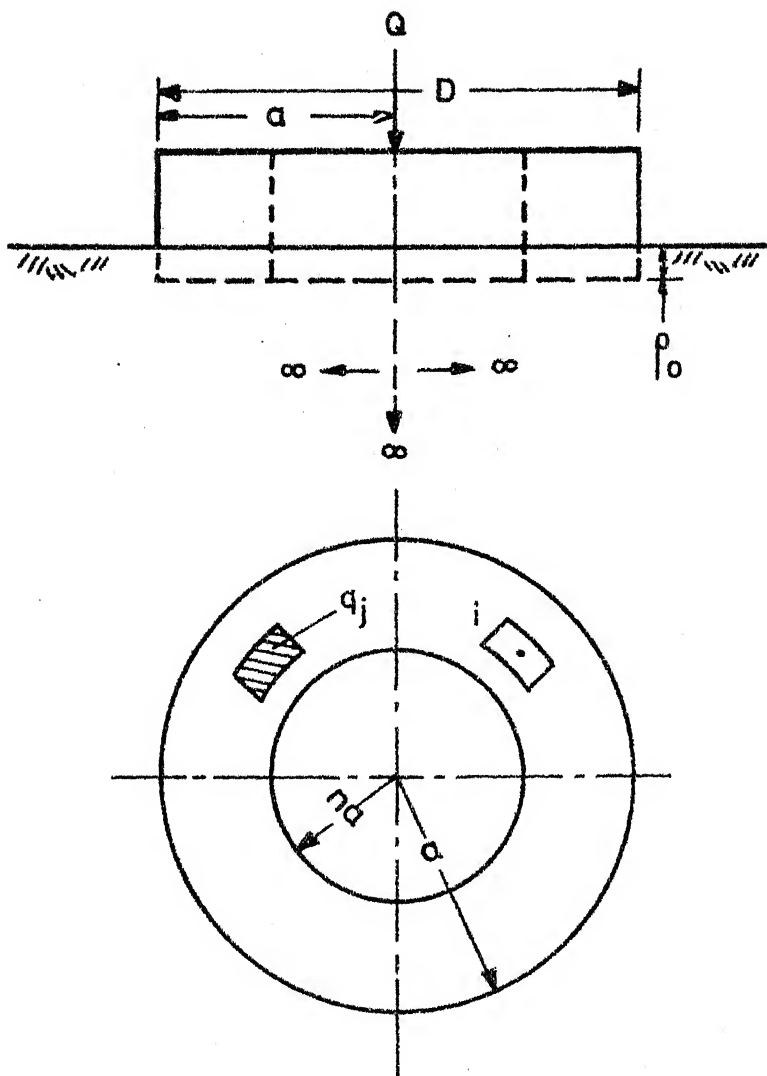
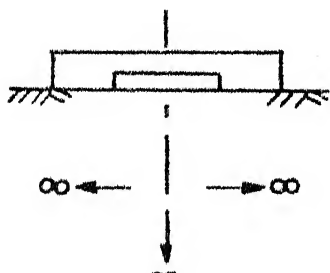
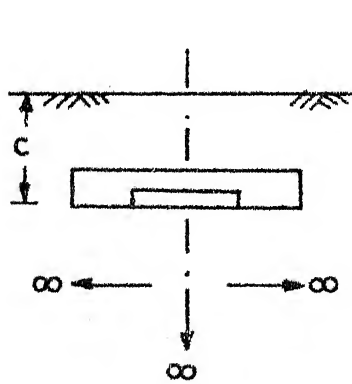


FIG.3.1 RIGID ANNULAR FOOTING ON SEMI-INFINITE CONTINUUM

TYPE A



TYPE B



TYPE C

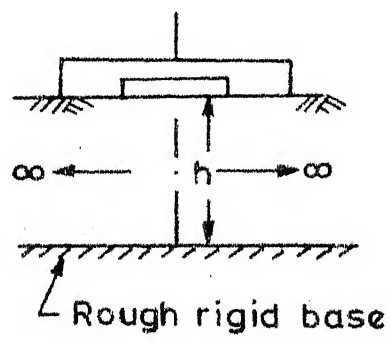


Fig.3.2 Problem type definition sketch

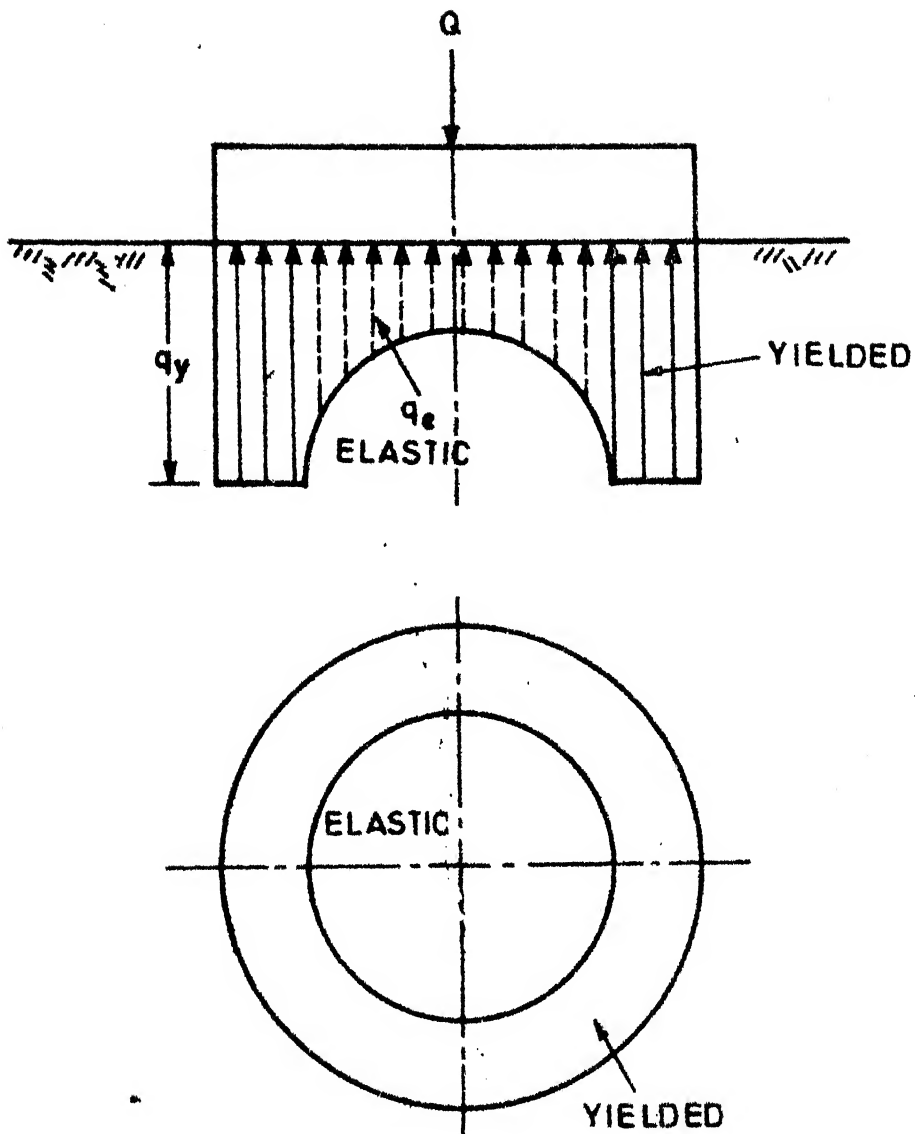


FIG-3.3 YIELDED AND ELASTIC PORTIONS OF SOIL PRESSURES

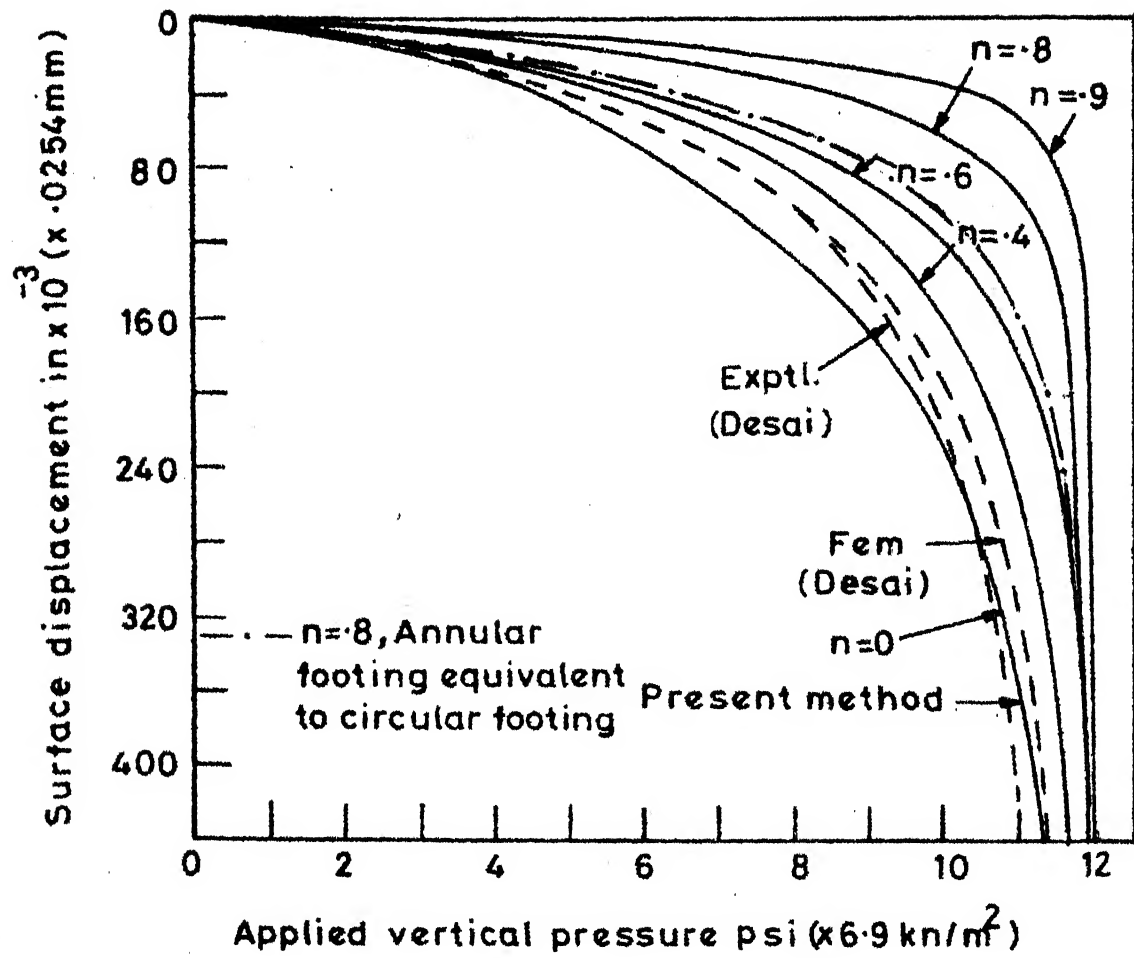
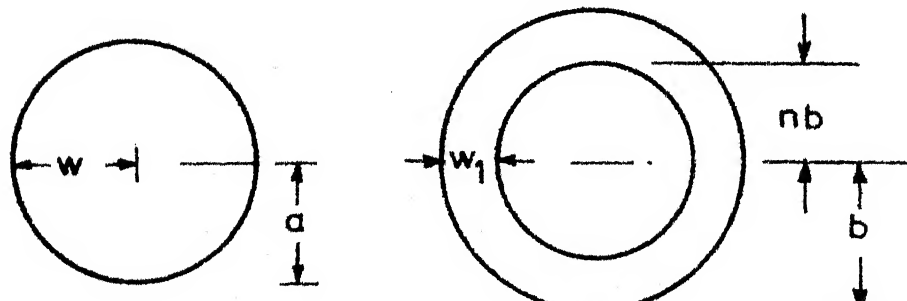


FIG.3.4 TYPICAL LOAD SETTLEMENT CURVES



$$\text{AREA} = \pi a^2 = \pi b^2 (1 - n^2)$$

$$\text{WIDTH RATIO } w_1/w = (1-n)/\sqrt{1-n^2}$$

FIG.3.5 EQUIVALENT CIRCULAR AND ANNULAR

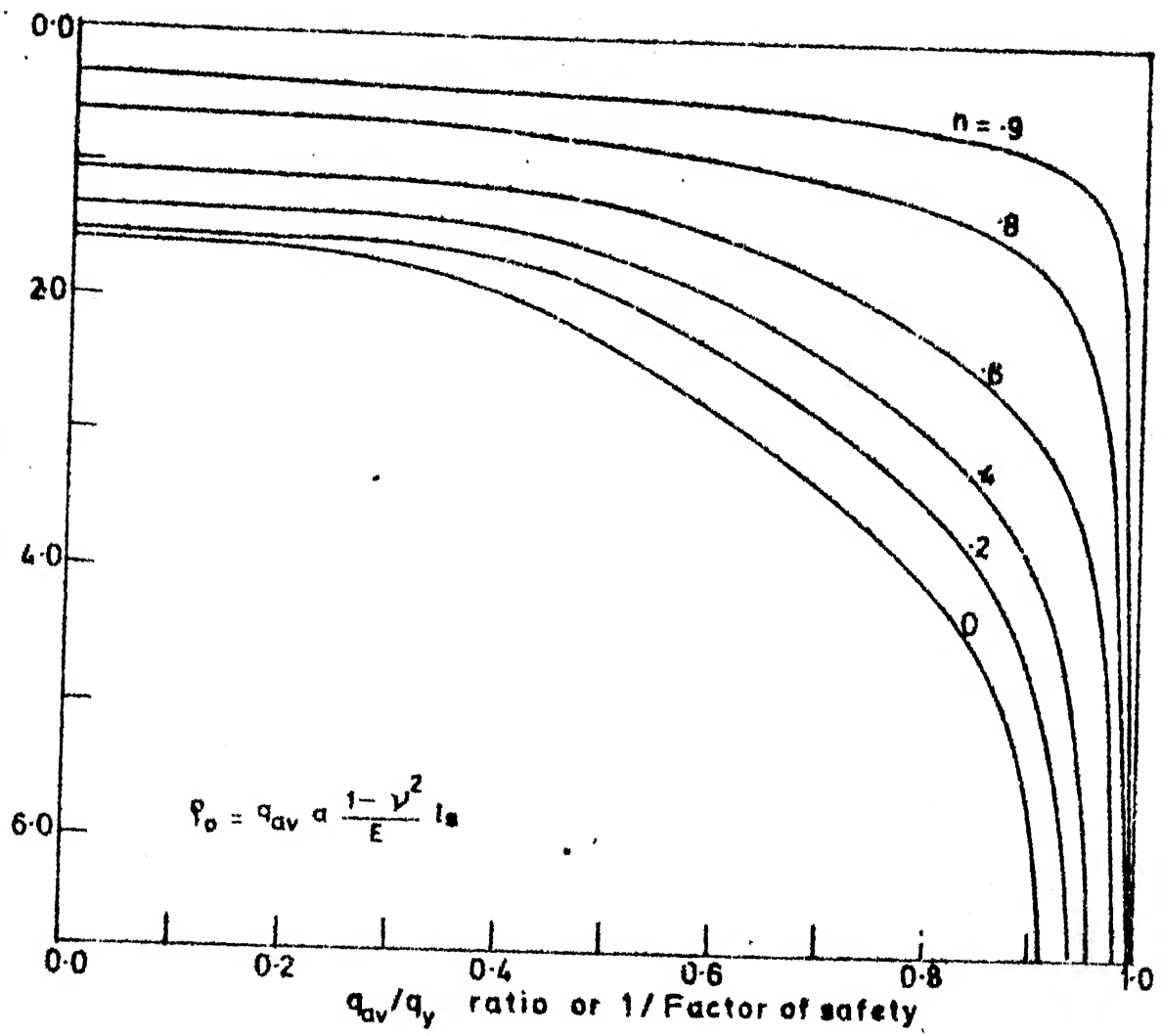
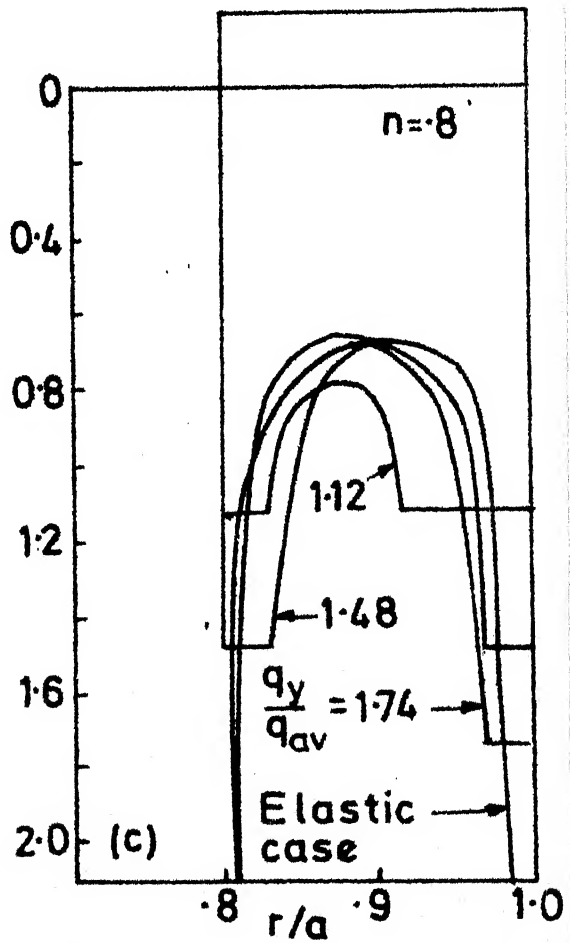
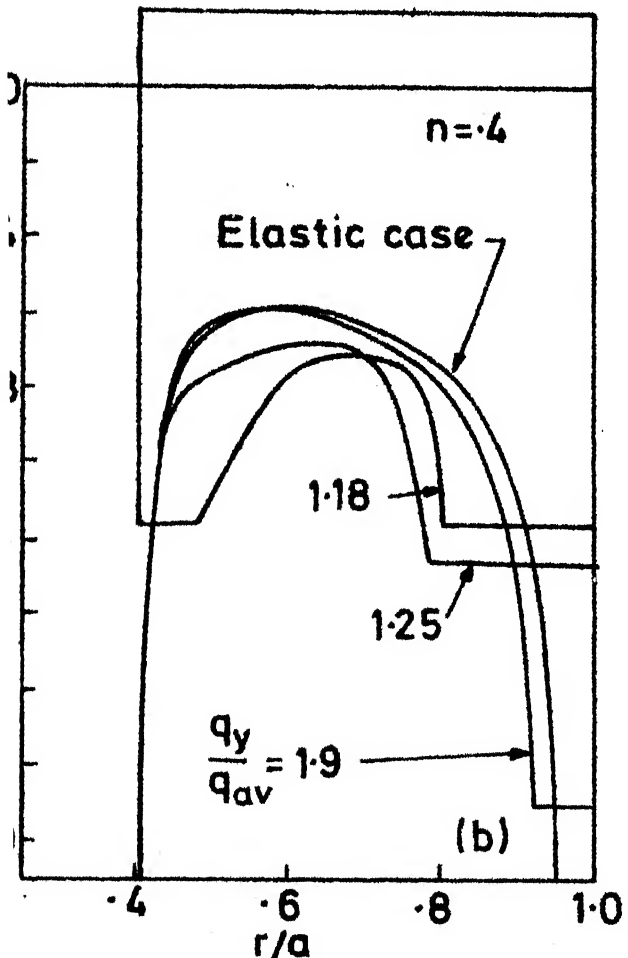
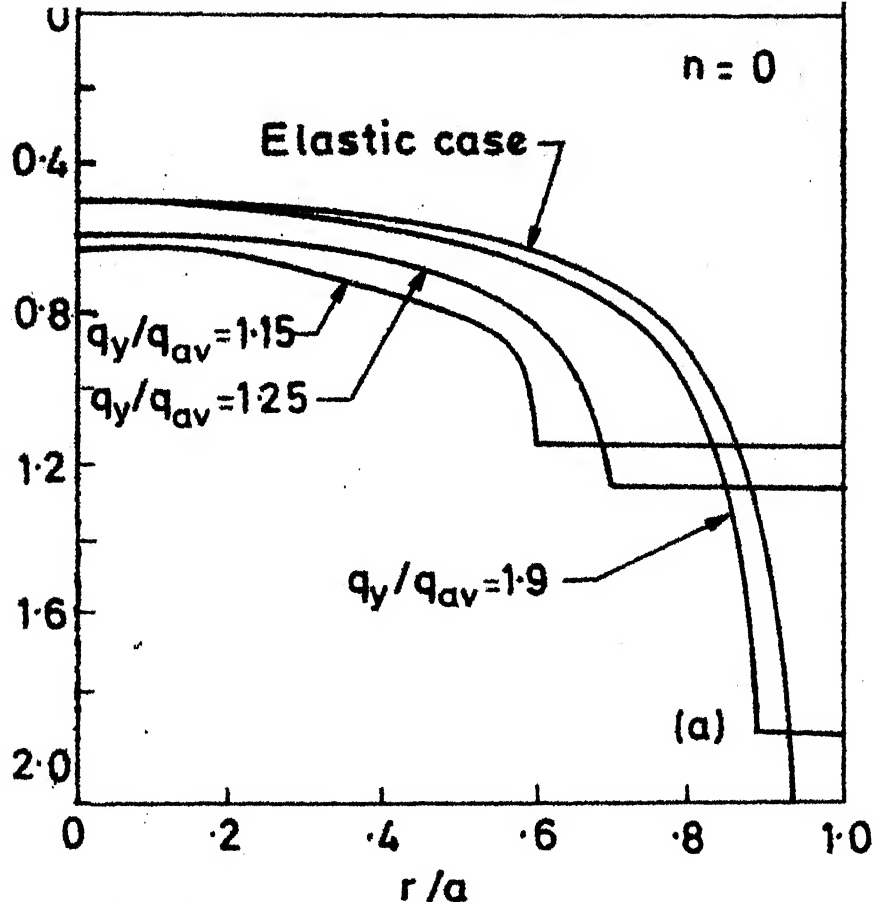


FIG. 3-6 DESIGN CHART FOR SETTLEMENT OF CENTRALLY LOADED RIGID ANNULAR SURFACE FOOTING



.37 TYPICAL CONTACT PRESSURES BENEATH RIGID FOOTINGS

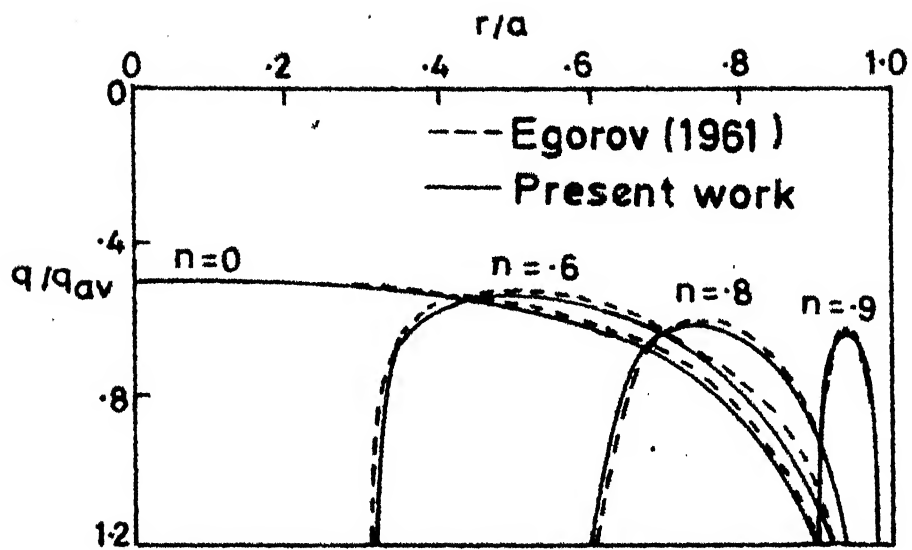


FIG.3.8 CONTACT PRESSURE BENEATH
RIGID RING ON SEMI-INFINITE SOIL

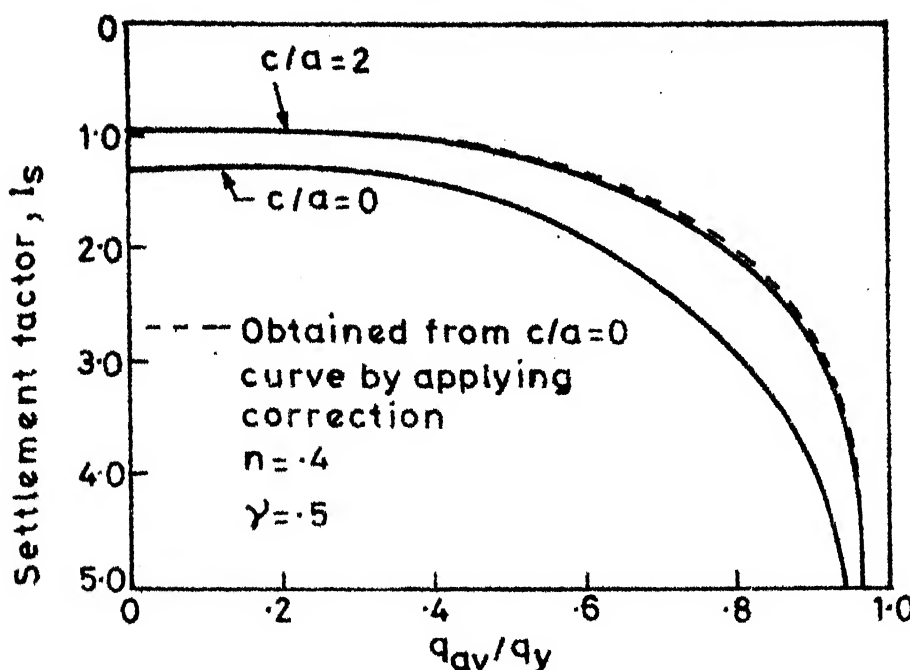


FIG. 3.9 a EMBEDDED FOOTING-COMPARISON OF LOAD SETTLEMENT RESPONSE WITH SURFACE FOOTING

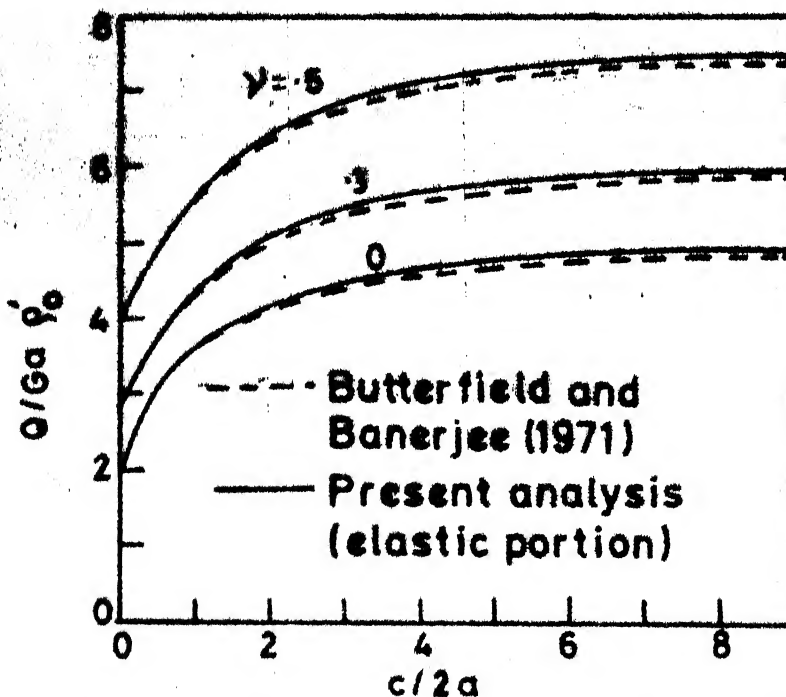


FIG. 3.9 b EMBEDDED FOOTING -COMPARISON OF ELASTIC SETTLEMENTS OF CIRCULAR FOOTING

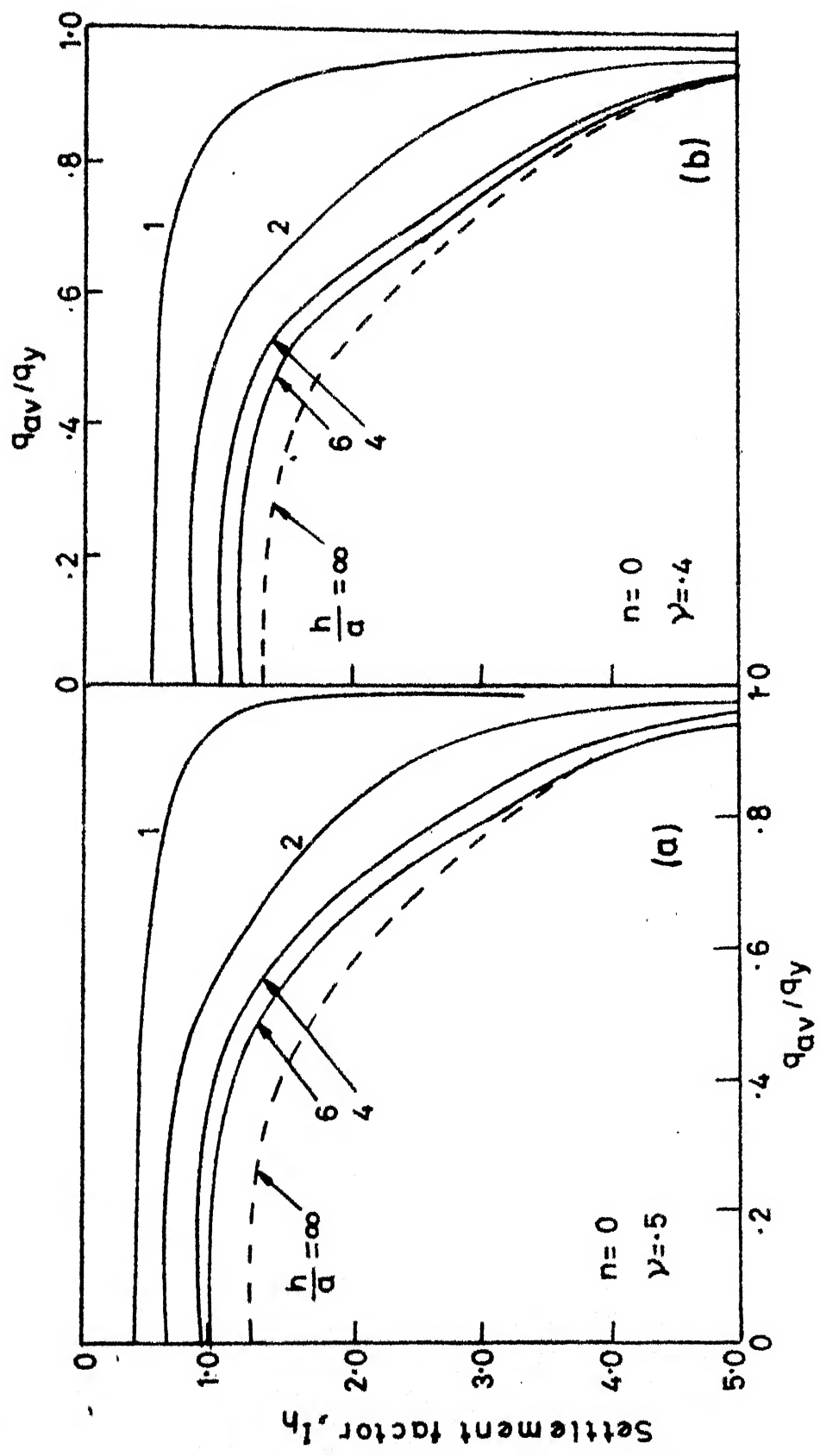


FIG. 3.10 FINITE DEPTH SETTLEMENT FACTORS

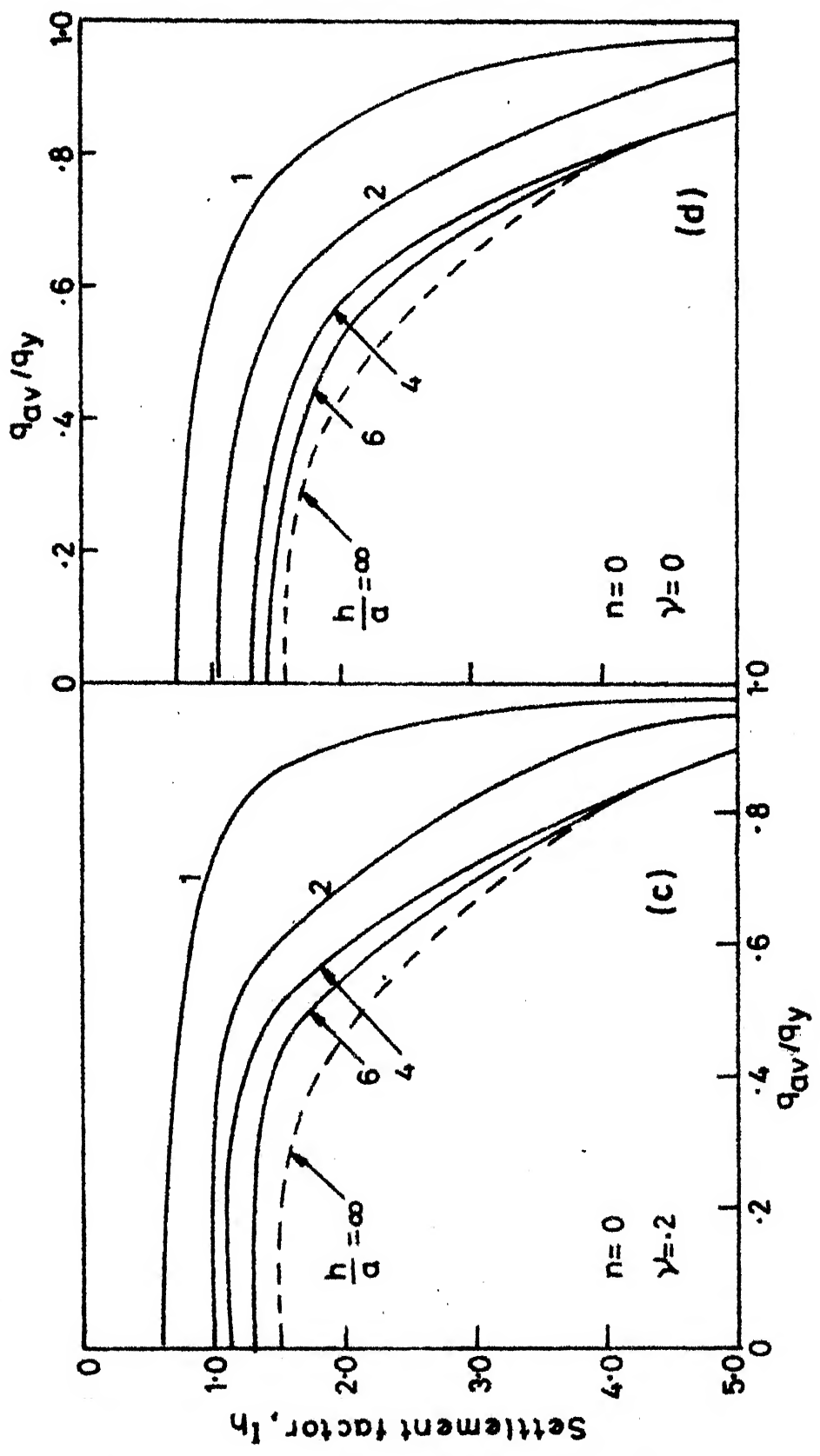


FIG. 3.10 FINITE DEPTH SETTLEMENT FACTORS

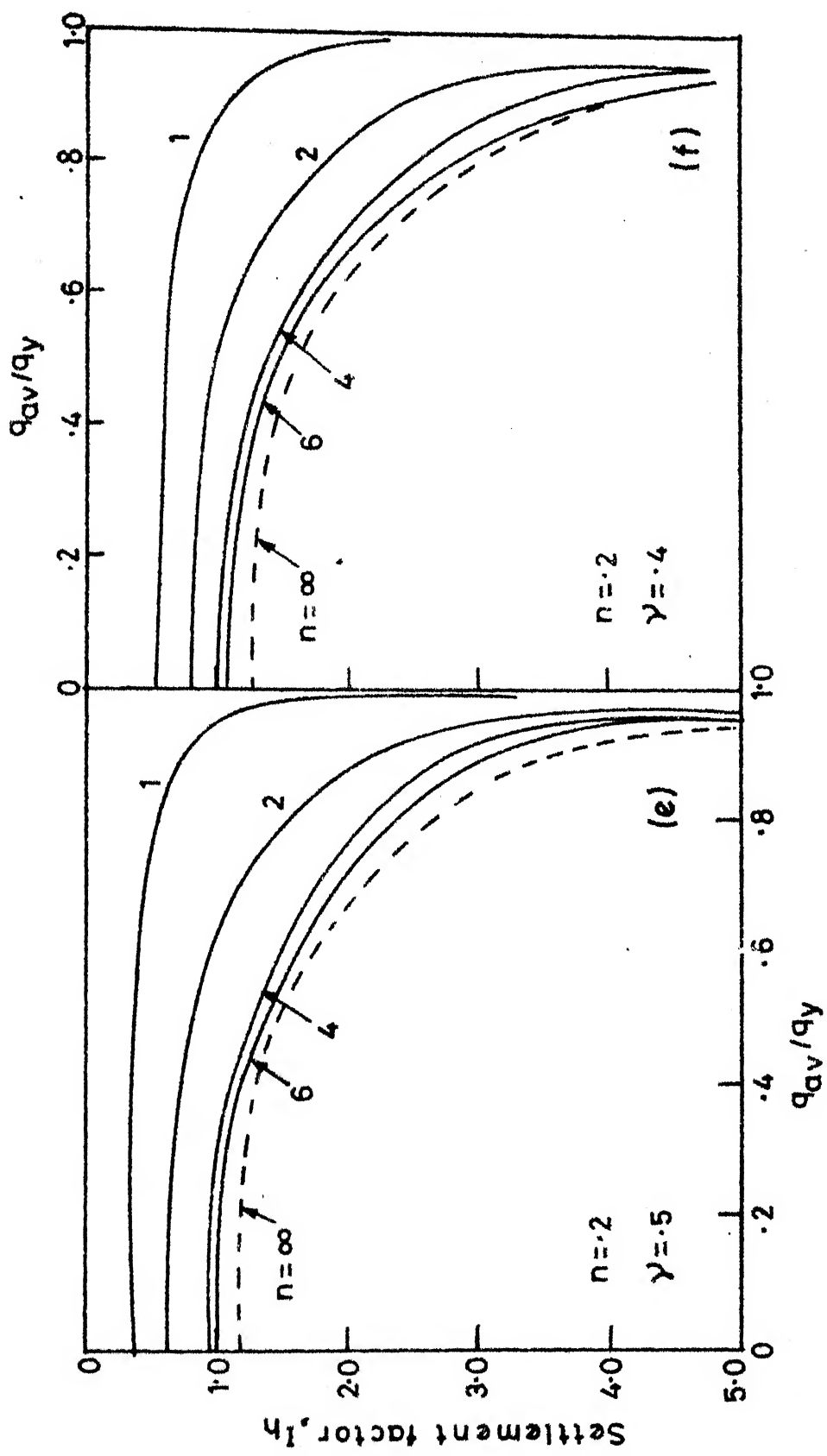


FIG. 3.10 FINITE DEPTH SETTLEMENT FACTORS

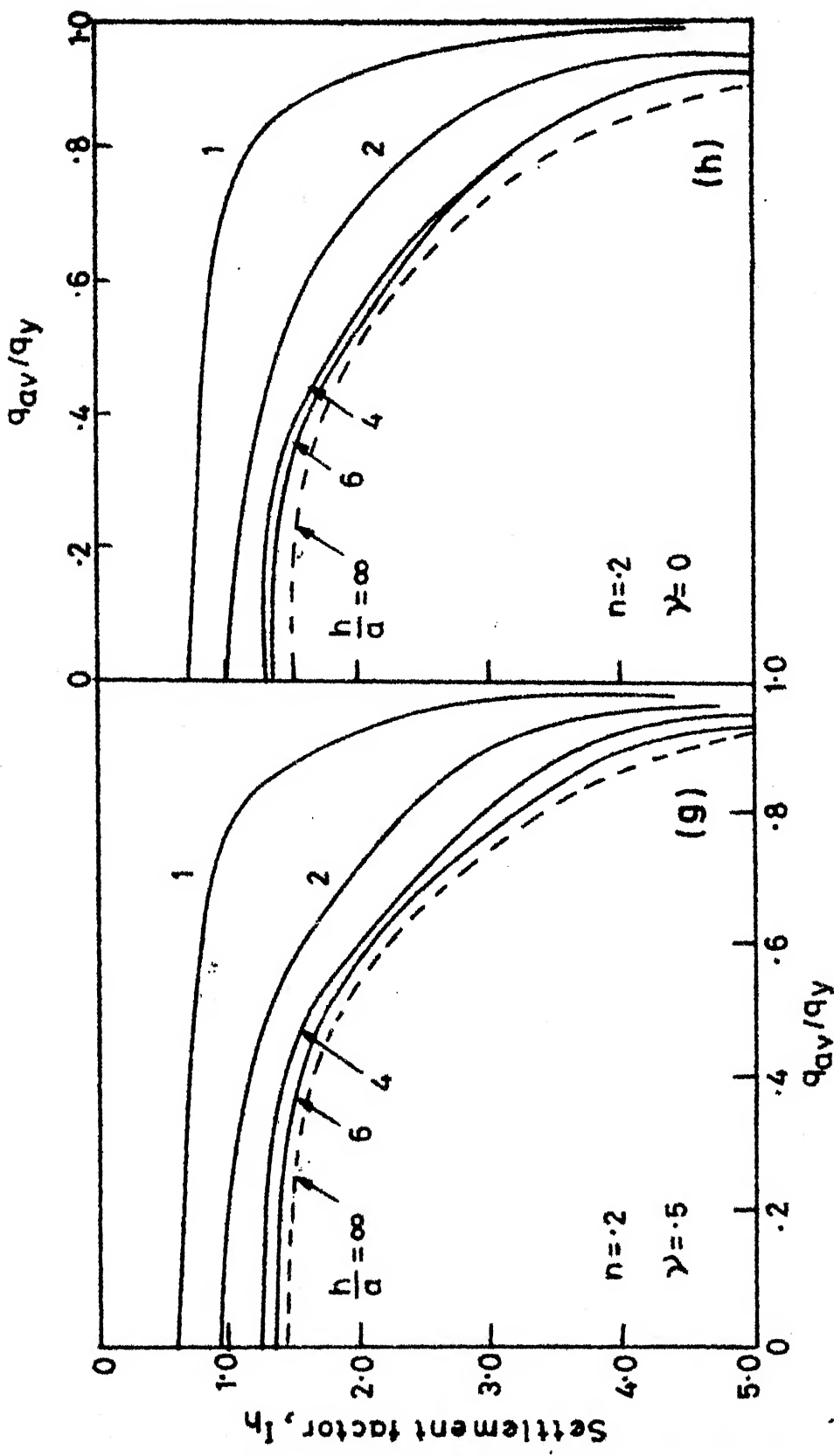


FIG. 3.10 FINITE DEPTH SETTLEMENT FACTORS

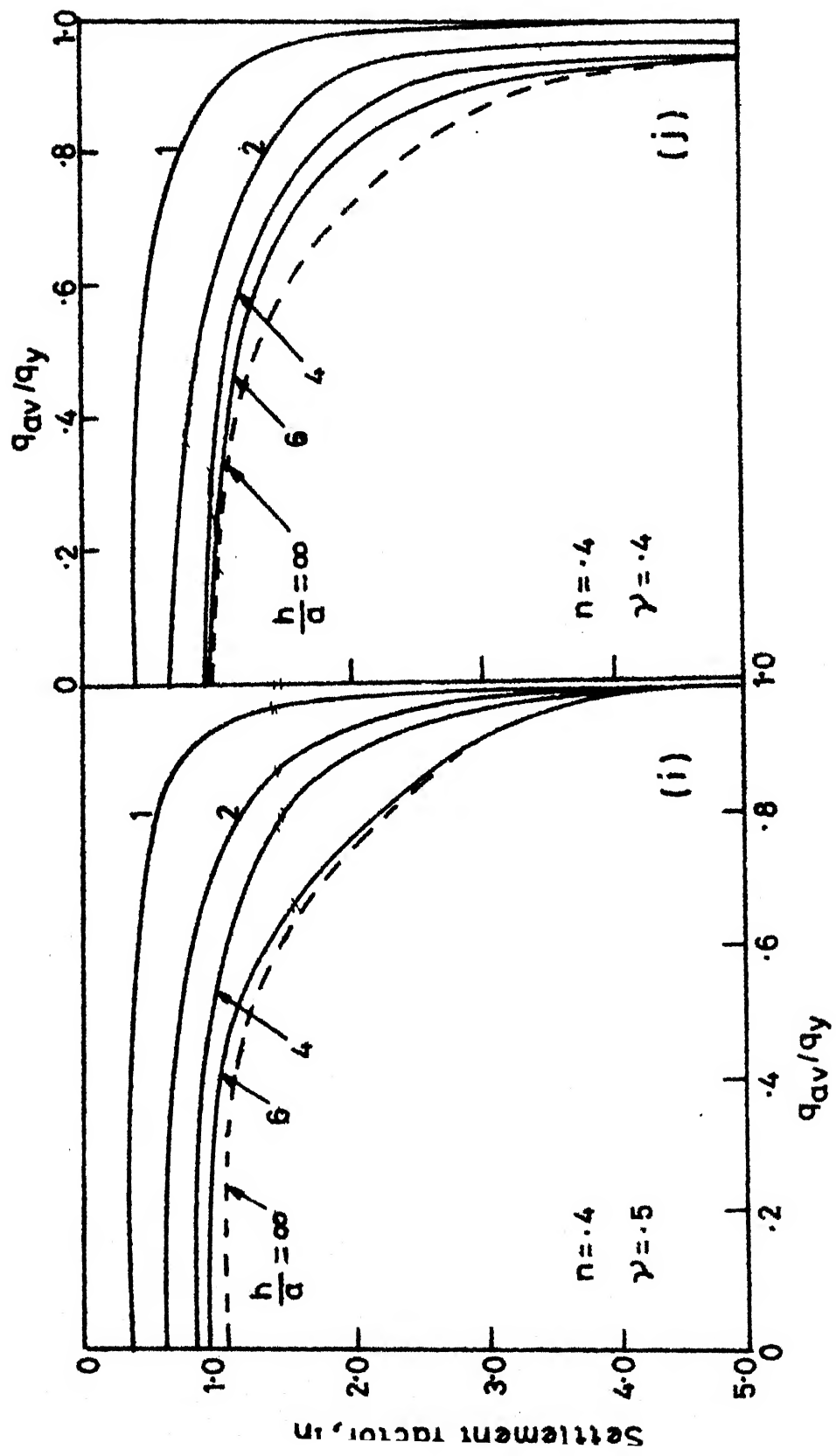


FIG 3.10 FINITE DEPTH SETTLEMENT FACTORS

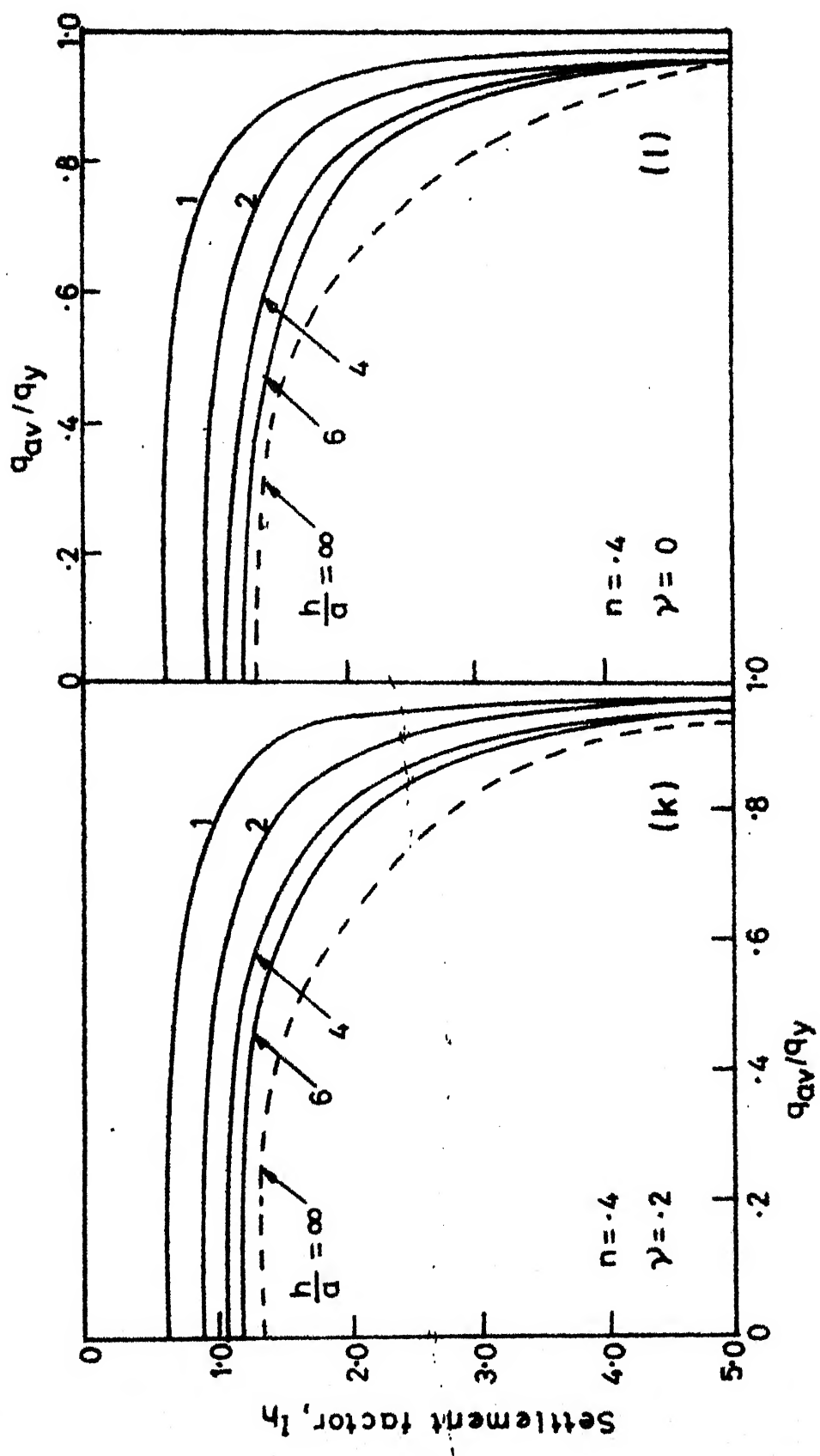


FIG 3.10 FINITE DEPTH SETTLEMENT FACTORS

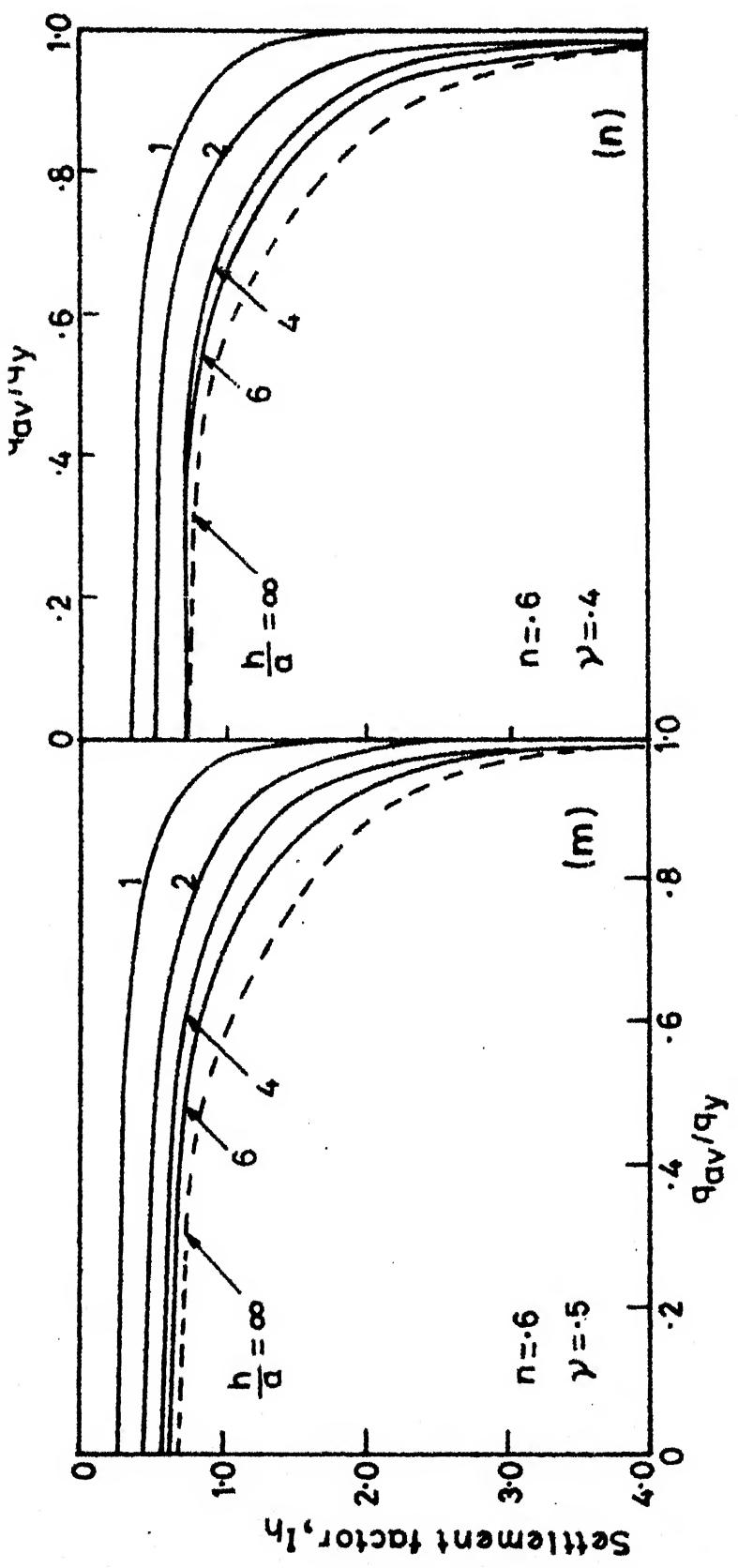


FIG. 3.10 FINITE DEPTH SETTLEMENT FACTORS

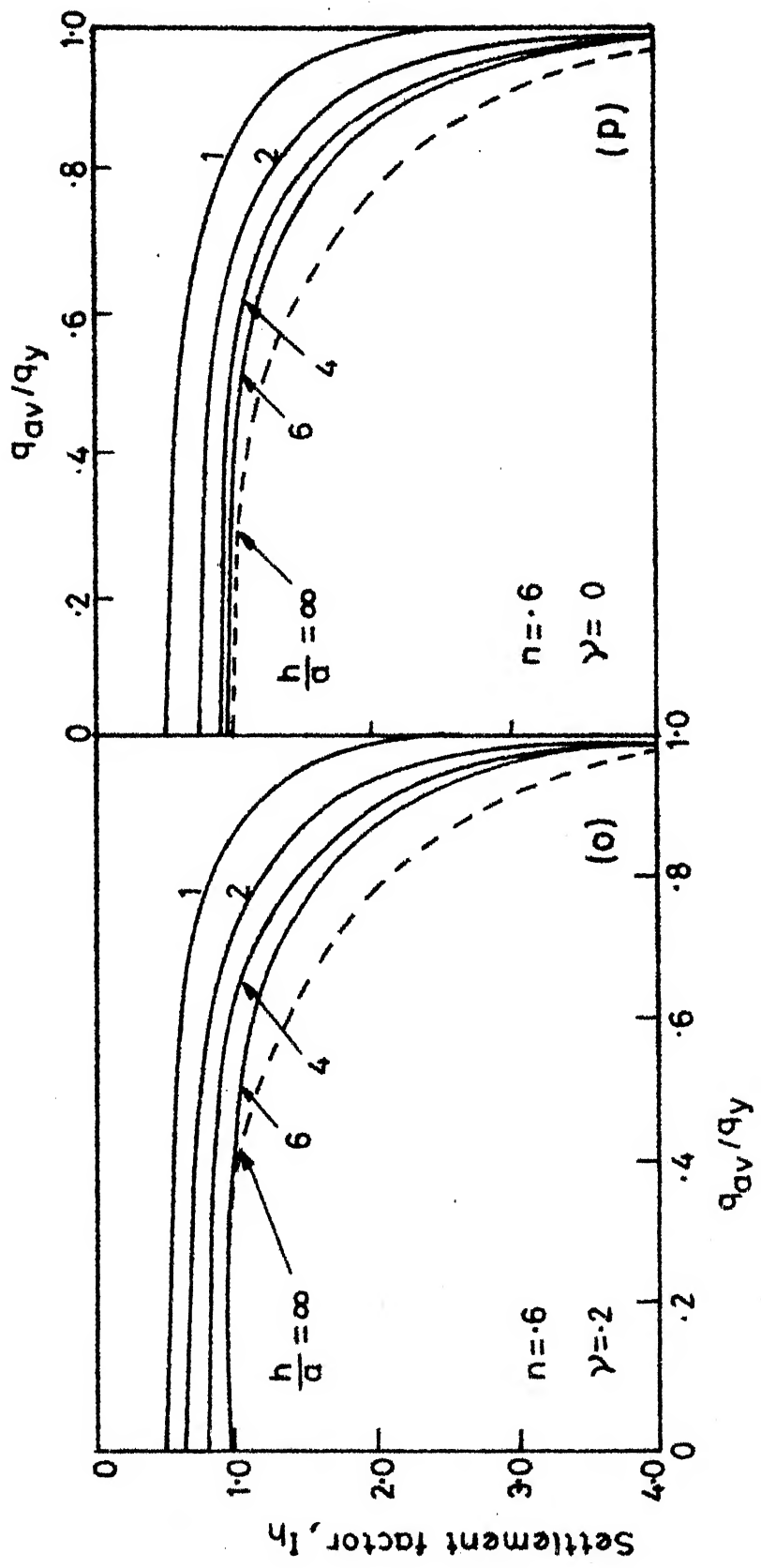


FIG. 3.10 FINITE DEPTH SETTLEMENT FACTORS

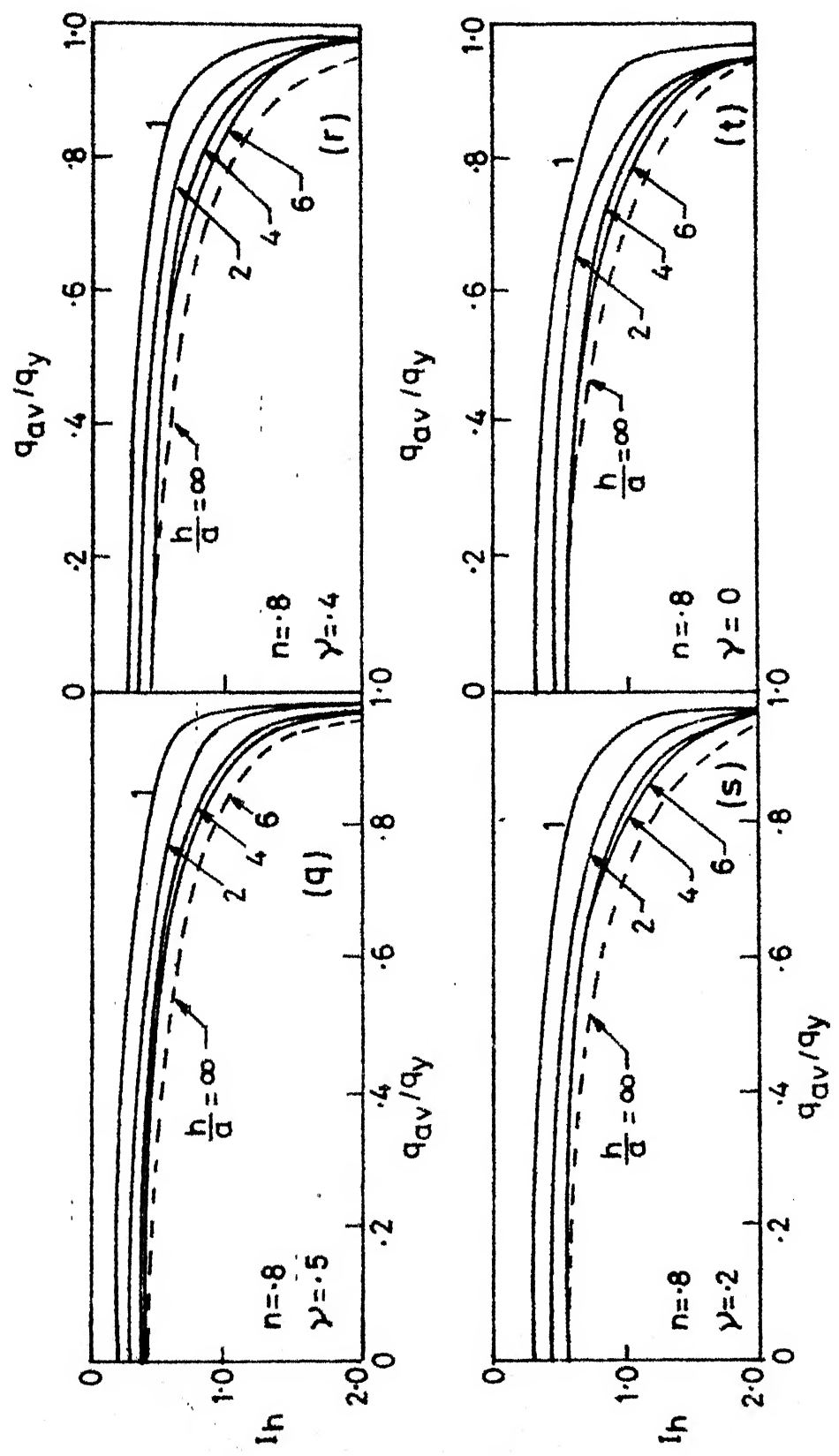


FIG.3.10 FINITE DEPTH SETTLEMENT FACTORS

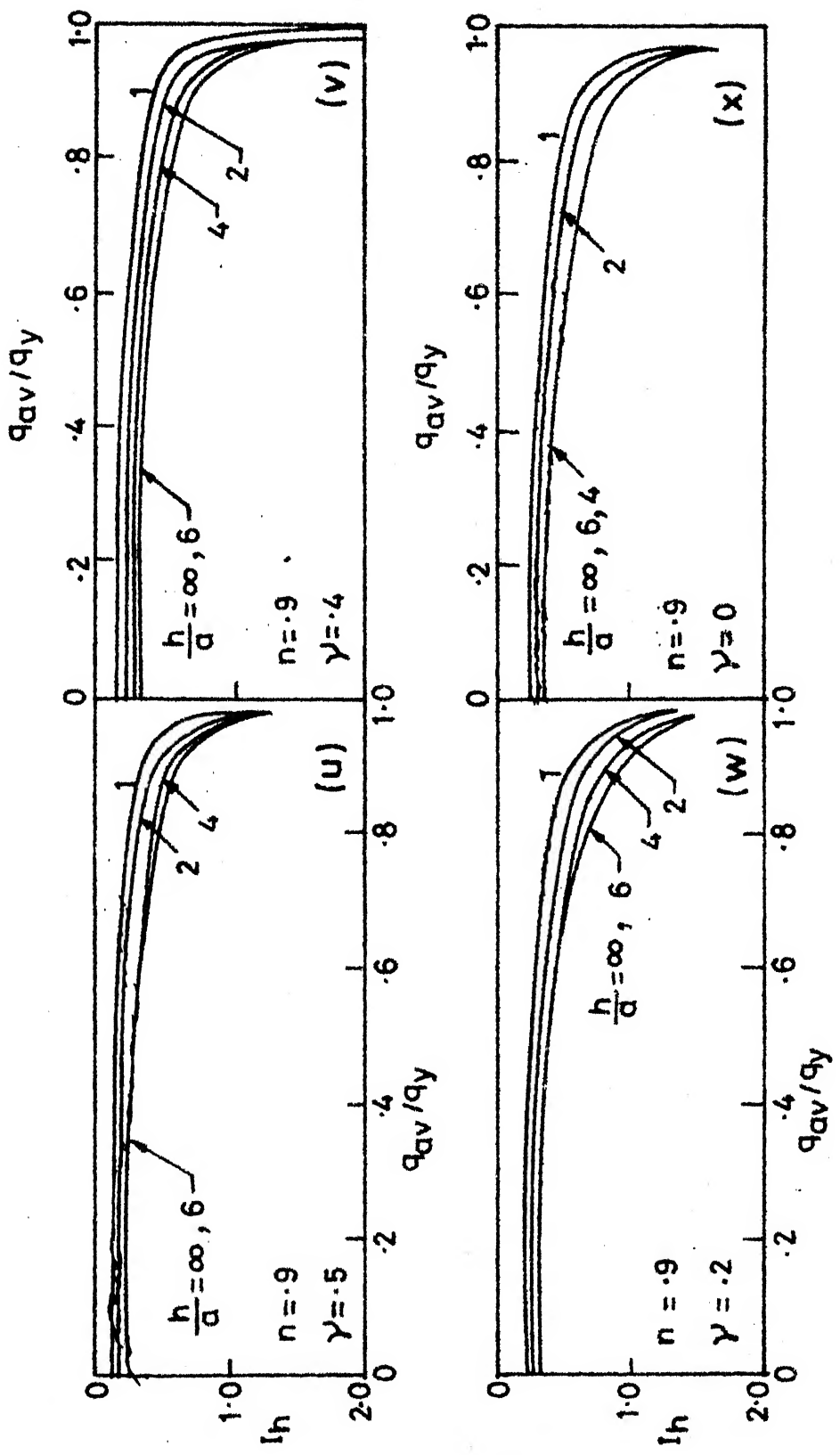


FIG.3.10 FINITE DEPTH SETTLEMENT FACTORS

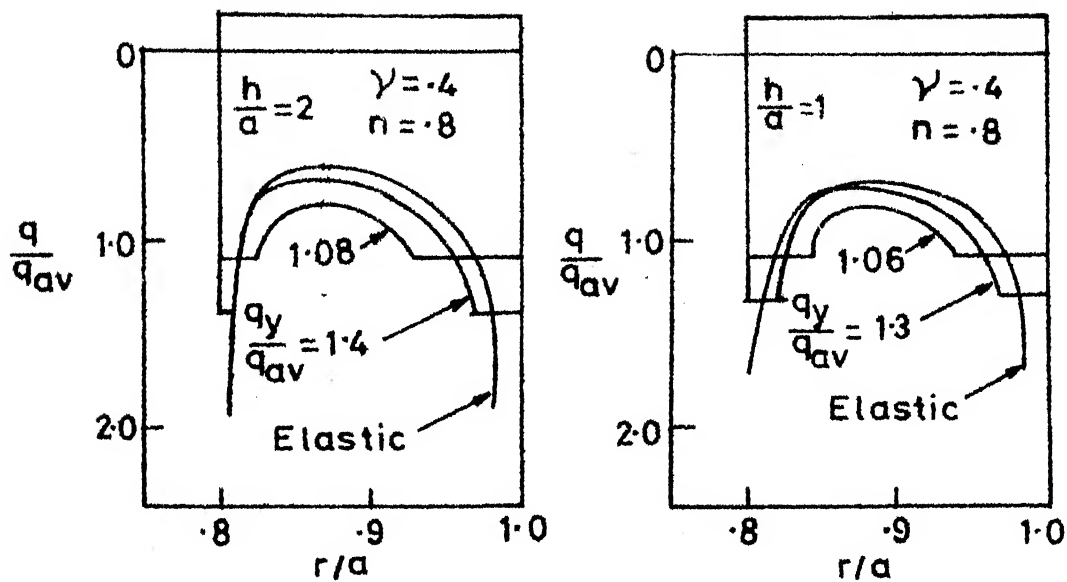


FIG.3.11 TYPICAL CONTACT PRESSURES BENEATH
RING FOOTING ON FINITE LAYER

CHAPTER 4

ELASTO-PLASTIC SETTLEMENT ANALYSIS OF CENTRALLY LOADED ANNULAR FOOTINGS OF FINITE RIGIDITY

4.1 INTRODUCTION

The footing slabs used as foundations for heavy structures have to be strong enough and therefore can be classified as rigid. But rigidity of a footing relative to the rigidity of soil is an important consideration for the analysis of settlements—maximum and differential—and of bending moments and shear forces in the footing. Also in certain cases like storage tanks at or below ground level, the bottom slab or plate resting directly on the soil can be thin. It is therefore necessary to study the effect of relative rigidity of a footing. With increasing flexibility of the footing, the contact pressure distribution tends to be uniform and this aspect is important from the point of view of the elasto-plastic analysis and several design aspects.

Since the study of finite flexibility of footing involves interaction between soil settlements and plate displacements, a study of bending moment and shear is also included along with the elasto-plastic analysis of settlement. The nature and positioning of the imposed

load on the footing has a significant effect and is also made a part of the study. Another specific feature of the study of footings with finite rigidity is the possibility of loss of contact of the footing from the soil under certain values of relative rigidity and certain loading configurations.

One of the earliest important studies of flexural rigidity in connection with smooth circular footing is found in the work of Borowicka (1939). In this study, the load is in the form of a central concentrated load and the footing rests on semi-infinite soil. For uniformly loaded circular footing, the solution is given by Brown (1969) for semi-infinite soil as well as for finite depth of soil. The bending moments are studied for rigid circular plates on finite layer by Egorov and Serebryanyi (1963) and Poulos (1968). All the solutions mentioned so far are based on the assumption of purely elastic behaviour of soil and these can be referred to in the compilation by Poulos and Davis (1974). Some of the studies based on elastic theory but considering loss of contact are by Cheung and Nag (1968), Svec (1974), Gladwell and Iyer (1974), Valliapan et al. (1975), Scott (1978).

The study of smooth annular footings of finite rigidity from the point of view of settlement, bending

51

moments and shear forces in the footing taking elasto-plastic behaviour of the soil into account is not found in the literature.

The use of thin plate theory to deal with the footing-soil interaction is in vogue and is presumed to be acceptable if the aim is an overall study of interaction behaviour and major structural design aspects of the footing and not the details of inplane stresses etc., in the footing.

The coupling of the plate-bending problem with that of soil deformations is achieved by inverting one of the plate rigidity or soil flexibility matrices and just adding if only elastic behaviour is involved. Since in the present work, elasto-plastic behaviour is considered, a somewhat complicated procedure had to be adopted, but since the size of the problem in terms of the size of the matrix to be solved is quite small, the computations are still within highly economic limits.

4.2 ASSUMPTIONS AND STATEMENT OF THE PROBLEM

4.2.1 Assumptions

The assumptions contained in Section 3.2.1(A) (a) and (b) are applicable.

For the purpose of this Chapter, the following assumptions are also applicable.

- (i) The footing is in the form of an annular ring (a circle being a particular case).
- (ii) The footing is loaded vertically and axisymmetrically and has finite rigidity.
- (iii) The footing is treated as a thin plate.

4.2.2 Statement of the Problem

The statements contained in Section 3.2.2 and Figs. 3.1 and 3.2 are valid except that in this case the footing has finite rigidity and that the vertical loading may be positioned in any axisymmetric configuration.

Since several combinations and parameters are involved, only some cases of load distributions have been studied from which at least a qualitative conclusion of behaviour under any configuration of loading could be drawn. The following load configurations are studied (Fig. 4.1).

- (1) Uniformly distributed load (U.D.L.) over the entire area.
- (2) U.D.L. over the outermost one-ninth width of the ring (or circle).

- (3) U.D.L. over the innermost one-nineth width of the ring (or, over a circle of one-nineth the outer radius in case of a circle).
- (4) U.D.L. over the central one-nineth width of ring or circle.

4.3 ANALYSIS

4.3.1 The Soil Flexibility Matrix

As for rigid footing (Chapter 3), the footing is discretized into a number of small elements and subelements. The settlement, ρ_{ij} of an element i due to contact pressure p_j on element j is expressed by

$$\rho_{ij} = p_j a \frac{1 - v_s^2}{E_s} I_{ij} \quad (4.1)$$

Here subscript s has been used to indicate parameters pertaining to soil.

The above Eq. 4.1 in matrix form, for all the elements of the footing, condensed to the size $m \times m$, where m is the number of radial elements, can be written as

$$\{\bar{\rho}\} = (1 - v_s^2) [I] \{\bar{p}\} \quad (4.2)$$

where $\{\bar{\rho}\} = \frac{1}{a} \{\rho\}$ is the non-dimensional settlement

vector, $\{\bar{p}\} = \frac{1}{E_s} \{p\}$ is the non-dimensional contact pressure vector and $[I]$ is the influence coefficient matrix.

The condensation of [I] matrix into mxm size is possible because of axisymmetry.

For convenience, Eq. 4.2 is cast into the following form

$$\{\bar{p}\} = [Z] \{\bar{p}\} \quad (4.3)$$

where [Z] represents non-dimensional soil flexibility matrix of size mxm.

4.3.2 Footing Rigidity Matrix

For an axisymmetric ring shaped thin plate, the governing plate equations are (Timoshenko and Krieger, 1959) :

$$D \left(\frac{d^4 w}{dr^4} + \frac{2}{r} \frac{d^3 w}{dr^3} - \frac{1}{r^2} \frac{d^2 w}{dr^2} + \frac{1}{r^3} \frac{dw}{dr} \right) = q-p \quad (4.4)$$

$$M = -D \left(\frac{d^2 w}{dr^2} + \frac{v_p}{r} \frac{dw}{dr} \right) \quad (4.5)$$

$$F = D \left(\frac{d^3 w}{dr^3} + \frac{1}{r} \frac{d^2 w}{dr^2} - \frac{1}{r^2} \frac{dw}{dr} \right) \quad (4.6)$$

where $D = E_p t^3 / 12(1 - v_p^2)$ is the flexural rigidity of the plate (footing), t is the thickness of the plate, E_p is the Young's Modulus of the plate, v_p is the Poisson's ratio of the plate, w is the deflection of an element situated at a radial distance r from the centre, q is the intensity of load on the element, p is the contact pressure

on the element, M and F are the bending moment and shear force per unit length respectively.

Using Taylor's expansions and central difference scheme, Eq. 4.4 is converted into finite difference form, for node i (Fig. 4.2) as

$$\frac{D}{(\delta r_i)^4} \left(w_{i-2}(1-y_i) + w_{i-1}(-4+2y_i - y_i^2 - \frac{y_i^3}{2}) + w_i(6+2y_i^2) + w_{i+1}(-4-2y_i - y_i^2 + \frac{y_i^3}{2}) + w_{i+2}(1+y_i) \right) = q_i - p_i \quad (4.9)$$

where $y_i = \delta r/r_i$, r_i being radial distance of i^{th} element.

Eq. 4.9 can be written, in matrix form, as

$$\frac{D}{\delta r^4} \begin{bmatrix} a_i & b_i & c_i & d_i & e_i \end{bmatrix} \begin{bmatrix} w_{i-2} & w_{i-1} & w_i & w_{i+1} & w_{i+2} \end{bmatrix}^T = \{ q - p \} \quad (4.10)$$

$$\begin{aligned} a_i &= 1 - y_i \\ b_i &= -4 + 2y_i - y_i^2 - \frac{y_i^3}{2} \\ c_i &= 6 + 2y_i^2 \\ d_i &= -4 - 2y_i - y_i^2 + \frac{y_i^3}{2} \end{aligned}$$

$$\text{and } e_i = 1 + y_i .$$

For convenience, the m radial elements are denoted by numbers $3, 4 \dots m+2, 1, 2, m+3$ and $m+4$ are the fictitious nodes added (Fig. 4.2). Eq. 4.10 embodies m equations for m nodes but would include 4 unknown deflections at the fictitious nodes $1, 2, m+3$ and $m+4$. To eliminate these, the following (free edge) boundary condition for the footing (plate) are used, i.e.

- 1) Moments at the inner and outer edges of ring footing are zero.
- 2) Shear forces at the inner and outer edges of ring footing are zero.

Considering the inner edge, (Fig. 4.2 one can write) the boundary conditions as

$$M_A = M_{i-1/2} = -D \left(\frac{d^2 w}{dr^2} + \frac{v_p}{r} \frac{dw}{dr} \right) = 0 \quad (4.11)$$

$$F_A = F_{i-1/2} = D \left(\frac{d^3 w}{dr^3} + \frac{1}{r} \frac{d^2 w}{dr^2} - \frac{1}{r^2} \frac{dw}{dr} \right) = 0 \quad (4.12)$$

Using central difference, these equations are converted into the following finite difference matrix forms.

$$\begin{vmatrix} (1/2)(-1/2 - v_p y_a) & (-1/2 + v_p y_a)(1/2) & [w_{i-2} \ w_{i-1} \ w_i \ w_{i+1}]^T \end{vmatrix}^T \\ = [0 \ 0 \ 0 \ 0]^T \quad (4.13)$$

$$\begin{vmatrix} (-1 + \frac{y_a}{2})(3 - \frac{y_a}{2} + y_a^2) & (-3 - \frac{y_a}{2} - y_a^2) & (1 + \frac{y_a}{2}) & . \end{vmatrix}$$

$$[w_{i-2} \ w_{i-1} \ w_i \ w_{i+1}]^T = [0 \ 0 \ 0 \ 0]^T \quad (4.14)$$

where $y_a = \delta r/r_a$, r_a being radial distance of A from centre.

Similar expressions are written for the outer edge.

For a circular footing the above boundary conditions for the inner edge are replaced by the following:

- 1) Because of symmetry about the centre, the deflection at the fictitious node 2 is mirrorimage of deflection at 3 i.e. $w_2 = w_3$.
- 2) Similarly $w_1 = w_4$.

Thus using the four equations obtained from boundary conditions, w_1 , w_2 , w_{m+3} and w_{m+4} are eliminated from Eq. 4.10 leaving m equations to be solved.

For convenience, Eq. 4.10 after incorporating the boundary conditions, is cast into the following form

$$[P] \{ \bar{w} \} = \{ \bar{q} - \bar{p} \} = \{ \bar{q} \} - \{ \bar{p} \} \quad (4.15)$$

where $\{ \bar{w} \} = \frac{1}{a} \{ w \}$ represents non-dimensional deflections vector, $\{ \bar{q} - \bar{p} \} = \frac{1}{E_s} \{ q - p \}$ is the nondimensional net pressure vector and $[P]$ represents nondimensional plate rigidity matrix of size $m \times m$.

4.3.3 Coupling of Soil and Plate Responses:Elastic Case

Inverting Eq. 4.3

$$[Z]^{-1} \{ \bar{p} \} = \{ \bar{p} \} \quad (4.16)$$

For compatibility of vertical displacements of plate and soil, the deflections of plate should be equal to settlements of the soil, hence

$$\{\bar{w}\} = \{\bar{\rho}\} \quad (4.17)$$

Using Eqs. 4.15 through 4.17,

$$[Z^{-1} + P] \{\bar{\rho}\} = \{\bar{q}\} \quad (4.18)$$

This equation is solved to get settlements. Contact pressures are obtained from Eq. 4.16.

4.3.4 Coupling of Soil and Plate :Elasto-Plastic Case

For the elements where the contact pressure exceeds yield stress q_y of the soil, say k in number, the displacement compatibility is not to be satisfied and at these elements the contact pressure is held at q_y . It is necessary to remove the equations corresponding to yielded elements from Eqs. 4.15 and 4.16 before coupling is done. Considering Eq. 4.16, the rows corresponding to yielded elements, are eliminated, one by one, and in doing so, using the known value q_y , the $[Z]$ matrix as well as the right hand side of the equation get modified. Let $\{\bar{p}_1\}$ indicate the modification to the r.h.s. vector. After removing the k rows corresponding to yielded elements,

$$[Z'^{-1}] \{\bar{\rho}\} = \{\bar{p}\} - \{\bar{p}_1\} \quad (4.19)$$

where $[Z'^{-1}]$ is now a matrix of size $(m-k) \times (m-k)$.

The effect of contact pressures acting on yielded elements is now contained in the vector $\{\bar{p}_1\}$.

Similarly, Eq. 4.15 is treated to obtain

$$[P'] \{\bar{w}\} = \{\bar{q}\} - \{\bar{p}\} - \{\bar{p}_2\} \quad (4.20)$$

where $\{\bar{p}_2\}$ indicates the effect of yielded elements and $[P']$ is the modified form of $[P]$ matrix, now reduced to the size $(m-k) \times (m-k)$.

The settlements $\{\bar{p}\}$ in Eq. 4.19 and the plate deflections $\{\bar{w}\}$ in Eq. 4.20 can now be equated since they belong to elements of elastic zone only. Therefore, from Eqs. 4.19 and 4.20 one gets,

$$[Z'^{-1} + P'] \{\bar{p}\} = \{\bar{q}\} - \{\bar{p}_1\} - \{\bar{p}_2\} \quad (4.21)$$

Eq. 4.21 written for compatibility in elastic region only (see Chapter 3) is solved to get the settlements (=plate deflections) in the elastic region. The contact pressures in elastic region are obtained by using Eq. 4.19. The contact pressures in the yielded region are all equal to q_y . The plate deflections in the region where soil has yielded are obtained by solving Eq. 4.15 for $\{\bar{w}\}$.

4.3.5 Separation or Tension Cut-off

In footings with finite rigidity, situations can arise, such as when the load is concentrated at the centre of

a circular footing, creating separation of the footing from the soil in some region. This occurs since soil can not take tension. To account for this, first one can find, from elastic solution, elements where contact pressures become negative. At these elements say k' in number, the contact pressure value is held at zero. The compatibility of displacements at these elements is not satisfied and hence the procedure follows exactly on the lines of yielded elements. For the case of elasto-plastic analysis with separation, Eqs. 4.19 and 4.20 are obtained by excluding the k' elements so that the size of the matrices obtained becomes $(m-k-k') \times (m-k-k')$. The rest of the procedure remains the same.

4.3.6 Bending Moments and Shear in the Footing

While plate deflections are obtained directly from the solution of Eqs. 4.18 or 4.21, the deflections at the fictitious points are obtained from the appropriate expressions used for boundary conditions as given in Section 4.3.2 above.

Finally Eqs. 4.⁵ and 4.⁶ in Finite Difference form as given below are used to get bending moments and shear forces at any node (centre of element) i of the ring footing.

$$M_i = - \frac{D}{(\delta r)^2} \left(\left(1 - \frac{v_p}{2}\right) y_i w_{i-1} - 2w_i + \left(1 + \frac{v_p}{2}\right) y_i w_{i+1} \right) \quad (4.22)$$

$$\begin{aligned} F_i &= \frac{D}{(\delta r)^3} \left(-\frac{1}{2} w_{i-2} + \left(1 + y_i + \frac{1}{2} y_i^2\right) w_{i-1} - 2y_i w_i \right. \\ &\quad \left. + \left(-1 + y_i - \frac{1}{2} y_i^2\right) w_{i+1} + \frac{1}{2} w_{i+2} \right) \end{aligned} \quad (4.23)$$

where $y_i = \delta r/r_i$, r_i being radial distance of node i from centre.

For a circular footing, the bending moment at the centre is the only important quantity, for which instead of Eq. 4.22 the following equation is used

$$M_0 = \frac{D(1+v_p)}{(\delta r)^2} (w_4 - w_3) \quad (4.24)$$

The bending moments referred to above so far are radial bending moments. The tangential bending moments are easily obtained from the following relations

$$M_T = -D \left(v_p \frac{d^2 w}{dr^2} - \frac{1}{r} \frac{dw}{dr} \right) \quad (4.25)$$

Eq. 4.25 in Finite Difference form for node i of a ring footing will be

$$M_{Ti} = - \frac{D}{(\delta r)^2} \left(\left(v_p + \frac{y_i}{2}\right) w_{i-1} - 2v_p w_i + \left(v_p - \frac{y_i}{2}\right) w_{i+1} \right) \quad (4.26)$$

where $y_i = \delta r/r_i$ as before

At the centre of a circular footing, the radial and tangential moments are equal.

$$M_{T_0} = M_0 \quad (4.27)$$

The values of radial or tangential bending moments will be maximum at certain points and further, the higher of the two will be of particular interest. The absolute maximum values of bending moment and shear force have been denoted by M_c and F_c respectively.

4.4 RESULTS AND DISCUSSION

4.4.1 General

The parameters used in the present study are the Poisson's ratios for soil and footing, (ν_s and ν_p) and the relative rigidity K defined as

$$K = \frac{E_p}{E_s} (1 - \nu_s^2) \left(\frac{t}{a}\right)^3 \quad (4.28)$$

All the other required elastic derived quantities are expressed in terms of ν_s , ν_p and K .

For brevity, ν_s and ν_p are assigned the values 0.5 and 0.25 respectively in major portion of the work included herein.

During the numerical solution in each case, the settlements, contact pressures, bending moments, and shear forces at all the elements are calculated. However, for the purpose of presentation, more stress is laid on certain quantities as mentioned below, in which a geotechnical or

a structural engineer may be interested most.

The maximum settlement is of particular interest and settlement refers to maximum settlement unless otherwise stated. For this purpose of settlement, it is expressed as

$$\rho = \frac{q_{av}^a}{E_s} I_f \quad (4.29)$$

where I_f is the maximum settlement influence coefficient for footing of finite rigidity. The differential deflection is also a quantity of importance and it is expressed in the dimensionless form as

$$D_f = \text{Differential Deflection Factor} \\ = \frac{\text{Maximum Differential Deflection} \times E_p s}{(1 - v_s^2) q_{av} a} \quad (4.30)$$

The results of the present work corresponding to elastic portion are compared in Figs. 4.3(a) to (g) with available elastic solutions for circular footings. An agreement within a range of about 3.5 percent is found to exist in all the cases.

The various aspects of the results obtained from the present work are discussed below in an order convenient for comparative study.

4.4.2 Footings of Finite Rigidity Resting on Semi-Infinite Soil

4.4 .2.1 Effect of plastic yielding of soil on bending moments and shear forces

Except for an extremely flexible footing, the contact

pressures obtained by elastic theory are very high near the edges of the footing (Brown, 1969). The soil near and under the edges is bound to yield. Under increasing loads, more and more portion of soil under the footing yields and in the limit the entire soil in contact with the footing yields so that the contact pressure becomes uniform and equal to q_y - the yield stress of the soil. Thus the magnitude as well as the distribution of contact pressure depends on the relative level of loading. This gives rise to very significant changes in moments and shear forces in the footing under varying load. In some cases it would be highly erroneous to calculate these quantities on the basis of elastic theory alone, neglecting yielding of soil.

(a) Uniformly loaded footing

Fig. 4.4(a) shows the value of critical (absolute maximum) moment, in a circular/ring footing loaded uniformly, against values of q_{av}/q_y (load level). This moment M_c is expressed in non-dimensional form as $M_c/q_{av} a^2$. The value of non-dimensional moment reduces with increasing load and equals zero at failure ($q_{av}/q_y = 1$).

A similar trend is seen for the critical shear force expressed in nondimensional form as $F_c/q_{av}a$ plotted against load level q_{av}/q_y (Fig. 4.4(b)). The changing nature of

moment and shear with load level can be brought out better by plotting the nondimensional moment and shear in terms of $M_c/q_y a^2$ and $F_c/q_y a$ since in these terms q_y and a are constants for a given soil and geometry of footing.

Fig. 4.4 shows the nondimensional moment and shear plotted versus load level (q_{av}/q_y) for a uniformly loaded annular footing. It is seen that the nondimensional moment for a relatively rigid circular footing ($K = 10$) increases from zero to about .037 at $q_{av}/q_y = .65$ and then reduces to become finally zero at $q_{av}/q_y = 1$. The corresponding maximum value for $K = .1$ is about .011 at $q_{av}/q_y = .87$ and for $n = .4$ and $K = .1$ it is about .0065 at $q_{av}/q_y = .8$. A similar trend is seen for nondimensional shear.

When the loading intensity is less, the contact pressure distribution is more like elastic, with very high values near the edges. This distribution tends to give higher values of moment and shear but the load itself is small and so the values of $M_c/q_y a^2$ or $F_c/q_y a$ are small. With increasing load, they increase but the contact pressure distribution also changes. With more and more region being plastic under increasing load, the contact pressure tends to become uniform and equal to q_y everywhere. Therefore, in the limit, the footing is loaded with q_y and the contact pressure becomes also equal to q_y resulting in no moment or

shear anywhere in the footing. In between the extreme conditions associated with no load and failure load, maximum values are obtained. These are the design values of nondimensional moment and shear. Fig. 4.6 shows the design moment values indicated by M_d and plotted as dimensionless quantity $M_d/q_y a^2$ versus the radius ratio, n , for various values of relative rigidity, K . In this figure, the curves for $h/a = \infty$ apply to the case of footing resting on semi-infinite soil. Similarly the design shear can be obtained from the curves for $h/a = \infty$ in Fig. 4.7.

The critical bending moment obtained from elastic theory for a circular footing with $K = 10$ and $\nu_s = .5$, $\nu_p = .25$ would be given by $M_c/q_{av} a^2 = .07$. In elastic treatment of the problem, this value is independent of the load level and hence the maximum value of M_c , which is the design value M_d is given by $M_d = .07 = q_y a^2$. From elasto-plastic analysis M_d for this data is (Fig. 4.6), $M_d = .037 q_y a^2$, which is only about 53 percent of that based on elastic theory. Table 4.1 gives some values of the design moment and shear as percentages of those based on elastic theory alone.

TABLE 4.1 : DESIGN MOMENT AND SHEAR VALUES BASED ON ELASTO-PLASTIC ANALYSIS EXPRESSED AS PERCENTAGE OF VALUES BASED ON ELASTIC THEORY

(Loading-uniform, $v_s = .5$ or 0 , $v_p = .25$, $h/a = \infty$)

n	Design value based on elasto-plastic analysis as percent of that based on elastic theory alone					
	Bending Moment			Shear Force		
	K=10	K=1	K=.1	K=10	K=1	K=.1
0.0	52.9	60.0	78.6	56.4	62.7	69.7
0.4	47.6	51.8	92.9	51.8	55.1	59.2

From this Table and from Figs. 4.5 and 4.6 can be seen that a design based on elasto-plastic analysis will be highly economical, more so far $K \geq 1$ which is the more likely range of K values in practice. In the conventional current design practice, the elasto-plastic behaviour is not considered, although it is quite significant as shown in the present study.

From Figs. 4.6 and 4.7 it can also be seen that the design nondimensional moment and shear values are less for lower values of K and higher values of n. For example, the values of $M_d/q_y a^2$ for $n=.4$ are .0295 and .0215 for $K=10$ and $K=1$ respectively and for $n=.8$ they are .014 and .005 for

$K=10$ and $K=1$ respectively.

In all the cases it has been found that out of the radial and tangential moments, the latter is critical and that it occurs at the inner edge (centre in case of a circle). Except for circular footing ($n=0$), in which case both these moments are maximum and equal at the centre, the maximum radial moments are less than the maximum tangential moments. This is evident from the typical values shown in Fig. 4.8. It has been found that the maximum radial moments are much smaller than the maximum tangential moments for higher values of n . It can be said in general that the maximum tangential moment is critical in all the cases.

It has been found that, for the case under consideration, the critical shear occurs near mid-width of the footing (near half-radius in case of circular footing).

(b) Loading at the inner edge of ring footing

For the purpose of comparative study of various loading configurations the footing is divided into annular rings of equal width. The programme developed for this thesis has provision for loading these rings in any desired proportion. However for brevity, the 3 cases mentioned in Section 4.2.2 are discussed herein.

Fig. 4.9(a) shows the effect of width of uniformly loaded area on the maximum dimensionless shear and moment, the loading being on the innermost portion of a ring or a circular footing. The values shown in this figure are for q_{av}/q_y value of about .45 but a similar trend is found to exist under other load levels (q_{av}/q_y values). As the width of loaded area reduces, the maximum dimensionless moment and shear increase at increasing rate. For example, the maximum moment in terms of $M_c/q_{av} a^2$ is about .07, .32 and .8 for load covering 100 percent, 50 percent and 10 percent radius respectively of a circular footing with $K=10$. A situation of very narrow loaded area at the inner edge or centre should therefore be avoided.

Fig. 4.9(b) shows the effect of positioning of loaded annular area of width equal to one-tenth of outer radius, on maximum dimensionless moment and shear. For this figure q_{av}/q_y is about .4, but values for other load levels are found to show similar trend. The maximum moment and shear have small negative values for loading at the outer edge. These values reduce to zero and then increase on the positive side as the loading moves from the outer edge to the inner edge. The values of $F_c/q_{av} a$, for example, are about -.15, .75 and 3.8 for circular footing with $K=10$ with loading at the outer edge, centre of width (half radius) and inner edge respectively.

In both the cases mentioned above, the effects of load position on maximum moment and shear are less for higher values of n and a little less for lower values of K (Fig. 4.9).

An extensive study of maximum moment and shear under elasto-plastic conditions of soil revealed that they remain fairly constant at all load levels e.g. Fig. 4.10. This behaviour is explained as below.

Under smaller loads, the contact pressure is much higher near the edges, whereas under higher loads, because of plastic yield of soil, the contact pressure tends to be uniform. The effects of these two factors oppose each other in changing the maximum bending moment and shear force and hence the change remains small (within 10 percent).

A study of a large number of cases has led to the conclusion that the footing under this type of loading could be either designed on the basis of elastic solution or on the basis of complete yield condition of soil amounting to uniform contact pressure of intensity q_y . The latter is recommended being easier to deal with.

The critical shear force is calculated easily at any radial distance r as equal to the unbalanced force outside this radius, divided by the perimeter ($2\pi r$) at this section (vide Fig. 4.11). The force due to the contact pressure is

calculated easily on the basis of uniform stress of intensity q_y (yield stress of soil). The critical shear occurs at the outer edge of the loading and this would be the design shear. The design moment occurs, as tangential bending moment, at the inner edge (centre in case of circular footings) and can be calculated by assuming uniform contact pressure q_y and then using, and superimposing if necessary, standard elastic thin plate solutions (e.g. Timoshenko Krieger (1959)).

The design procedure suggested above, amounts to replacing soil by a uniform pressure q_y and the moment and shear become independent of K .

(c) Other positions of annular loading

An extensive study under elasto-plastic conditions revealed that the critical moment and shear remain fairly constant or slowly increase as load increases. Therefore, the design procedure given in (b) above is satisfactory. For loading on a thin annular ring, it can be assumed, without much loss of accuracy, that this loading is replaced by an annular line support. For example, the design moment for a ring footing loaded on a thin annular ring at the outer edge can be found out fairly accurately from the formula (Timshenko- Krieger, 1959)

$$\frac{M_T}{q_y a^2} = \frac{(3 + v_p) (1 - n^2)}{16}$$

The above solution is for a thin annular plate simply supported at the outer edge and loaded uniformly with intensity q_y .

For annular loading at the outer edge, the maximum shear occurs at the inner edge of the loading and the maximum moment (tangential) occurs at the inner edge, both being negative.

For annular loading at the centre of width of a ring footing (at half radius for circular footing), the maximum shear occurs at the outer edge of the loading. The radial and the tangential moments are maximum and nearly equal under the loading.

In all types of loadings, the design moment and shear force values reduce with increasing value of n . This aspect is discussed in detail later.

4.4.2.2 Elasto-plastic settlement: Effect of relative rigidity

The settlement is expressed as (Eq. 4.29)

$$\phi = \frac{q_{av}^a}{E} I_f$$

Except for an infinitely rigid footing, the settlement under a footing is non-uniform and refers to the maximum settlement under a footing unless otherwise specified. The settlement has been generally found to be maximum at the inner edge (centre in case of circle) except in some

cases like annular loading at the outer edge in which case it is maximum under the load.

For footings with finite rigidity, the differential settlement is an important design consideration and it is indicated by D_f (Differential Deflection Factor) given in Eq. 4.30.

In Fig. 4.12 are given the plots of I_f and D_f for two values of K ($K = 10$ and 1) and for uniformly loaded ring footing with $n = 0, .4$ and $.8$; the curves corresponding to $h/a = \infty$ being applicable for the case under consideration. The settlement (indicated by I_f) is more for lower values of K in the lower range of values of q_{av}/q_y . For example, at $q_{av}/q_y = .2$, the values of I_f for $n = 0$ are 1.0 and 1.1 for $K = 10$ and 1 respectively (Fig. 4.12). This difference is small and it is due to sagging of a flexible footing near the centre.

In case of a flexible footing, the contact pressure is uniform-like and hence under increasing load, the pressures increase somewhat equally without causing yielding, giving rise to very slow increase in I_f . The curve for I_f therefore goes somewhat straight until failure develops over appreciable area after which settlement increases at a fast rate. On the contrary, for a comparatively rigid footing, because of highly non-uniform contact pressure,

yielding spreads even under small load increments, giving rise to a drooping curve for I_f . The settlement in this case increases in a uniform manner. This explains the difference in nature of curves for $K = 10$ and $K = 1$ in Fig. 4.12. This difference in behaviour due to K is less dominant for higher values of n which can also be seen from Fig. 4.12. This is mainly because of already lower I_f values for higher values of n .

The differential settlement, indicated by D_f is however found to be highly sensitive to K (Fig. 4.12). For example, considering the load level $q_{av}/q_y = .5$, the value of D_f for $n = .4$ is .0165 for $K = 10$ as against .11 for $K = 1$, for $n = 0$ it is .0185 for $K = 10$ as against .15 for $K = 1$, and for $n = .8$, it is .0025 for $K = 10$ as against .01 for $K = 1$. As the load approaches the failure load, the differential settlement under a uniformly loaded footing tends to vanish since a situation of uniform contact pressure equal and opposite to uniform loading on the footing is approached. The differential settlement under a uniformly loaded footing is therefore most critical under working loads.

Figs. 4.13 and 4.14 show the plots of I_f and D_f for three types of annular loadings, for two values of K (10 and 1) and two values of n (0 and .8). Apart from n , the maximum

settlement is controlled by the load position, relative rigidity K , and the load level indicated by q_{av}/q_y . Referring to Fig. 4.13 ($n=0$ case) and considering the effect of K on I_f , it is seen that for loading at the outer edge, I_f is more for lower value of K and the difference increases rapidly beyond $q_{av}/q_y > .3$. For example, at $q_{av}/q_y = .7$, I_f is 4.2 for $K = 1$ as against 2.1 for $K = 10$. In the other two cases of loading, I_f is less for $K = 10$ than for $K = 1$ upto $q_{av}/q_y \leq .5$ and vice versa beyond $q_{av}/q_y > .5$. One of the effects of load position on I_f is already mentioned above (loading at the outer edge). I_f is less sensitive to load position, at any load level, for higher value of K as seen from Fig.4.13 where the corresponding curves are close to each other.

From Fig. 4.13 it is seen that D_f is low and fairly constant for all load positions and levels for higher value of K . However it can be seen that D_f is highly sensitive to load position for lower values of K . For $K = 1$, D_f at $q_{av}/q_y = .4$ is about 4.7, 2.1 and 1.5 for loading at the inner edge, centre of width and outer edge respectively. The corresponding values for $K = 10$ are .6, .3 and .2. This shows that loading at the innermost portion is critical from the point of view of differential settlement, more so for lower values of K .

Fig. 4.14 is similar to Fig. 4.13 except that it is for $n=.8$ instead of $n = 0$. It is seen from this Figure (Fig. 4.14) that D_f is sensitive to load position for lower value of K ($K=1$) and the rest of the curves show less sensitivity at all load levels to load position or K . It is also seen that in this case ($n=.8$), D_f is minimum for load position at centre of width.

Considering I_f and D_f at all load levels it can be said that the position near the centre of width of ring footing (near half radius for circular footing) of an annular loading is better than any of the other positions of load. This applies particularly, for relatively more flexible footings.

4.4.2.3 Effect of radius ratio n

From Figs. 4.3 to 4.6 and 4.8 to 4.14, it can be seen that the maximum or design moment and shear values decrease with increasing values of n , the reduction being faster as n approaches unity. For the sake of comparison, some design values for $n=.8$, obtained from the present work are quoted in Table 4.2 in terms of percentage of corresponding values, for a circular footing after applying the correction R_{eq} (Section 3.4.3 and Fig. 3.5). The comparison stands for equivalent footings i.e. for equal total loading on the ring and circular footing and equal area for ring and circular

footing. The design shear for loading other than uniform loading is calculated as explained in section 4.4.2.1(b) and Fig. 4.11.

TABLE 4.2 : TYPICAL DESIGN MOMENT AND SHEAR VALUES FOR A RING FOOTING WITH $n=0.8$ EXPRESSED AS PERCENTAGE OF CORRESPONDING VALUES FOR CIRCULAR FOOTING, UNDER EQUAL AREA AND TOTAL LOAD CONDITIONS

Quantity	Loading	K	Percentage
Design shear	Uniform	10	10
	Uniform	1	13
	A	Any value	20
	B	Any value	14
	C	Any value	36
Design moment	Uniform	10	100
	Uniform	1	25
	C	Any value	36

Note: A : Annular loading of one tenth width of ring footing at inner edge (loading within .1 a of circular footing).

B : Annular line loading at centre of width of ring (at .5a for circular footing).

C : Annular line loading at outer edge.

From the above Table, it can be seen that the design moment and shear values are considerably less for the ring footing in almost all the cases.

From Fig. 4.13 and Fig. 4.14 and Table 4.2 it can be seen that the settlement of footing is less for higher values of n for any K , position of load and load level q_{av}/q_y even after applying correction R_{eq} for equivalence of footings. The differential settlement, represented by D_f in these figures, is also seen to be highly sensitive to n , being very much less as n approaches unity. For a rational comparison, the quantity $D_f/\text{unit width of footing}$ should be compared for equal total load. To account for this, D_f for ring footing/ D_f for circular footing is to be multiplied by $\sqrt{(1-n^2)/(1-n)}$ (Fig. 3.5). If this is done, it is found that the real advantage is obtained if n is greater than about .6. Referring to Fig. 4.11 it can be found out, after applying the correction, that

$$\frac{D_f/\text{unit width for } n=.8}{D_f/\text{unit width for } n=0} = .154 = 15.4 \text{ percent}$$

for equal total load with $K = 10$ and $q_{av}/q_y = .5$. For $K = 1$, this percentage works out to 20 percent. This is a substantial advantage in favour of ring footing.

Thus ring footings are better suited than circular footings for carrying the same total load. This is true

from the point of view of moment and shear in the footing, as well as settlement and differential settlement.

4.4.3 Footing Resting on a Soil Layer of Finite Depth Underlain by Rough Rigid Base

As for the case of infinitely rigid footing in the previous Chapter the only change due to finite depth comes in through the use of the appropriate elastic solution.

The entire discussion given in Section 4.4.2 above for semi-infinite soil holds good, in general, for the case under consideration. The discussion below is therefore aimed at only a comparative study involving the effect of depth h , of the layer.

The design moment and shear values are shown in Figs. 4.4 and 4.5 for two values of h/a , three values of K against n for uniformly loaded footing. It is seen than those values are lower for lower values of h . For example, the values of design moment as percentage of those for $h/a = \infty$ are, for $n = 0$, $K = 10$, about 87 percent and 69 percent for $h/a = 2$ and 1 respectively. These percentages work out to about 80 percent and 50 percent for $K = 1$. Thus for lower values of h the design moment and shear values are less. This effect is less prominent for higher values of n (narrow ring footings). The design values drop considerably for very low values of depth of layer.

Under loadings other than uniform loading, an extensive study of maximum moment and shear has revealed results similar to those for $h/a = \infty$. Therefore, the design values be better based on uniform contact pressure q_y . Thus for the loadings considered (other than uniform) the design moment and shear values would be independent of K and depth ratio h/a also. For finding the design values, the procedure given in Section 4.4.2.1(b) and Fig. 4.11 is to be followed.

The settlement and differential deflection are expressed as in Eq. 4.29 and Eq. 4.30 respectively. Fig. 4.15 and Fig. 4.16 show the plots for I_f and D_f for uniform loading for various parameters and two values of h/a . The curves for $h/a = \infty$ shown in Figs. 4.13 and 4.14 can be used for comparison. From these figures it can be seen that I_f is appreciably affected by h/a . For example, for $q_{av}/q_y = .5$, I_f for $h/a = 1$ expressed as percentage of value for $h/a = \infty$ is about 33 percent for all the values of K and n shown in the figure. (This percentage is however not constant for all values of K and n at all other values of q_{av}/q_y). It is observed that the effect of h/a on I_f is significant and it remains so at all load levels. For uniform loading the differential settlement represented by D_f is also highly sensitive to h/a . For example, D_f for $n=0$ and $q_{av}/q_y = .4$

expressed as percentage of D_f for $h/a = \infty$ is about 87 percent for $h/a = 2$ and 55 percent for $h/a = 1$. The corresponding values of D_f for $n = .4$ are 81 percent for $h/a = 2$ and 45 percent for $h/a = 1$. D_f for higher values of n which is already low even for $h/a = \infty$ is further reduced very much with decreasing values of h/a .

Figs. 4.15 and 4.16 show plots for I_f and D_f for two values of h/a , the loading being at the inner edge on one-nineth width. The curves for uniform loading are also shown for the sake of comparison. Since loading on one nineth width presents considerably different situations for various values of n , a direct comparison with respect to n is not advisable. Broadly it can be said, referring to Figs. 4.15 and 4.16, that I_f is less sensitive to loading configuration and load level for higher values of K , lower values of n and lower values of h/a . D_f is high for loading at the inner edge even for low values of h/a , except for n values of about .8 and above.

In short, the effect of radius ratio n as discussed for $h/a = \infty$ is similar for finite values of h/a . As mentioned earlier, the design nondimensional values of moment and shear under uniform loading are lower for higher values of n . Under other loading positions, h/a does not affect these design values (since the design is to be based on

uniform contact pressure equal to q_y) and the discussion for $h/a = \infty$ holds good. Both I_f and D_f are reduced, the latter considerably with increasing values of n , and even considering equivalence, narrow ring footings will give very small values for design moment and shear, as well as settlements and differential settlements, in comparison to circular footing. All these values reduce further for lower values of h/a .

All the design values discussed above depend on q_y and since q_y for finite values of h/a , is to be corrected as explained in Section 3.4.5 for thickness of layer will be lower than those for $h/a = \infty$.

4.4.3 Effect of Embedment of Footing in Semi-Infinite Soil

For this case Mindlin's solution has been used in place of Boussinesq's solution. The behaviour agrees in general with that of a surface footing except for some differences which are discussed below.

Fig. 4.17 shows the bent portions of the footing near the centre of a uniformly loaded circular footing embedded at depths of .3, .6 and 1 times the outer radius ($c/a = .3, .6$ and 1). It is seen that the curvature is sharper for $c/a = .6$ than for $c/a = .3$ or $c/a = 1$. (Although settlements are less for higher values of c/a). This type of

behaviour is found to exist for all values of K , n and q_{av}/q_y . The bending moments are very sensitive to the deformed shape of the footing (Eqs. 4.5, 4.25). It is therefore found that the dimensionless design moment ($M_d/q_y a^2$) is maximum for a certain value of q_{av}/q_y for c/a values between a range of .3 to .6 for uniformly loaded embedded footings. Fig. 4.18 gives these maximum values for $K = 10, 5$ and 1 and $n = 0, .4$ and $.8$. It is seen that these values increase as c/a increases, become maximum between $c/a = .3$ to $c/a = .6$ and then decrease at a slower rate as c/a increases, being almost constant for $c/a > 2$. All the above discussion holds good for dimensionless design shear ($F_d/q_y a$) also and the maximum values are shown in Fig. 4.18. As pointed out in the earlier Chapter, the value of q_y appropriate to c/a should be used.

For loadings other than uniform loading, it is again found that the design moment and shear should be found from the basis of uniform contact pressure q_y , on the lines given in Section 4.4.2.1(b) and Fig. 4.11. Thus for such loadings, the design moment and shear values are independent of depth of embedment.

I_f and D_f follow the same overall pattern as for surface footing, the values being lesser with increasing

value of depth of embedment. However, the curves, if plotted as for earlier cases do not show a simple pattern of variation with q_{av}/q_y . It is suggested that the correction be applied to values found for surface footings as given in Chapter 3 for rigid footings.

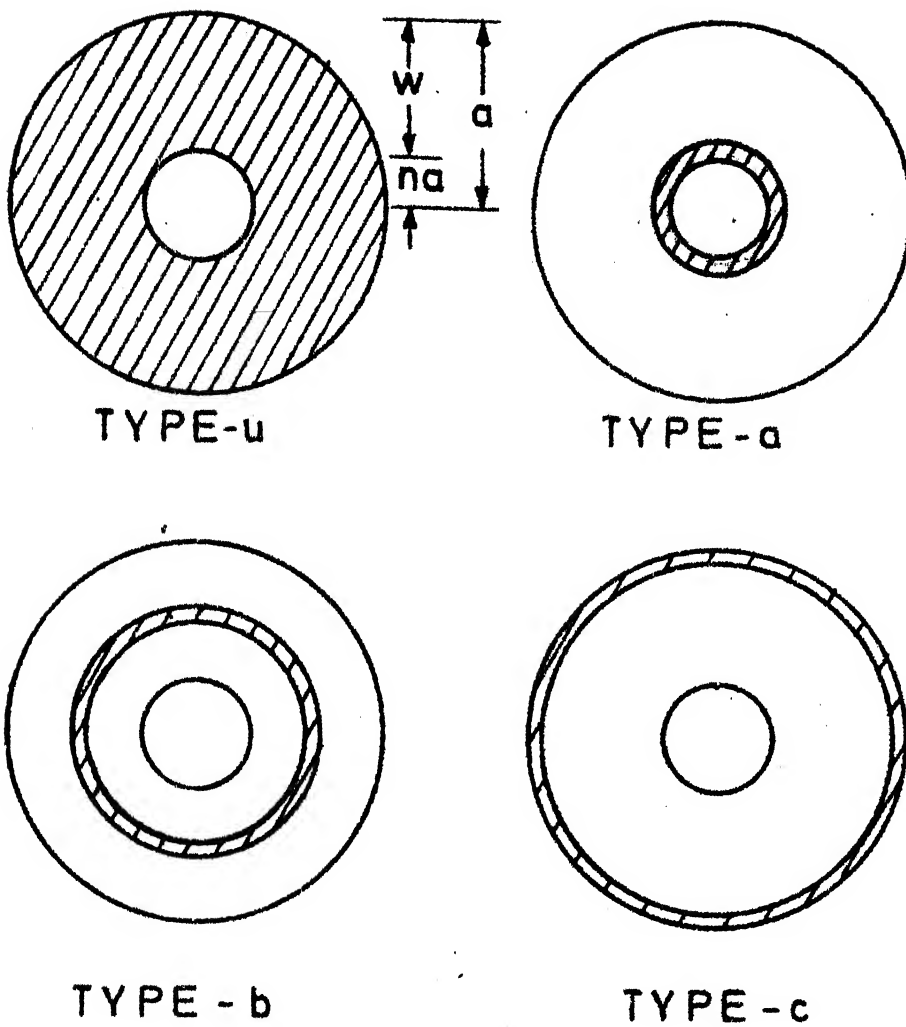
4.5 CONCLUSIONS

- (1) A study of axisymmetrically loaded annular footings of finite rigidity resting at or below the surface of a semi-infinite soil or resting on a compressible soil layer of finite depth has been made using thin plate theory for the footing. The Bending Moments and Shear Forces in the footing and the settlements are studied under various loading configurations and under elasto-plastic soil condition and with tension cut-off wherever applicable.
- (2) It is found that differential settlement and design moment and shear under uniform loading are highly sensitive to relative rigidity K of footing. Maximum and differential settlements are higher and design moment and shear are lower for lower values of K .
- (3) It is found that in all the cases, a ring footing, especially with inner radius more than about .6 times the outer radius gives lesser design bending

moment and shear force and settlements and are advantageous over a circular footing of the same area and carrying the same total load.

- (4) Under uniform load, it is found that the footing need be designed for values much lower than those obtained from elastic theory alone. Design charts for some values of parameters are presented.
- (5) Under annular loadings, it is found that the design moment and shear in all the cases should be found by assuming uniform contact pressure equal to yield stress of soil.
- (6) For the loadings considered, the locations of maximum moment and shear are investigated. Under uniform loading the maximum shear occurs near the centre of width of ring footing or near half radius of circular footing. The maximum moment occurs at the inner edge (or the centre) except for annular loading at half width in which case the maximum moment as well as shear occur near/under the load.
- (7) Out of the maximum radial and tangential bending moments, the latter are found to be critical in all the loading cases considered.
- (8) The design moment, shear and settlements are smaller for lower values of depth of layer or for higher values of depth of embedment.

- (9) The settlement of embedded footing can be approximately found by applying correction procedure given for rigid footing (Chapter 3).
- (10) A design procedure has been given for evaluating the design moment and shear in the footing and the maximum and differential settlements of footings of finite rigidity resting on or in semi-infinite soil or on soil layer of finite thickness.



TYPE - b

TYPE - c

u - Uniformly distributed load

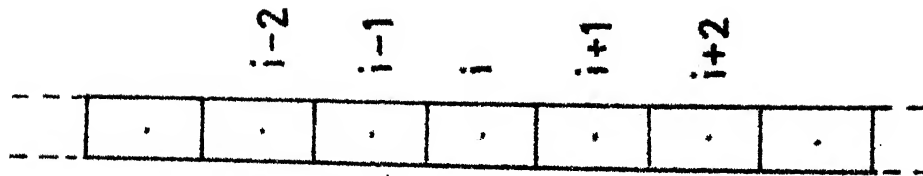
a - Annular load at inner edge

b - Annular load at centre of width

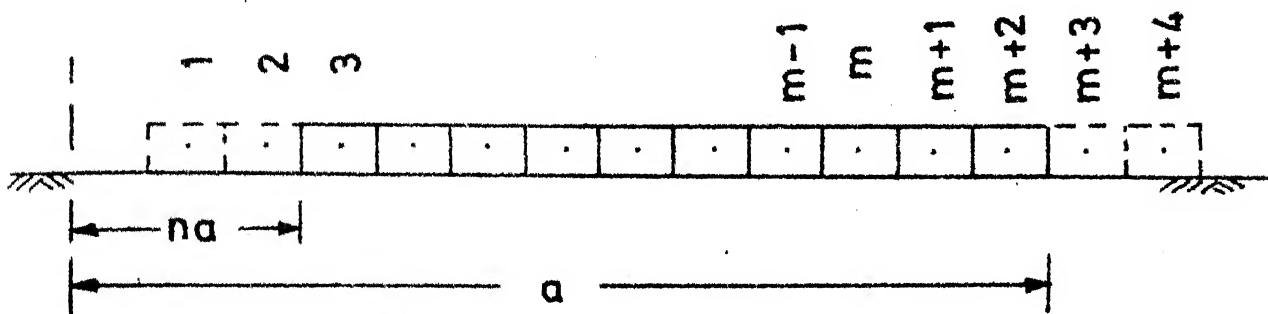
c - Annular load at outer edge

w - Width of ring

FIG.4.1 TYPES OF LOADING CONFIGURATION
ON FOOTING OF FINITE RIGIDITY

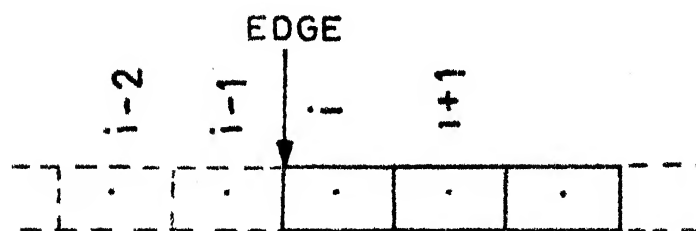


(a) Elements in the neighbourhood of i



Fictitious elements $1, 2, m+3, m+4$

(b) Numbering of plate elements



Fictitious
elements

(c) Elements in the neighbourhood
of edge

FIG. 4.2 PLATE DISCRETIZATION

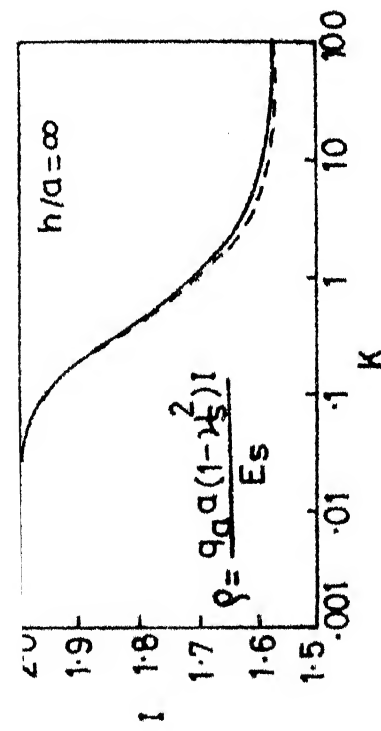


FIG. 4.3 a CENTRAL VERTICAL DISPLACEMENT
FACTOR FOR CIRCULAR RAFT

— BROWN (1969)
— PRESENT WORK

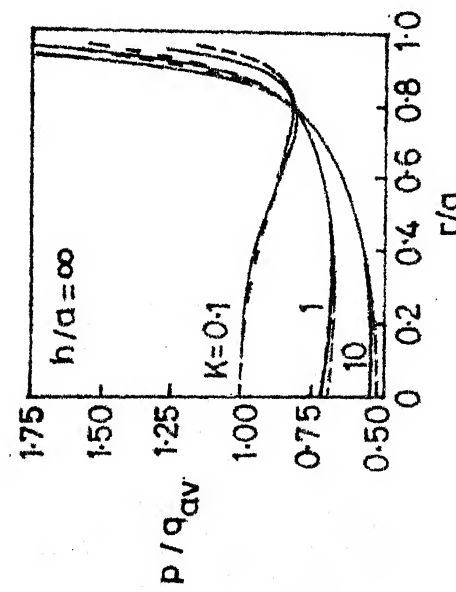


FIG. 4.3 b CONTACT PRESSURE BENEATH
CIRCULAR RAFT $\gamma_p = .3$

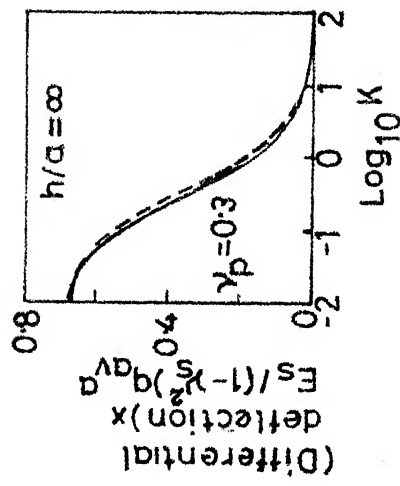


FIG. 4.3 c DIFFERENTIAL DEFLECTION
IN CIRCULAR RAFT $\gamma_p = .3$

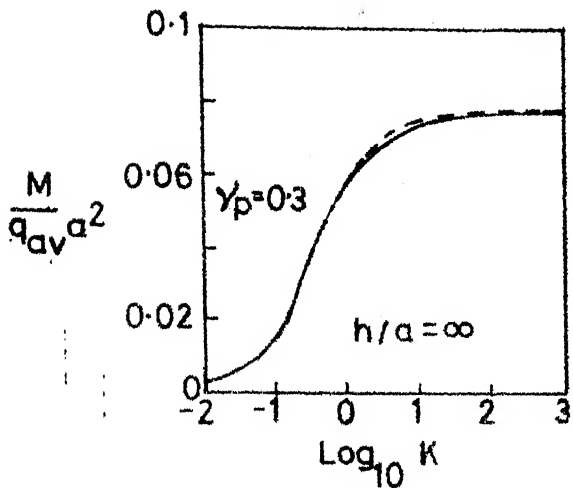


FIG. 4.3 d MAXIMUM MOMENT IN CIRCULAR
RAFT $\gamma_p = 0.3$

— BROWN (1969)
- - - PRESENT WORK

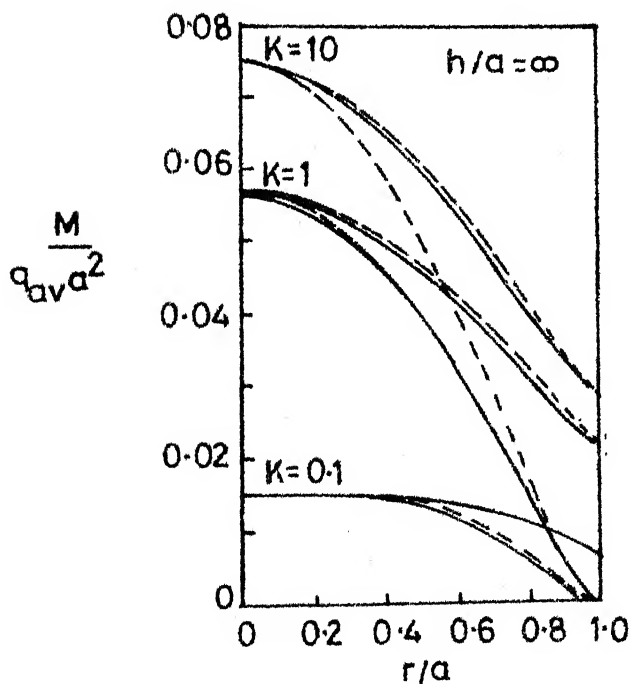


FIG. 4.3 e BENDING MOMENT DISTRIBUTIONS
IN CIRCULAR RAFT $\gamma_p = 0.3$

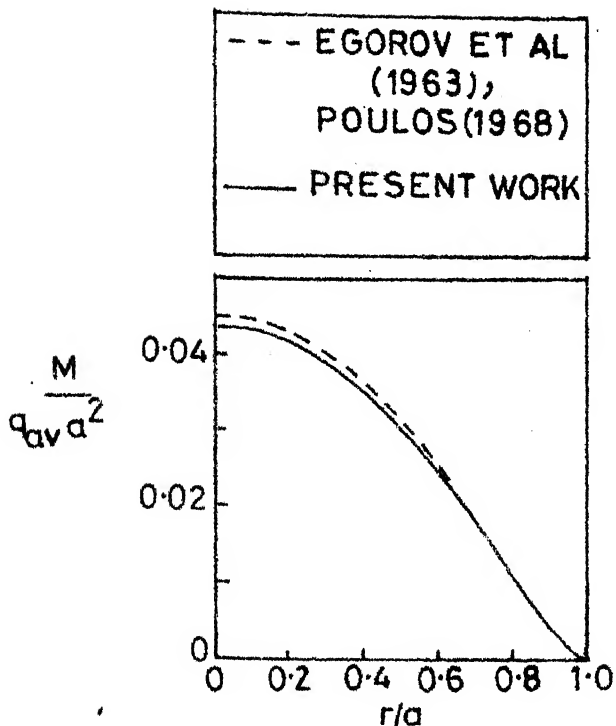


FIG.4.3 f RADIAL BENDING MOMENT DISTRIBUTION IN UNIFORMLY LOADED RIGID CIRCULAR RAFT. $\gamma_s=0.4$, $\gamma_p=0.25$, $h/a=1$

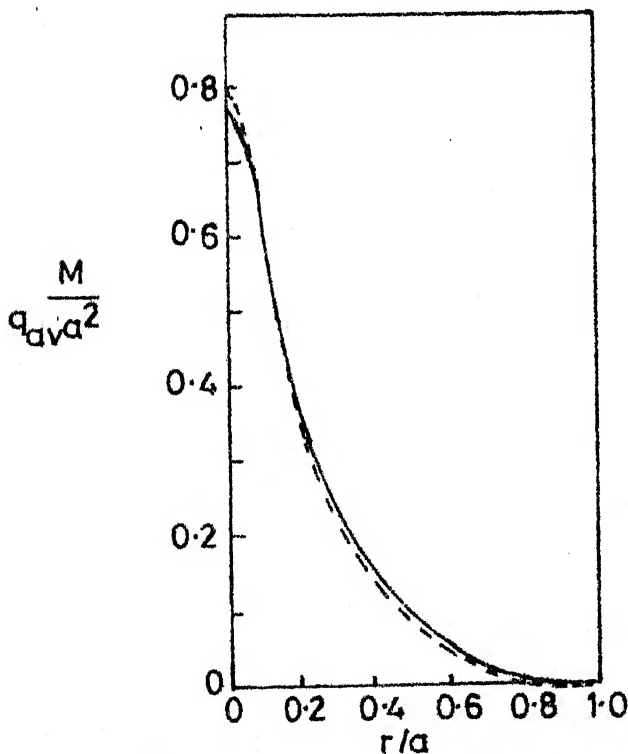


FIG.4.3 g RADIAL BENDING MOMENT DISTRIBUTION FOR CONCENTRATED LOAD WITHIN $r=0.1a$

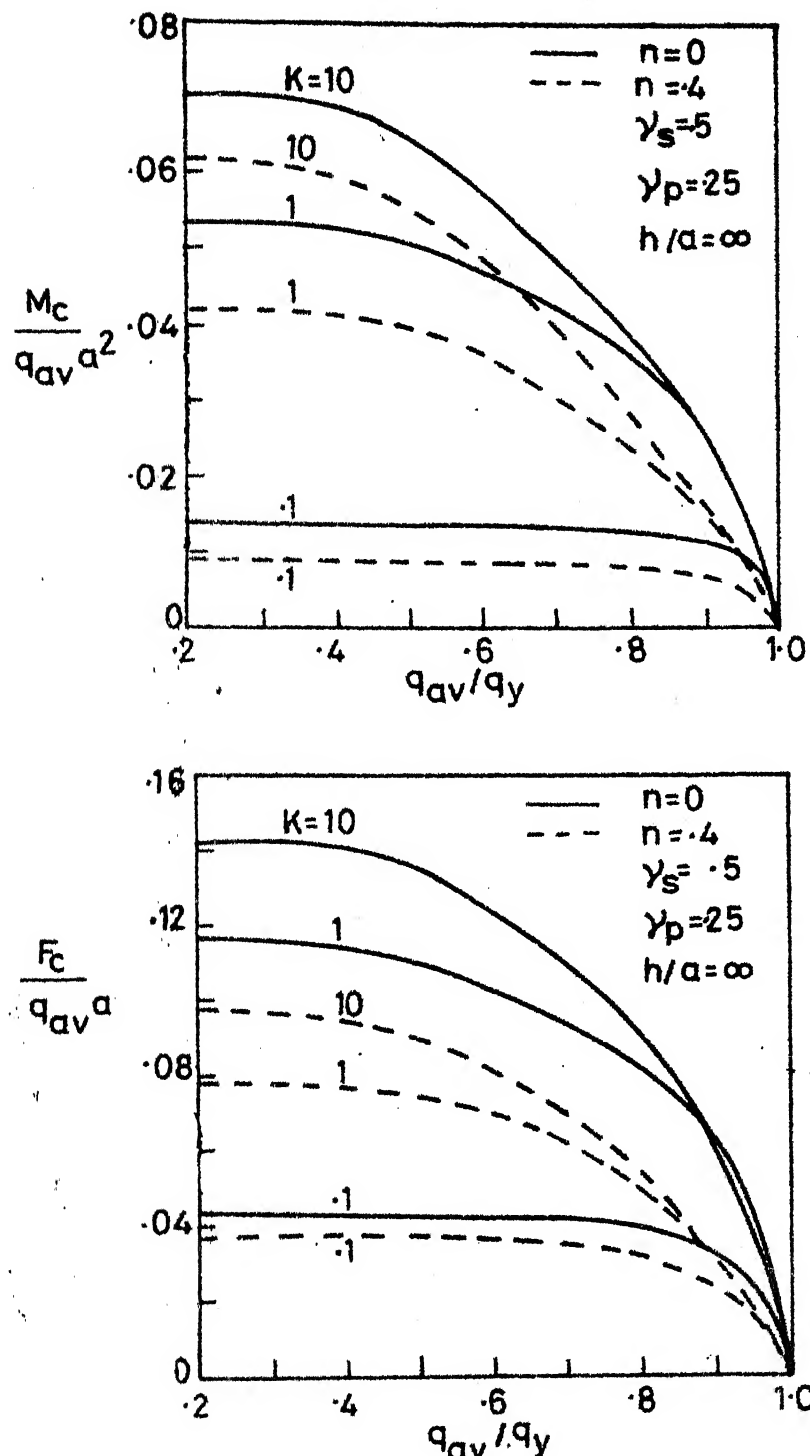


FIG.4.4 MAXIMUM (Critical) BENDING MOMENT AND SHEAR AT VARIOUS LOAD LEVELS IN A UNIFORMLY LOADED FOOTING

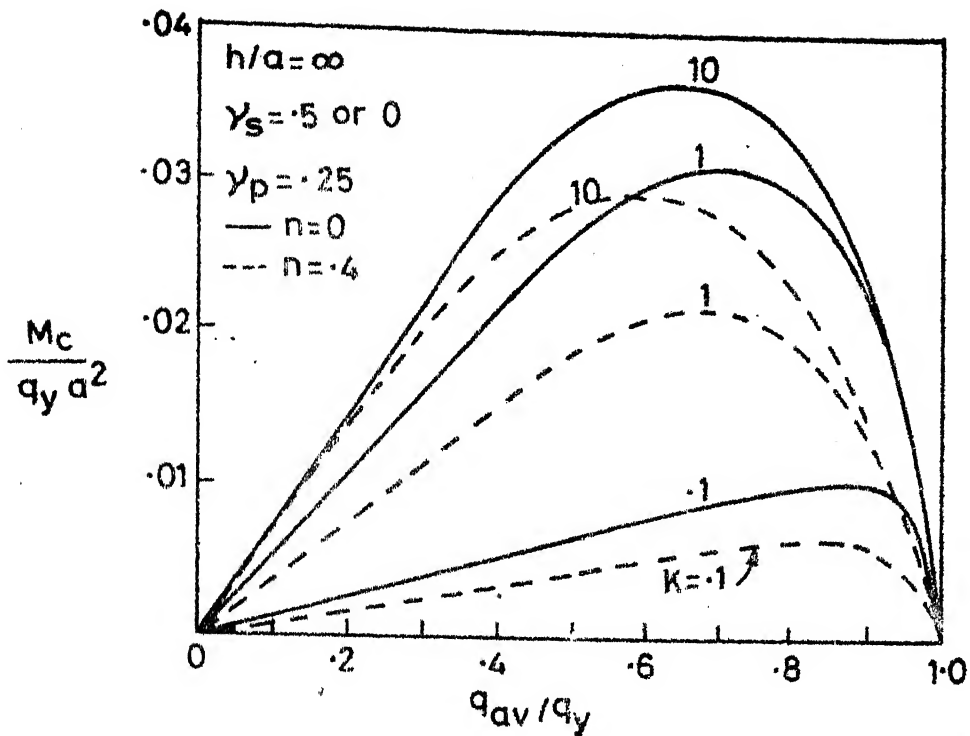


FIG. 4.5 (a) DEPENDENCE OF CRITICAL B.M. ON LOAD LEVEL

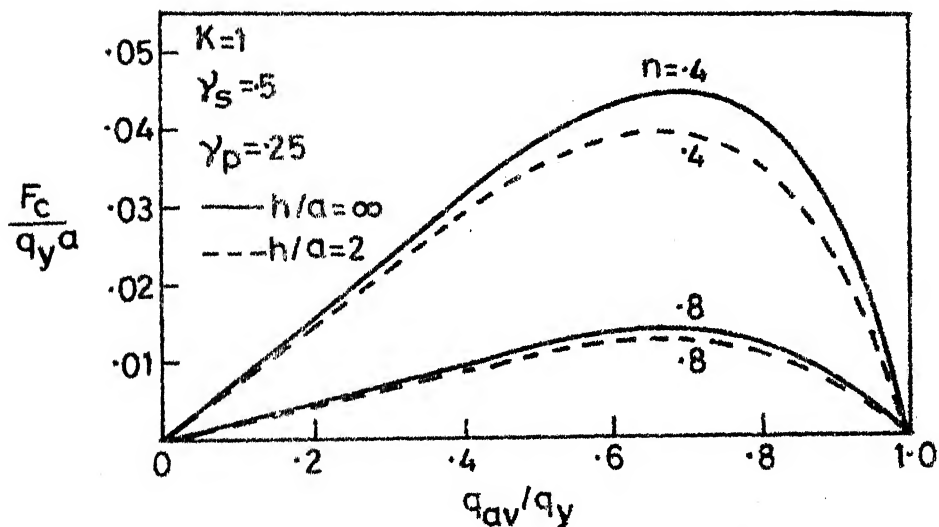


FIG. 4.5 (b) DEPENDENCE OF CRITICAL SF ON LOAD LEVEL

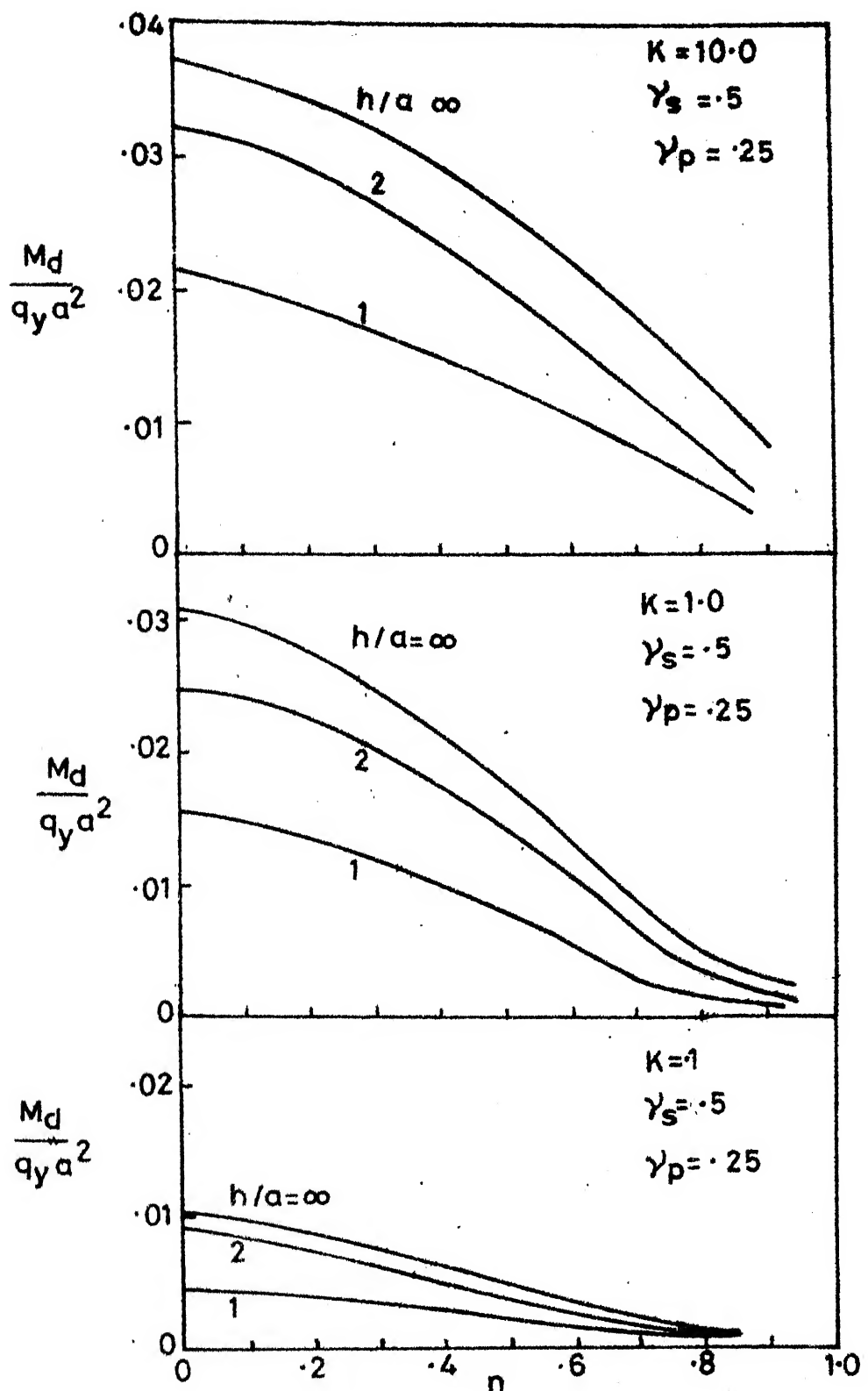


FIG.4.6 DIMENSIONLESS DESIGN MOMENT FOR UNIFORMLY LOADED RING FOOTINGS

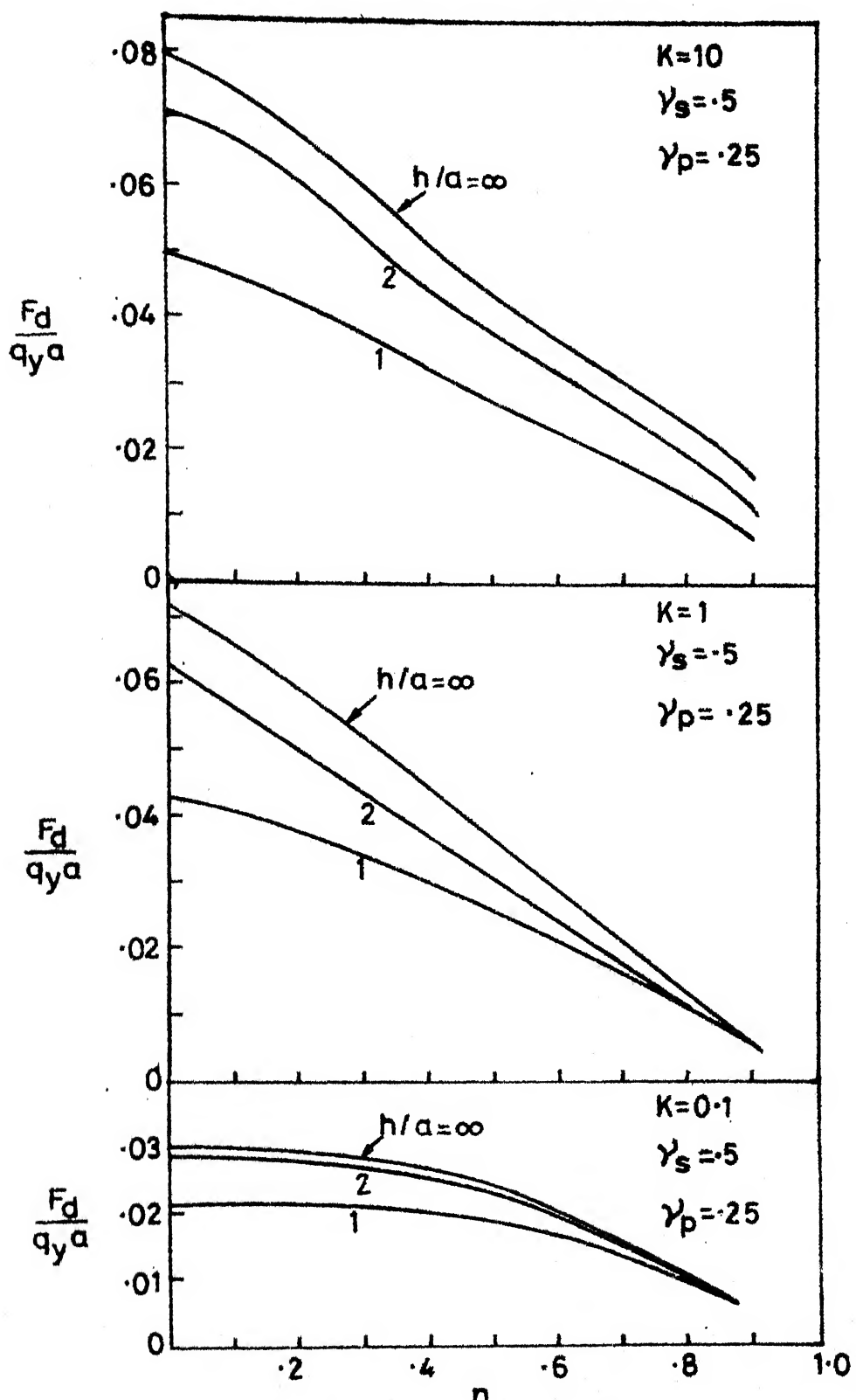
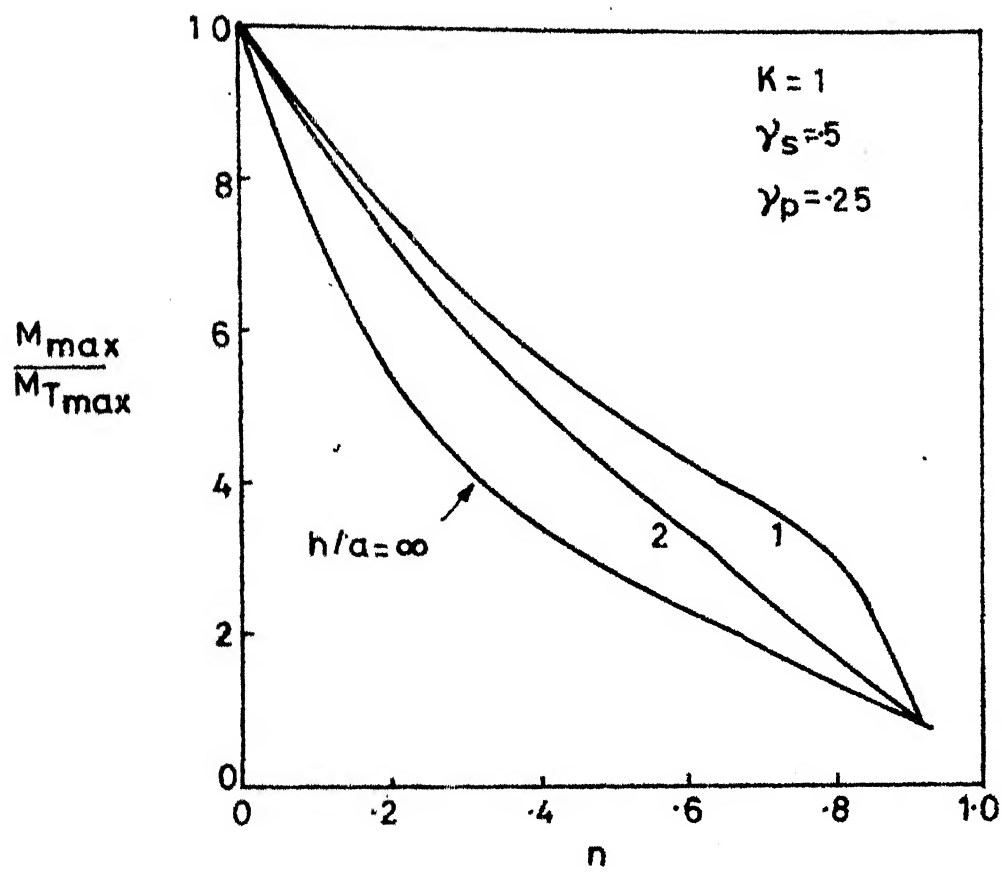


FIG. 4.7 DIMENSIONLESS DESIGN SHEAR FOR UNIFORMLY LOADED RING FOOTINGS



**FIG. 4.8 COMPARISON OF TYPICAL MAXIMUM VALUES
OF RADIAL AND TANGENTIAL BENDING
MOMENTS**

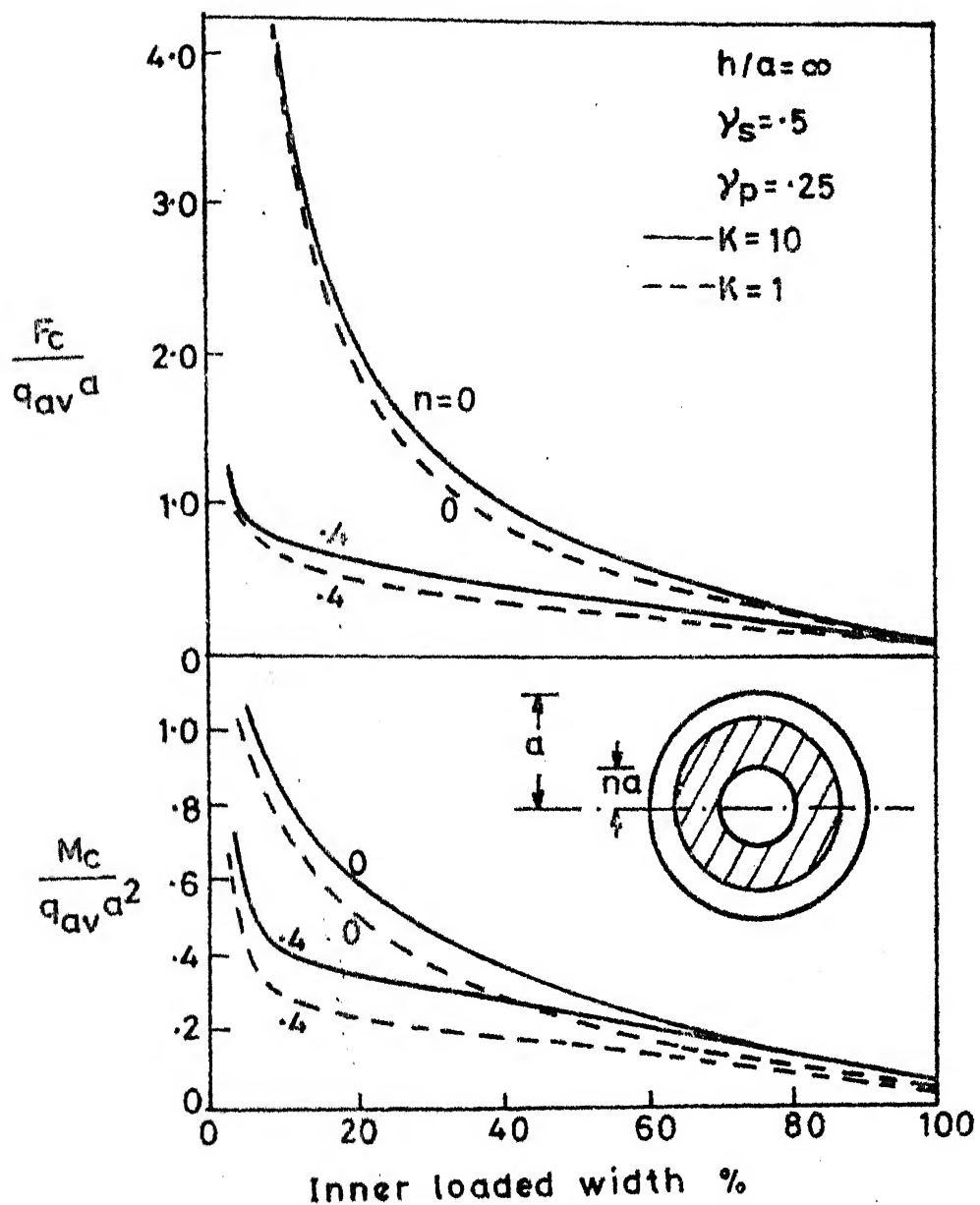


FIG. 4.9(a) EFFECT OF WIDTH OF UNIFORMLY LOADED AREA (innermost portion) ON MAXIMUM SHEAR AND MOMENT

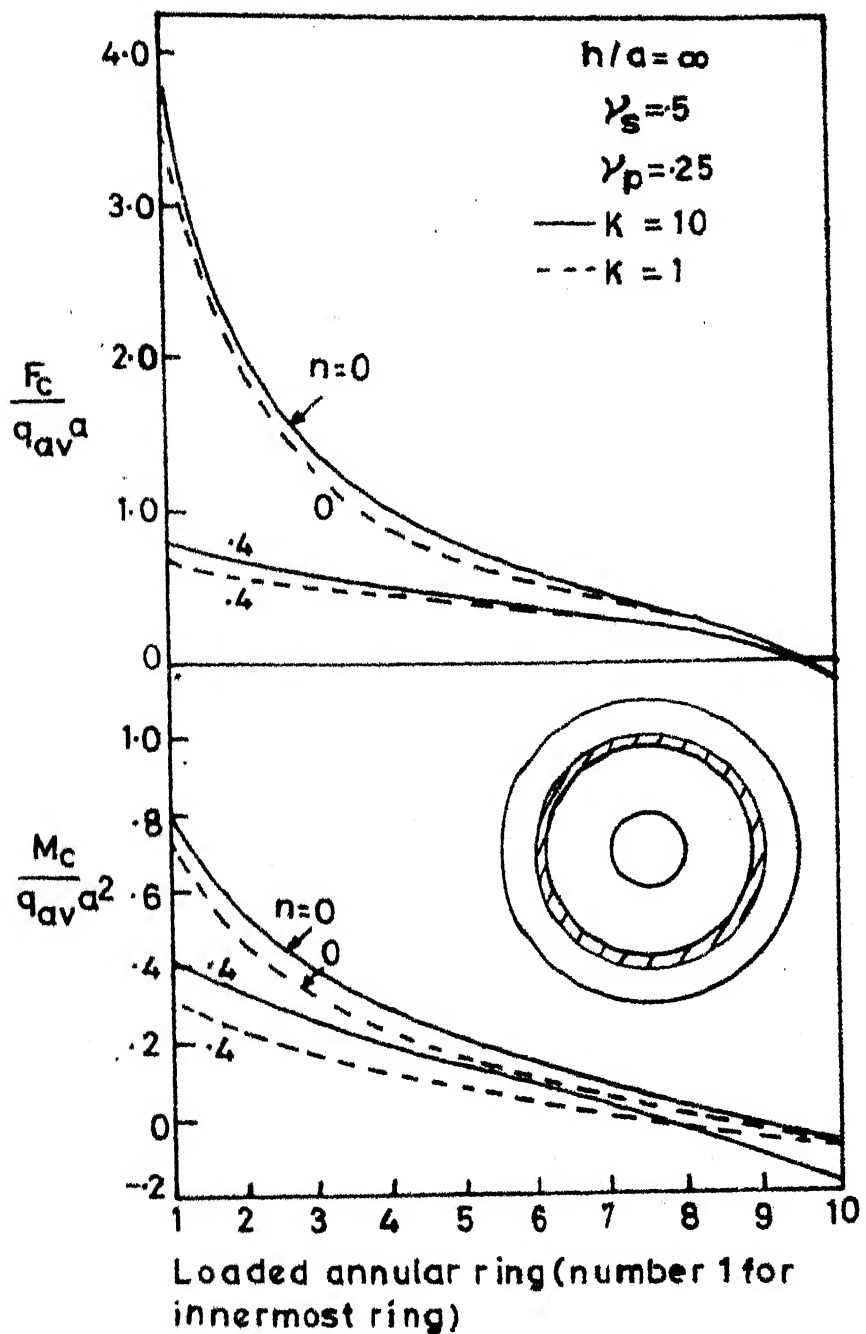


FIG. 4.9(b) EFFECT OF POSITION OF SINGLE LOADED ANNULAR RING

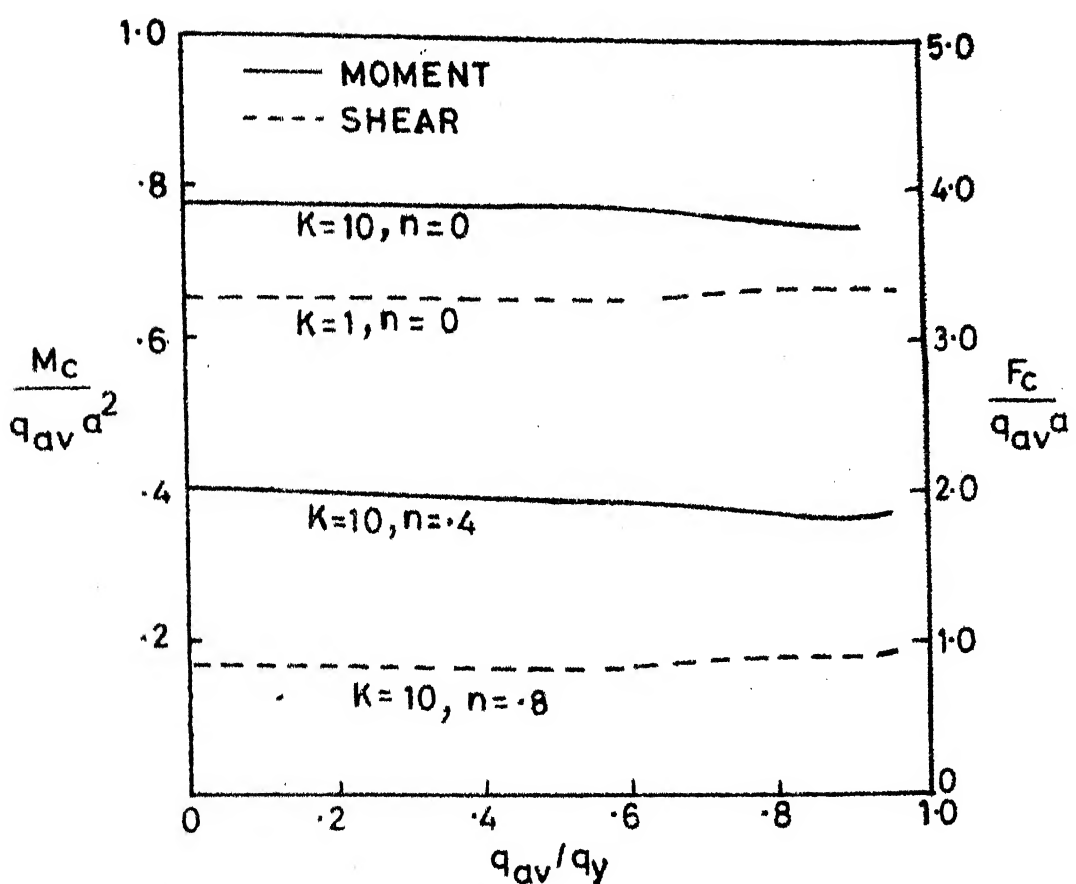


FIG. 4.10 MAXIMUM MOMENT AND SHEAR VARIATION
WITH LOAD LEVEL FOR INNERMOST ONE
NINETH WIDTH LOADED

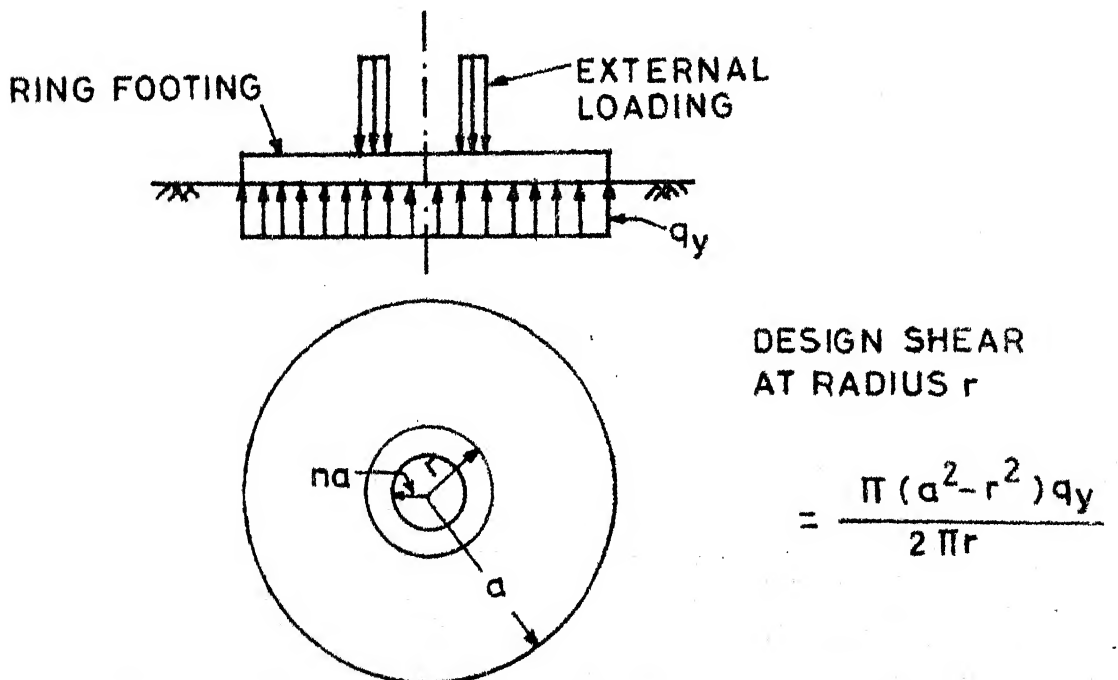


FIG. 4.11 METHOD OF CALCULATING DESIGN SHEAR
FOR RING FOOTING LOADED AT INNER EDGE

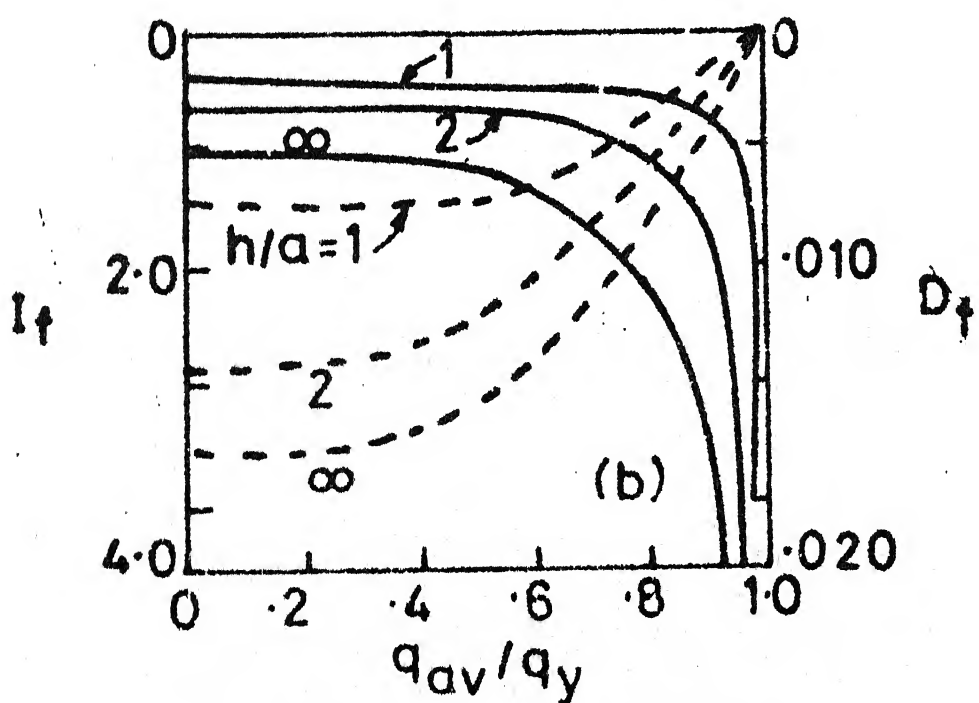
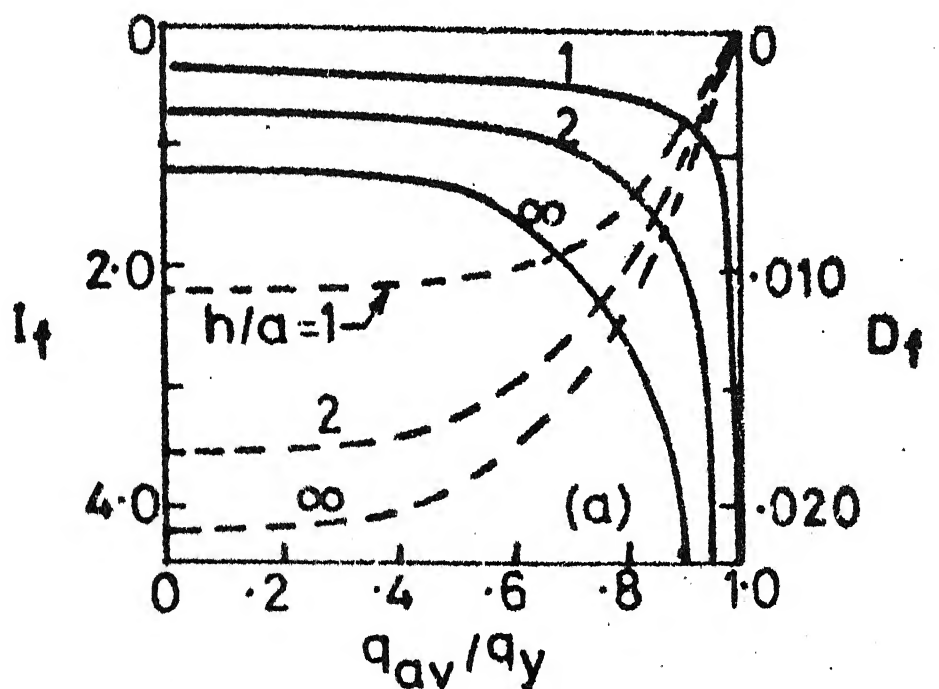


FIG.4.12 DESIGN CHARTS FOR SETTLEMENT
INFLUENCE FACTOR AND DIFFERENTIAL
DEFLECTION FACTOR FOR UNIFORMLY
LOADED RING FOOTING

(a) $K=10, n=0$ (b) $K=10, n=.4$

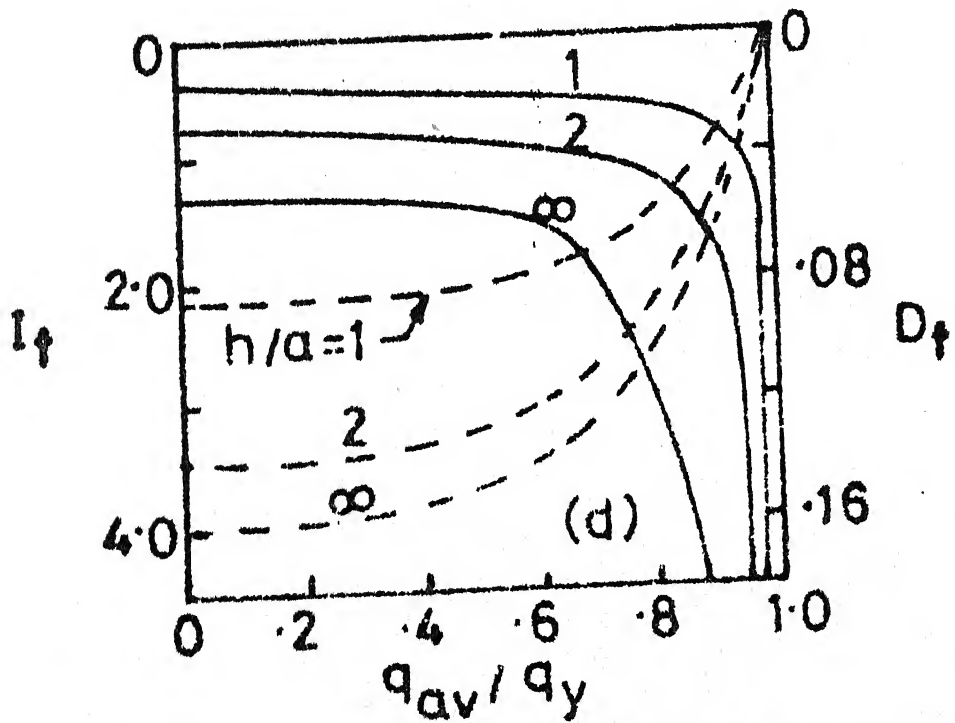
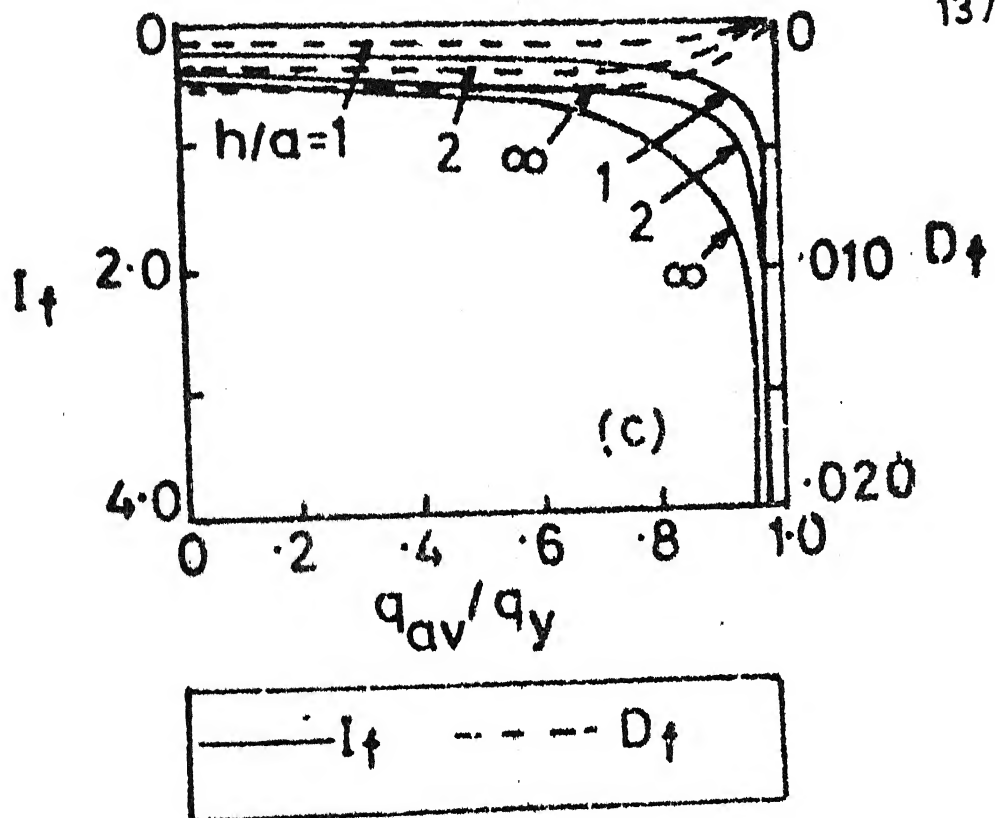
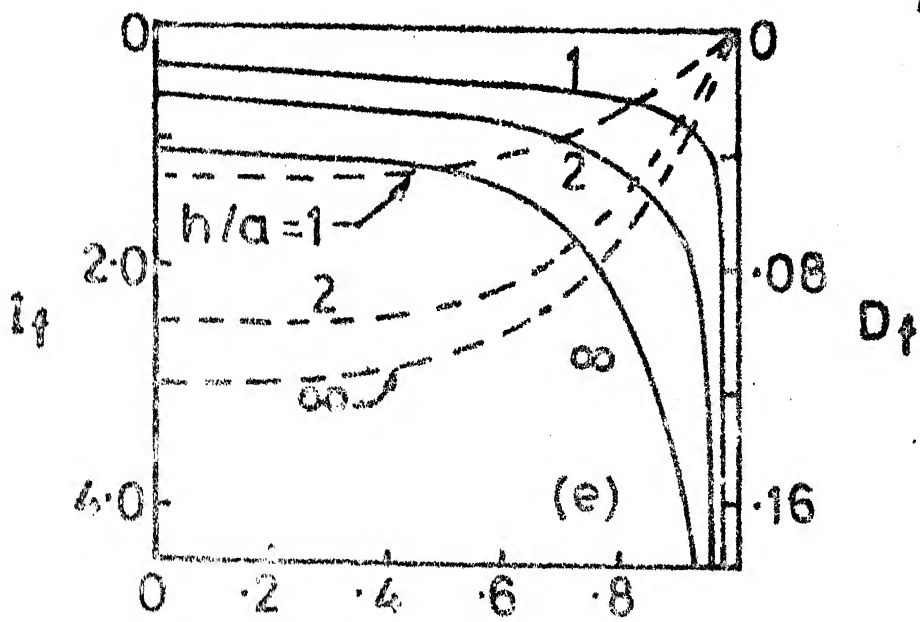


FIG. 4.12 DESIGN CHARTS FOR SETTLEMENT
INFLUENCE FACTOR AND DIFFERENTIAL
DEFLECTION FACTOR FOR UNIFORMLY
LOADED RING FOOTING
(c) $K=10, n=8$ (d) $K=1, n=0$


 q_{av}/q_y

— I_f - - - D_f

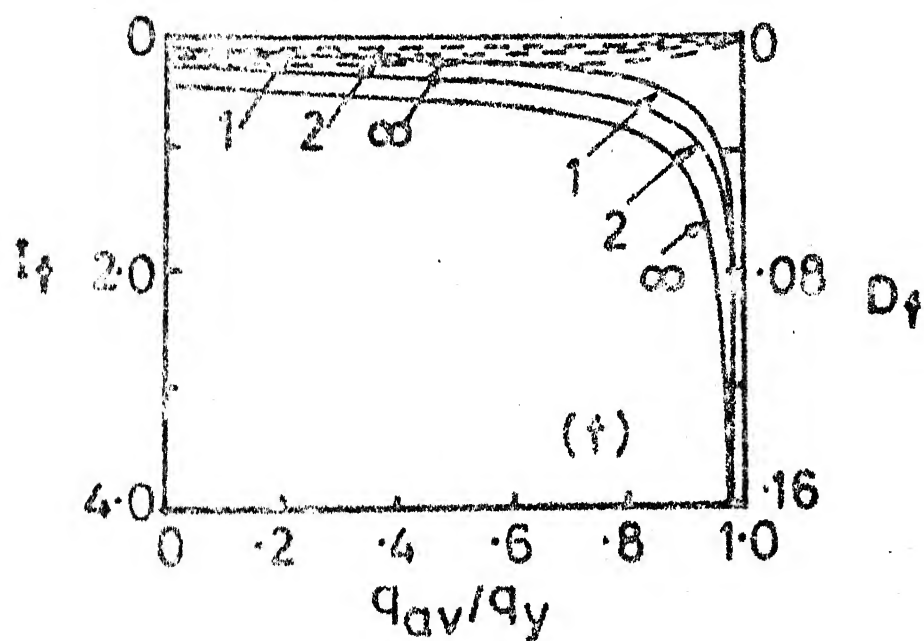


FIG. 6.12 DESIGN CHARTS FOR SETTLEMENT INFLUENCE FACTOR AND DIFFERENTIAL DEFLECTION FACTOR FOR UNIFORMLY LOADED RING FOOTING
 (e) $K=1, n=0.4$ (f) $K=1, n=0.8$

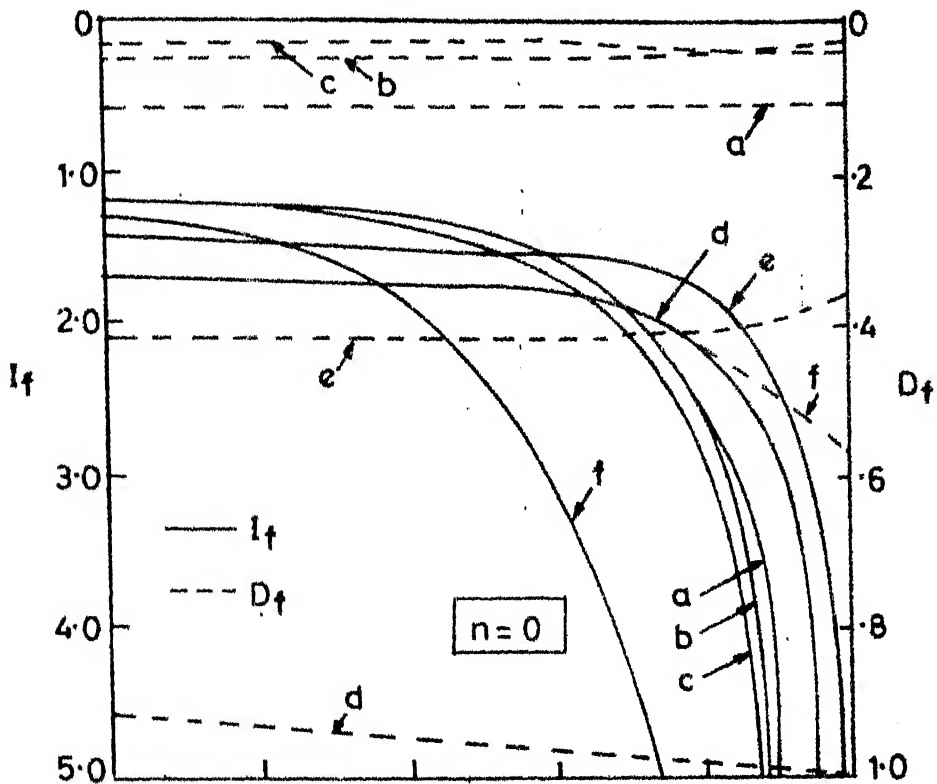


FIG.4.13 MAXIMUM SETTLEMENT FACTOR AND DIFFERENTIAL DEFLECTION FACTOR FOR VARIOUS LOADINGS ON FOOTING ON SEMI-INFINITE SOIL

Loading on one nineth width

Inner edge-a,d ; Centre of width-b,e

Outer edge-c,f; $K=10$ for a,b,c ; $K=1$ or d,e,f

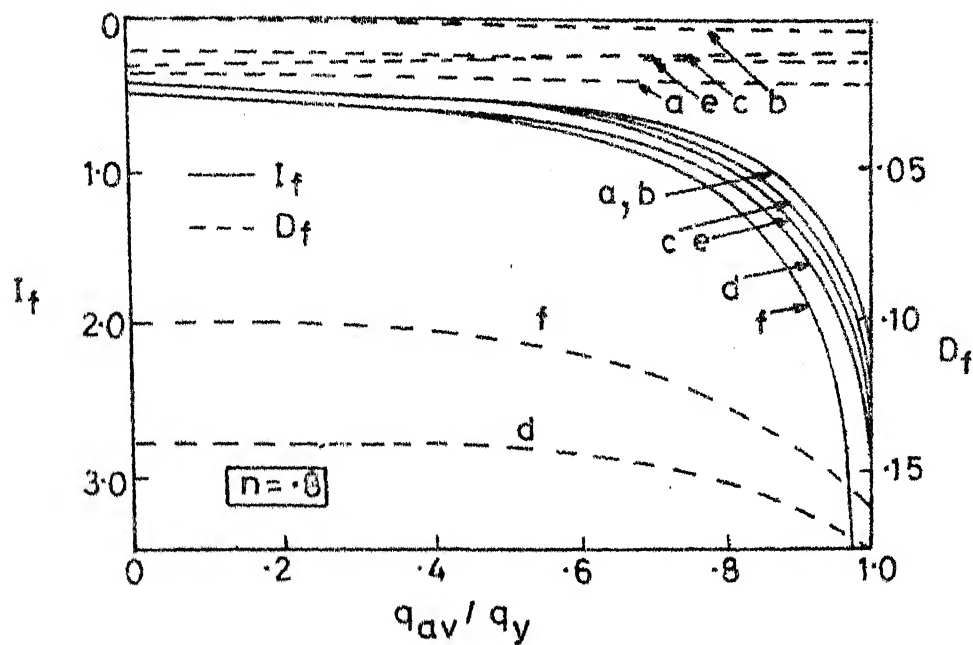


FIG. 4.14 MAXIMUM SETTLEMENT FACTOR AND DIFFERENTIAL DEFLECTION FACTOR FOR VARIOUS LOADINGS ON FOOTING ON SEMI-INFINITE SOIL

Loading on one-nineth width :

Inner edge-a,d; Centre of width-b,e

Outer edge-c,f ; K=10 for a,b,c ; K=1 for d,e,f

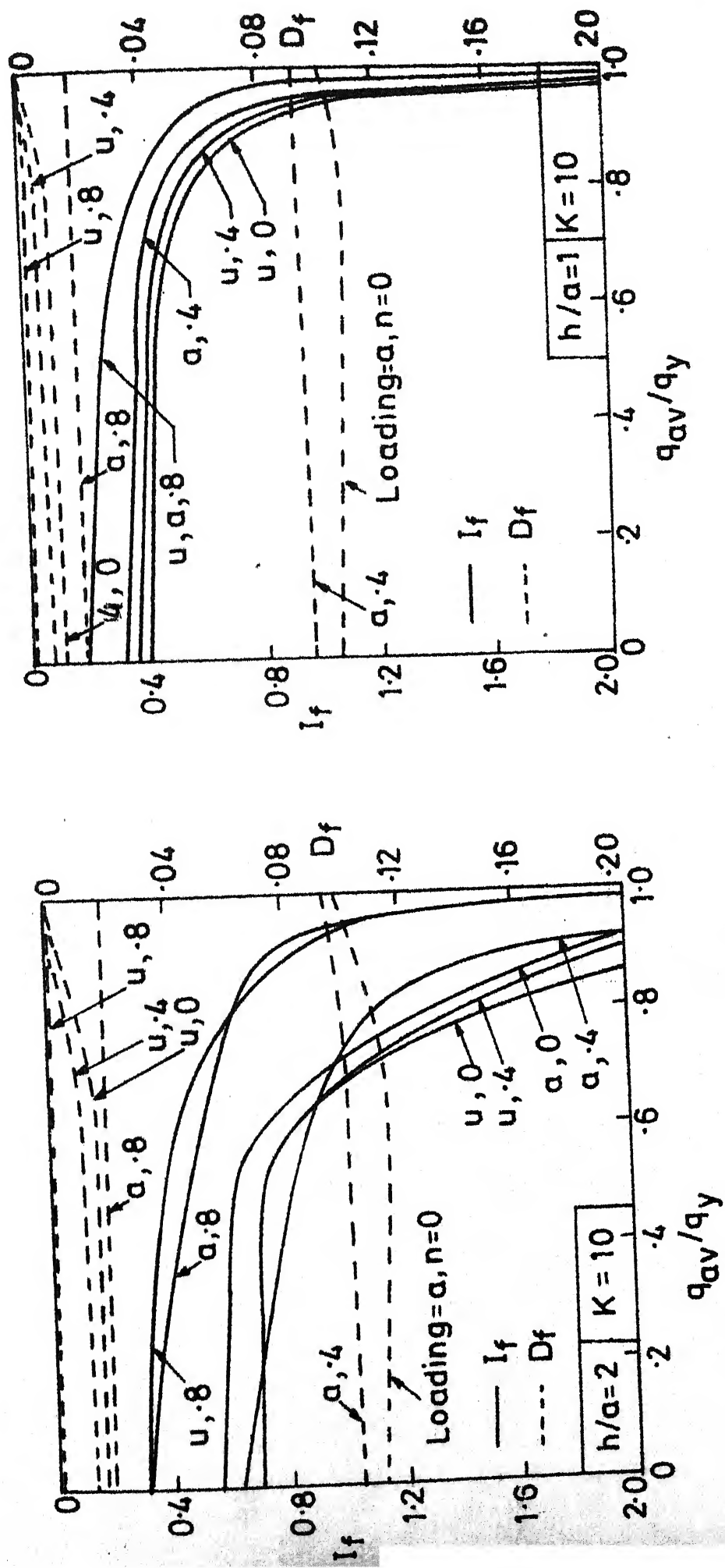


FIG. 4.15 SETTLEMENT CURVES FOR FOOTING RESTING ON SOIL OF FINITE DEPTH ($K = 10$)

u - Uniformly distributed load
 α - One-nineth width at inner edge loaded

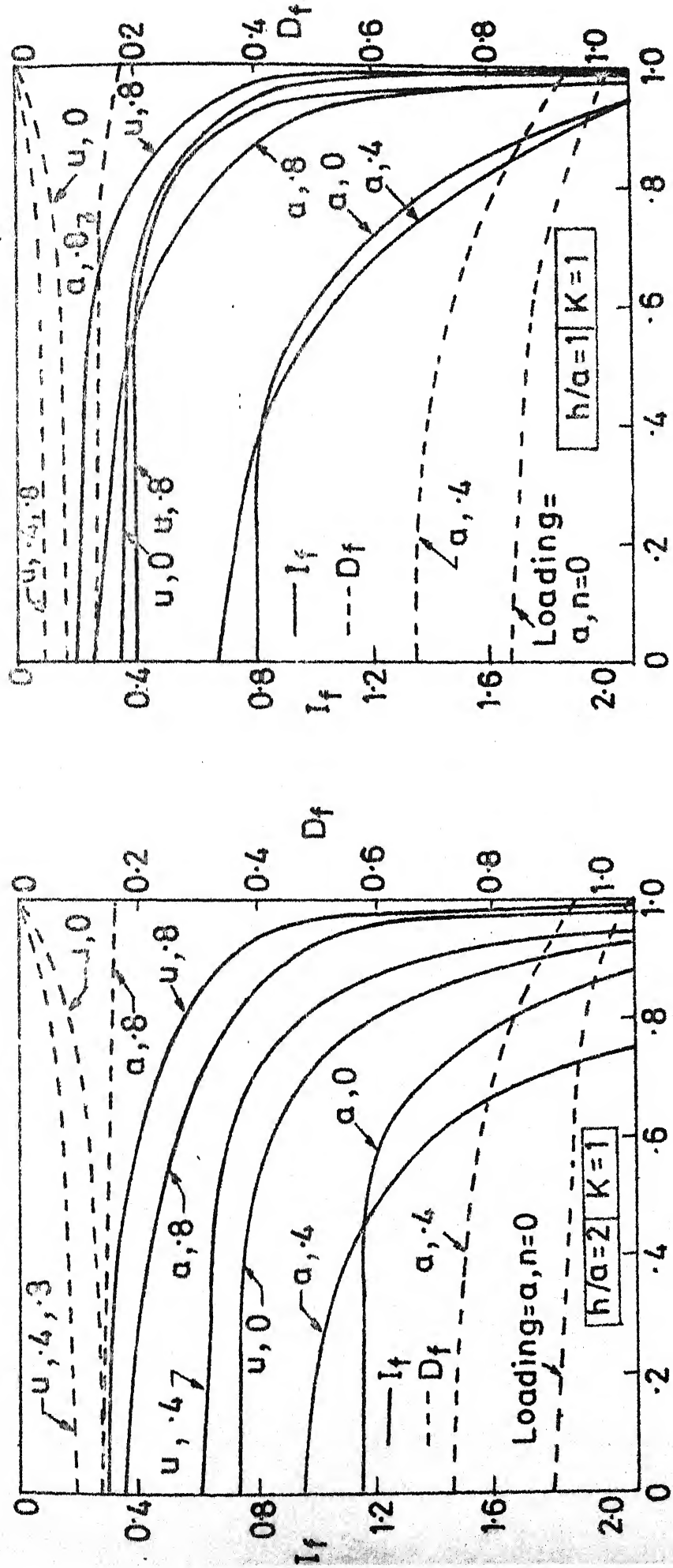


FIG.4.16 SETTLEMENT CURVES FOR FOOTING RESTING ON SOIL OF FINITE DEPTH (K=1)

U - Uniformly distributed load
 a - One ninth width at inner edge loaded

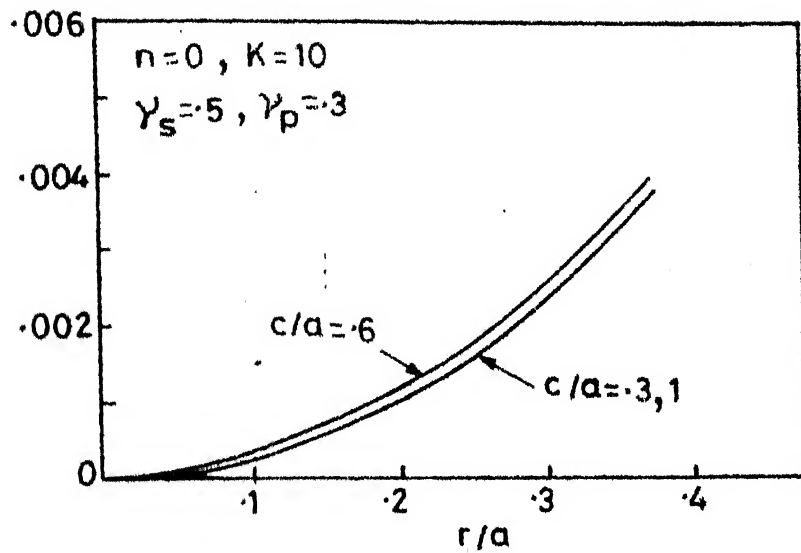
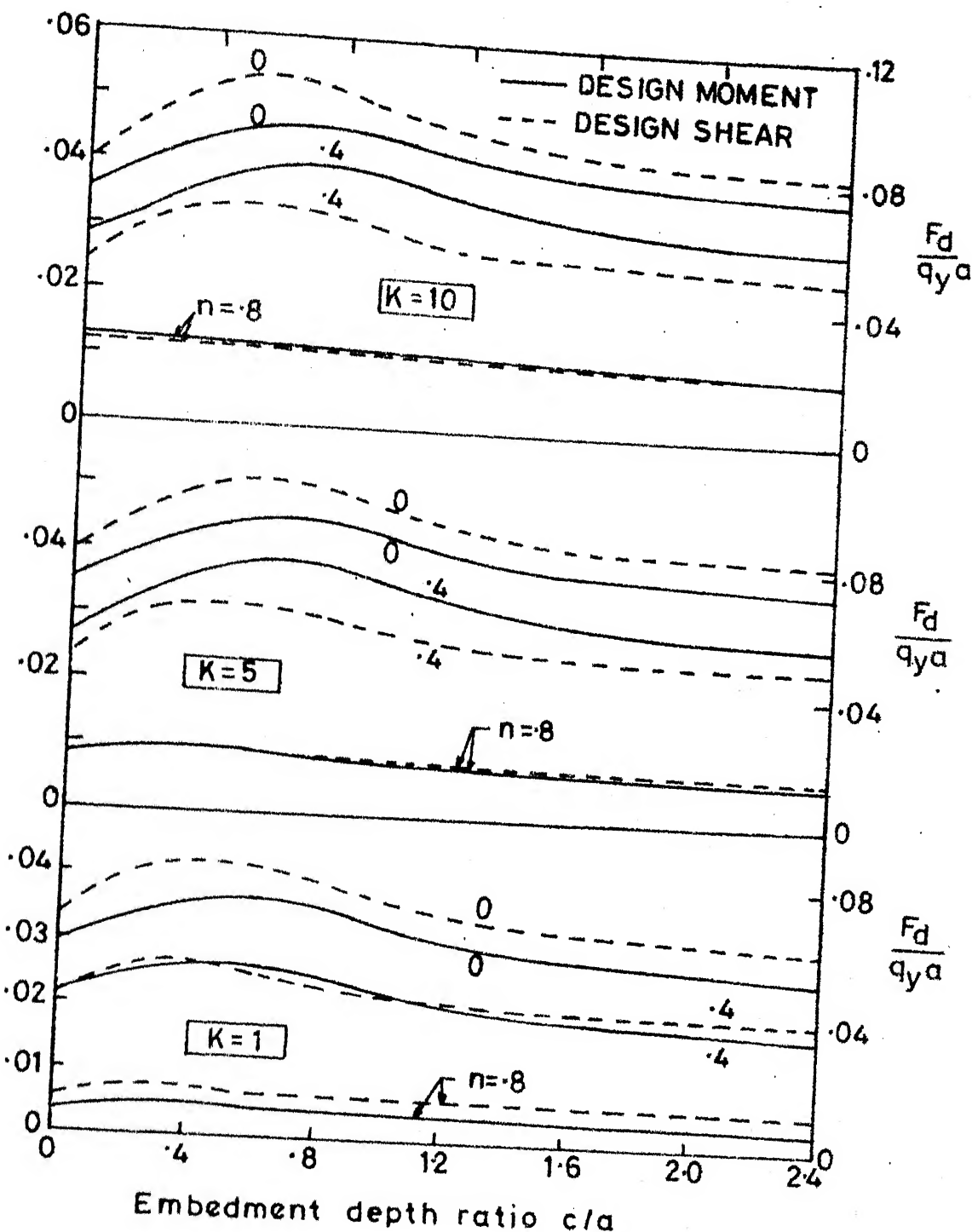


FIG. 4.17 SETTLEMENT OF EMBEDDED CIRCULAR
UNIFORMLY LOADED FOOTING RELATIVE
TO CENTRE OF FOOTING
(r = distance from the centre)



4.18 VARIATION OF DESIGN MOMENT AND SHEAR WITH DEPTH OF EMBEDMENT FOR UNIFORMLY LOADED FOOTING

CHAPTER 5

ELASTO-PLASTIC ANALYSIS OF CENTRALLY LOADED PILED RIGID ANNULAR FOOTINGS

5.1 INTRODUCTION

In the design of the foundation for a heavy structure on a deep deposit of clay or for a medium structure on a deep deposit of soft clay, it may be found that excessive settlement and not bearing capacity failure is the deciding design criterian. In order to restrict the settlement it is advisable to provide a few short piles. In such cases, traditionally the piles are designed to carry all the load, which is not logical. In fact in the pile-raft system, the aim is to take best advantage of the load bearing capacity of the raft and the settlement restricting capacity of piles. An integrated analysis, taking into account the load sharing between the raft and piles and the extent of plastic yield in each component of the system at all load levels, is justified for predicting the behaviour of the system.

Pile raft foundations have been reported (Poulos and Davis, 1977) to have been successfully used in Mexico (Zeevaert, 1957), and London (Hooper, 1973).

A brief description of the various approaches used for analysing the pile-raft systems has been given by Poulos and Davis (1980), which includes the comparative study made by Brown et al. (1975). The method of 'Plate on piles and continuum' (Hain, 1975) was assumed by Brown et al. (1975) as reference solution since it involved the least approximation and the elasticity based method by Poulos and Davis was reported to be comparatively the most satisfactory from settlement point of view among the methods considered (which excluded finite-element analyses). In simplified finite element analyses (Hooper, 1973, Desai et al. 1974), the piles have been replaced, in an approximately axially-symmetric problem, by an equivalent continuous annulus. However, choosing an appropriate stiffness for the annulus simulating the piles is difficult. A complete three-dimensional analysis can give a satisfactory solution, but the cost involved, if a generalised or parametric study is aimed at would be definitely prohibitive. A method which considers the interaction at all load levels between piles, raft and soil; the nature and extent of plastic yield at all the contact points; is able to predict directly the load settlement behaviour throughout the entire load range upto failure and which is not computationally expensive, is therefore needed. An attempt is made in this study to develope

such a method, although some assumptions are made regarding the rigidity of the raft and piles.

For a proper load transfer from above the footing to the piles, it is necessary and advantageous to have the footing of relatively high rigidity. If the footing is quite flexible, a load, if it is located above a pile, will not be shared by the footing and if it is not above the pile, it will not be transmitted to the pile. In this study, therefore, the footing is idealised to be fully rigid. Also, relative to the heavy loading and/or soft soil for which the pile-raft combination is intended, the piles can also be treated, in the first instance, as rigid. Hence the piles are assumed incompressible. If necessary, corrections for compressibility of piles (and flexibility of footing) can be applied as outlined by Poulos and Davis (1980).

The advantage of annular footings over circular footing with regard to settlements is brought out in the earlier Chapters and if they are provided with even a small number of short piles, the settlement is likely to be reduced considerably. Hence piled annular footings are ideally suited for many heavy tower like structures. An integrated elasto-plastic analysis for piled annular footings is not available presently in literature. An integrated analysis becomes all the more necessary when the piles are

arranged in more than one concentric circle and would be having different loads and plastic slips.

Piled annular footings are expected also to exhibit excellent resistance to eccentric loading. However, this aspect has not been tackled in the present work.

Basically, numerical integration of available elastic solutions has been employed in this study. Hence the size of the problem, for the axisymmetric cases considered in this Chapter, in terms of size of matrix is equal to the number of annular rings in which the footing is discretized plus the number of elements in which dissimilar piles are discretized. Therefore the size of the problem still remains relatively small, and the computer programme developed for the purpose of this thesis can be used to analyse any specific case at a very low computational cost.

5.2 ASSUMPTIONS AND STATEMENT OF THE PROBLEM

5.2.1 Assumptions

In addition to all the assumptions contained in Section 3.2.1 (Chapter 3), the following assumptions are also made for the purpose of the study in this Chapter.

- (1) The soil is semi-infinite in extent.
- (2) The raft rests on the piles and the surface of the soil and is perfectly rigid and smooth.

147

- (3) The piles are incompressible.
- (4) The pile-raft system and the loading form an axisymmetric arrangement.
- (5) The shear strength of the soil is constant with depth.
- (6) The inclusion effect of piles is neglected.
- (7) Displacement compatibility is satisfied only in the vertical direction.

5.2.2 Statement of the Problem

A rigid ring footing of external radius 'a' and internal radius 'na' rests simply on incompressible piles and on the surface of a semi-infinite soil mass (Fig. 5.1). The pile-raft system and the central loading form an axisymmetric arrangement. All the piles in a system are assumed, for the sake of simplicity, to have the same size (Length = L, diameter = d).

5.3 ANALYSIS

5.3.1 General

In addition to the discretization of the footing, the piles are also discretized (Fig. 5.2(a)). Each pile is divided into a suitable number of elements of equal length plus an element representing the base of the pile.

The vertical displacement of an element i due to contact pressure q_j on element j is expressed, as in Eq. 3.4, Chapter 3, by

$$\rho_{ij} = q_j a \frac{1-v^2}{E} I_{ij} \quad (5.1)$$

which, in the matrix form is written as (Eq. 3.5, Chapter 3)

$$\{\bar{\rho}\} = (1-v^2) [I] \{\bar{q}\} \quad (5.2)$$

where $\{\bar{\rho}\} = \frac{1}{a} \{\rho\}$ is the non-dimensional displacement vector, $\{\bar{q}\} = \frac{1}{E} \{q\}$ is the non-dimensional contact stress vector and $[I]$ is the influence coefficient matrix. $\{q\}$ includes contact pressures at the bottom of the footing, the stresses along the periphery of the piles and the stresses at the bases of the piles.

5.3.2 Influence Coefficients

The settlements or displacements of various elements are found out as below. The stress on an element is assumed to act as a concentrated force at the geometric centre of the element except for finding the influence of an element on itself in which case, the mathematically integrated formulae are used.

(a) Influence of footing elements on footing elements

Although Boussinesq's solution is applicable, Mindlin's solution with depth equated to zero is used for

the sake of generalisation (Poulos and Davis, 1974). In general, the settlement at a point in the soil mass due to a point load P (Fig. 5.2(b)) is given by

$$\rho_z = \frac{P(1+\nu)}{8\pi E(1-\nu)} \left(\frac{3-4\nu}{R_1} + \frac{8(1-\nu^2)-(3-4\nu)}{R_2} + \frac{(z-c)^2}{R_1^3} \right. \\ \left. + \frac{(3-4\nu)(z+c)^2-2cz}{R_2^3} + \frac{6cz(z+c)^2}{R_2^5} \right) \quad (5.3)$$

where z is the depth of the point under consideration below the surface, c is the depth of the point below the surface where the point load is acting and R_1 and R_2 are distances, as given below, in terms of c , z , and the horizontal distance between the two points under consideration, r (Fig. 5.2(b)).

$$R_1 = (r^2 + (z-c)^2)^{1/2} \quad | \\ R_2 = (r^2 + (z+c)^2)^{1/2} \quad | \\ P = q_j \times dA_j \quad | \quad (5.4)$$

where dA_j is the area of the element j .

For the particular case under consideration,

$$c = 0 \quad | \\ z = 0 \quad | \\ R_1 = R_2 = r \quad | \quad (5.5)$$

The influence coefficients are obtained by using Eq. 5.3 for various elements in the form of Eq. 5.1 and finally of Eq. 5.2.

For $i = j$, Eq. 5.3 is not valid and the Mindlin's solution integrated over a rectangular area is used assuming the small element to be rectangular. The settlement at the centre of the element is obtained using this solution (Poulos and Davis, 1974) as

$$\rho_{ij} = \frac{2q_j}{E} \times I \quad (5.6)$$

where

$$I = K_0 [K_1 \left(\beta \ln \frac{1+\sqrt{1+\beta^2}}{\beta} + \ln (\beta + \sqrt{1+\beta^2}) \right) + K_2 \left(\ln \frac{(\beta+t)}{\sqrt{1+4\alpha^2}\beta^2} + \beta \ln \frac{1+t}{\beta s} - 2\alpha\beta \tan^{-1} \left(\frac{1}{2\alpha\beta} \right) + 4\alpha\beta \tan^{-1} \frac{(1-s)(\beta s-t)}{2\alpha} \right) + 2\alpha\beta K_1 \tan^{-1} \left(\frac{1}{2\alpha t} \right) + \frac{8\alpha^4\beta t}{s^2(1+4\alpha^2t^2)} \times \left(2 + \frac{1}{4\alpha^2} - \frac{1}{t^2} \right)] \quad (5.7)$$

$$\text{where } K_0 = \frac{1+\nu}{8\pi(1-\nu)}$$

$$K_1 = 3-4\nu$$

$$K_2 = 5-12\nu + 8\nu^2$$

$$\alpha = 2c/y, \beta = y/x, s = \sqrt{1+4\alpha^2},$$

$$t = \sqrt{1+\beta^2 \cdot (1+4\alpha^2)} \quad (5.8)$$

where x and y are the lengths of shorter and longer sides of the rectangular area respectively.

(b) Influence of footing element on pile element

For the whole pile-raft system, it is rational to consider the centre of a pile element as the centre of the cylindrical element of the pile. Eqs. 5.3 and 5.4 are used in which, for the particular case under consideration,

$$c = 0$$

z = depth of centre of pile element,

r = horizontal distance between centre of the footing element and the centre of pile.

(c) Influence of pile element on element of another pile

Eqs. 5.3 and 5.4 are used in which, for the particular case under consideration,

z = depth of centre of pile element on which influence is being found out,

c = depth of centre of pile element whose influence is being found out,

r = horizontal distance between centres of piles

$dA = \pi d \cdot dL$ where

d = diameter of pile and

dL = length (height) of pile element,

$dA = \pi d^2/4$, for the base element.

(d) Influence of pile element on footing element

Eqs. 5.3 and 5.4 are used in which, for the particular case under consideration,

$$z = 0$$

c = depth of centre of pile element,

r = horizontal distance between centres of pile and footing elements

$dA = \pi d \cdot dL$ as in (c) above

$dA = \pi d^2/4$ for tip element of pile.

(e) Influence of pile element (other than base) on pile element of the same pile

For this case, the pile element surface is divided into subelements (Fig. 5.2(c)) and the concentrated force on the subelements has been integrated mathematically to get the influence of the pile element on an another element of the same pile, as

$$\begin{aligned} p_{ij} &= \frac{(1+v)q_j d}{8E(1-v)} \left[8(1-v)^2 \ln \tan\left(\frac{\beta}{2} + \frac{\pi}{4}\right) \right. \\ &\quad - 4(1-v) \ln \tan\left(\frac{\alpha}{2} + \frac{\pi}{4}\right) + \sin \alpha \\ &\quad - (3-4v) \sin \beta - \frac{4z}{d} \cos \beta \\ &\quad \left. - \frac{4z}{d} \sin^2 \beta \cos \beta + \frac{8z^2}{d^2} \sin \beta \cos^2 \beta \right]_{c_1}^{c_2} \end{aligned} \quad (5.9)$$

$$\text{where } \alpha = \tan^{-1} \frac{2(z-c)}{d}, \quad \beta = \tan^{-1} \frac{2(z+c)}{d},$$

$$c_1 = c - \frac{dL}{2}, \quad c_2 = c + \frac{dL}{2},$$

z = depth of centre of pile element on which influence is being found out,

c and dL are depth to centre and length (height) of pile element whose influence is being found out respectively.

(f) Influence of base element of pile on an element of the same pile

For this case, the base element circle is divided into subelements (Fig. 5.2(d)) and the concentrated force on the subelement has been integrated mathematically to get the influence as

$$\rho_{ij} = \frac{(1+\nu) q_j}{4E(1-\nu)} \left[(3-4\nu) \sqrt{A} + 8(1-\nu)^2 \sqrt{B} - (3-4\nu) \sqrt{B} - (z-c)^2 / \sqrt{A} - (3-4\nu) (z+c)^2 / \sqrt{B} + 2cz / \sqrt{B} - 2cz(c+z)^2 B^{-3/2} \right]_0^{d/2} \quad (5.10)$$

$$\text{where } A = (c-z)^2 + r^2$$

$$B = (c+z)^2 + r^2$$

$r = d/2$ for the upper limit

$r = 0$ for the lower limit

c = depth of pile base below surface = L = length of pile

z = depth of centre of pile element on which influence is being found out.

(g) Influence of base of pile on itself

This is obtained by using the same formula derived in Section 5.3.1 (f) with $z = c = L$, but multiplying by the factor $\pi/4$ to account for the rigidity of the base assuming that this factor true for surface area is approximately applicable for embedded area also (Poulos, 1977).

5.3.3 Final Form of Equations to be Solved

Since the footing is assumed as rigid and the piles as incompressible, the settlement will be equal to say, r_0 . Hence Eq. 5.2 can be written as

$$\bar{\rho}_0 \{U\} = (1 - v^2) [I] \{\bar{q}\} \quad (5.11)$$

where $\bar{\rho}_0 = \rho_0/a$ and $\{U\}$ is unit vector.

For overall equilibrium,

$$\sum q_j dA_j = Q \quad (5.12)$$

where Q is the external load and the summation is taken over all the elements of the footing and the piles.

5.3.4 Elastic Case

Equations 5.11 and 5.12 can now be solved to obtain unknown stresses $\{\bar{q}\}$ as well as $\bar{\rho}_0$.

5.3.5 Elasto-Plastic Case

Even under very small load, the contact pressures near the edges of the footing and the tips of the pile may

reach a very high value giving rise to yielding of the soil. Under higher loads, more and more soil elements yield and as per the assumption made, the stress is to be held at the yield value of the soil, for such elements.

In case of a pile-raft system, the yield value of the soil for the footing and the pile will be different. In the present study, the yield stress along the pile is assumed to remain constant. The yield stresses are as below .

- (a) For the footing $q_{yf} = 5.69 c_u$
- (b) For the pile shaft $q_{ys} = \alpha c_u = \frac{q_{yf}}{5.69}$ for $\alpha = 1.0$
- (c) For the pile base $q_{yb} = 9 c_u = \frac{9 q_{yf}}{5.69}$.

Under increasing load, as soon as the value of stress at any element reaches the corresponding yield value as given above, it is held constant at that value and partitioning and partial inversion of modified influence matrix is done as given in Chapter 3.

The settlement is expressed in the following form

$$\delta_o = \frac{Q}{d \cdot E} I_p \quad (5.13)$$

where I_p is the settlement influence factor for the pile-raft, Q is the total load on the system and d is the diameter of a reference pile.

A quantity of particular interest is the load sharing between the footing and the various sets of piles. A set of piles for this purpose is one having piles that carry equal loads due to their concentric placement and such a set will be denoted as a 'pile-ring'.

The piles in different rings will not only carry different loads, but they will be at different stages of failure under any load. Therefore interaction factors found out on the basis of equal loads on two piles are not applicable. Hence for a more rigorous analysis an integrated pile-raft analysis is necessary and the same is adopted in this work.

5.4 RESULTS AND DISCUSSION

5.4.1 General

For a combined pile raft system, the load level is indicated rationally by the ratio of total load on the footing to the total ultimate load, Q_u (and not by q_{av}/q_y as in case of footing alone). The ratio Q_y/Q indicates overall factor of safety.

Q_u calculated on the basis of yield-stress being reached at all the points of contact between the soil and the pile-raft system is given by

$$Q_u = \pi A' q_{yf} + m\pi dL q_{ys} + m\pi d^2 q_{yb}/4 \quad (5.14)$$

where m is the number of piles, A' is the net area of the footing ($A' = A - m\pi d^2/4$), q_{yf} , q_{ys} and q_{yb} are yield stresses as defined in Section 5.3.5 and A is the area of the footing.

Although the computer programme developed in this thesis allows for unequal diameters and lengths of piles, the diameter and length of all the piles in a system are assumed, for the purpose of simplicity, as equal.

The load shared by a pile ring expressed as a percentage of the total load is denoted by 'p'. The value of p is assumed as .5 throughout.

It was sufficient to divide the pile into a small number of elements (Poulos and Davis, 1977). Depending on the length, each pile was divided into 5 to 20 elements.

5.4.2 Single Floating Pile in Semi-Infinite Soil

Some results have been obtained for the purpose of studying the settlement response of piles under various load levels upto failure. Fig. 5.3 shows the case of a single pile, the load-settlement curves for which are drawn as $P/c_u d^2$ versus $\phi E/c_u d$, where P is the load on the pile, c_u is the ultimate shaft resistance (assuming $\alpha = 1$) and d is the diameter of the pile. It can be seen that,

- (i) The load-settlement curves are almost linear upto about 55 percent, 68 percent and 75 percent

of ultimate load for L/d values of 9.2, 18 and 25 respectively. Thus the linear-like response is over a larger range of load level for higher values of L/d .

(ii) Beyond the linear-like range, the curves become nonlinear at increasing rate as the load increases.

In Fig. 5.3, the load-settlement curves obtained from field tests for a stiff clay by O'Neill and Reese (1972) for two values of L/d are shown. For drawing these curves the values of E and c_u are obtained by back-figuring. It is assumed that the soil is semi-infinite in extent. A curve obtained from FEM (Desai, 1977) for the case of $L/d = 9.2$ is also shown in which the back-figured values for the corresponding field test are again used. These curves also show a high non-linearity beyond the initial linear portion, and a rapidly increasing settlement as failure is approached. A large number of field tests such as those by Whitaker and Cooke (1966) and Burland et al. (1966) show the same trend, although the tests are in different types of soils. Recently Boek Madsen and Lagoni (1981) have reported from a field test on pile in white chalk that the settlement varies in cubic proportion to the load. The present analysis gives results conforming to these trends and the agreement as seen from Fig. 5.3 with the results

from field test and from FEM, is satisfactory, thus validating the analysis. A load-settlement curve for $L/d = 25$ based on the method of Poulos and Davis (1980) is also shown in Fig. 5.3. It agrees well with the curve obtained from the present analysis upto a load level of about 76 percent of ultimate load.

5.4.3 Effect of Radius Ratio n on Settlement Response of Pile-Ring Footing System

Figure 5.4 shows the load settlement responses of three footings with $n = 0, .6$ and $.8$. The outer radii of the three footings are selected in such a way that the area of the footings for all the cases remains the same. Each of the footing is provided with a ring of piles consisting of six identical piles and hence the footings can be treated as equivalent systems. From Fig. 5.4 it can be seen that the settlement response improves with n under all load levels (denoted by Q/Q_u). For example for $Q/Q_u=.2$ the values of I_p (which indicates settlement) are about $.036$, $.029$ and $.025$ for $n=0, .6$ and $.8$ respectively and for $Q/Q_u=.5$, the values of I_p are about $.087$, $.068$ and $.05$ for $n=0, .6$ and $.8$ respectively; thus higher n being more advantageous for higher values of Q/Q_u . It is better to adopt a value of n as high as possible subject to considerations of availability of space in plan and structural design of

the ring. In the same figure (Fig. 5.4) , the settlement response expressed in terms of I_p for an equivalent footing with no piles has been shown; equivalence being attained by designing the unpiled footing also for the same total ultimate load Q_u as for piled footing. Even though a high value of n is chosen ($n=.8$), it is seen that the settlement of unpiled footing is much more than that of piled footing. For example, I_p for piled footing with $n=.8$ and six piles of diameter .15a and L/d value of 25 is about 19 percent of that of unpiled footing at $Q/Q_u=.2$, this percentage being about 33 percent at $Q/Q_u=.7$.

The percentage pile load (relative to total load on the system), p , is shown in Fig. 5.4 for three equivalent systems. It is seen that p is higher, at all load levels except at failure, for higher values of n . For example, at $Q/Q_u = .5$, p is about 50 percent for $n = 0$ and about 63 percent for $n=.8$. Thus for higher values of n , the participation and utilization of piles is better. It is also seen that in comparison to working load range, the pile load would be overestimated if based on elastic analysis and underestimated if based on failure load. In any case it is illogical to design the piles for the entire load.

5.4.4 Effect of Positioning of Pile-Ring

Figure 5.5 shows the effect of positioning a pile ring, on the settlement (indicated by L_p) and the load shared by piles (indicated as percentage p) for two cases of n ($n=0$ and $.5$). For $n = 0$ case, d the diameter of pile is $0.075 a$ and there are 6 piles with $L/d = 25$. For $n=.5$ case, $d = .075 a$ and there are 6 piles with $L/d = 30$. The position of pile ring is defined by 's', (Fig.5.1), such that

$$\begin{aligned} s &= \frac{\text{Radius of pile ring - Inner radius of ring}}{\text{Width of ring} (= \text{outer radius - inner radius})} \\ &= \frac{r_p - na}{(1-n) a} \end{aligned} \quad (5.15)$$

The settlement of the system (Fig. 5.5) in the lower range of load level (Q/Q_u) is a little lower for higher value of s but in the higher range of Q/Q_u , it is lower for smaller value of s (Pile-ring near inner edge). This difference in settlements for various values of s, is very low for higher values of n except near failure.

The minimum settlement in the range of Q/Q_u values greater than $.25$ occurs roughly for $s = .75$ and $.5$ for $n=0$ and $.5$ respectively. It can be said that if the pile ring is placed at a position dividing the footing area inside and outside into equal regions, minimum settlement is obtained (although p is not a maximum). For narrow ring

footings the pile ring can be placed at the centre of width of ring. This would be advantageous from the point of view of positioning the load also near the centre of the width and causing minimum design bending moment and shear in the footing.

In the same Figure (Fig. 5.5), the values of p (percentage load shared by piles) are plotted for the case of $n=5$, for 3 values of s ($s=.1, .5$ and $.9$). These curves join together at failure but at low values of Q/Q_u the difference is considerable for various values of s . For example, at $Q/Q_u=.3$, p values are about 42 percent, 50 percent and 59 percent for $s = .1, .5$ and $.9$ respectively. However the settlements at this Q/Q_u are almost same for 3 values of s . It appears that the load sharing between the piles and the footing and the distribution of contact stresses in various cases produce some balancing effects on settlement for various values of s .

5.4.5 Combined Effect of Length and Number of Piles in

Nearly Equivalent Systems

One can think of alternative systems of piled ring footings, keeping the size of the footing, the diameter of piles and the number of piles times L/d the same. Such systems will be nearly equivalent since their ultimate load bearing capacity will be approximately equal.

Figure 5.6 shows the load settlement response of two sets of such systems. For the sake of general comparison the dominance or otherwise of piles can be represented by percentage pile load at failure, denoted by p_f . The values of p_f are about 76 percent and 4.6 percent for the $n=.8$ systems and $n=.5$ systems respectively. For lower value of p_f , the settlement response for the two equivalent systems ($L/d = 10$, 3 piles and $L/d=5$, 6 piles) is almost identical, whereas for the higher value of p_f , the I_p for $L/d = 40$, and 3 piles is lower than that for $L/d = 20$ and 6 piles, being about 67 percent at $Q/Q_u = .3$ and 50 percent at $Q/Q_u=.7$. Since the cost of piles per unit length increases with increasing depth, a cost analysis will be required to decide which of the equivalent alternatives is economical in the long run for the sets of equivalent systems having high pile loads. For lower values of pile load one can say that it would be preferable to use an equivalent alternative having more number of shorter piles than having less number of longer piles provided the piles are not very near to each other.

5.4.6 Ring Footing with Two or More Pile Rows (Rings)

It may be necessary to provide piles in 2 or more rows if the number of piles desired to be provided is large causing too less spacing between piles. It may also be

convenient to provide the piles in more than one row even though they could be accommodated in a single ring. The piles in different rings will carry different loads and will be at different stages of failure.

Figure 5.7 shows the effect of positioning piles in two rows. The pile radius is $.06a$ where a is the outer radius of the footing. For each system, there are 12 piles with $L/d = 5$. The three systems are equivalent. From this figure it is seen that the best positioning of the two pile rings (rows) is at the inner and outer edge. In the same figure, the response for 3 pile rings with 4 piles each, two being placed near the edges and one at the centre of width (in staggered angular location) is shown. It shows that this arrangement is, in an overall way, better than that of placing 2 pile rings, with 6 piles each, near the edges.

Some of the values of load carried by piles are given in Table 5.1 for the above cases.

From the Table 5.1 , it can be seen that, the load shared by the pile ring near the inner edge is less and that for pile ring near the outer edge is more in all the cases, except at failure.

TABLE 5.1 : LOAD SHARING BY PILE RINGS

System Number	Pile-Ring Position	No. of Piles in the Ring	s	Load Shared(Percentage of total load)		
				At $Q/Q_u = .2$	At $Q/Q_u = .67$	At $Q/Q_u = 1$
1	Outer	6	.9	28.5	19.1	13.5
	Centre		.5	17.5	16.9	13.5
2	Outer	6	.9	29.5	19.3	13.5
	Inner		.1	14.5	15.7	13.5
3	Centre	6	.5	18.8	17.0	13.5
	Inner		.1	14.2	15.0	13.5
4	Outer	4	.9	19.0	17.0	9.0
	Centre		.5	11.8	11.8	9.0
	Inner		.1	7.8	8.2	9.0

Provision of more pile rings with staggered arrangement is the best arrangement.

5.5 CONCLUSIONS

- (1) An integrated elasto-plastic analysis of a rigid ring footing supplemented by incompressible piles in one or more annular rows or rings, is presented.
- (2) Providing even a few short piles below a footing reduces the settlements considerably. The benefit of the use

of the combination of advantages of the piles and the raft will be lost if either of the component dominates.

- (3) It is highly advantageous to increase n (keeping the area same) of a piled ring footing.
- (4) To provide more number of short piles or less number of long piles (keeping number of piles $\times L/d = \text{constant}$) makes little difference from settlement point of view unless the piles share a high percentage of load (more than about 50 percent). Hence the former alternative may be preferable. For pile dominating systems a cost analysis will be necessary.
- (5) It is preferable, from the point of view of overall settlement response, to place the piles in as many number of pile rings as possible (subject to possibility of accommodating in the width of ring footing). In such cases, angular staggering of piles in various rings is essential.
- (6) Charts for settlement response as provided in the present study can be used for the purpose of design.

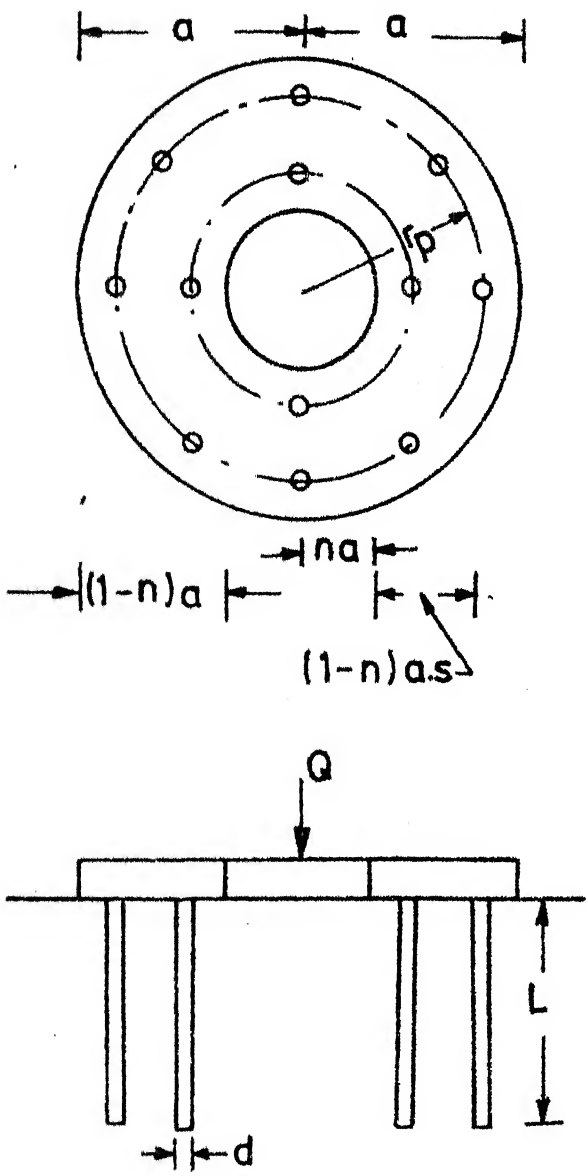
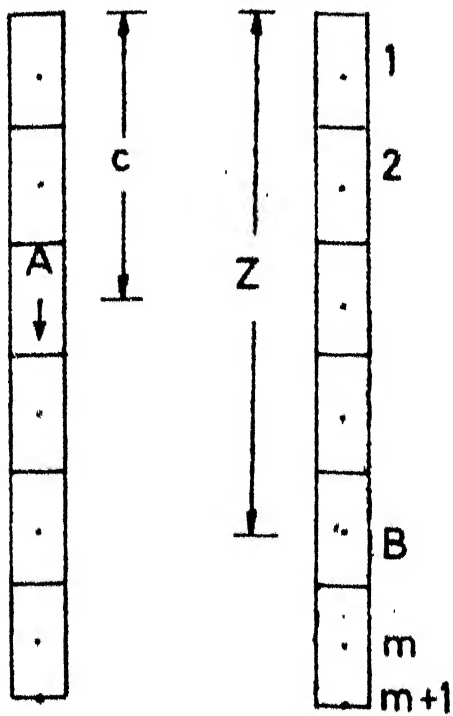
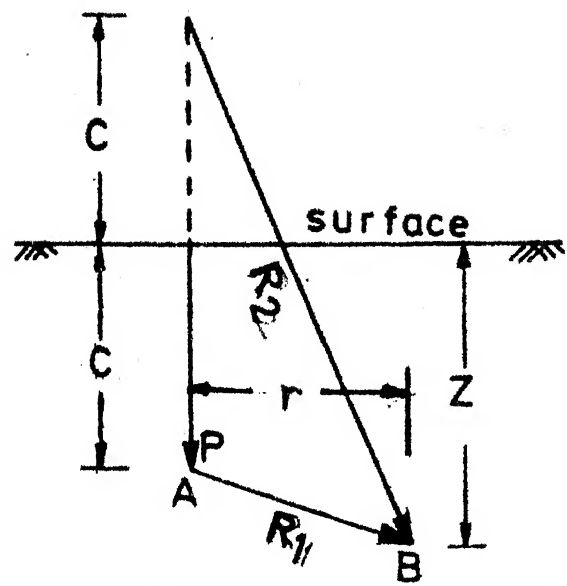


FIG.5.1 DEFINITION SKETCH OF PILED RIGID RING FOOTING

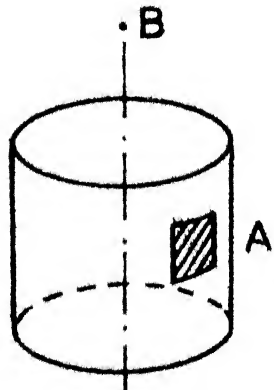


(a) PILE DISCRETIZATION

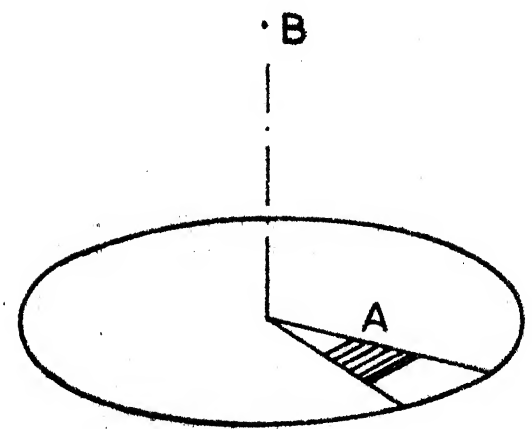


A - Point where load acts
 B - Point where settlement is found out

(b) MINDLIN PROBLEM



(c) INFLUENCE OF PILE ELEMENT ON ELEMENT OF SAME PILE



(d) INFLUENCE OF BASE ELEMENT OF SAME PILE

FIG. 5.2 APPLICATION OF MINDLIN'S SOLUTION

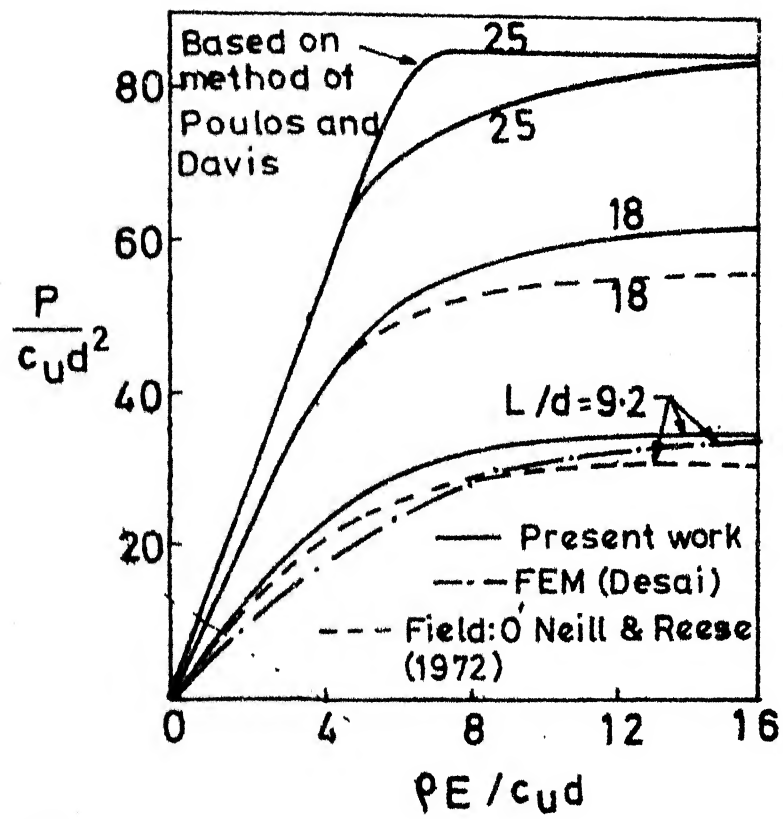


FIG. 5.3 LOAD SETTLEMENT RESPONSE FOR SINGLE FLOATING PILE

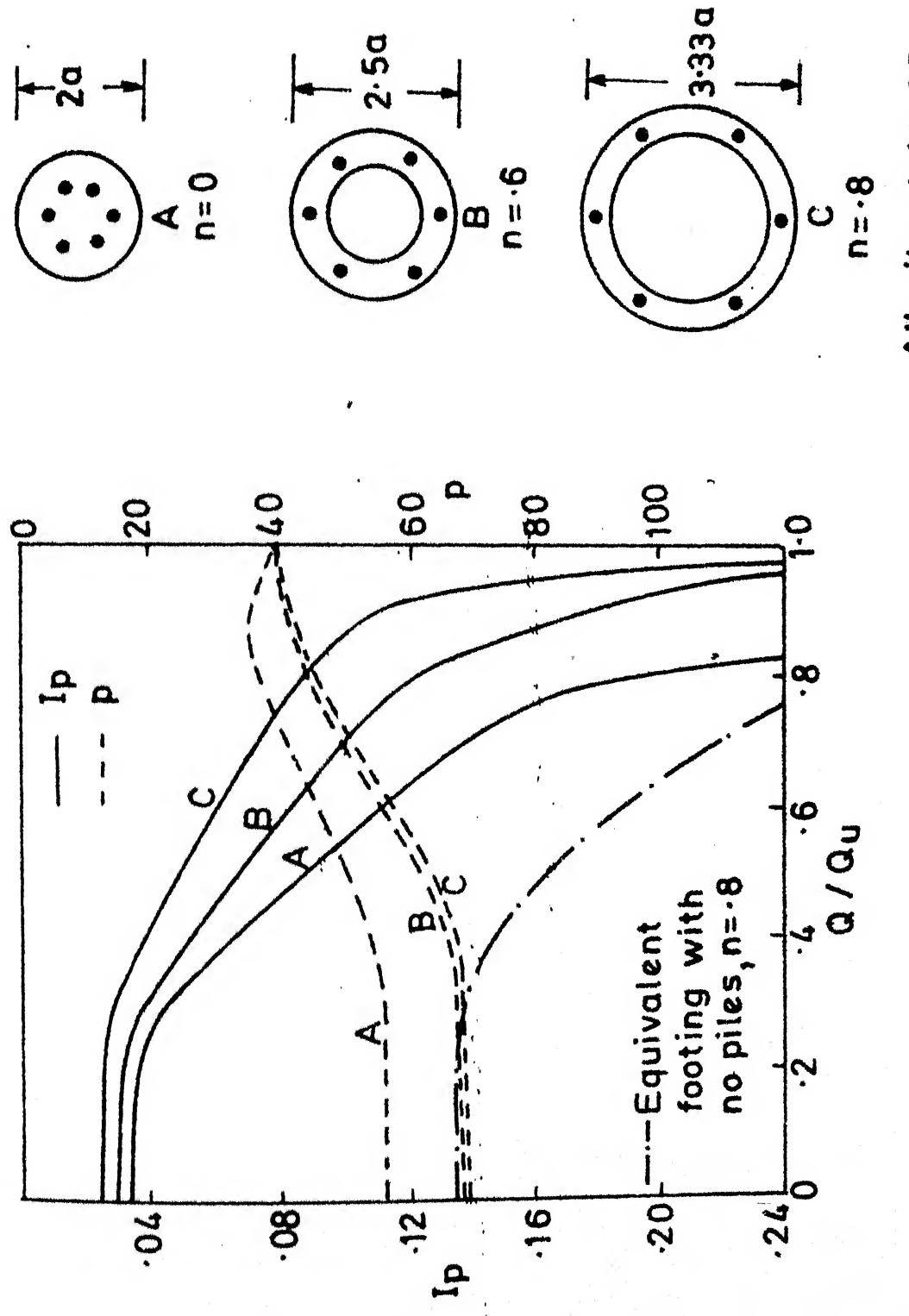
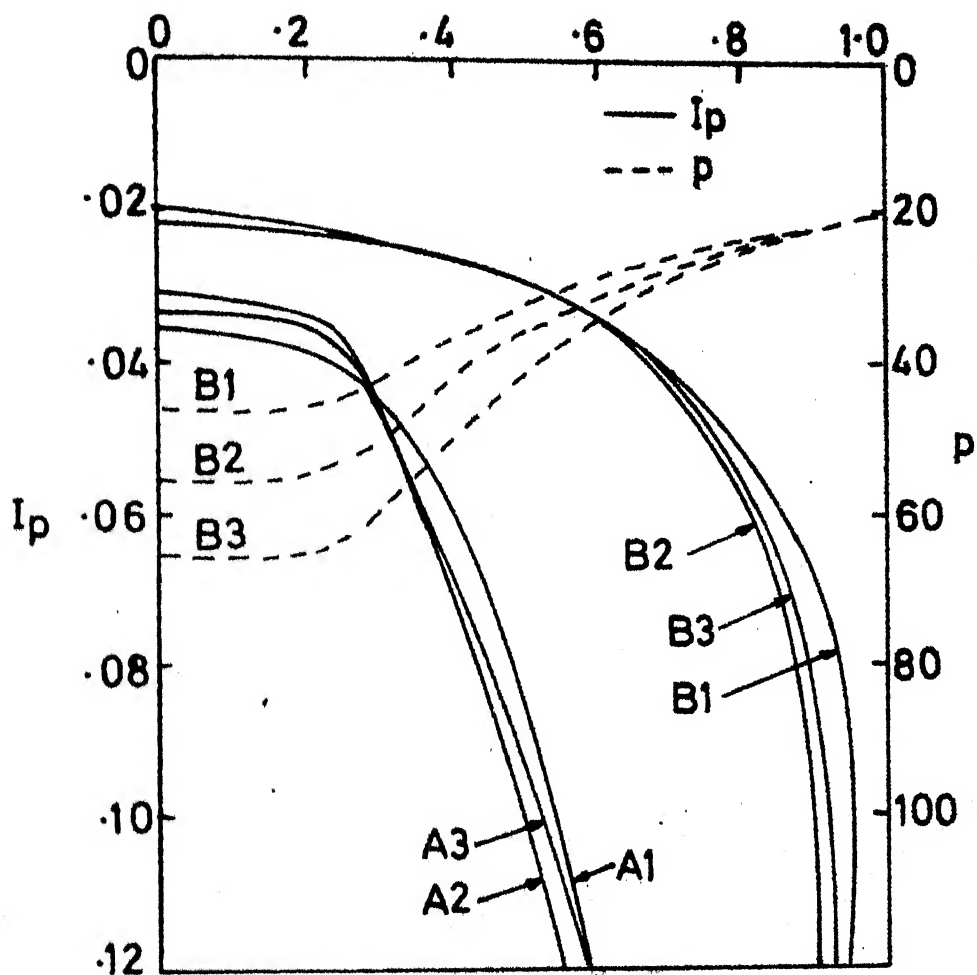


FIG. 5-4 SETTLEMENT FACTOR AND PERCENTAGE PILE LOAD FOR EQUIVALENT PILE RAFT SYSTEMS



$A_1 - n=0, S=.5$	6 Piles $d=.025a$ $L/d=25$
$A_2 - n=0, S=.75$	
$A_3 - n=0, S=.875$	
$B_1 - n=5, S=.1$	6 Piles $d=.075a$ $L/d=30$
$B_2 - n=5, S=.5$	
$B_3 - n=5, S=.9$	

FIG. 5.5 EFFECT OF POSITIONING OF PILE RING ON SETTLEMENT AND PILE LOAD SHARE

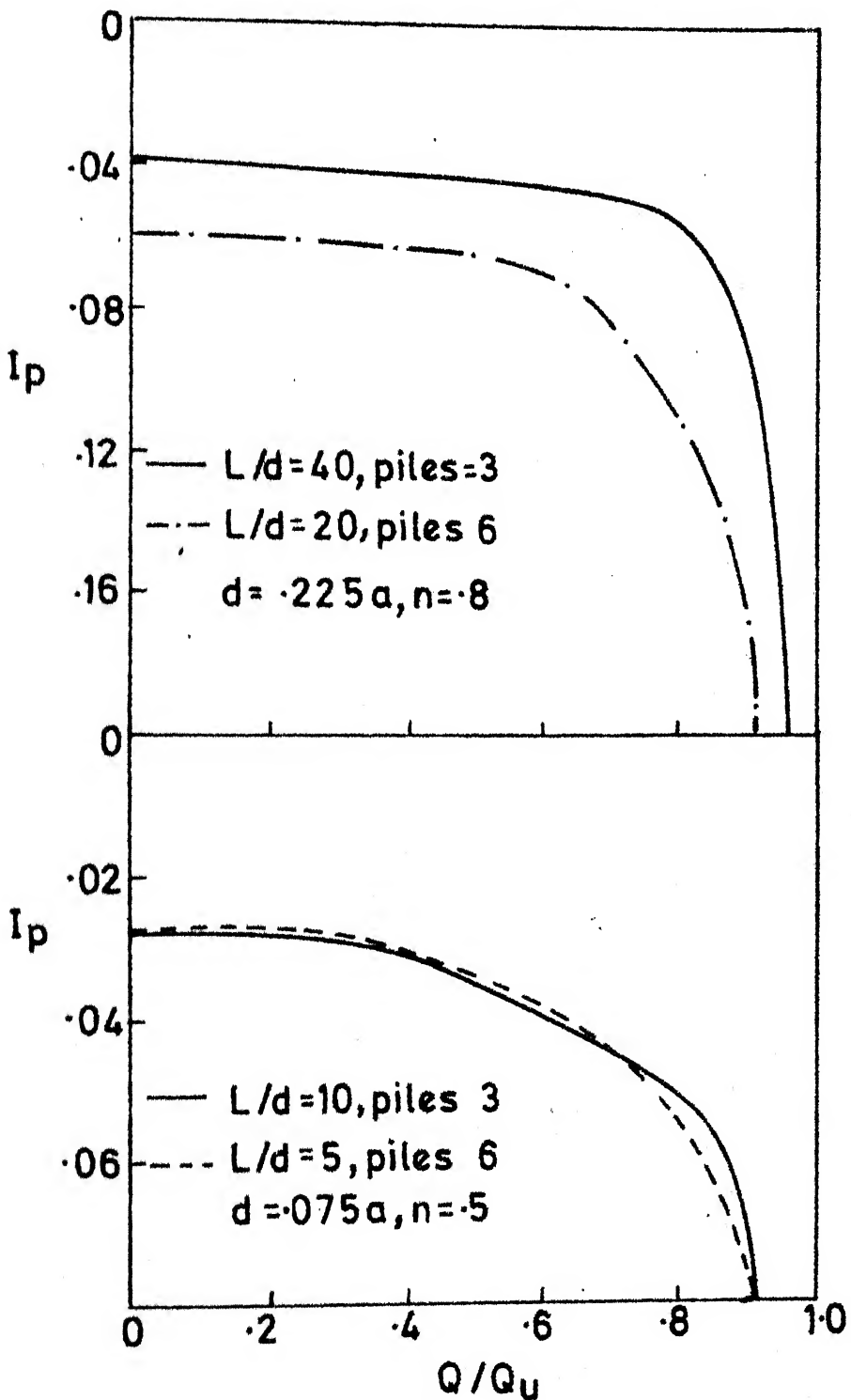


FIG.5·6 COMPARISON OF NEARLY EQUIVALENT SYSTEMS OF PILED RING FOOTINGS

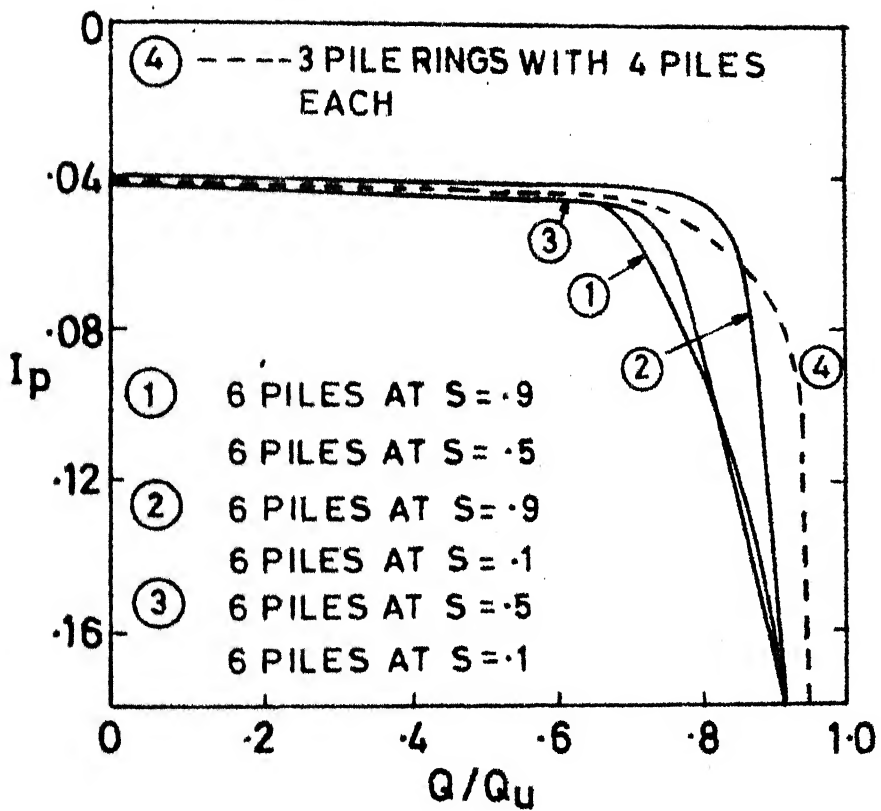


FIG.5.7 EFFECT OF POSITIONING OF PILE RINGS

CHAPTER 6

ELASTO-PLASTIC ANALYSIS OF SETTLEMENT OF ECCENTRICALLY LOADED RIGID ANNULAR FOOTINGS

6.1 INTRODUCTION

Annular or circular footings which are well suited for tall tower like structures are generally centrally loaded. However forces such as wind load may cause eccentric loading on the footing. Because of the tall nature of the structure, a high eccentricity under such load can not be over-ruled at least occasionally. Also for such structures, the footing has to be strong (rigid) enough. Hence it is appropriate to study the settlement response of eccentrically loaded footings which are highly rigid.

The elasto-plastic analysis of centrally loaded footings has been made in Chapter 3 and the same is extended in this Chapter for eccentric loading. Because of eccentric loading, rotation is caused. This, and the possibility of lift-off under high eccentricity on the tension side of the footing are the two important aspects introduced because of eccentricity of loading.

Even though soil can be treated generally as an elastic continuum, it would be erroneous to assume that it could take tension. This aspect of tension cut-off has to

be therefore taken into account in any rational and realistic analysis of settlement.

For a rigid circular footing the elastic solutions for moment loading are given by Borowicka (1943) and Sneddon (1946). The solution given by Yegorov and Nichiporovich (1961), although approximate, is of particular interest since it is applicable to a footing on a finite layer of soil. Both these solutions do not take into consideration the plastic yielding of soil or the lift-off or separation. There is no solution available presently for eccentrically loaded rigid annular footing taking these factors into account.

In the present study, the horizontal forces, if any, on the footing are not considered. These forces are not expected to contribute appreciably to the vertical settlement and the effect on the rotation is considered in the form of eccentricity.

6.2 ASSUMPTIONS AND STATEMENT OF THE PROBLEM

6.2.1 Assumptions

In addition to the assumptions contained in Section 3.2.1(A) and (B) (Chapter 3), the following additional assumptions are made for the purpose of study in this Chapter.

- (1) The external force acting on the footing is vertical but not central.
- (2) Wherever tensile stresses tend to develop at the contact face between the footing and the soil, the stress is held at zero value.

6.2.2 Statement of the Problem

A smooth rigid annular footing of outer radius ' a ' and inner radius ' n_a ' carries a vertical load Q at an eccentricity ' e ' (Fig. 6.1).

Three types of problems as in Section 3.2.2 (Chapter 3) are considered, the only difference being that the load is eccentric.

6.3 ANALYSIS

6.3.1 General

The analytical procedure outlined in Chapter 3 and the portion of Chapter 4 involving tension cut-off are generally applicable. The elastic solutions mentioned in earlier Chapters are all applicable.

6.3.2 Elastic Case

The footing is discretized into small elements (Fig. 3.1) and the stress q_j over a small element is assumed uniform and acting at the centre of the element as a point load, except for the case when a formula is available for

finding the influence of an element on itself.

The settlement ρ_{ij} at the centre of element i due to stress q_j on element, j , is expressed (Eq. 3.4) as

$$\rho_{ij} = q_j a \frac{1-v^2}{E} I_{ij} \quad (6.1)$$

This equation in matrix form for all the elements is written as (Eq. 3.5),

$$\{\bar{\rho}\} = (1-v^2) [I] \{\bar{q}\} \quad (6.2)$$

where $\{\bar{\rho}\}$ and $\{\bar{q}\}$ are non-dimensional settlement and contact stress vectors respectively.

Since the footing is assumed to be rigid, the settlement at any point at a distance x from the centre can be expressed as

$$\bar{\rho} = \alpha \bar{x} + \bar{k} \quad (6.3)$$

where $\bar{x} = x/a$, \bar{k} is the non-dimensional vertical displacement of the centre of the footing and α is the rotation of the footing about its centre.

The settlement-contact stress relationship in matrix form (Eq. 6.2) along with Eq. 6.3 can be written as

$$(1-v^2) [I] \{\bar{q}\} = \{\phi \bar{x} + \delta\} \quad (6.4)$$

For overall equilibrium of forces and moments on the footing,

$$\sum q_j dA_j = Q \quad (6.5)$$

$$\sum q_j dA_j x_j = Q \cdot e \quad (6.6)$$

where dA_j is the area of element j , and x_j is the distance of centre of element j from the centre of the footing measured in the direction of eccentricity, and Q is the vertical force acting on the footing at eccentricity e .

If m is the total number of elements into which the footing is divided, $m+2$ equations contained in (6.4) to (6.6) above are solved to yield m values of contact pressures and also the two unknowns α and k which give the settlements. The solution can be written in the following form

$$p = \frac{Q}{a} \frac{1-v^2}{E} (\phi \bar{x} + \delta) \quad (6.7)$$

where ϕ and δ are rotation and settlement influence factors respectively.

6.3.3 Elastic Case with Tension Cut-off

If the eccentricity of the load is high enough, the solution of Eqs. 6.4 to 6.6 above would indicate some negative values of contact pressure on the other side of eccentricity. Since soil can not take tension, such a solution would stand invalid. To avoid this situation, the contact pressures over all such elements are assigned zero value (Fig. 6.2),

and the equations are resolved, keeping in mind that compatibility of displacements for these elements need not be satisfied. It may turn out that after the redistribution of contact pressures obtained after the solution, some other elements may indicate negative contact pressures, for which the procedure is to be repeated until satisfactory solution with no tensile contact stresses is obtained.

6.3.4 Elasto-Plastic Case Without Tension Cut-off

Even under a small load, the contact stresses near the edges of a rigid footing are extremely high and the soil under some of the elements of the footing would yield. Let suffixes e and y indicate elastic and plastically yielded values respectively. Eq. 6.2 is converted, for convenience of the analysis, into partitioned form as below (same as Eq. 3.10, Chapter 3).

$$\{ -\frac{\bar{\rho}_e}{\bar{\rho}_y} \} = (1 - v^2) [I] \{ -\frac{\bar{q}_e}{\bar{q}_y} \} \quad (6.8)$$

In the above equation, \bar{q}_y indicates the value of yield stress of soil to which, as per assumption made in this analysis, the contact stress is held (Fig. 6.2) after yielding takes place. (\bar{q}_y = nondimensional yield stress = q/E).

Since compatibility of displacements is satisfied in the elastic region only, Eq. 6.8 above is written as

$$\{\bar{\rho}_e\} = (1 - v^2) [I'] \left\{ -\frac{\bar{q}_e}{q_y} \right\} \quad (6.9)$$

where $[I']$ is the modified coefficient matrix corresponding to the rows of elastic elements only (Eq. 3.11).

The equilibrium equations 6.5 and 6.6 can be re-written, after dropping the suffix j for brevity, as

$$\sum q_e \cdot dA + \sum q_y \cdot dA = Q \quad (6.10)$$

$$\sum q_e \cdot dA \cdot x + \sum q_y \cdot dA \cdot x = Q \cdot e \quad (6.11)$$

Where subscripts e and y denote elements in elastic and yielded zones respectively.

Equations 6.9 through 6.11 can now be solved, along with Eq. 6.3 to get the values of contact pressure in the elastic region (the value being known and equal to q_y in yielded region) and the unknown settlement components in the form of central settlement and rotation. It may turn out that the solution thus obtained contains contact pressure values higher than yield stress q_y . In that case, the procedure is to be repeated until satisfactory solution with contact pressure not exceeding q_y anywhere is obtained.

6.3.5 Elasto-Plastic Case with Tension Cut-Off

Under higher values of eccentricity and at any loading (even small) both lift-off and plastic yielding of soil would take place. After applying the conditions, namely, for any element j ,

$$q_j = q_y, \text{ if } q_j > q_y \quad (6.12)$$

$$\text{and} \quad q_j = 0, \text{ if } q_j < 0, \quad (6.13)$$

it may turn out, after the first trial solution using the techniques given in Section 6.4.3 and Section 6.4.4 above, that (i) some contact pressures exceed q_y and /or , (ii) some contact pressures are negative.

The contact pressure values at these elements are made to take up the values as in Eqs. 6.12 and 6.13 above and the solution is obtained again. If the required conditions are not found to be satisfied, the procedure is repeated until the conditions of Eqs. 6.12 and 6.13 are nowhere violated.

6.4 RESULTS AND DISCUSSION

6.4.1 Minimisation of Computational Effort

At the outset, only half of the footing symmetrical about the diameter on which the resultant external load acts is considered.

The redistribution of contact pressures at the beginning of each trial solution, along with the involvement of two components of settlement and two restrictions on the contact pressure values is expected to run into a long iterative procedure. However, it was found that the zone of lift-off (or separation) marches with an almost straight front towards

the centre of the footing in all the cases considered. Therefore it was possible to adopt the following procedure and reduce the interactions normally to 2 to 3 only.

Equation 6.4 is split as below, without loss of generality .

$$(1 - v^2) [I] \{c_1 \bar{q} + c_2 \bar{\bar{q}}\} = \{\emptyset \bar{x} + \delta\} \quad (6.14)$$

$$(1 - v^2) [I] \{c_3 \bar{q}\} = \{\bar{x}\} \quad (6.15)$$

$$(1 - v^2) [I] \{c_4 \bar{q}\} = \{U\} \quad (6.16)$$

where , $\{U\}$ is unit vector and c_1 , c_2 , c_3 and c_4 are constants such that

$$c_3 = c_1 \emptyset ; \quad c_4 = c_2 \delta \text{ and } c_3 + c_4 = 1 \quad (6.17)$$

For convenience, a beginning is made with an assumed extent of tension cut-off or zone of separation. For the plastically yielded zone, the procedure given in section 6.4.4 is adopted. In case some negative values of contact pressure occur, c_1 and c_2 are simply chosen in such a way that, while Eqs. 6.17 are satisfied, the recombining of Eqs. 6.15 and 6.16 would give all positive contact pressures and exactly zero pressures on the boundary of the separation zone. Partitioning and elimination of the yielded and separation zones from the computations reduces the matrix size successively under higher loads and/or eccentricities.

A computer run for the entire range of loading and eccentricities under given geometry of footing took on DEC 10 system only about 2 minutes of CPU time.

It may be mentioned that, even allowing for the diametric symmetry, a FEM solution of the three-dimensional nature as involved in the present problem, even under simplified elasto-plastic or non-linear elastic analysis involves enormous computations in terms of computer memory as well as CPU time.

6.4.2 Footing Resting on the Surface of Semi-Infinite Soil

6.4.2.1 General

Figure 6.3 shows typical load settlement responses of centrally and eccentrically loaded footings. The particular case of $e = 0$ of the present analysis is seen to tally well with experimental and FEM results given by Desai (1968) (curves 1 to 3, Fig. 6.3). In the same figure, some load settlement curves for typical values of radius ratio n and eccentricity \bar{e} ($\bar{e} = e/a$) are also shown (Curves 4 to 8 Fig. 6.3). For \bar{e} other than zero, the settlement refers to the maximum settlement of the footing (which occurs at the outer edge of the footing). It is seen that the settlement response for $n=0.9$ remains nearly linear upto about 85 percent, 70 percent and 60 percent of failure load

for $\bar{e} = 0, .2$ and $.3$ respectively and then shows a tendency of rapid increase to failure. The settlement response for $n=0$, on the other hand shows a steadily increasing trend. For comparing the performance under equal load, the settlement obtained under the same load level for a ring footing with a certain value of n is to be multiplied by the Equivalence Factor (Section 3.5.3), given by $1/\sqrt{1-n^2}$. Using this and the curves of Fig. 6.3, it is seen that the settlement of ring footing with $n = .9$, at 50 percent of ultimate load, is about 44 percent, 28 percent and 24 percent of that for $n=0$ (carrying the same load and having the same area) for $\bar{e} = 0, .2$ and $.3$ respectively. This shows that the settlements of a ring footing are much less than those of a circular footing at all eccentricities and load levels.

From the elasto-plastic analysis it is found that the settlement components indicated by central settlement factor δ and rotation ϕ depend on eccentricity, radius ratio and load level.

$$\phi, \delta = f(n, \bar{e}, q_{av}/q_y) \quad (6.18)$$

The results of the present investigation are presented in compact form to serve as design charts (Figs. 6.4 to 6.7). In these charts, the values of δ and ϕ are given against \bar{e} ($=e/a$) for various values of n and q_y/q_{av} . The

settlement at any point x from the centre measured in the direction of eccentricity can be found out from Eq. 6.7, namely,

$$\rho = \frac{Q}{a} - \frac{1 - v^2}{E} (\phi \bar{x} + \delta)$$

where $\bar{x} = x/a$ and ϕ and δ are to be read directly from the design charts (Figs. 6.4 to 6.7). These charts can be used in a number of ways. For example, for a given size of a ring footing, the permissible load and/or eccentricity for a desired ratio q_y/q_{av} (Factor of Safety) can be worked out using the charts and the above equation.

The results from the present analysis, in the lower range of load level, nearly represent elastic behaviour and the value of δ in this range is found to be equal to .5 for circular footing (same as in Chapter 3) and the value of ϕ/\bar{e} for circular footing allowing tension is found to be .75 which tally with solutions by Borowicka (1943) and Yegorov and Nichiporovich (1961).

A discussion about the settlement response is made below on the basis of the design charts (Figs. 6.4 to 6.7), with reference to various parameters. It ought to be mentioned here, that since the parameters are not explicitly operative the discussion is only meant for broad comparative study.

6.4.2.2 Effect of radius ratio n

Since the values of ϕ and δ are to be used in Eq. 6.7, a comparison at the same load Q and the same load intensity q_{av} between a circular and a ring footing can be made by applying the Equivalence Factor as below.

The outer radius for a ring footing equivalent to a circular footing (same area) is given by (Section 3.5.3)

$$b = a/\sqrt{1-n^2}$$

Therefore, the settlement of ring footing equivalent to circular footing of radius a (carrying the same load and having equal area) can be written as

$$\rho = \frac{Q}{b} \frac{(1-v^2)}{E} \left(\phi \frac{x}{b} + \delta \right) \quad (6.19)$$

where $b = a/\sqrt{1-n^2}$.

The maximum settlement is given by ($x=b$)

$$\rho_{max} = \frac{Q}{b} \frac{(1-v^2)}{E} (\phi + \delta) \quad (6.20)$$

This can be written as

$$\rho_{max} = \frac{Q}{a} \frac{(1-v^2)}{E} (\phi_{eq} + \delta_{eq}) \quad (6.21)$$

where $\phi_{eq} = \phi\sqrt{1-n^2}$ and $\delta_{eq} = \delta\sqrt{1-n^2}$.

Thus the ϕ and δ for an annular footing are to be multiplied by $\sqrt{1-n^2}$ to get equivalent values for circular footing.

Some of the equivalent values worked out using the above relations and the design charts are given in Table 6.1 assuming that the values of non-dimensional eccentricity (e/a or e/b) are the same.

TABLE 6.1 : EQUIVALENT CENTRAL SETTLEMENT AND ROTATION COEFFICIENTS ($q_y/q_{av} = 3$)

n	b/a	e/b	Equivalent values		$\phi_{eq} + \delta_{eq}$
			ϕ_{eq}	δ_{eq}	
0.0	1.00	.1	0.20	0.60	0.80
		.3	0.40	0.63	1.03
		.5	1.70	1.10	2.80
0.8	1.67	.1	0.06	0.39	0.45
		.3	0.20	0.42	0.62
		.5	0.70	0.40	1.10

From the Table it can be seen that the central settlement, rotation and maximum settlement, indicated by δ_{eq} , ϕ_{eq} and $\phi_{eq} + \delta_{eq}$ respectively are much less for $n=0.8$ than for $n=0$. This difference will be more if e instead of \bar{e} is taken same for the ring and the circular footings.

A study of design charts (Figs. 6.4 to 6.7) shows that ring footings are advantageous over circular footings

from the consideration of settlement and rotation for all values of e/a and q_y/q_{av} .

6.4.2.3 Effect of eccentricity

From the charts for ϕ in Figs. 6.4 to 6.7), it is observed that ϕ (rotation coefficient) increases with e/a at any load level, as expected. The increase in ϕ with e/a is very rapid after a certain eccentricity for low load levels and it is so for even for a small value of eccentricity for higher load levels. Both these types of behaviour are explained on the basis of elasto-plastic nature of soil. The contact pressures which are already very high at the edges increase further on the compression side under eccentric load even if the load is small in magnitude. This induces larger yielding of soil under increasing eccentricity causing more rotation. In addition to this, tension cut-off is created on the tension side which also accentuates rotation. Under loads close to failure, a large portion of the soil remains yielded due to which the rotation is sensitive to even small changes in eccentricity.

For the same reason involving plastic yielding of soil, the central deflection also increases with eccentricity as seen from Figs. 6.4 to 6.7. However, this alone does not give the correct idea of the movement of the

footing, since the settlements must be looked upon as the sum of $\phi\bar{x}$ and δ . Thus the following quantities are of particular interest.

$$\text{Maximum settlement coefficient} = \phi + \delta \quad (x/a=1) \quad (6.22)$$

$$\text{Minimum settlement coefficient} = -\phi + \delta \quad (x/a=-1) \quad (6.23)$$

$$\text{Differential settlement coefficient} = 2\phi \quad (6.24)$$

Distance of point of rotation from the centre

$$= \frac{\delta}{\phi} a . \quad (6.25)$$

These quantities can be obtained from the design charts. It can be found that the centre of rotation moves from infinity (no rotation) to smaller distances from the centre under increasing values of e/a .

Some typical values obtained from Eqs. 6.21 to 6.25 above are given in Table 6.2 after converting to equivalent values as given in Section 6.4.2.2.

From Table 6.2 it is also seen that at large values of eccentricity and/or load levels (q_{av}/q_y), even a physical lift-off-the-ground can take place (indicated by negative values of minimum settlement).

TABLE 6.2 : TYPICAL VALUES OF MAXIMUM AND MINIMUM COEFFICIENT OF SETTLEMENT AND DISTANCE OF POINT OF ROTATION

n	q_y/q_{av}	e/a	ϕ_{eq}	δ_{eq}	Maximum Settle- ment Coeffici- ent = $\phi_{eq} + \delta_{eq}$	Minimum Settle- ment Coeffici- ent = $-\phi_{eq} + \delta_{eq}$	Distance of Point of Rotation from Centre = $(\delta_{eq}/\phi_{eq})a$
0	4	0.0	0.00	0.51	0.51	0.51	∞
		0.3	0.23	0.57	0.80	0.34	2.480a
		0.5	1.00	0.75	1.75	-0.25	0.750a
0	3	0.0	0.00	0.52	0.52	0.52	∞
		0.3	0.40	0.63	1.03	0.23	1.575a
		0.5	1.70	1.10	2.80	-0.60	0.295a
.8	3	0.0	0.00	0.55	0.55	0.55	∞
		0.3	0.20	0.42	0.62	0.22	2.100a
		0.5	0.70	0.40	1.10	-0.30	0.570a

6.4.2.4 Marching of yielded and tension cut-off zones

As a part of the solution, the contact pressures and the extents of yielded zone and tension cut-off zone (if any) are also obtained for any stage of loading and eccentricity. Typical yielded and lift-off zones are also sketched in Fig. 6.8. The nature of typical contact pressure distribution

under yielded and separation conditions is shown in Fig. 6.9. Whereas the first yielded zone develops near the entire outer edge of a circular footing under central loading, it develops only on the side of eccentricity for eccentric loading. It then proceeds towards the centre with increasing load. For an eccentrically loaded ring footing the first yield starts at the inner and outer edges on the side of eccentricity.

The tension cut-off zone starts on the tension side and under increasing load or eccentricity it marches towards the centre, with almost a straight front. Fig. 6.10 shows the relationship between q_y/q_{av} and eccentricity at impending tension cut-off. It is seen that tension cut-off starts, at q_y/q_{av} value of 5 at e/a values of about 0.34 and 0.39 for $n=0$ and 0.8 respectively. For any load level, the tension cut-off starts at higher values of e/a for footings with higher values of n (ring footings with narrow width) which is in favour of ring footings. Another interesting observation from this figure (Fig. 6.10) is that for values of q_y/q_{av} high enough (infinity in the limit) which indicates close to elastic conditions, the e/a necessary to cause tension cut-off is seen to be about .39 for $n=.8$, whereas, when elasto-plastic analysis is made, it is found that tension cut-off can be caused at e/a values of about .385, .375, .36 and .2 at q_y/q_{av} ratios of 2.5, 2, 1.5 and 1.25 respectively.

Thus tension cut-off is likely to occur at values of eccentricities lower than those arrived at from elastic theory.

6.4.3 Effect of Embedment of Footing

For the purpose of this study, the embedment amounts to application of net load Q on the footing embedded at a depth c below the surface of semi-infinite soil which is basically treated as elastic medium and the Mindlin's solution is applied instead of Boussinesq's solution.

Figure 6.8 shows a typical contact pressure distribution for $c/a = 0$ and $c/a = 5$ (The contact pressures are almost same for the two cases). The contact pressure distribution as well as the behaviour of the embedded footing is found to be very similar to that of a surface footing at all load levels and hence it has been found possible to correlate it to that of surface footing after applying correction factors. The procedure for applying the correction factors is given in Section 3.4.4 and the correction factors to be applied for depth and for radius ratio and v for central loading are given in Table 3.2 and Table 3.3.

For eccentric loading, the settlement of a rigid footing, at any point at a distance x from the centre of the

footing measured in the direction of eccentricity is expressed as

$$\sigma' = \frac{Q}{a} \cdot \frac{1-\nu^2}{E} C_c (C_n C_v \delta' + R_n R_v \phi' \bar{x}) \quad (6.26)$$

where Q = Load on the footing

a = External radius of footing

E, ν = Elastic constants of soil

C_c = Correction factor for depth of embedment
(Table 3.2, Chapter 3)

C_n, C_v = Settlement correction factors for n and v
(Table 3.3, Chapter 3).

R_n, R_v = Rotation correction factors for n and v

\bar{x} = x/a

δ', ϕ' = Central settlement, and rotation coefficients obtained for surface footing (Figs. 4.4 to 4.7), but for appropriate c_y value at depth c as explained in Section 3.4.4.

The values of R_n and R_v are given in Table 6.3.

The effect of n on R_n is not much as apparent from Table 6.3; however the effect of n on other parameters such as ϕ is significant.

The effect of depth of embedment alone on rotation is of the same proportion as for central settlement and is included through the correction factor C_c .

TABLE 6.3 : ROTATION CORRECTION FACTORS R_n AND R_v FOR RADIUS RATIO (n) AND POISSON'S RATIO (v) (EQ. 6.26)

c/a	R _n						R					
	n=0	n=.2	n=.4	n=.6	n=.8	n=.9	v=.5	v=.4	v=.3	v=.2	v=.1	
0.00	1	1	1.00	1.00	1.00	1	1	1.00	1.00	1.00	1.00	1.00
0.05	1	1	1.00	0.99	0.98	0.94	1	0.99	0.97	0.95	0.95	0.95
0.10	1	1	0.99	0.98	0.95	0.89	1	0.98	0.96	0.93	0.93	0.91
0.25	1	1	0.99	0.97	0.90	0.84	1	0.96	0.92	0.88	0.88	0.85
0.50	1	1	0.99	0.95	0.89	0.84	1	0.95	0.89	0.84	0.79	0.79
0.75	1	1	0.99	0.96	0.90	0.86	1	0.94	0.88	0.82	0.82	0.76
1.00	1	1	0.99	0.96	0.93	0.89	1	0.94	0.88	0.81	0.81	0.76
2.00	1	1	1.00	0.99	0.98	0.97	1	0.96	0.90	0.84	0.84	0.78
3.00	1	1	1.00	1.00	0.99	0.99	1	0.97	0.91	0.85	0.85	0.80
6.00	1	1	1.00	1.00	1.00	1.00	1	0.97	0.92	0.86	0.86	0.80
10.00 or more	1	1	1.00	1.00	1.00	1	1	0.97	0.92	0.86	0.86	0.80

The contact pressure distribution, changes in it at various load levels and the nature and the extent of yielded and separated zones for embedded footings are similar to those for surface footing. Also the discussion for surface footings applies to the case of embedded footings except for the effect of the correction factors. The load level and eccentricities at which tension cut-off is caused is the same as for surface footings (see the curves for $h/a = \infty$ in Fig. 6.10). However here again, since the reference q_y itself is higher, tension cut-off in case of embedded footings will be caused at higher load/eccentricity levels in comparison to surface footings.

6.4.4 Footing Resting on Soil Layer of Finite Depth Underlain by Rough Rigid Base

6.4.4.1 General

Solutions for this case are obtained by using the appropriate elastic solutions for finite layer.

The settlement in this case is expressed as

$$\rho_h = \frac{Q}{a} \frac{1-v^2}{E} (\alpha \delta_h + \phi_h \bar{x}) \quad (6.27)$$

where the subscript h is employed to indicate finite depth and α is the correction factor for effect of Poisson's ratio. It is found that it is not necessary to apply correction to ϕ_h .

Also, $\alpha = 1$ for $v = .5$

6.4.4.2 Settlement and rotation response for Poisson's ratio = .5

Figures 6.11 to 6.16 give the values of ϕ_h and δ_h for various parameters and for Poisson's ratio = .5 ($\alpha=1$). The nature of the curves is generally similar to that for semi-infinite soil except for the following:

- (i) Depth of layer has a considerable effect on the settlement and rotation of the footing. For example, if ϕ_h and δ_h are to be restricted to say .5 each at a load level $q_y/q_{av}=2$, then for a circular footing, e/a has to be less than about 0.01, 0.25 and 0.31 for $h/a = \infty$, 2 and 1 respectively. For the same data, if e/a is .2, q_y/q_{av} values are 5, 1.8 and 1.5 for $h/a = \infty$, 2 and 1 respectively (Figs. 6.4, 6.11 and 6.12).
- (ii) The effect of higher values of n is similar to that for the case of semi-infinite soil; however, this effect and the effect of depth of layer are additive giving rise to much less settlement and rotation for a narrow ring resting on soil of finite depth. For example, the ϕ_h value, at $q_y/q_{av}=2$ and $e/a = .2$, is about .57 for $h/a=\infty$, $n=0$. The value is .3 for $h/a = \infty$, $n=.8$ and it is .18 for $h/a = 1$, $n=.8$ (Figs. 6.4, 6.6 and 6.16).

6.4.4.3 Effect of and correction for Poisson's ratio

Figure 6.17 shows typical values of ϕ_h obtained directly for $h/a = 2$, $n=0$ and Poisson's ratio = .5 and 0. It is seen that the curves for Poisson's ratio of .5 and 0 are nearly the same for the case considered, for two values of q_y/q_{av} . This trend is found in general and therefore it is not found necessary to apply any correction to ϕ_h on account of Poisson's ratio. Also in this Figure (Fig.6.17) are shown typical curves for δ_h obtained directly as well as obtained by applying the correction α (Eq. 6.27). The value of α is obtained as follows:

$$\alpha = \frac{I_{h_v}}{I_{h_{.5}}} \times \frac{(1-(.5)^2)}{(1-v^2)} \quad (6.28)$$

where v = Poisson's ratio under consideration.

I_{h_v} = Value of settlement influence coefficient obtained from design charts for centrally loaded rigid annular footings (Figs. 3.10, Chapter 3) against required value of Poisson's ratio and for the required values of n and q_{av}/q_y .

$$I_{h_{.5}} = \text{As above for Poisson's ratio} = .5$$

$$\alpha = 1 \text{ for } v = .5 \quad (6.29)$$

It is seen from Fig. 6.17 that the values of δ_h obtained for $v = 0$ by applying the correction as above tally fairly well with those obtained directly for $v = 0$.

Similar trend is found to exist generally. Hence, the simplified correction procedure as above is suggested.

While finding out the value of q_{av}/q_y in all the cases of footing resting on finite layer of soil, if the corrected value of q_y for depth as given in Section 3.4.5 is used, the value of corrected load level q_{av}/q_y will be reduced on account of this correction and all the design values of settlement, moment etc. will also reduce.

6.5 CONCLUSIONS

- (1) A simplified elasto-plastic analysis has been conducted to obtain the entire response of settlements and rotations of rigid annular footings (circular footing being a particular case) under vertical eccentric loading.
- (2) The contact pressures at the edges of the rigid footing which are very high under central loading are further increased on the compression side if the load is eccentric and this gives rise to plastic yielding of soil even at lower load levels and to non-linear settlement/rotation characteristics with increasing load and/or eccentricities.
- (3) Design procedure and charts are presented for the three cases considered.

- (4) Tension cut-off occurs at eccentricity values lower than those predicted by elastic theory when elasto-plastic behaviour of soil is taken into consideration.
- (5) Annular footings are found to be better suited than circular ones from the consideration of not only settlements but rotation also under eccentric loading.
- (6) The settlements and rotations are less for footings resting on finite layer of soil and embedded footings in comparison to surface footings on semi-infinite soil.

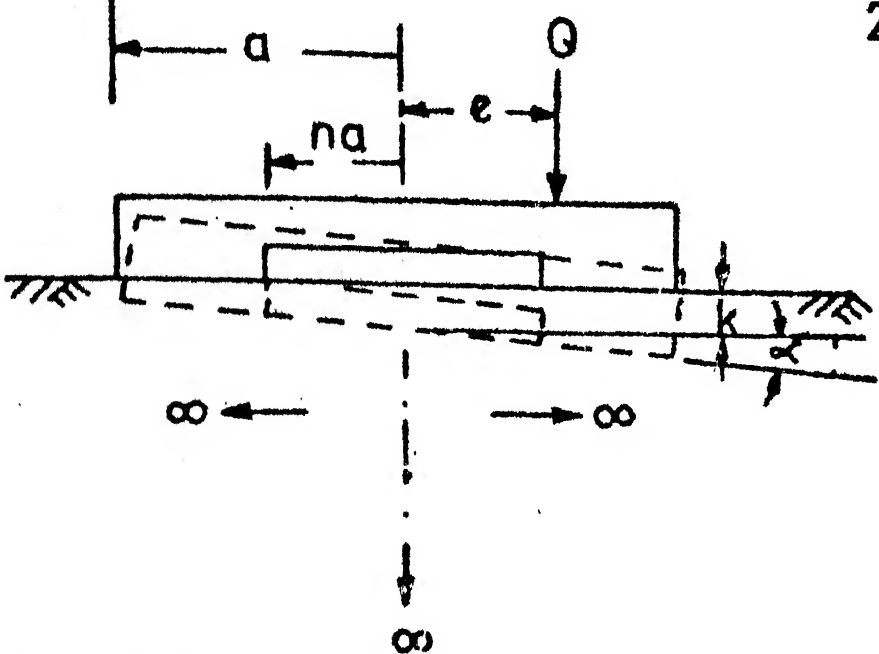
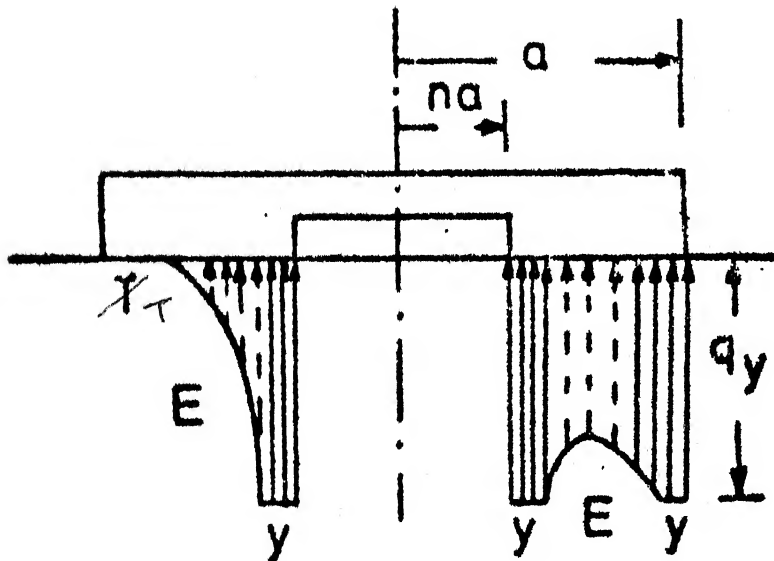


FIG. 6.1 ECCENTRICALLY LOADED RIGID ANNULAR FOOTING: DEFINITION SKETCH (Problem type A)



T-Tension cut-off zone

E-Elastic zone

y-yielded zone

FIG. 6.2 CONTACT STRESSES

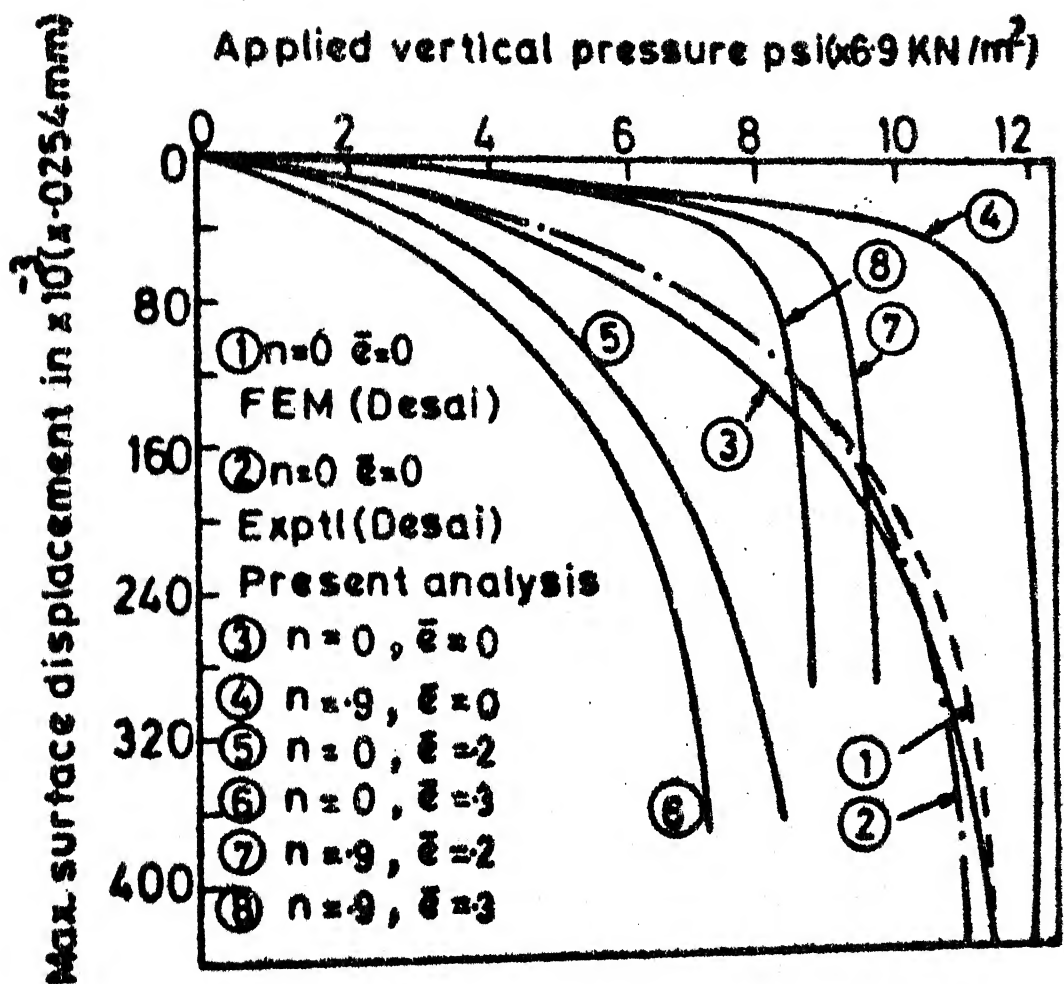


FIG. 6.3 TYPICAL LOAD SETTLEMENT CURVES

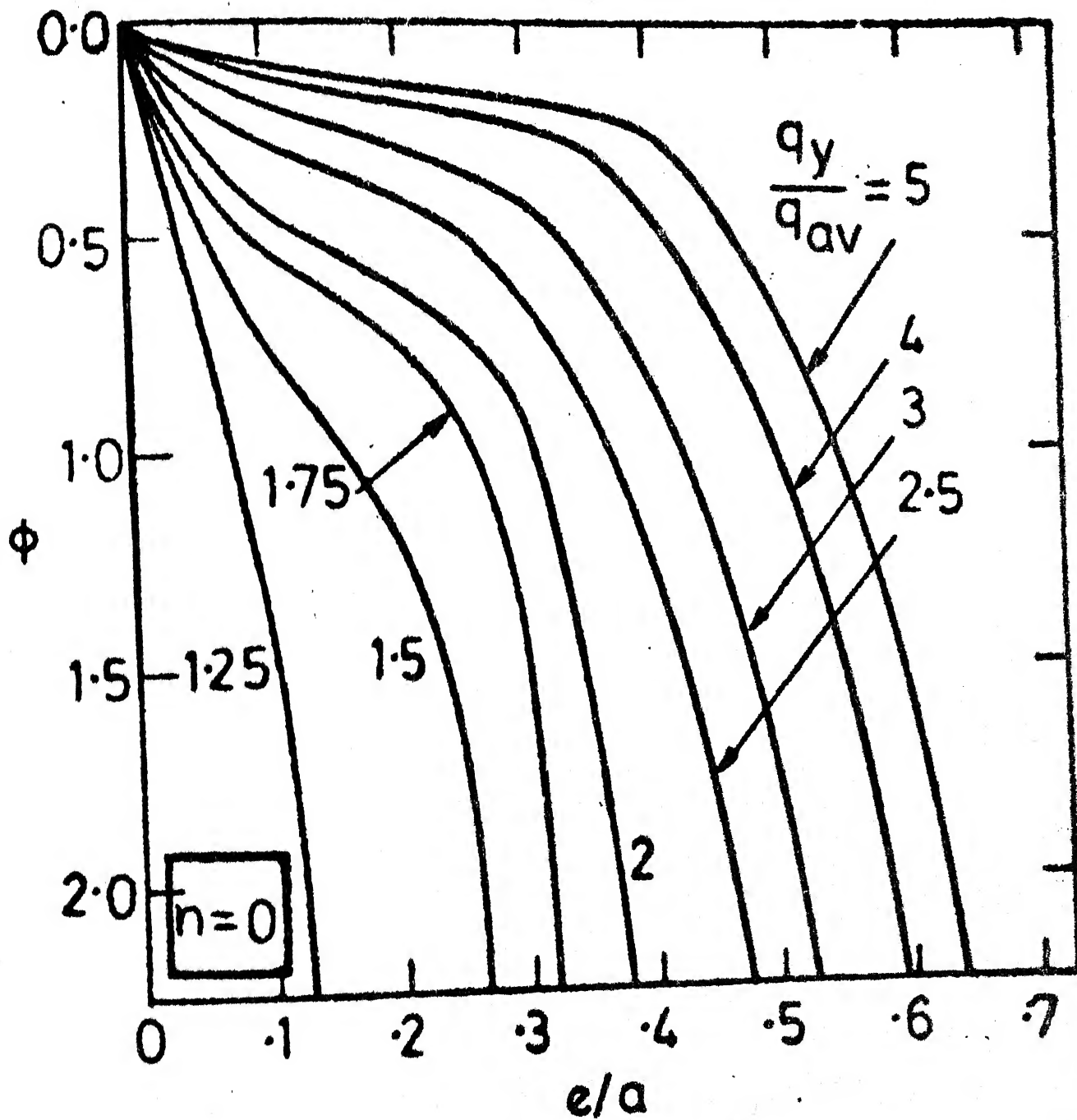


FIG. 6.4(a) ROTATION ECCENTRICITY CURVES

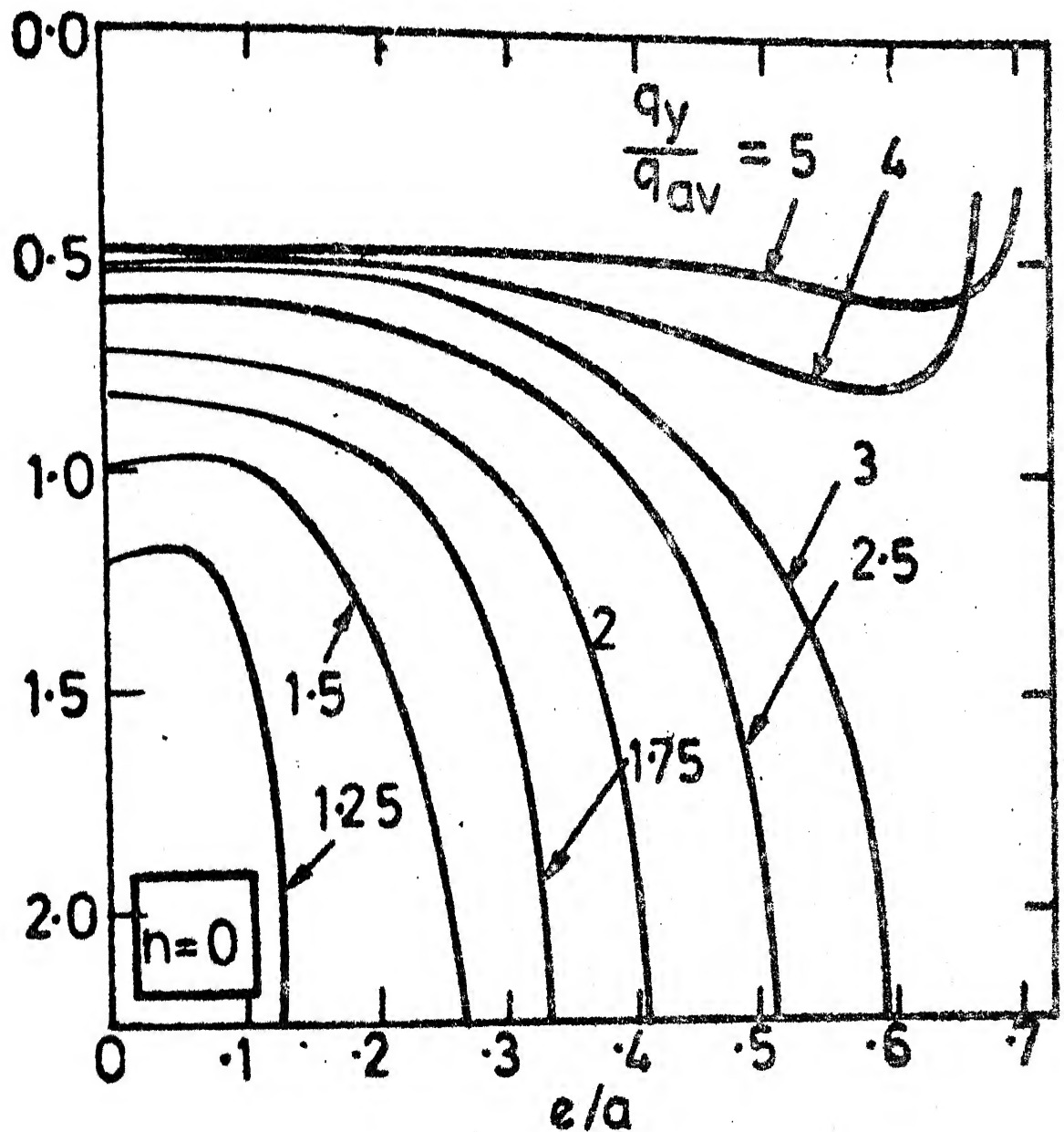


FIG. 6.4 (b) SETTLEMENT ECCENTRICITY CURVES

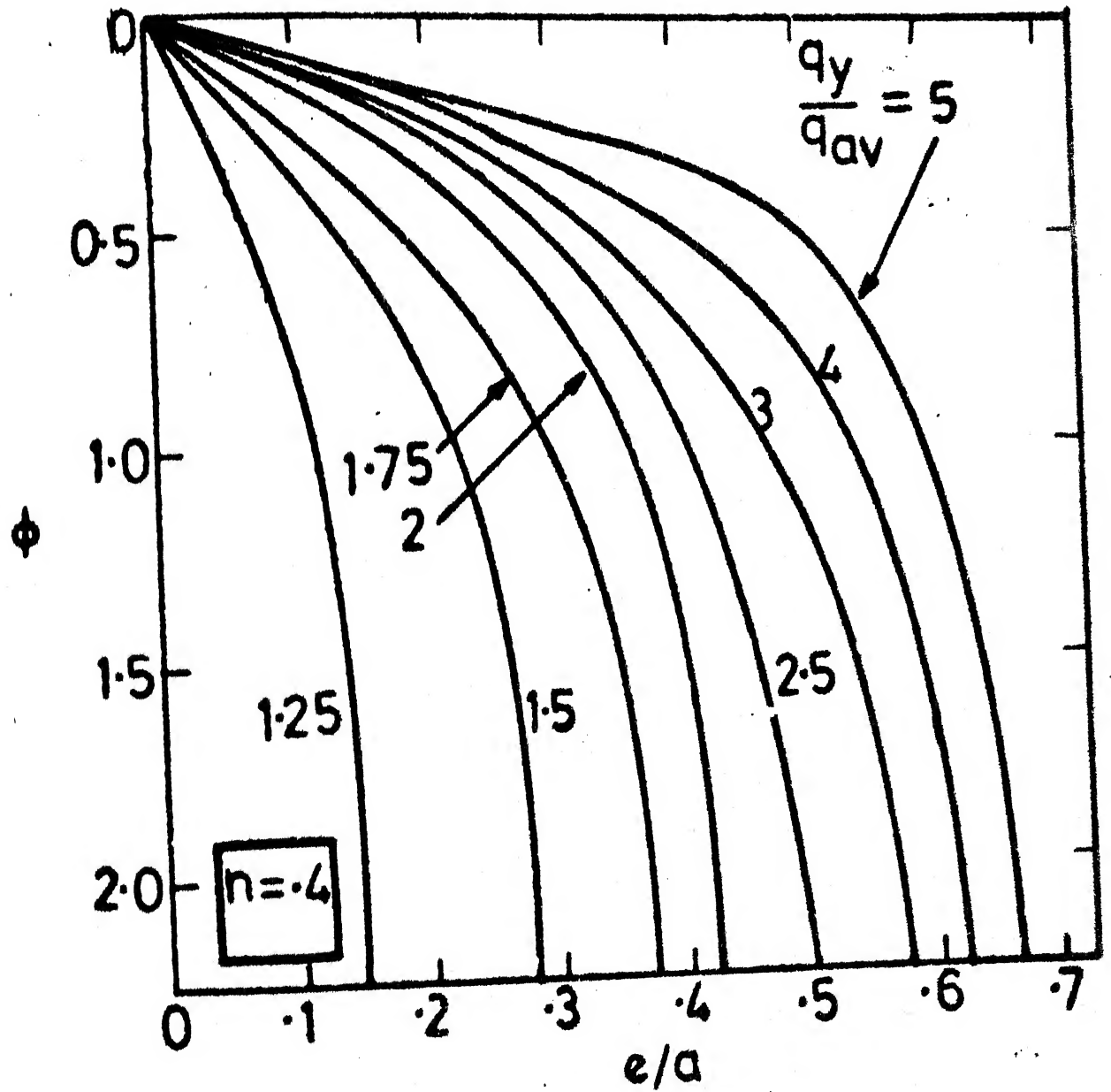


FIG. 6.5(a) ROTATION ECCENTRICITY CURVES

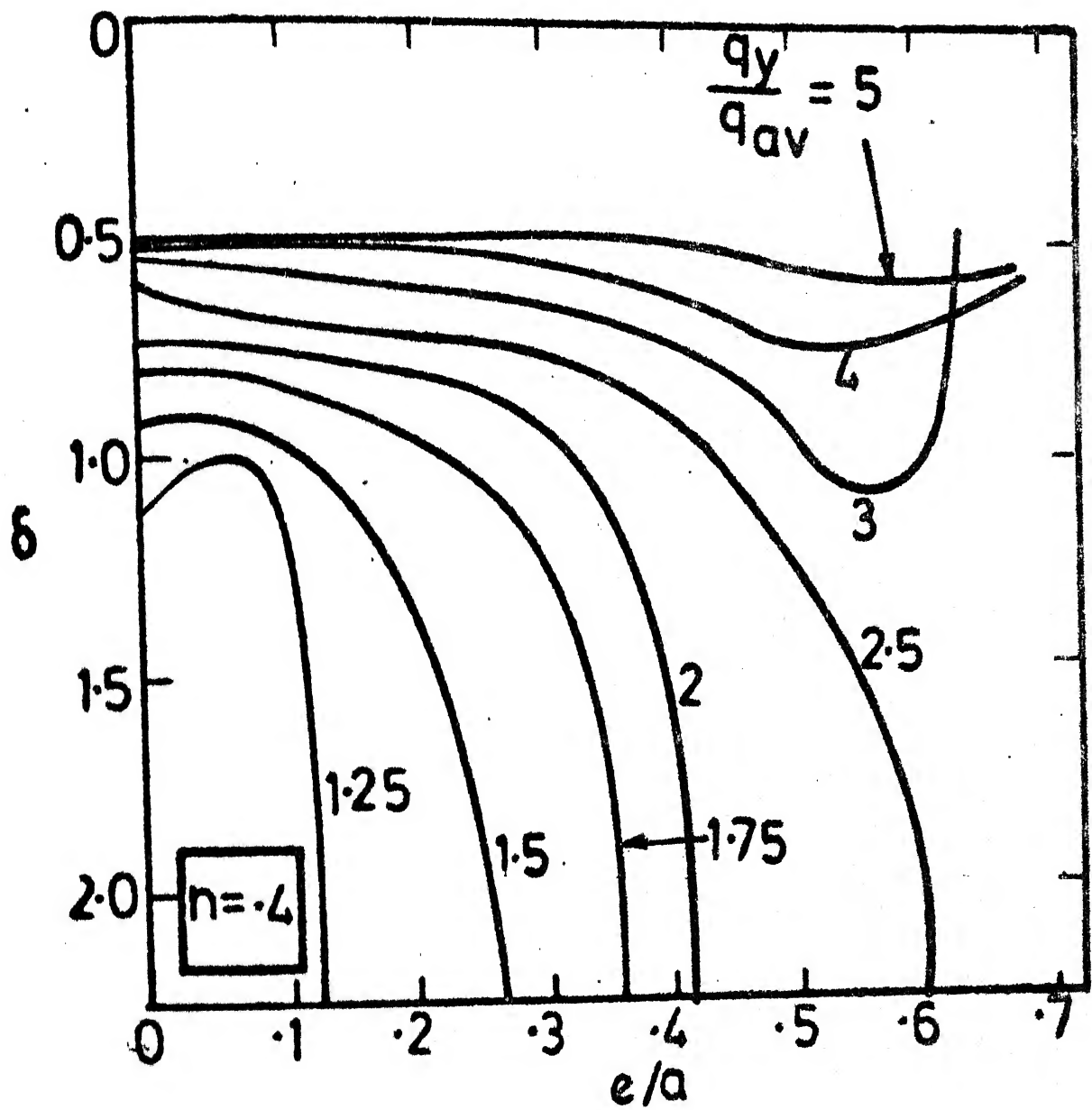


FIG. 6.5 (b) SETTLEMENT ECCENTRICITY CURVES

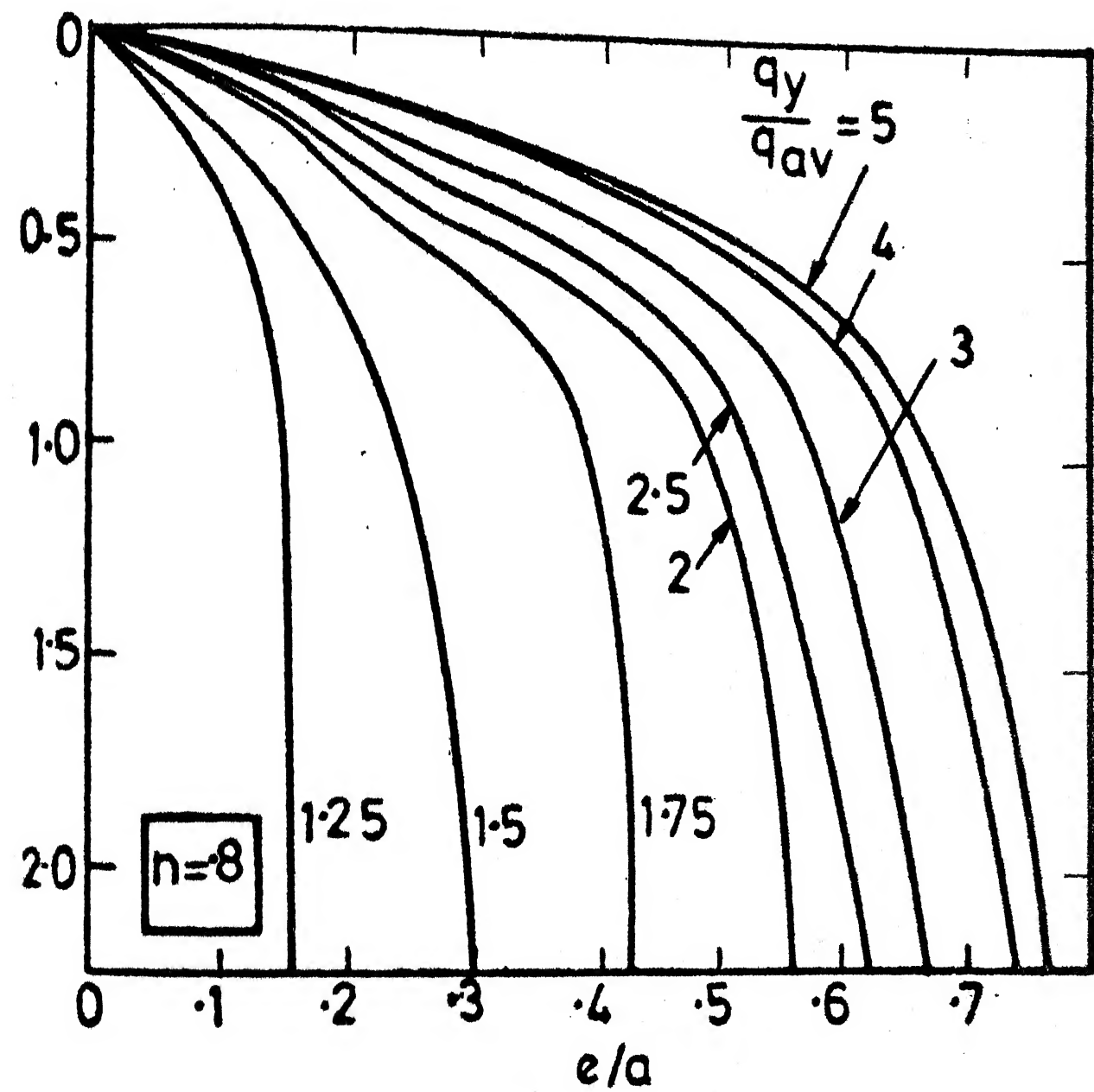


FIG. 6.6(a) ROTATION ECCENTRICITY CURVES

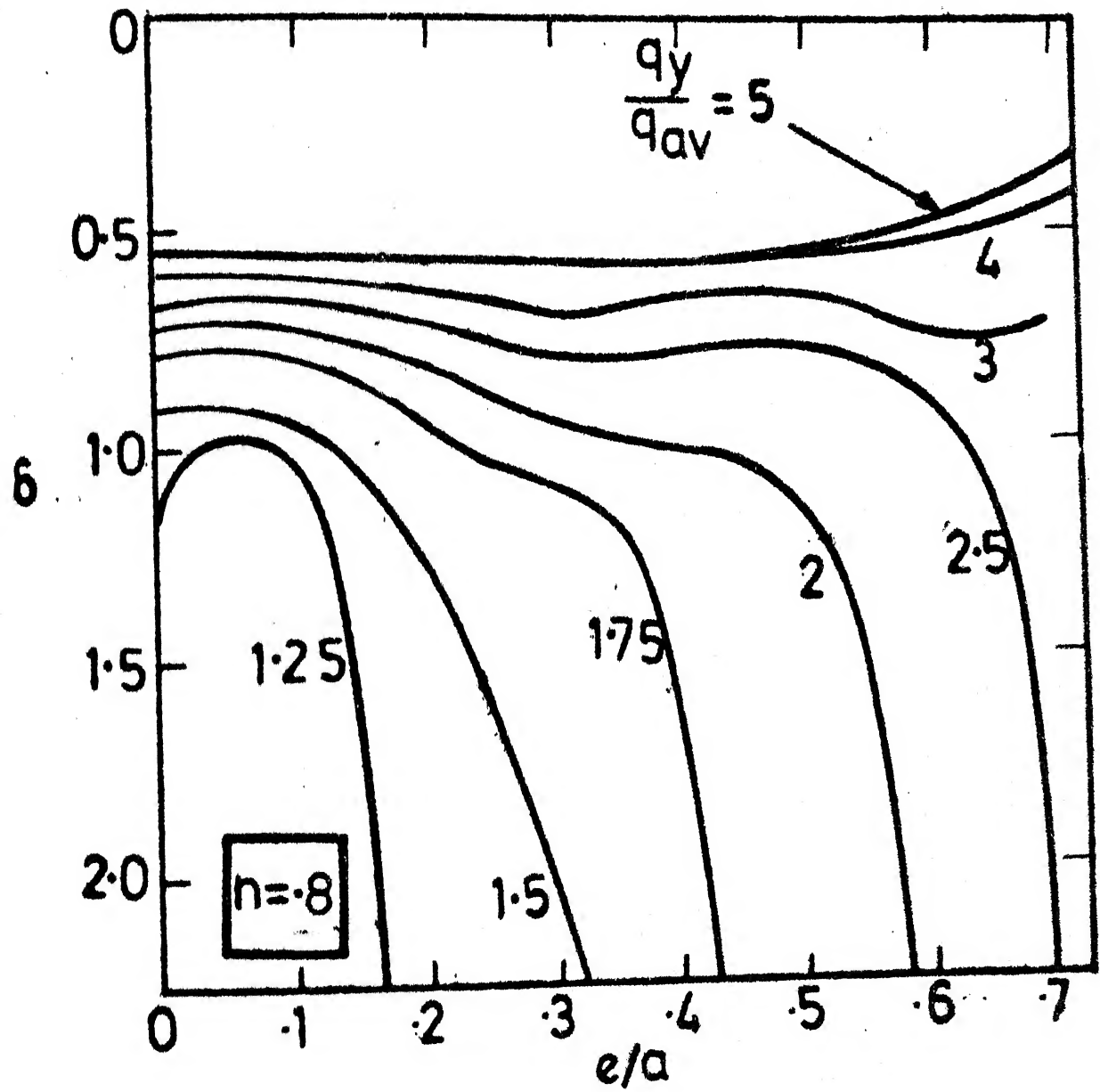


FIG. 6.6 (b) SETTLEMENT ECCENTRICITY CURVES

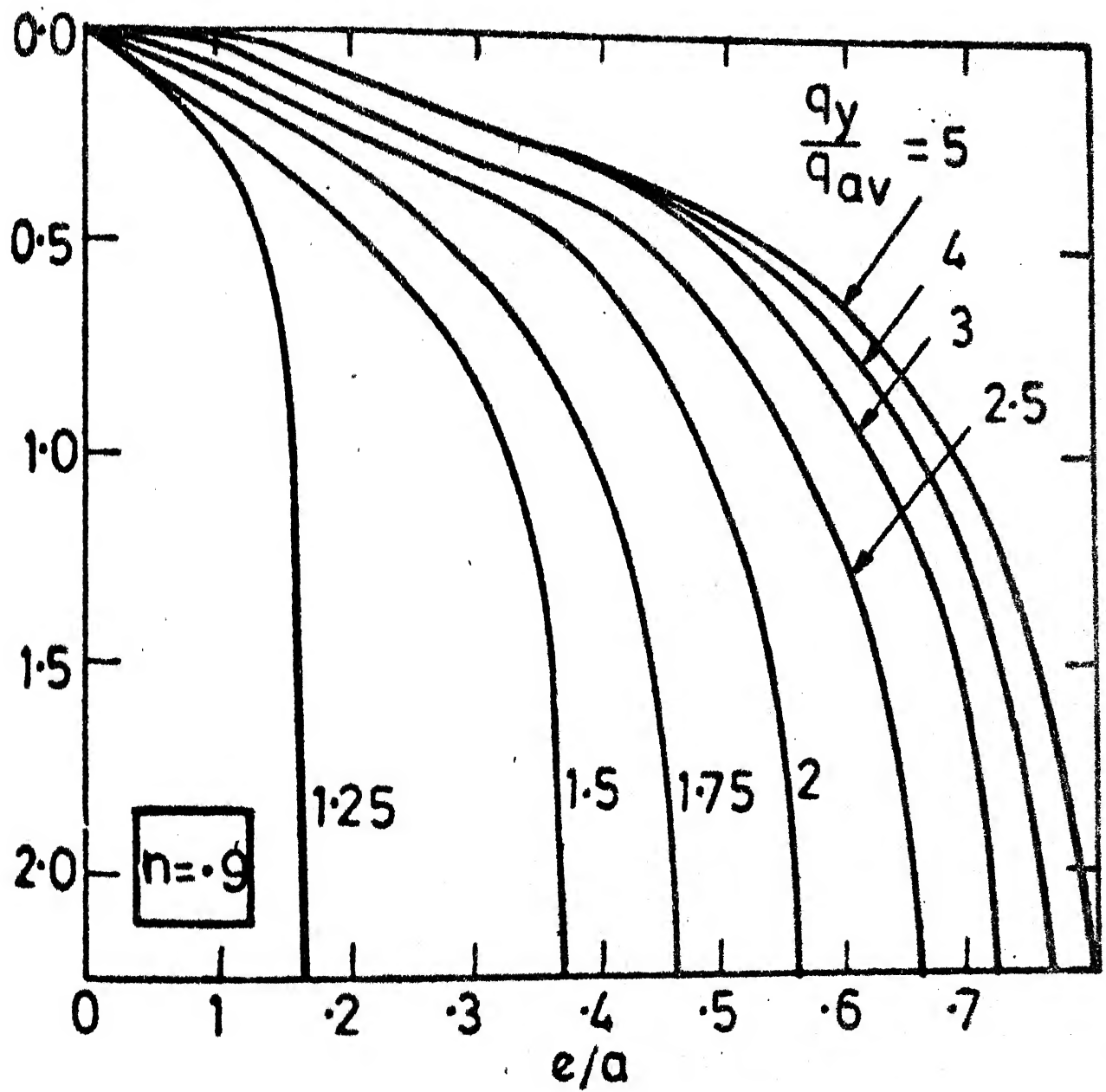


FIG. 6.7(a) ROTATION ECCENTRICITY CURVES

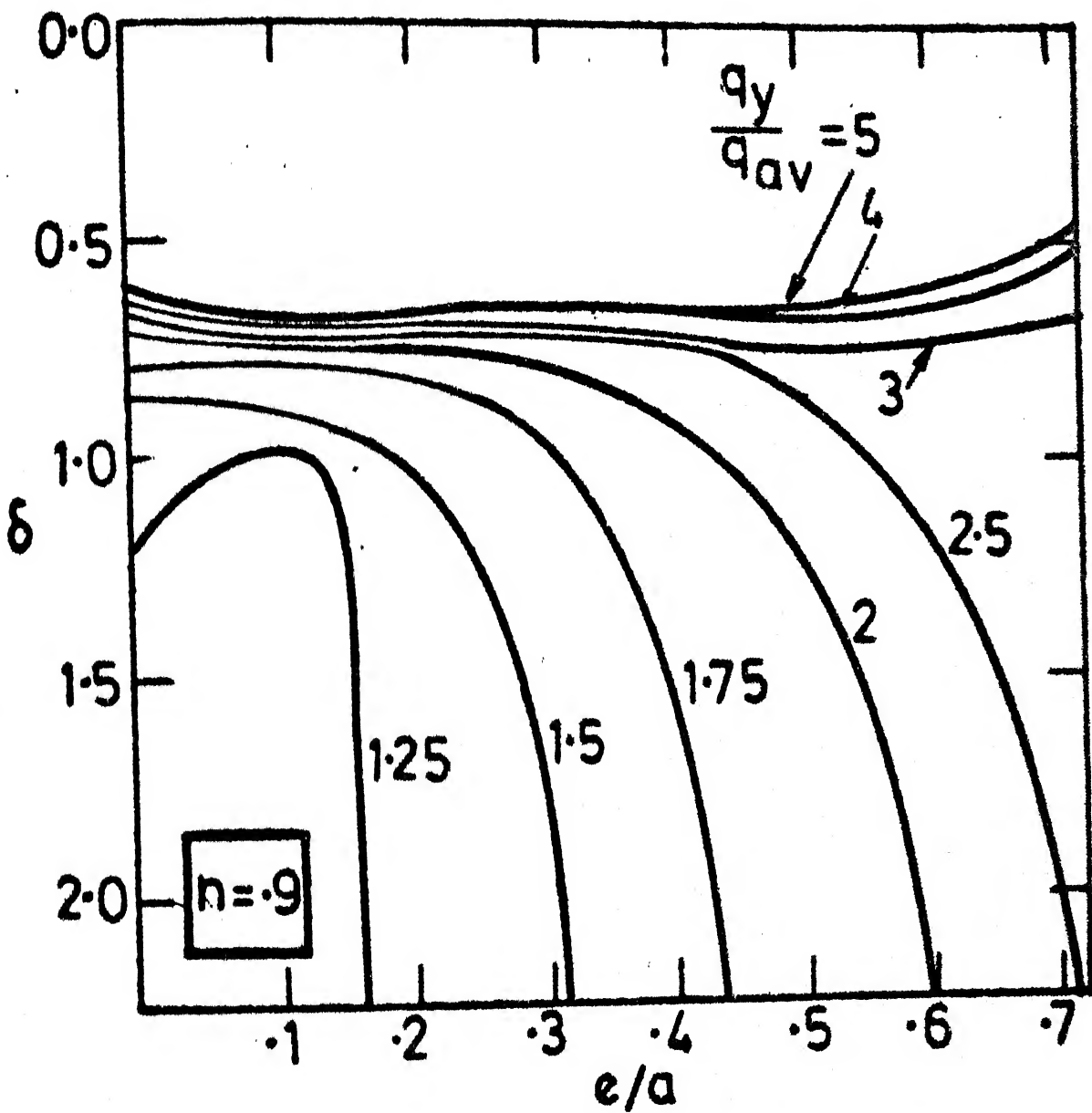
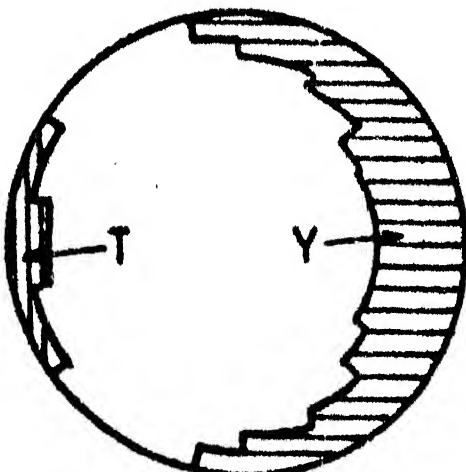
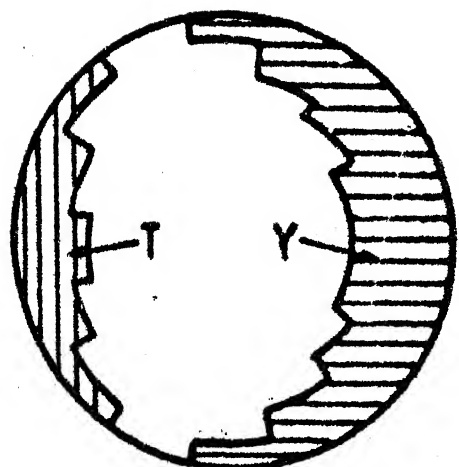


FIG. 6.7 (b) SETTLEMENT ECCENTRICITY CURVES



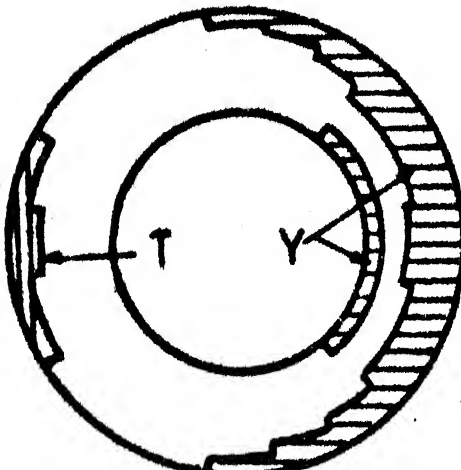
$$n=0, \frac{q_y}{q_{av}} = 2.0$$

$\bar{\epsilon} = .297$



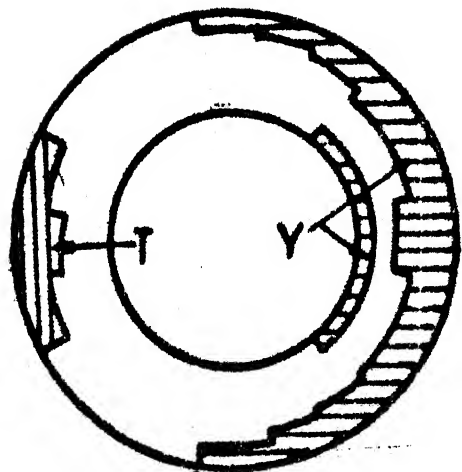
$$n=0, \frac{q_y}{q_{av}} = 2.0$$

$\bar{\epsilon} = .326$



$$n=.6, \frac{q_y}{q_{av}} = 2.0$$

$\bar{\epsilon} = .34$



$$n=.6, \frac{q_y}{q_{av}} = 2.0$$

$\bar{\epsilon} = .37$

Y-Yielded zone

T-Tension cut-off zone

**FIG.6.8 MARCHING OF TENSION CUT-OFF
AND YIELDED ZONES**

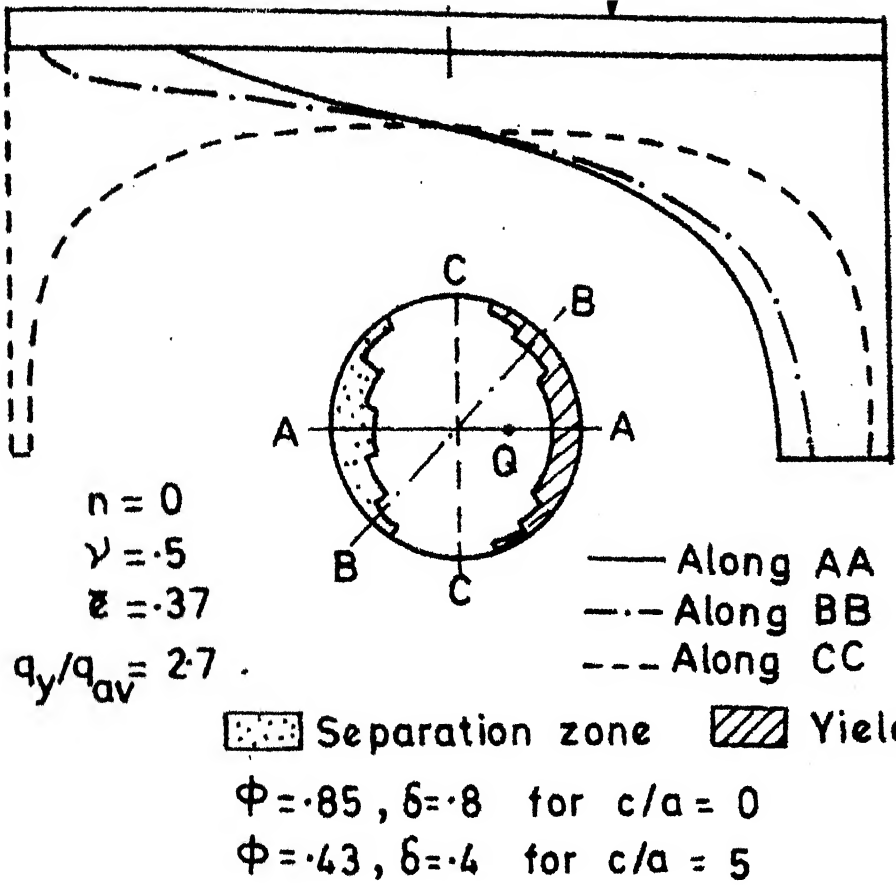


FIG. 6.9 TYPICAL CONTACT PRESSURES UNDER RIGID CIRCULAR FOOTING UNDER ECCENTRIC LOAD FOR $c/a=0$ AND $c/a=5$

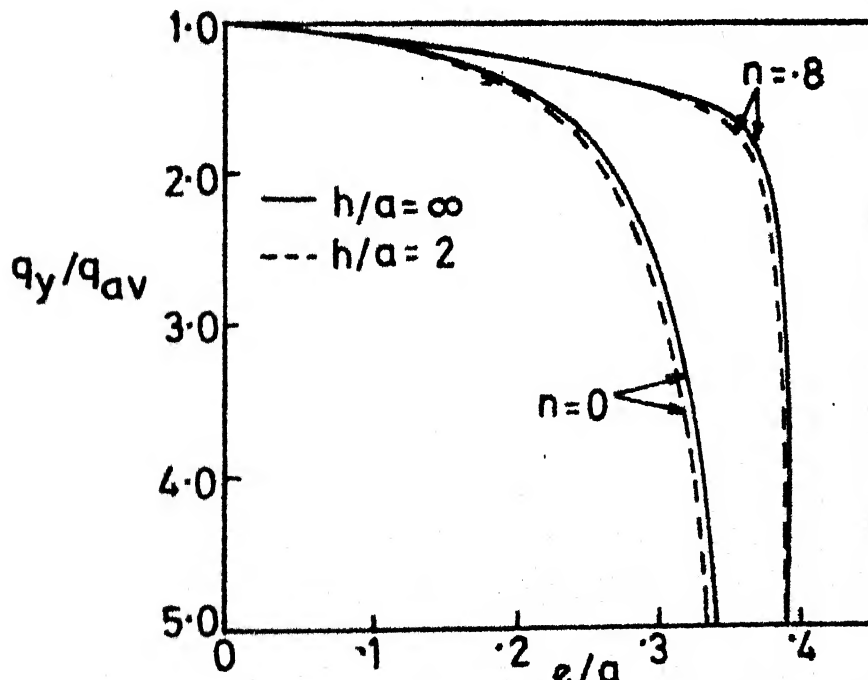


FIG. 6.10 LOAD ECCENTRICITY RELATION AT TENSION CUT-OFF CONDITION

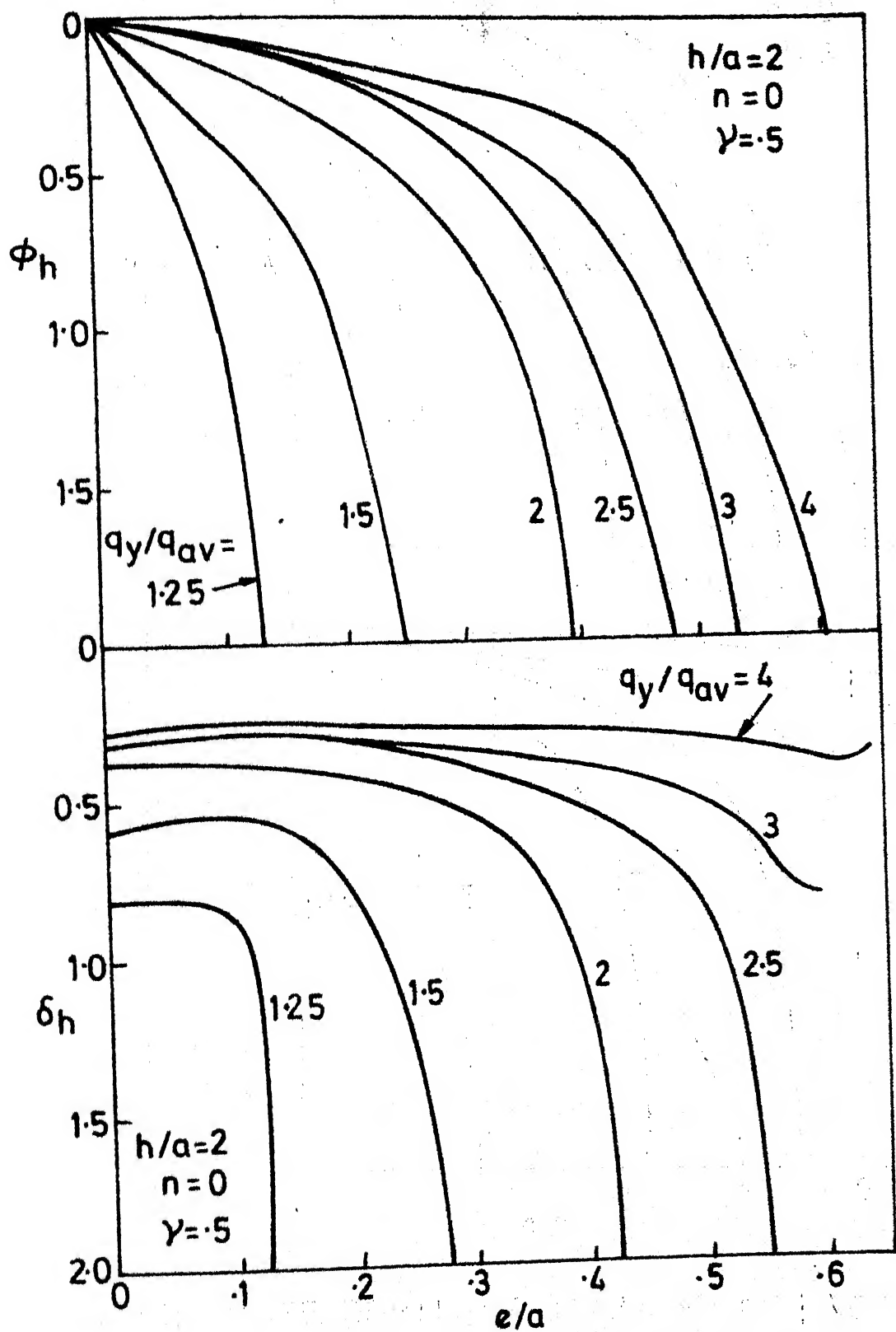


FIG. 6.11 FINITE DEPTH SETTLEMENT AND ROTATION FACTORS

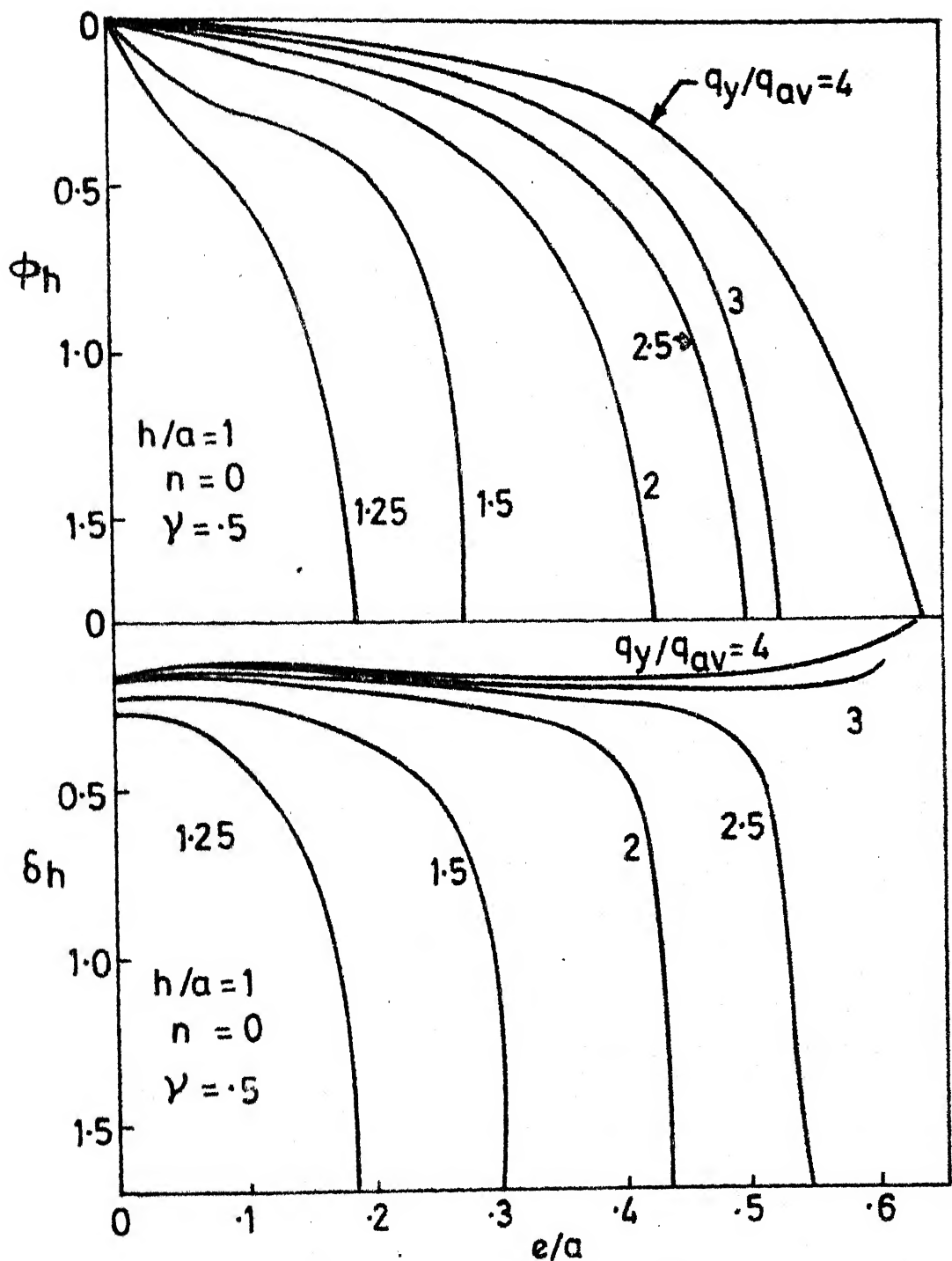


FIG. 6.12 FINITE DEPTH SETTLEMENT AND ROTATION FACTORS

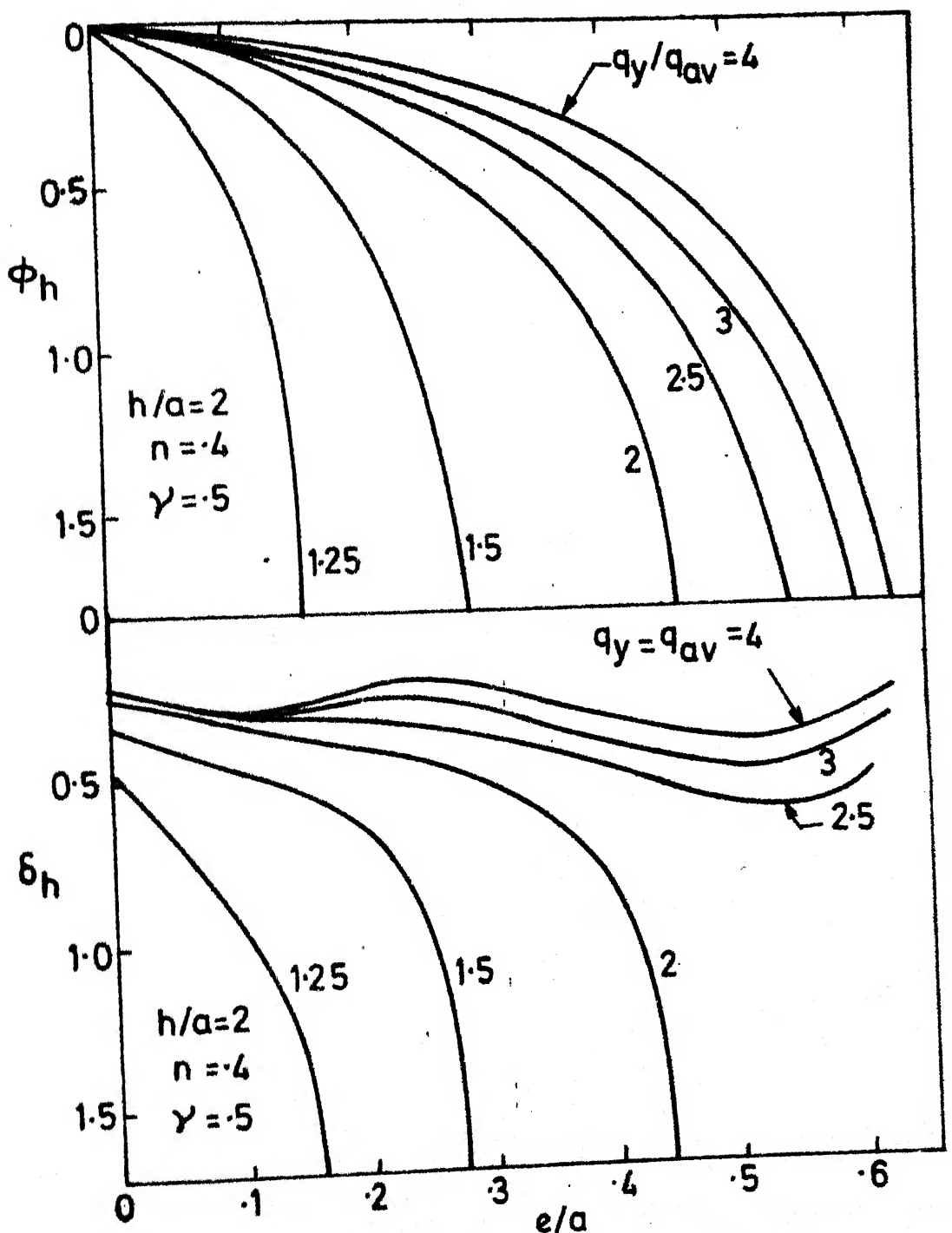


FIG. 6.13 FINITE DEPTH SETTLEMENT AND ROTATION
 FACTORS

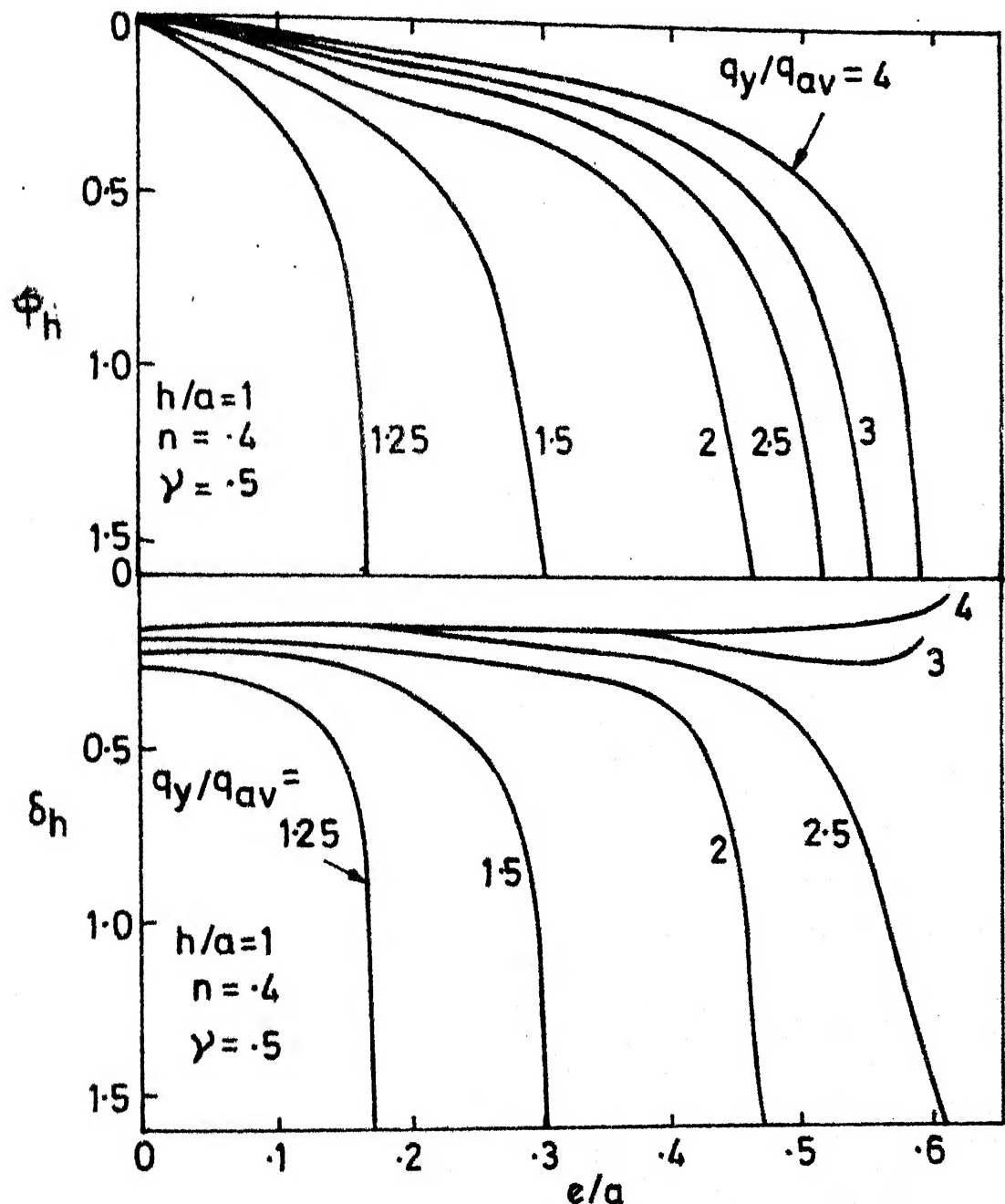


FIG. 6.14 FINITE DEPTH SETTLEMENT AND ROTATION FACTORS

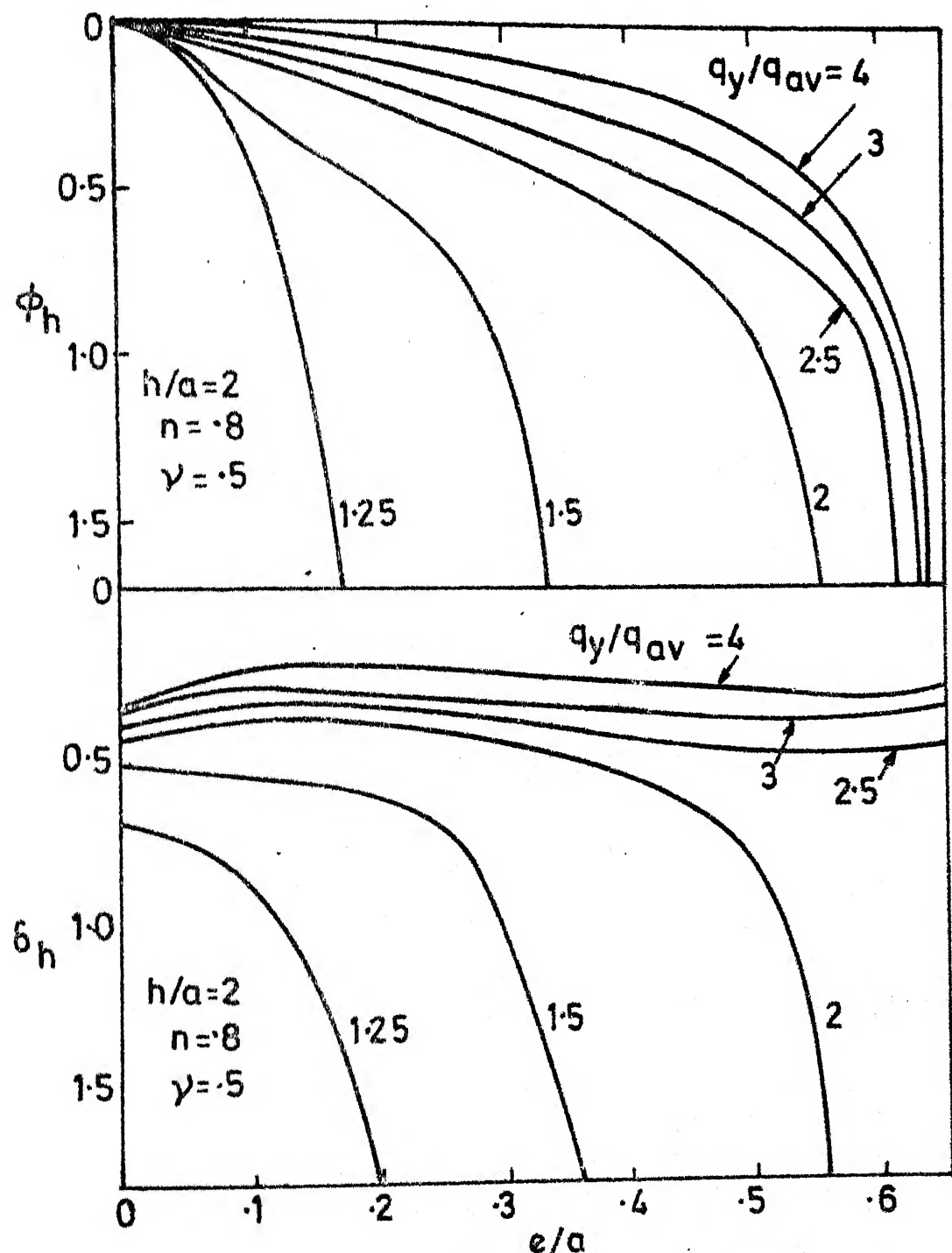


FIG. 6.15 FINITE DEPTH SETTLEMENT AND ROTATION FACTORS

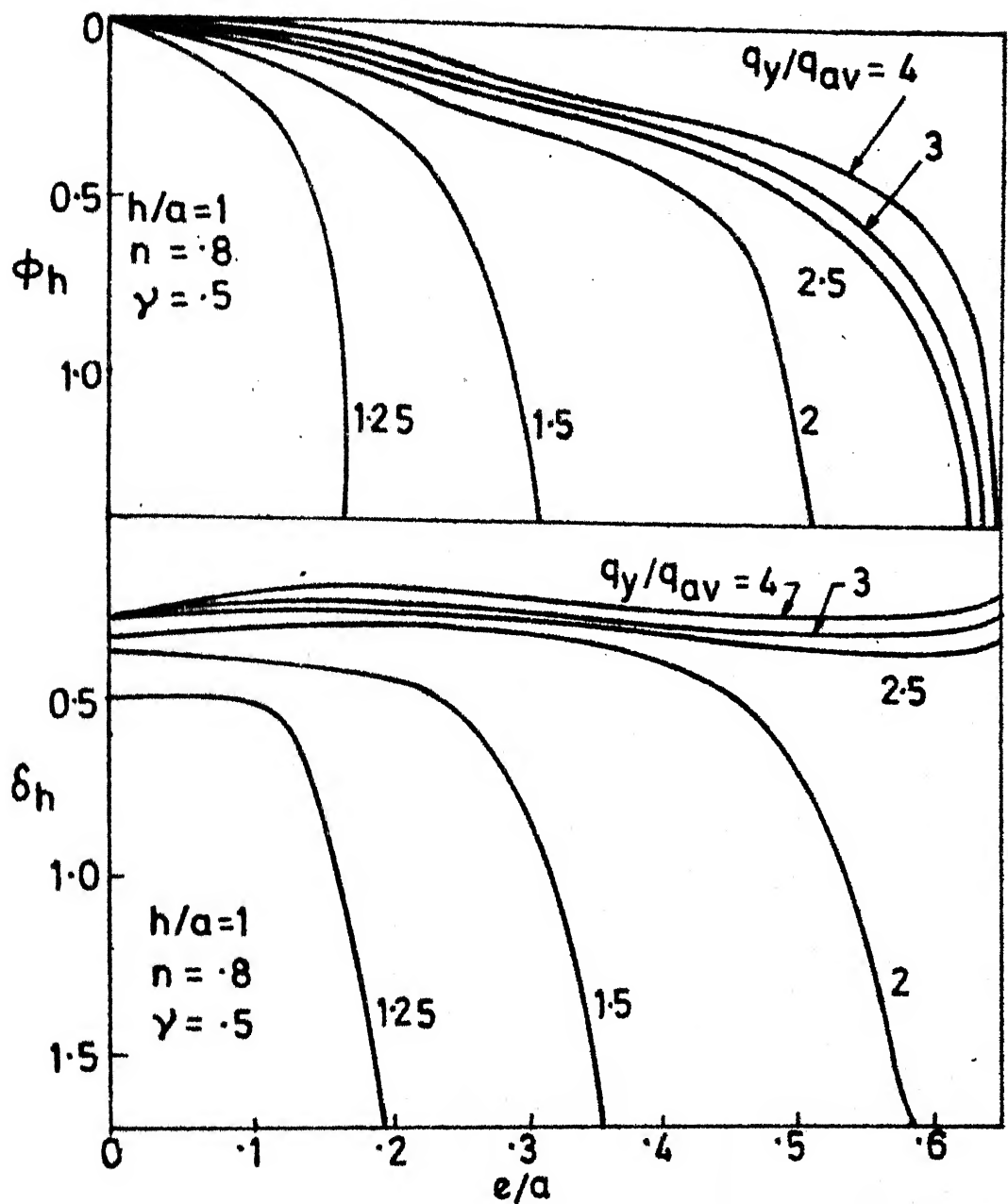


FIG. 6-16 FINITE DEPTH SETTLEMENT AND ROTATION FACTORS

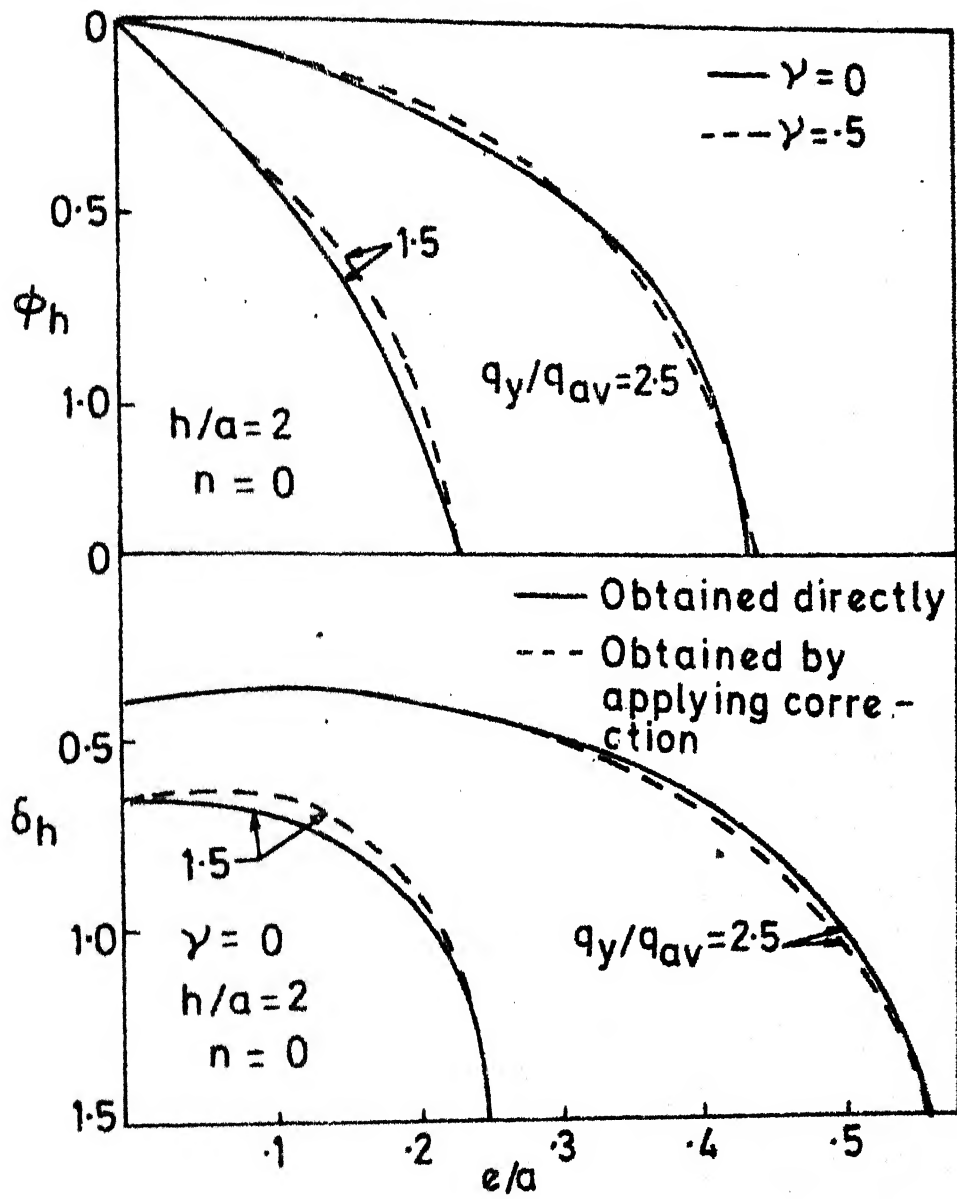


FIG. 6.17 EFFECT OF γ ON SETTLEMENT FACTORS FOR ECCENTRICALLY LOADED RIGID ANNULAR FOOTING ON FINITE DEPTH OF SOIL

CHAPTER 7

CONSOLIDATION SETTLEMENT OF ANNULAR FOOTINGS

7.1 INTRODUCTION

7.1.1 General

In addition to immediate or final settlements, the time rate of settlement is an important aspect requiring investigation for the purpose of predicting the behaviour of a footing with respect to time and for the purpose of design.

Although footings will have finite rigidity, it is convenient to study the extreme cases of fully flexible and fully rigid footings and these are the cases which are considered in this study. For a flexible or rigid footing, an aspect which needs due attention is the effect of period of construction on consolidation. Except for soils of very low permeability, a considerable amount of consolidation settlement takes place during the construction period itself. A study of this aspect is included in the present work with reference to annular footings.

Many types of soils, due to their formation process, are more permeable in the horizontal direction than in the vertical direction. Thus the effect of anisotropy also

needs consideration.

7.1.2 Consolidation Under Flexible Annular Footings

For the general three-dimensional consolidation analysis, two major types of approaches are available. The pseudo-three-dimensional approach (Terzaghi-Rendulic) assumes three-dimensional flow but one dimensional settlement caused due to flow of fluid only. This approach is comparatively simple and has been successfully used, to predict time-rate of settlements. For predicting the overall time-settlement response, this approach, after corrections to time scale etc., has been used for three-dimensional problems and it has been reported (Davis, 1969) that the results are fairly accurate when compared to the more rigorous approach (Biot). In this approach a simple Finite Difference numerical scheme can be used to solve the governing differential equation. The Terzaghi-Rendulic approach has been used by Madhav and Vitkar (1981) for flexible circular footings with special reference to period of construction and anisotropy of soil with respect to permeability. In the present work, the same approach is used for the analysis of consolidation of flexible annular footings.

In the other approach (Biot, 1941), the flow of fluid and the elastic displacements of the soil are treated together

as a coupled problem. The governing differential equation is complex enough and can be solved in closed form only under a number of simplifying assumptions; else the help of numerical techniques such as Finite Element Method is to be sought. Once the soil is discretized and FEM is applied, the pore pressures and displacements in the soil mass are obtainable at any time. The discretization in time domain involves the choice of a weightage coefficient which decides the variation of pore pressures between two time steps. Due to the discretization of soil mass and the necessity to modify and solve a large matrix, high computational costs are involved in this procedure. However for a study of pore pressures and three-dimensional displacements in a specific problem, the approach with FEM solution is the only choice. The manifestation of Mandel-Cryer effect is possible due to the coupling of flow and elastic deformation problems in the Biot's approach. This effect is not indicated in the Terzaghi-Rendulic approach in which the coupling is not there. However the difference between the two theories is never very large as far as the overall settlement response is concerned (Murray, 1978).

For the consolidation under a completely flexible circular raft quite a few solutions are available based on the simple diffusion theory (e.g. Gibson and Lumb (1953),

Davis and Poulos (1972)) as well as those based on Biot's theory (e.g. De Jong (1957), Mandel (1957, 1961), Paria (1957), McNamee and Gibson (1960), Gibson et al.(1970)). Madhav and Vitkar's (1980) solution takes into account the effects of construction time and anisotropy. However, no solution is found presently for consolidation under annular footing considering construction time and anisotropy with respect to permeability.

Enough evidence already exist (Davis, 1969) to show that there is good overall agreement between the results based on Biot's theory and Terzaghi-Rendulic theory in case of flexible circular (or strip) footings.

7.1.3 Consolidation Under Completely Rigid Annular Footings

The problem of consolidation under rigid footing becomes much more involved because of the conditional rigid settlement under the footing.

Analytical solutions for consolidation under rigid circular raft have been obtained by Agbezuge and Deresiewicz (1975) and Chiarella and Booker (1975). However these are for the condition of semi-infinite soil. No solution is found presently for the consolidation of finite layer under rigid annular (or even circular) footing taking into consideration construction time and anisotropy with respect to permeability.

The only available approach for this type of problem appears to be the FEM based on Biot's theory. Although it involves relatively higher computational cost, the contact pressure distribution, pore pressure distribution, deformation and stresses in the soil mass etc. can all be obtained by advancing the solution with respect to time. However, it is possible (as shown in the present work) to use the simpler Terzaghi-Rendulic approach and finite difference scheme of solution to tackle this type of problem, provided one is not interested in the spatial distribution of stresses and strains in the soil. The overall behaviour of consolidation settlement and the changes in contact pressure distribution which are the important aspects for the purpose of design can still be investigated. The limitations of the Terzaghi-Rendulic approach are noted.

The major considerations involved in dealing with consolidation under rigid footings are the requirement of uniform settlement and the consequent changes in contact pressure as consolidation proceeds and the changes in pore pressures which, in turn, are caused due to changes in contact pressures, in addition to those due to the process of consolidation. While these considerations are automatically handled in Biot's theory due to the coupling of flow and elastic deformation problems, they are to be indirectly introduced if the Terzaghi-Rendulic approach is used.

Firstly it must be recognized that the changes in contact pressure are mainly, if not entirely, due to the requirement of uniform settlement at all the times, under the rigid footing. This involves the response of the consolidating soil mass as a whole. The consolidation has to continue conditionally i.e. the Finite Difference scheme has to become implicit. Secondly, the changes in contact pressure have to introduce corresponding changes in pore pressures. It is found (D'Appolonia et al., 1971) that the pore pressures are predicted well as equal to octahedral total stresses calculated from the theory of elasticity. The calculation of changes in pore pressure due to changes in contact pressure at each time step would therefore involve elastic solution considering the elastic parameters of the soil and the geometry of the problem. The changes in pore pressure have been calculated in the present work on this basis and therefore a coupling, although indirect, has been achieved between the flow and the elastic deformation problems. Thus the changes in pore pressures due to consolidation, the changes in contact pressure and the consequent changes in octahedral total stresses in the soil mass and changes in pore pressures due to changes in contact pressure get implicitly coupled. Although ~~Mandel-Cryer effect is not manifested directly, changes in total stresses do take~~

place corresponding to changes in contact pressures. Due to all this, this approach, with the indirect coupling employed in the present work, is presumed to predict the behaviour of the rigid footing fairly accurately, as far as settlement and changes in contact pressure are concerned.

7.2 CONSOLIDATION SETTLEMENT OF FLEXIBLE ANNULAR FOOTING

7.2.1 Assumptions and Statement of the Problem

7.2.1.1 Assumptions

- (1) The consolidating layer of soil is homogeneous and of uniform thickness.
- (2) The consolidation is governed by Terzaghi-Rendulic theory.
- (3) The loading can be instantaneous or time-dependent, and in case of time-dependent loading, its variation is linear with time.
- (4) The soil is anisotropic only with respect to permeability.
- (5) The loading is uniform giving rise to axisymmetric problem.

7.2.1.2 Statement of the problem

A uniformly distributed load in the form of an annular ring of outer radius ' a ' and inner radius ' n_a ' is applied on a homogeneous layer of thickness ' h ' underlain by a rigid base (Fig.7.1(a)).

The load is applied in a linearly increasing manner (Fig. 7.2(b)) during the construction period t_c , which in non-dimensional form is expressed as

$$T_c = \frac{c_v t_c}{a^2} \quad (7.1)$$

where c_v is the coefficient of consolidation of the soil.

$T_c = 0$ refers to the case of instantaneous loading.

The following types of drainage conditions at the boundaries are considered:

- (a) IFIB - Impervious footing and base
- (b) IFPB - Impervious footing, pervious base
- (c) PTIB - Pervious top, impervious base
- (d) PTPB - Pervious top and base.

The anisotropy with respect to permeability is defined as

$$m = \frac{k_r}{k_z} = \frac{c_{vr}}{c_{vz}} \quad (7.2)$$

where r indicates radial (horizontal) direction, z indicates vertical direction, and k and c_v are the coefficient of permeability and consolidation respectively.

7.2.2 Analysis

For a homogeneous isotropic elastic soil, the general differential equation for 3-D consolidation is

$$\frac{\partial u}{\partial t} = c_3 \left(\frac{\partial^2 u}{\partial x^2} + \frac{\partial^2 u}{\partial y^2} + \frac{\partial^2 u}{\partial z^2} \right) + \frac{1}{3} \frac{\partial \theta}{\partial t} \quad (7.3)$$

where, θ is the total bulk stress ($= \sigma_x + \sigma_y + \sigma_z$),

c_3 is the three dimensional coefficient of consolidation

and u is the excess pore pressure.

The Terzaghi-Rendulic theory amounts to assuming $\frac{\partial \theta}{\partial t} = 0$, which is approximately valid for all practical purposes and is fairly accurate as far as overall consolidation process is concerned, (Davis, 1969). With this assumption, Eq. 7.3 written for axisymmetric case reduces to

$$\frac{\partial u}{\partial t} = c_3 \left(\frac{1}{r^2} \frac{\partial^2 u}{\partial r^2} + \frac{1}{r} \frac{\partial u}{\partial r} + \frac{\partial^2 u}{\partial z^2} \right) \quad (7.4)$$

The average degree of pore pressure distribution, U_p , on any selected vertical line is obtained, after solving Eq. 7.4, from the expression,

$$U_p = \frac{\int u(z,0)dz - \int u(z,t)dz}{\int u(z,0)dz} \quad (7.5)$$

where t refers to the instant under consideration and zero refers to reference time. The average degree of settlement, U_s , is approximately equal to U_p for 3-D case if the time scale is adjusted in such a way that the time factor is defined as (Poulos and Davis, 1972; Christian, 1972).

$$T = \frac{c_1 t}{a^2} \quad (7.6)$$

where c_1 is one dimensional coefficient of consolidation.

The governing differential equation for anisotropic axisymmetric case is,

$$\frac{\partial u}{\partial t} = c_{vr} \left(\frac{1}{r^2} \frac{\partial^2 u}{\partial r^2} + \frac{1}{r} \frac{\partial u}{\partial r} \right) + c_{vz} \frac{\partial^2 u}{\partial z^2} \quad (7.7)$$

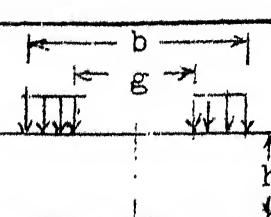
In the present study, it is necessary to know the initial excess pore pressures induced in the soil mass under a given loading on the surface. These can be obtained from the Henkel's empirical relation (D'Appolonia et al. (1971),

$$u = \sigma_{oct} + f \tau_{oct} \quad (7.8)$$

where f = a coefficient depending on the compressibility of soil.

A study by the author (Table 7.1) for consolidation under a strip footing showed that the effect of taking the term $f \tau_{oct}$ into consideration is quite less and it reduces as consolidation advances. If consolidation of two closely spaced strip footings is considered, a situation somewhat similar to ring footing, the effect of $f \tau_{oct}$ is slightly more but still quite small.

TABLE 7.1 : EFFECT OF τ_{oct} ON CONSOLIDATION UNDER FLEXIBLE STRIP LOADING

	b/h	g/h	Percentage degree of consolidation			
			f=0	f=.1	f=0	f=.2
	2	0	10.00	10.37	20.00	20.42
	1	0	10.00	10.18	20.00	20.10
	1	0.5	10.00	9.80	20.00	19.70

In the evaluation of pore pressures beneath an embankment, D'Appolonia et al. (1971) also observed that the pore pressures are predicted well by the relation, based on three dimensional theory of elasticity, between pore pressures and σ_{oct} only. Therefore, the initial pore pressures were obtained from the relation

$$u = \sigma_{oct} = \frac{\theta}{3} \quad (7.9)$$

where θ is the total bulk stress. The values of bulk stresses are easily obtained by numerical integration of available solutions from theory of elasticity (Poulos and Davis, 1974). Thus pore pressure (or the change in it) at any point in the soil mass can be expressed as the product of a constant coefficient and the load (or the load increment).

7.2.3 Solution Procedure

For solving the governing differential equation (7.7), it is written, using the usual Taylor's expansions and the approximations, in the Finite Difference form as

$$\begin{aligned} u_{i,j,t+\delta t} &= \beta \left\{ \left(\frac{\delta z}{\delta r} \right)^2 (u_{i,j+1,t} + u_{i,j-1,t} - 2u_{i,j,t}) \right. \\ &\quad + \frac{\delta z}{2r\delta r} (u_{i,j+1,t} - u_{i,j-1,t}) \\ &\quad \left. + \frac{c_{vz}}{c_{vr}} (u_{i+1,j,t} + u_{i-1,j,t} - 2u_{i,j,t}) \right\} + u_{i,j,t} \end{aligned} \quad (7.10)$$

$$\text{where, } \beta = \frac{c_{vr} \delta t}{(\delta z)^2} \quad (7.11)$$

On the axis of symmetry ($r=0$), Eq. 7.7 in Finite Difference form becomes,

$$u_{i,j,t+\delta t} = \beta \left\{ 2\left(\frac{\delta z}{\delta r}\right)^2 (u_{i,j+1,t} + u_{i,j-1,t} - 2u_{i,j,t}) \right. \\ \left. + \frac{c_{vz}}{c_{vr}} (u_{i-1,j,t} + u_{i+1,j,t} - 2u_{i,j,t}) \right\} + u_{i,j,t} \quad (7.12)$$

The time and time steps are given by

$$T = \frac{c_{vz} t}{a^2}; \quad \delta T = \frac{c_{vz} \delta t}{a^2} = \beta \frac{(\delta z)^2}{a^2} \cdot \frac{c_{vz}}{c_{vr}} \quad (7.13)$$

The soil mass is represented by a grid (Fig. 7.1(a)) made up of square units ($\delta r = \delta z$). A lateral extent to represent infinite soil mass with sufficient accuracy is chosen and the consolidation is marched forward through one time step using Eq. 7.12 and Eq. 7.13 and the given drainage conditions on the boundaries. The average load increment during the next time step is now applied so that additional pore pressures will be generated, which can be expressed as,

$$\delta u_{i,j} = b_{i,j} \cdot \delta p \quad (7.14)$$

where $b_{i,j}$ indicate coefficients of pore pressure generation and δp is the change in the imposed load ($\delta p = 0$ for instantaneous loading and $b_{i,j}$ depend only on the geometry

of the problem). The next time step is taken up after adding the pore pressures so generated to the existing pore pressures and the process is continued until consolidation is almost complete.

The finite difference grid and the time steps are so chosen that numerical stability and accuracy are achieved at reasonable computational cost. A value of $\beta = c_{vr} \delta t / (\delta z)^2 = .16$ was used and found satisfactory. A lateral extent of 5 times the outer radius of the ring was found to be sufficient to represent soil of infinite lateral extent.

7.2.4 Results and Discussion

7.2.4.1 General

Although the present work is oriented to solution of problems involving annular footings, some results were taken for circular footing and they were found to tally well with those of Poulos (1967). (Typical curves are shown in Fig. 7.2).

The settlement under the flexible footing is not uniform and the degree of settlement in all the cases herein refers to the maximum settlement below the annular footing.

The effects of various parameters are discussed below in brief.

7.2.4.2 Effect of drainage boundary conditions

Figure 7.3 shows for $T_c = 0$, $n=.75$ and $h/a = 4$ the effect of drainage boundary conditions on the rate of settlement. It is seen that the drainage boundary conditions have a significant effect on the rate of settlement (indicated by the degree of settlement U_s or degree of pore pressure dissipation U_p). IFIB and PTPB represent, as expected, the two extreme cases. For the particular case shown in Fig. 7.3, the degree of settlement, expressed as percentage, for PTPB case is about 29, 61 and 96 percent for $T = c_1 t/a^2 = .02, .2$ and 2 respectively, whereas the corresponding percentages for IFPB case are 6, 49 and 87 percent. The curves for IFPB and PTIB are found to lie between the two extreme cases. A similar trend exists for all values of T_c , n , h/a but the difference in rate of settlement due to drainage conditions is less for higher values of T_c , n and h/a .

IFPB case is similar to IFIB case in the early time range but approaches PTPB case towards the end of consolidation. PTIB is similar to PTPB at small times but approaches IBIB towards the end of consolidation, i.e. in the beginning of consolidation the permeability condition of the footing or the top surface dominates and towards the end of consolidation the permeability of the base

dominates. Since the IFPB and PTIB cases are intermediate between the extreme IFIB and PTPB cases, the latter are hereafter taken up for discussion unless otherwise mentioned.

7.2.4.3 Effect of radius ratio n

Figures 7.4(a) and 7.4(b) bring out the effect of n on time rate of consolidation settlement. From these figures it can be seen that a small opening at the centre of a circular footing (n less than about .25) has negligible effect on the rate of consolidation. As n increases, the consolidation tends to be faster, more so in case of IFIB case than PTPB case. As n approaches a large value closer to 1, the ring acts like a narrow strip footing and the consolidation is very rapid. For example, the degree of consolidation expressed as percentage, achieved at $T = 0.1$ is about 41.5, 51 and 66 percent for $n=.5$, .75 and .9 respectively for PTPB case ($h/a=4$, $T_c=0$). The corresponding Figures for IFIB case are 21, 34 and 58.5 percent.

The final maximum elastic settlement of a flexible ring footing with $=.9$, $h/a = 4$ (obtained by the author by numerically integrating tabulated values for point load (Poulos and Davis, 1974) is of the order of 27 percent of that for an equivalent circular footing (both the footings being of equal area and carrying equal load). For IFIB case, and $n = .9$, U_s from Fig. 7.4(a) is about .13 and .585

for $T = 0.01$ and 0.1 respectively. The corresponding figures for $n = 0$ are $.005$ and $.12$. Hence the settlements at $T = .01, 0.1$ and ∞ for $n = .9$ will be respectively about 7 , 1.3 and $.27$ times that for an equivalent circular footing. This shows the following two consequences which need attention from a practical point of view.

- (i) For ring footings, the consolidation settlement in the early stages is going to be faster in comparison to an equivalent circular footing.
- (ii) The settlement of a ring footing during the later major span of time will be much less in comparison to that of an equivalent circular footing.

7.2.4.4 Effect of Period of Construction T_c

Figure 7.5 shows the time-degree of settlement curves for $h/a = 4$ and 2 , IFIB and PTPB conditions, $n=.25, .5, .75$ and $.9$ and $T_c = .1, .5$ and 2 . The effect of time of construction on the nature of the time-settlement curves is appreciable. A higher value of T_c , which means slower rate of construction induces settlement at a slower rate. However, during the long time of construction a considerable amount of settlement takes place. This aspect has been brought out clearly in Fig. 7.6 in which the degree of consolidation achieved at the end of construction has been

plotted versus T_c . From Fig. 7.6, for PTPB and $h/a=2$ it can be seen that if the construction time $T_c = c_v t_c / a^2$ is equal to .1, about 60 percent consolidation would be over at the end of construction of a ring footing with $n = .9$. Some of the values are given in Table 7.2 for the purpose of comparison at a glance.

TABLE 7.2 : DEGREE OF CONSOLIDATION ACHIEVED AT THE END
OF CONSTRUCTION

h/a	Drainage Condition	T_c	Percentage Degree of Consolidation at T_c		
			n=.25	n=.5	n=.9
4	IFIB	0.1	5	10	38
		1.0	46	51	72
2	IFIB	0.1	6	12	45
		1.0	53	57	76
2	PTPB	0.1	33	37	60
		1.0	80	81	89

From Fig. 7.6 and Table 7.2 it is seen that the consolidation achieved during construction time is more for higher values of n and lower values of h/a .

Considering once again Fig. 7.5, it is seen that for higher values of T_c although consolidation is slower

initially, it becomes rapid some time before the end of construction (depending on T_c) and continues to show a somewhat fast rate of consolidation. For example, for $h/a=4$, $n=.5$, IFIB, the consolidation is advanced from 20 percent to 80 percent in time T of about 1.1 and 1.4 for $T_c = 0$ and $T_c = 0.5$ respectively. From Fig. 7.5 it can also be seen that the difference in time-settlement response in the extreme drainage cases IFIB and PTPB is lower for higher values of n , which means that narrow ring footings are less sensitive to drainage conditions, more so for higher values of h/a and higher values of T_c . In fact for very high values of T_c (greater than 5 for isotropic case), the curves for all values of h/a , n and all types of drainage conditions appear to merge into a single curve.

The charts as in Fig. 7.5 can be directly used to estimate the degree of settlement at any time for various values of depth of layer, outer and inner radii of loaded area and construction period T_c . Also charts, of Fig. 7.6 can be used directly to predict the degree of settlement at the end of construction.

7.2.4.5 Effect of depth of consolidating layer

Figure 7.7 brings out the effect of depth ratio h/a on the rate of consolidation settlement. When the depth of the consolidating layer is very small in comparison

to the dimensions of the loaded area, the consolidation except for IFIB case, is nearly one dimensional and the time required to attain a particular degree of consolidation is nearly in proportion to the square of the depth. However as the depth ratio h/a increase, the corresponding increase in time for attaining a particular degree of consolidation is lesser because of the three dimensional effect. For example, referring to Fig. 7.7, it can be seen that for $n=0.5$ and PTPB condition, the time for 80 percent consolidation with $h/a = 4$ is about 2.58 times and for $h/a = 10$ about 6.45 times that for $h/a = 2$; whereas, these figures for simple one dimensional consolidation would have been 4 times and 25 times respectively. The effect of h/a on rate of settlement is slightly lesser for higher values of n i.e. ring footings are less sensitive to h/a ratio than circular ones.

7.2.4.6 Effect of Anisotropy

The effect of anisotropy with respect to permeability, as defined in Eq. 7.2 , has been studied for instantaneous as well as linearly built up load. Figs. 7.8 shows typical curves for U_s versus $\log T$ for $m = 1$ (isotropic case), 10 and 100. The time-settlement characteristics change significantly as m increases from 1 to 10, this change being more for higher values of n . For values of m beyond about 10, the curves tend to become somewhat parallel to each other

for $T_c = 0$. However, it has not been possible to suggest a simple relationship to correlate the curves for various values of m even beyond $m = 10$.

Figure 7.8 also shows the U_s -log T curves for $m = 1, 10, 100$ and for $T_c = 0, .1$. It can be seen that the curves for various values of m tend to come closer to each other as T_c increases.

The curves such as in Fig. 7.8 can be directly used to estimate degree of settlement at any time for given values of h/a , n , T_c and m .

7.3 CONSOLIDATION SETTLEMENT OF RIGID ANNULAR FOOTING

7.3.1 Assumptions and Statement of the Problem

7.3.1.1 Assumptions

The assumptions contained in Section 7.2.1.1 except the last one about the loading are valid. In this case the assumption in connection with the loading (replacing (5) in 7.2.1.1) is as below.

The loading is in the form of a central load on a smooth rigid annular footing, giving rise to an axisymmetric problem.

7.3.1.2 Statement of the problem

It is the same as in Section 7.3.2.1 except that the footing is a smooth rigid footing carrying an axisymmetric

loading of any nature (Figs. 7.3).

7.3.2 Analysis

The governing differential equation for the consolidation process and the method of calculating pore pressures from elastic theory remain the same as for flexible footing and hence the analysis for the flexible footing remains valid. However two major factors required to be considered for the consolidation under rigid footing are:

- (1) The pore pressures generated due to external loading require revision at each time step since contact pressures under rigid footing keep on changing with time.
- (2) The consolidation process can not be explicitly marched forward in time since it has to incorporate the condition of uniform settlement under the rigid footing.

These major factors are incorporated in the solution procedure.

7.3.3 Solution Procedure

The consolidation under rigid footing has to continue in such a way that the settlement under the footing has to be uniform. To achieve this the contact

pressures must vary satisfying the following conditions:

- (1) Redistribution of contact pressures at each time step should take place so as to obtain a uniform change in degree of consolidation on vertical lines below the rigid footing under the combined effect of load increments (if any) and consolidation.
- (2) The overall change in contact pressure must be equal to the change in external loading during a time step.
- (3) The changes in contact pressure added up during the forward marching in time must yield the final contact pressure consistent with that obtained from elastic theory alone.

In order to couple the rigid-settlement of the rigid footing with the consolidation, the ring is divided into small annular rings (say, 'l' in number) and on each small ring, the contact pressure is assumed to be uniform (Fig. 7.9). Let δp_k indicate the average change in contact pressure for the k^{th} small ring, over a time step δT . Let $b_{k,i,j}$ indicate the coefficient of pore pressure generation such that at any nodal point (i,j) in the soil, the pore pressure generated due to incremental contact pressures on all the small rings is given by

$$\delta u_{i,j} = \sum_{k=1}^l b_{k,i,j} \delta p_k \quad (7.15)$$

Let t^+ indicate the instant just after the instantaneous pore pressure generation and just at the beginning of a consolidation step. The pore pressure at t^+ is given by

$$u_{i,j,t^+} = u_{i,j,t} + \delta u_{i,j} \quad (7.16)$$

Since changes in contact pressures and in pore pressures are introduced due to the rigid-settlement phenomenon in between the consolidation process the consolidation Eqs. 7.10 and 7.12 in finite difference form are firstly required to be modified using Eq. 7.16 above to get pore pressures at $t^+ + \delta t$ instead of at $t + \delta t$. Eqs. 7.10 and 7.12 after rearranging, will therefore be of the following form:

$$u_{i,j,t^++\delta t} = B_i + C_i \sum_{k=1}^1 \delta p_k \quad (7.17)$$

where corresponding to Eq. 7.10,

$$B_i = K_1 u_{i,j+1,t^+} + K_2 u_{i,j-1,t^+} + K_3 u_{i+1,j,t^+}$$

$$+ K_4 u_{i-1,j,t^+} + K_5 u_{i,j,t^+}$$

$$C_i = \sum_{k=1}^1 (K_1 b_{k,i,j+1} + K_2 b_{k,i,j-1} + K_3 b_{k,i+1,j} + K_4 b_{k,i-1} + K_5 b_{k,i,j})$$

$$K_1 = \beta \left(\frac{\delta z}{\delta r} \right)^2 + \beta \frac{\delta z}{2r\delta r}$$

$$K_2 = \beta \left(\frac{\delta z}{\delta r} \right)^2 - \beta \frac{\delta z}{2r\delta r}$$

$$K_3 = K_4 = \beta \frac{c_{vz}}{c_{vr}}$$

$$K_5 = -2\beta \cdot \frac{c_{vz}}{c_{vr}} \left(\frac{\delta z}{\delta r} \right)^2 - 1$$

Similarly, values of B_i and C_i can be written corresponding to Eq. 7.12.

The common change of degree of consolidation (assumed equal to change of degree of settlement) along any vertical line below the rigid footing is given by

$$\delta u = \frac{\int u_i(z,0) dz - \int u_i(z,t^+) dz}{\int u_i(z,0) dz} \quad (7.18)$$

where u_i indicates pore pressures on i^{th} vertical line.

The integrations are carried out numerically so that if 's' is the number of nodes on each vertical line, and if g_j indicates the coefficient of numerical integration for j^{th} node on the vertical line,

$$\int u_i(z,0) = \sum_{j=1}^s (u_{i,j,0} \times g_j) \quad (7.19)$$

$$\text{and } \int u_i(z,t^+) = \sum_{j=1}^s (u_{i,j,t^+} \times g_j) \quad (7.20)$$

In case of time dependent loading, the zero in Eq. 7.19 and in the numerator of Eq. 7.18 is to be replaced by the time at the beginning of the time step.

Indicating $\sum(u_{i,j,o} \times g_j)$ by U_{oi} and combining Eqs. 7.15 through Eq. 7.20, the following form of equation is obtained

$$C'_i \sum_{k=1}^l \delta p_k - U_{oi} \delta U = B'_i \quad (7.21)$$

where C'_i are known quantities in terms of coefficients of pore-pressure generation and coefficients of numerical integration and B'_i are known quantities in terms of pore pressures at the beginning of a time step.

The above equations are written for 'l' number of selected vertical lines below the rigid footing. One more equation is written for overall equilibrium of the footing

$$\sum_{k=1}^l A_k \delta p_k = \delta W \quad (7.22)$$

where A_k is the area of k^{th} small ring, δp_k is the corresponding change in contact pressure and δW is the change (if any) in the external load during a time-step under consideration,

Eqs. 7.21 and 7.22 are combined and written in the matrix form as,

$$\begin{bmatrix} d_{11} & d_{12} & \dots & \dots & U_{o1} \\ d_{21} & d_{22} & \dots & \dots & U_{o2} \\ \dots & \dots & \dots & \dots & \dots \\ \dots & \dots & \dots & \dots & \dots \\ d_{l1} & d_{l2} & \dots & \dots & U_{ol} \\ A_1 & A_2 & \dots & A_l & 0 \end{bmatrix} \begin{Bmatrix} \delta p_1 \\ \delta p_2 \\ \vdots \\ \vdots \\ \delta p_l \\ \delta U \end{Bmatrix} = \begin{Bmatrix} e_1 \\ e_2 \\ \dots \\ \dots \\ e_l \\ \delta W \end{Bmatrix} \quad (7.23)$$

In the above Eq. 7.23 , the matrix coefficients are derived from C'_i and are therefore calculated only once. The R.H.S. vector is derived from known pore pressures at the beginning of a time step and hence Eq. 7.23 is to be solved at each time step to get values of changes in contact pressure and change in degree of consolidation (settlement) of the rigid footing. The incremental pore pressures are evaluated using Eq. 7.15 and are added, after applying a weightage coefficient α as required in coupled problems involving time (Desai and Christian, 1977) to the original pore pressures and consolidation is advanced through a time-step. The process is continued until consolidation is almost complete. Fig. 7.10 shows the flow-chart for the computations involved.

7.3.4 Results and Discussion

7.3.4.1 General

The computer programme developed for this Chapter of the thesis is a general one covering flexible as well as rigid footings and for the latter, provision is made to generate a matrix, triangularize it and use it at the beginning of each time step. The size of the matrix is quite small being equal to the number of rings into which the footing is subdivided plus one (Eq. 7.23).

The soil is discretized as for flexible footing and as mentioned in Section 7.2.4.1 (Fig. 7.9).

The increase in contact pressures near the edge is critical since it may introduce increase in bending moment; hence the study and discussion is oriented to signify this aspect. The increase is found to be maximum for IFIB case of drainage and for instantaneous loading ($T_c = 0$) and the discussion refers to these cases unless otherwise stated.

The discussion made in Sections 7.2.4.2 to 7.2.4.5 applies broadly to rigid footings also.

7.3.4.2 Changes in contact pressure distribution

The ratio of contact pressure p to average contact pressure p_0 (total load divided by area of footing) is plotted versus dimensionless time factor T in Figs. 7.11 to 7.14. In Fig. 7.11, the contact pressure at a value of $T = .0225$ is shown for a ring footing ($h/a=2$) and at $T = .08$ for a circular footing ($h/a = 2$). At these time factors, the contact pressure shows an increase at the outer and inner edges of the ring footing and at the outer edge of the circular footing. In both the cases, the contact pressure away from the edge/edges has decreased. This change in the distribution is unfavourable from the point of view of moments induced in the footing. Figs. 7.12, 7.13

and 7.14 show the peaks of contact pressure averaged over the one fifth annular portion near the outer edge of the footing. In Fig. 7.12(a) the effect of h/a is brought out. It is seen that the maximum (peak) values of contact pressure are higher for larger values of h/a , the values of p/p_0 for $n=0$, $T_c=0$ being about 1.9, 1.84 and 1.61 for $h/a = 8, 4$ and 1 respectively. They work out to an increase of about 14, 12 and 9.5 percent over the initial contact pressures (which are already high near the outer edge). It is also seen that the peaks are attained at about $T = 0.08$ for the cases considered.

The peak p/p_0 values obtained from Fig. 7.12(b) for $h/a = 1$, $n=0$, $T_c = 0$ are about 1.61, 1.59, 1.58 and 1.56 for IFIB, PTIB, IFPB and PTPB boundary drainage conditions respectively. This shows that IFIB is the most critical condition.

Figure 7.13 shows the changes in contact pressures for $T_c = 0$, $n = 0$, IFIB, for the central ring and for an annular portion near the half radius of the circle. The average over one fifth width is plotted in this figure also. Whereas the edge contact pressures increase, attain a peak and decrease with time, the contact pressures away from the outer edge decrease, attain a minimum and then increase. This happens because the total load on the footing remains constant. It is seen from this figure that the minima do

not occur simultaneously with the peaks of outer edge pressures. For example, for $h/a = 2$, the peak of outer edge pressure occurs at about $T = 0.08$ (Fig. 7.12) whereas the minimum values at the central ring and at the half radius reach at about $T = 0.2$ and $T = 0.1$ respectively. This means that the most unfavourable contact pressure distribution may or may not coincide with the peaking of outer edge contact pressure. From the same figure (Fig. 7.13) it is seen that the contact pressures near the centre show a maximum decrease and that too for higher values of h/a . For example, for $h/a = 8$, the contact pressure near the centre drops from about .5 to .39 times average pressure on the footing.

Figure 7.14 shows the effect of radius ratio n on the changes in edge contact pressures. The peak p/p_0 values are about 1.915, 1.856 and 1.796 for $n=.5$, .2 and 0 respectively. These work out to an increase of about 13.3, 11.8, and 10.9 percent over initial values of edge contact pressure for $n = .5$, .2 and 0 respectively. This shows that the increase is more for higher values of n . However for a ring footing the bending moments are already less than those for a circular footing. Hence the change in contact pressure will be more critical for circular footings than for ring footings.

For an actual footing, the increase in contact pressure will not be so much as indicated in the preceding paragraphs because of several reasons:

- (i) The footing will have finite rigidity and hence the value of increase in edge contact pressure will lie inbetween that of perfectly rigid footing as analysed in this chapter and zero for fully flexible footing. (Also the initial edge contact pressure itself will be lower for flexible footings than for rigid footings).
- (ii) The real construction time being greater than zero, the peak values will drop (This aspect is discussed later).

Figure 7.15 shows the comparison between contact pressure changes for strip footing obtained from the present analysis applied to strip footing and from Biot's theory using the computer programme given by Verruijt (1977). The agreement is fairly good.

7.3.4.3 Effect of infinite rigidity in comparison to infinite flexibility on time rate of settlement

The present study shows that the consolidation under rigid ring footing with IFIB drainage condition would be faster than that under a uniformly loaded flexible footing

for the same drainage condition except towards later stages of consolidation when it becomes slightly slower (curves for $n = 0$). For $n = .5$ the difference is not much. The reason for faster consolidation under rigid ring footings (circular as a particular case) is that the high edge pressures, which also increase initially, increase the flow near the edges. The preferential outward radial flow under an axisymmetric loading is further accelerated due to high edge pressure at the outer edge.

In the cases shown in Figs. 7.16(a) and 7.16(b) the difference in the degree of settlement for rigid and flexible footings for the case of $T_c = 0$ is appreciable only in the earlier stages (T less than about .4), and this difference is less for higher values of h/a . In Fig. 7.16(b) the curves for $T_c = .5$ are also shown from which it is seen that for this T_c , the difference in the time rate of settlements for rigid and flexible footings is quite small as compared to that for $T_c = 0$. At high values of T_c (≥ 2) the behaviour of flexible and rigid footings with respect to time rate of settlement, is almost identical.

A comparison with available result for a rigid circular footing on semi-infinite soil (Agbezuge and Dercsiewicz, 1975) with the result from the present study for deep layer of soil is shown in Fig. 7.2. The agreement is seen to be good.

7.3.4.4 Effect of radius ratio n

Consolidation is faster for higher values of n in a way very similar to that for flexible footing (discussed in Section 7.2.4.3). The peaks in contact pressure show a higher percentage increase over initial values with higher values of n (Fig. 7.14 and discussion in Section 7.2.4.2). Fig. 7.17 also brings out this aspect. For $T_c = 0$, the percentage increase in edge contact pressure (taken over one fifth width of ring) is 113.0, 111.9 and 110.9 for $n = .5, .2$ and 0 respectively. Therefore the effect of increase in edge pressures on bending moments in the footing will be slightly more for higher values of n. However, as mentioned earlier, the moments are already lower for higher values of n. (For example for relative rigidity of 10, the nondimensional design moments ($M_d/q_y a^2$) for uniformly loaded footings for $h/a = 2$ are about .0205, .029 and .032 for $n = .5, .2$ and 0 respectively (Chapter 4)).

7.3.4.5 Dependence of peak contact pressure on construction time T_c

Figure 7.17 shows the effect of T_c on peak values. The figures in parentheses express the increase, in percentage, of peak contact pressure value, averaged over one fifth width of footing, over the initial contact pressure. The increase is less for higher values of T_c .

as expected, but the increase in peak contact pressure drops significantly for higher values of n . For example, the increase drops from 110.9 to 109.8 for $n = 0$ and from 113.0 to 108.7 for $n = .5$ as T_c increases from 0 to .2. Since T_c will be greater than zero in actual practice, the increase in contact pressures will not be as severe as for $T_c = 0$ and much less for higher values of n . This again goes in favour of providing footings with higher values of n .

7.3.4.6 Effect of anisotropy with respect to permeability

Figure 7.18 shows the effect of anisotropy on the time rate of settlement behaviour for a particular case of $h/a = 2$, $n = .5$, IFIB. The curves for flexible footing are also shown (dotted lines) for comparison. It is seen that consolidation is faster, for higher values of m ($m = k_r/k_z = c_{vr}/c_{vz}$) as expected. It is seen that the curves for m value more than 10 are somewhat parallel to each other. However it is not possible to suggest a simple correlation. The difference in behaviour of rigid and flexible footings shows the same trend as for isotropic case i.e., the consolidation for rigid annular footing being faster than that for uniformly loaded flexible footing, in the earlier period of consolidation.

Figure 7.19 shows the effect of anisotropy on peak values of contact pressure. It is seen that the increase in contact pressure at peaks (shown in parenthesis) is reduced with higher values of n . However, the difference is small and it could be said that anisotropy has little effect on peak contact pressures.

7.4 CONCLUSIONS

- (1) The consolidation settlement under flexible and rigid annular footings has been investigated using Terzaghi-Rendulic theory. For rigid footings, the flow due to consolidation is linked up with elastic behaviour of soil mass through pore pressure generation and the conditional uniform settlement.
- (2) Plots for time-settlement response for various parameters including construction time and degree of anisotropy are presented which could be used for the design of annular footings.
- (3) The consolidation under a flexible annular footing is faster for higher values of n especially in the earlier stages of consolidation.
- (4) Considerable consolidation settlement takes place by the end of the construction period, especially for higher values of n and lower values of depth of consolidating layer.

- (5) Ring footings are less sensitive to h/a ratio than circular ones in regard to time rate of settlement.
- (6) Anisotropy with respect to permeability has a significant effect on the time rate of settlement.
- (7) The contact pressure changes during the consolidation settlement of a perfectly rigid annular (or circular) footing are not insignificant. For ring footings, the peak percentage increase in edge contact pressures is slightly higher than for circular footings.
- (8) The peak contact pressures decrease considerably if time of construction is taken into account.
- (9) Consolidation under rigid annular (or circular) footings is faster than that under flexible footings in the initial stages (T less than about .4). Later the difference is quite less.

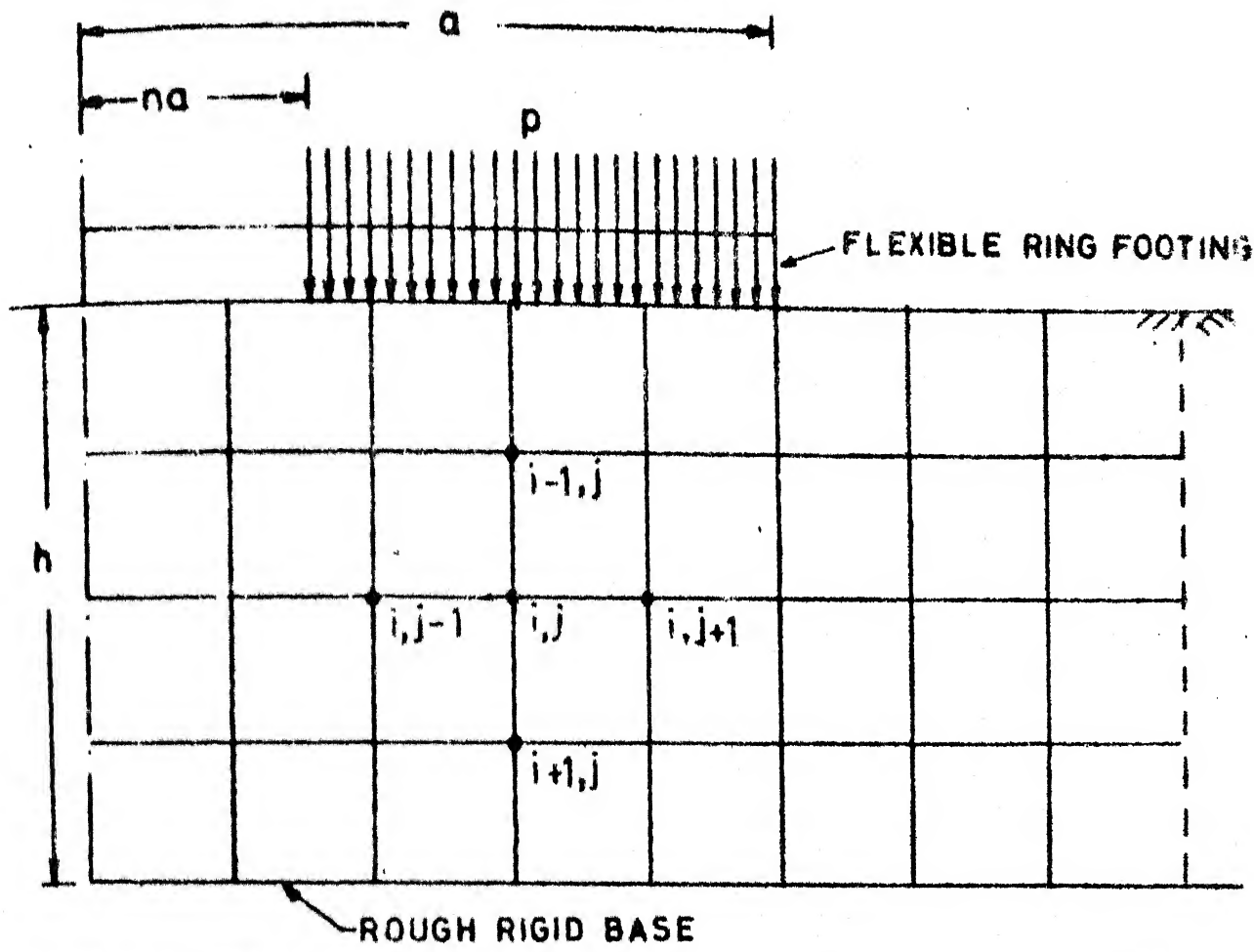


FIG.7.1(a) FLEXIBLE RING FOOTING ON A CONSOLIDATING FINITE LAYER AND FINITE DIFFERENCE GRID

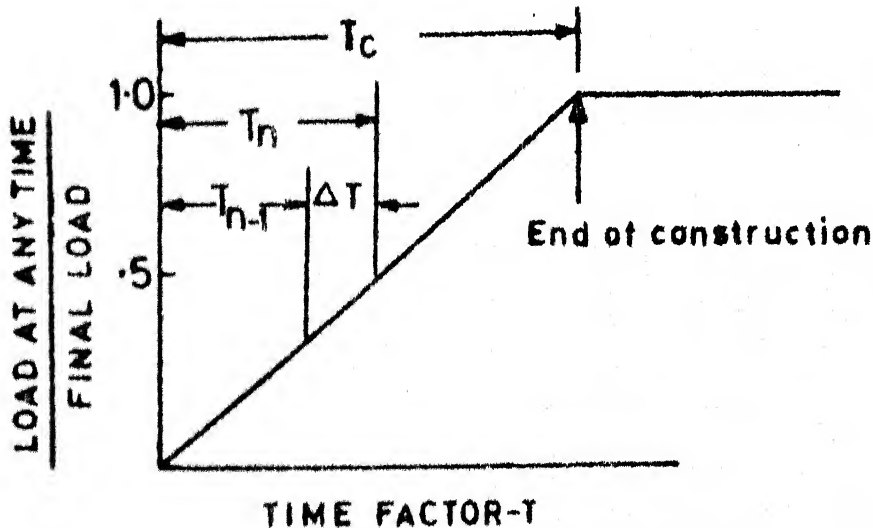


FIG.7.1 (b)

VARIATION OF CONSTRUCTION LOAD

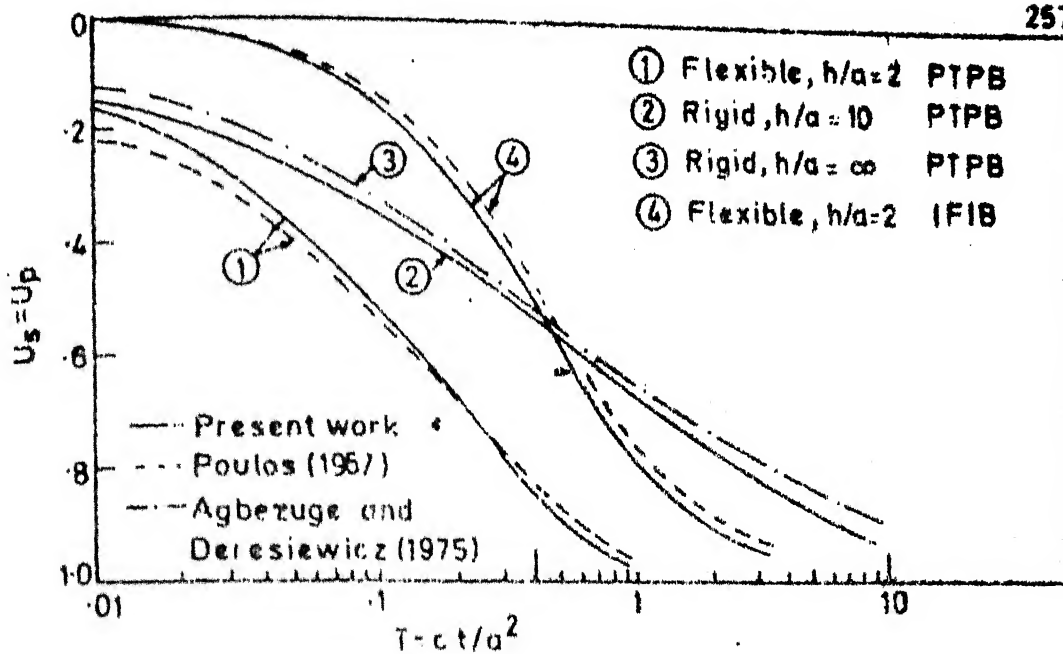


FIG.7.2 COMPARISON OF TYPICAL RESULTS FOR
CONSOLIDATION UNDER CIRCULAR FOOTING

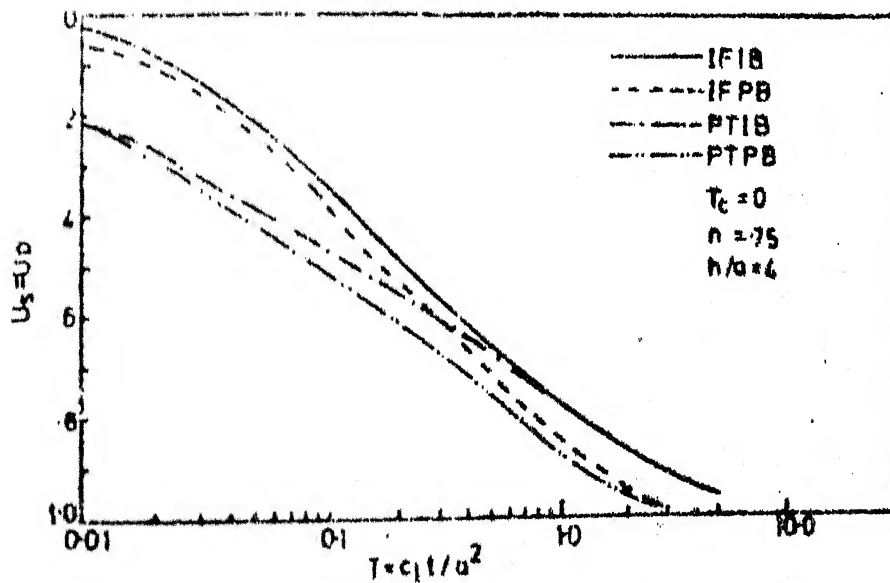


FIG.7.3 FLEXIBLE FOOTING-EFFECT OF
DRAINAGE BOUNDARY CONDITIONS

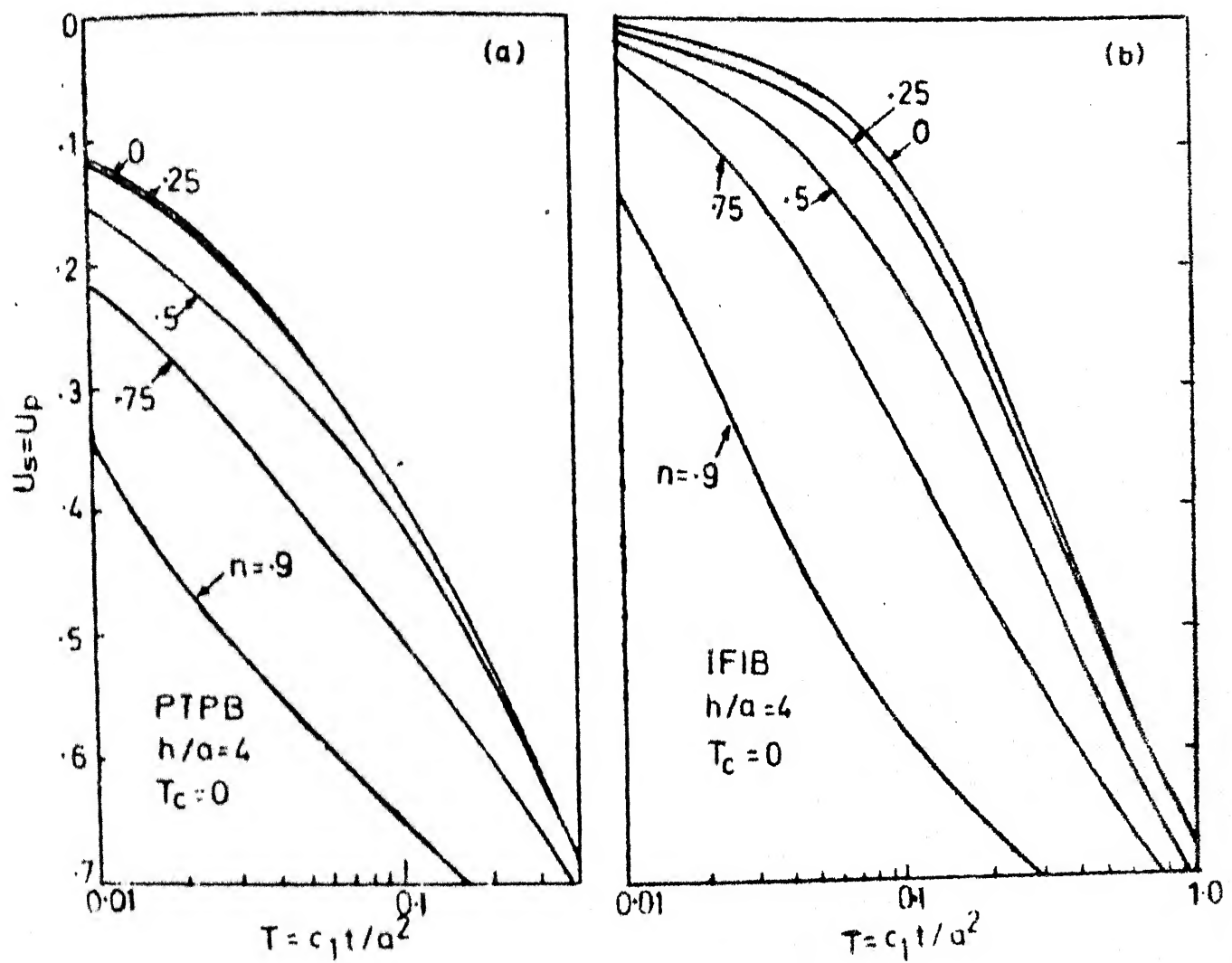


FIG.7.4 FLEXIBLE FOOTING-EFFECT OF RADIUS RATIO

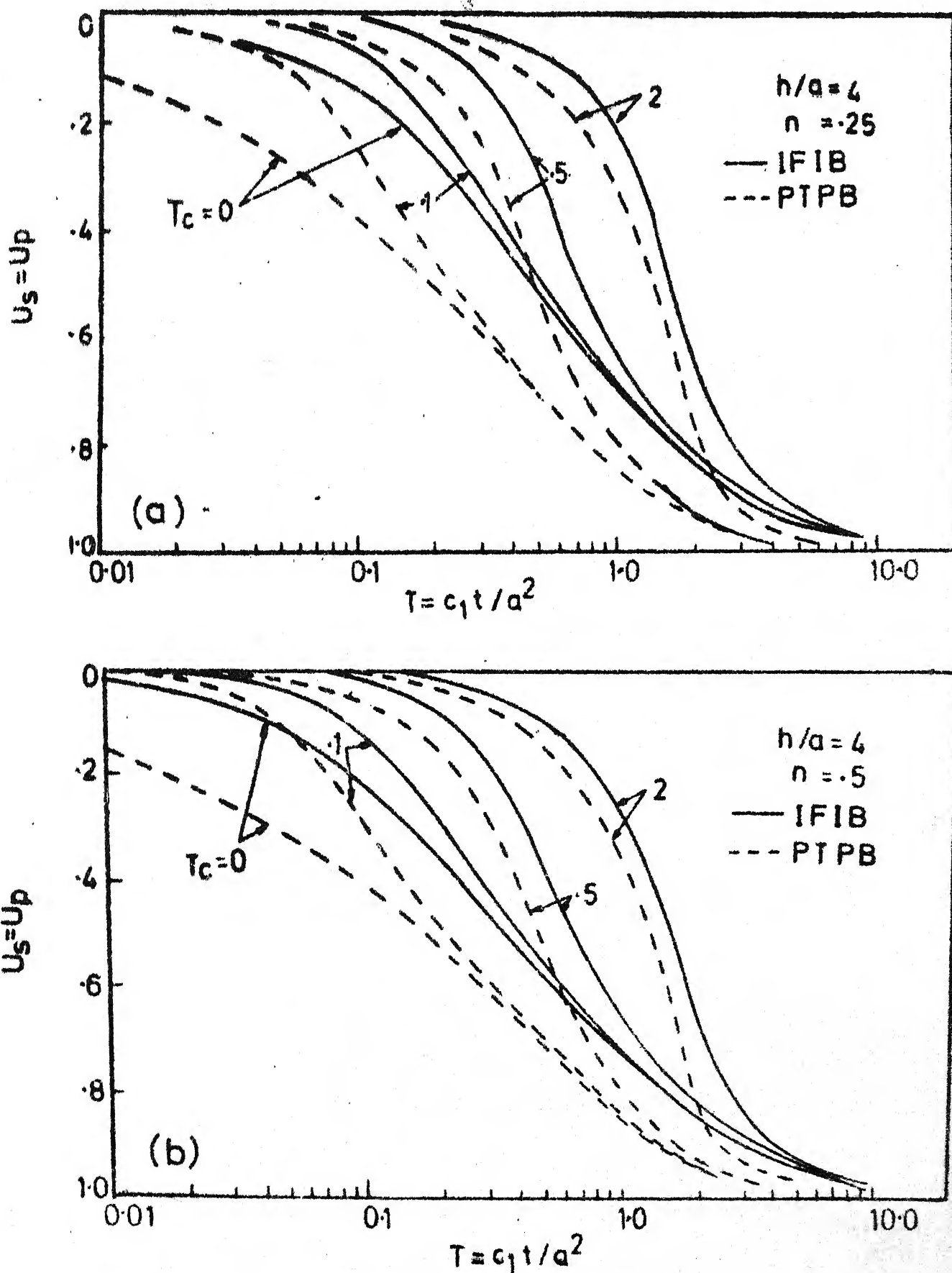


FIG. 7.5 CONSOLIDATION OF FLEXIBLE RING FOOTING UNDER CONSTRUCTION LOADING

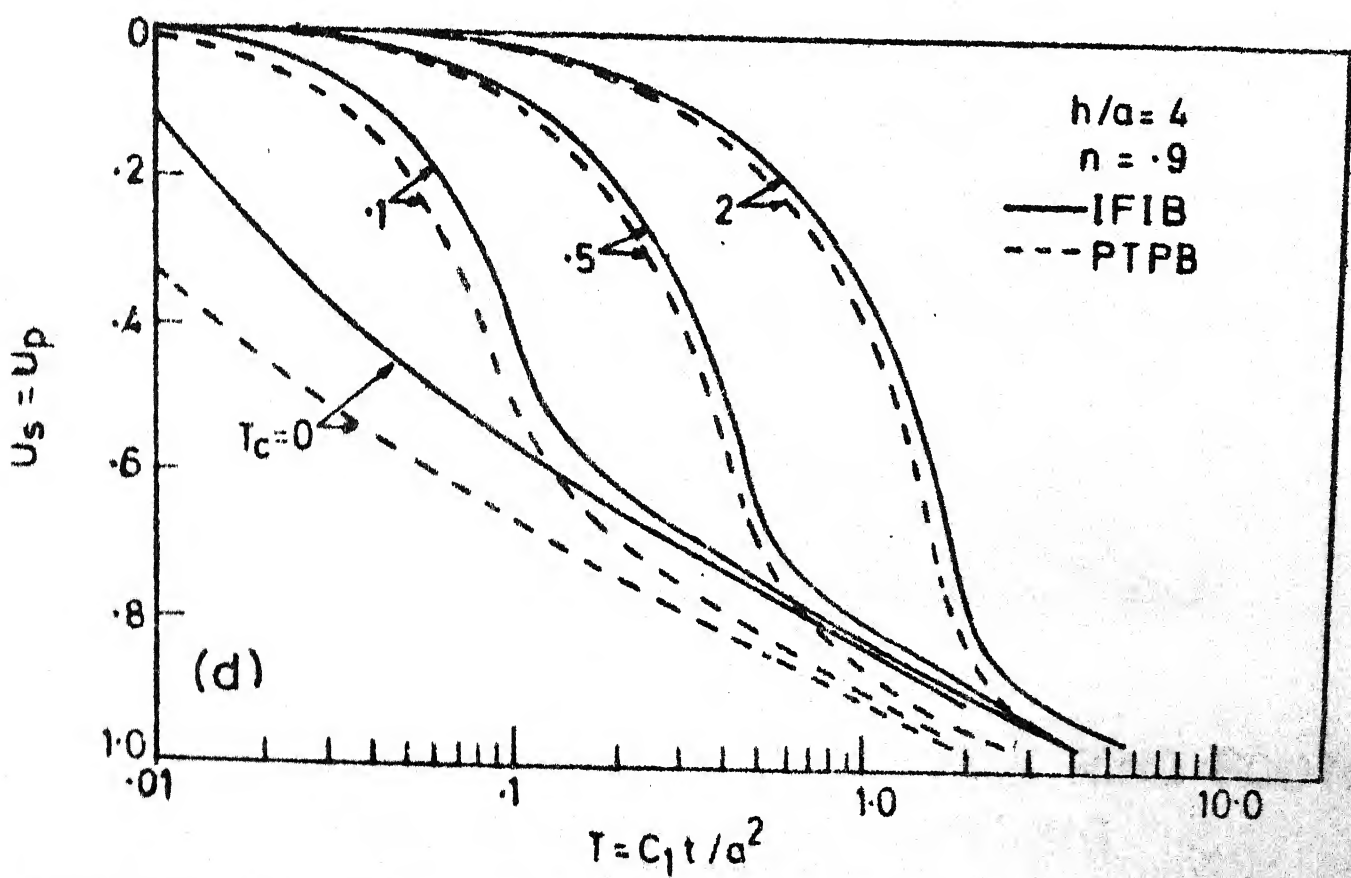
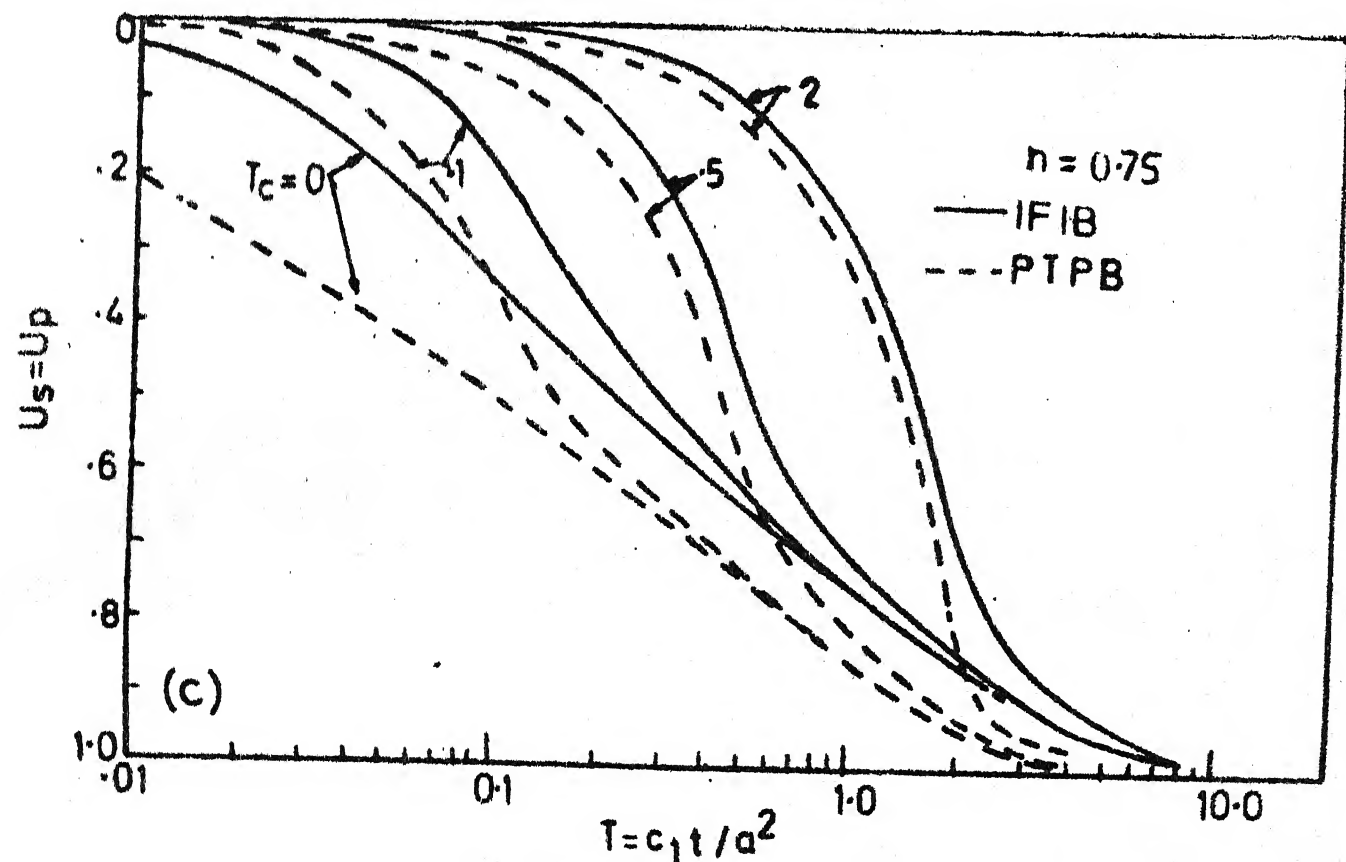


FIG.7.5 CONSOLIDATION OF FLEXIBLE RING FOOTING
UNDER CONSTRUCTION LOADING

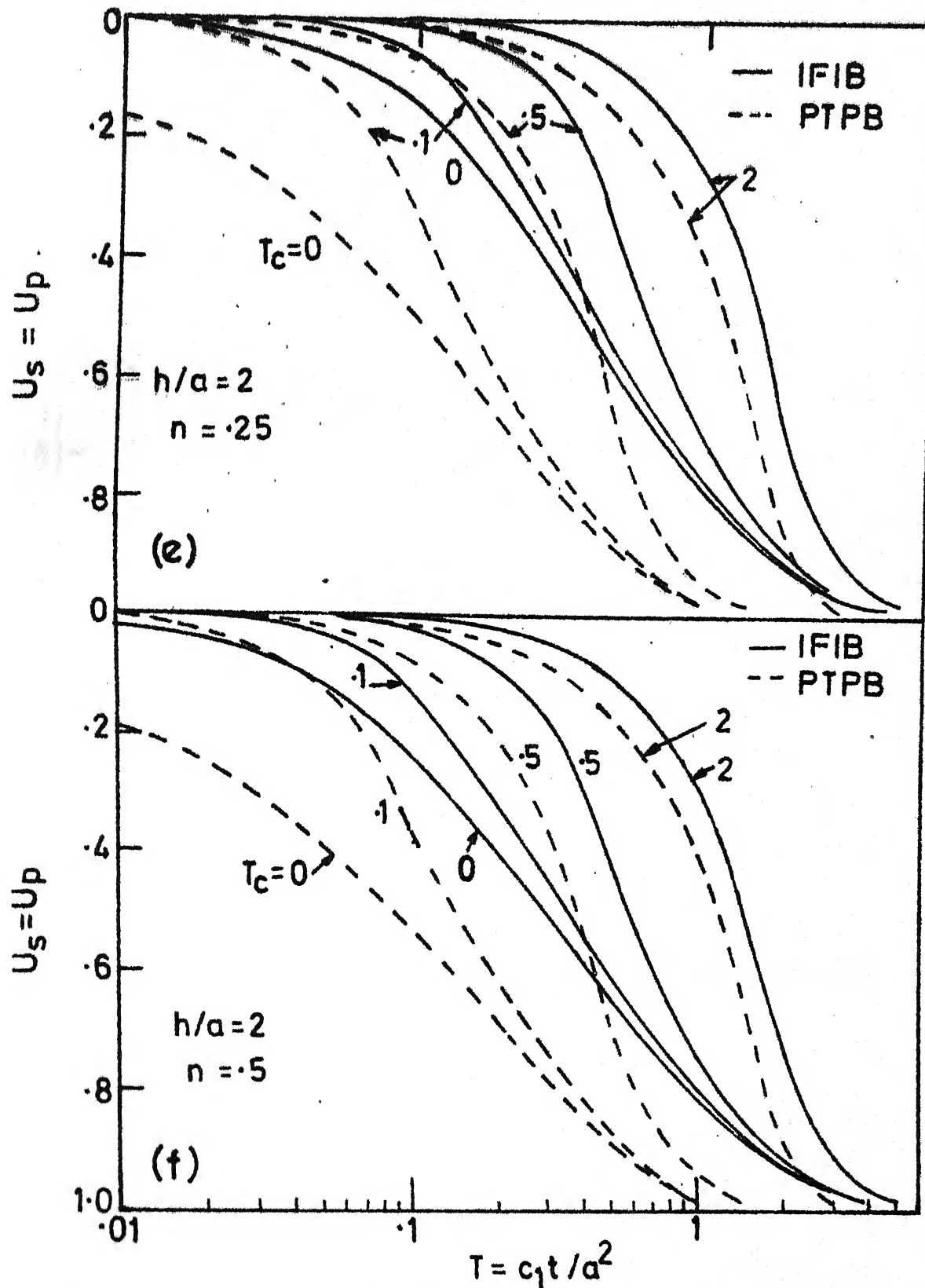


FIG. 7.5 CONSOLIDATION OF FLEXIBLE RING FOOTING
UNDER CONSTRUCTION LOADING

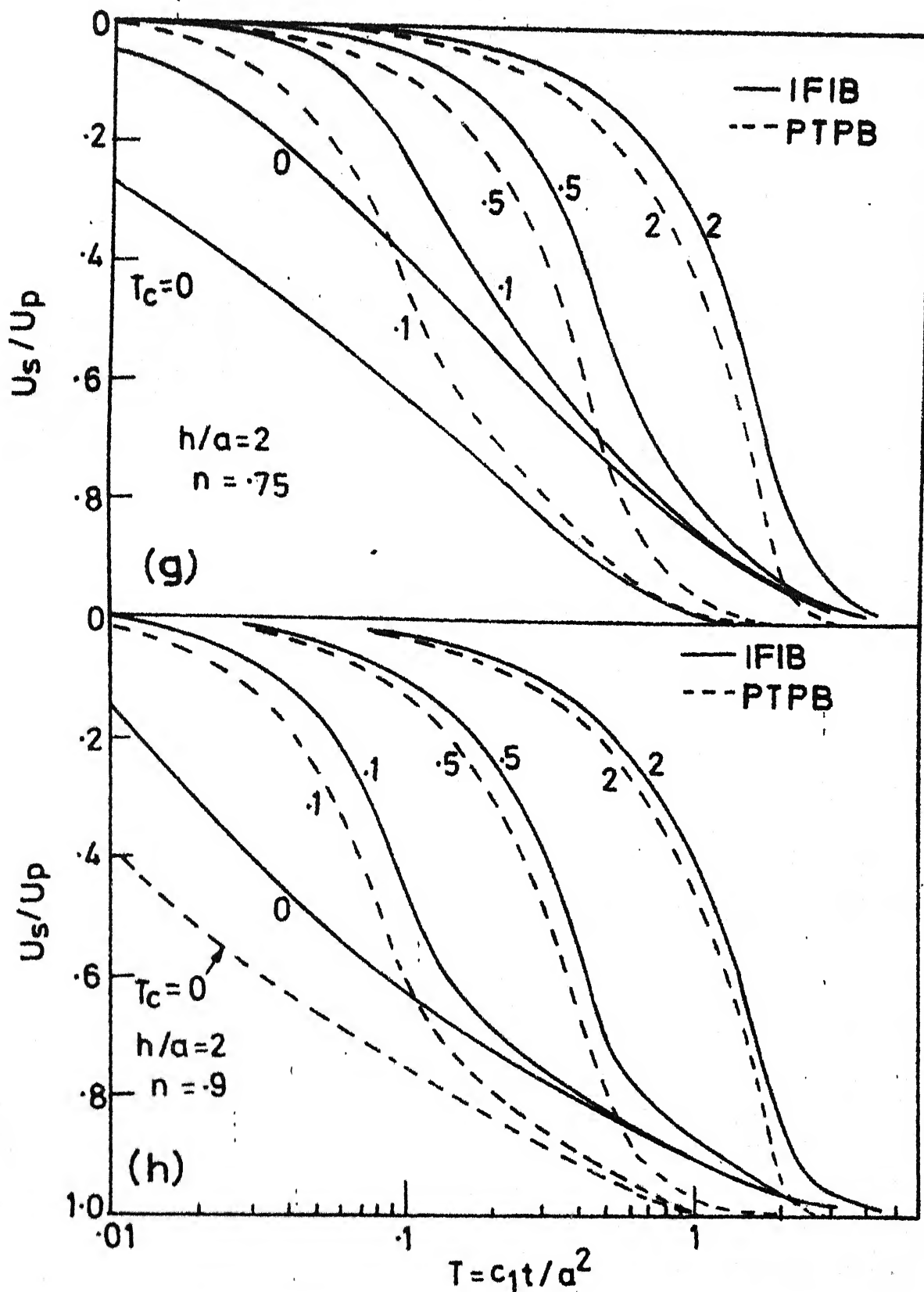


FIG. 7.5 CONSOLIDATION OF FLEXIBLE RING FOOTING
UNDER CONSTRUCTION LOADING

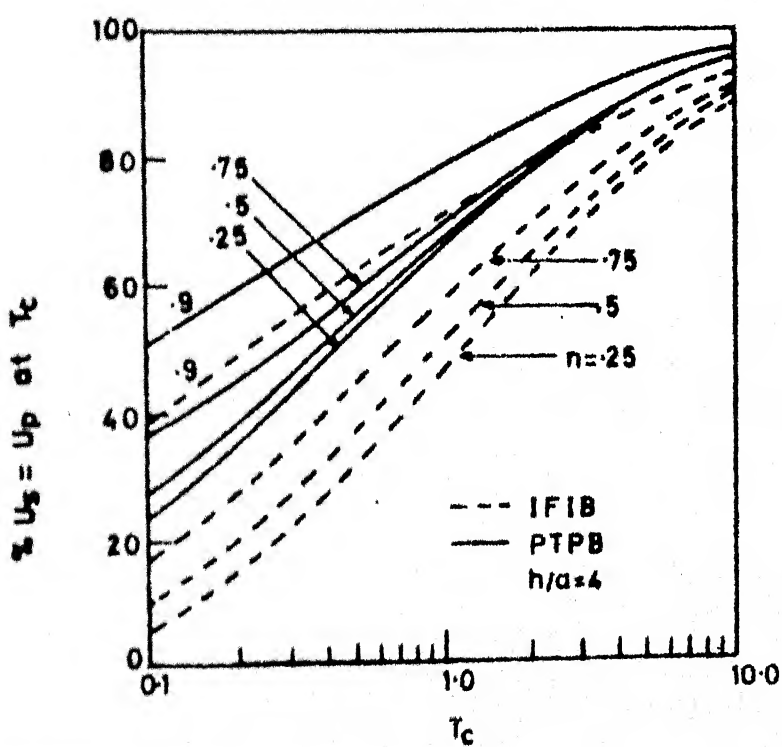
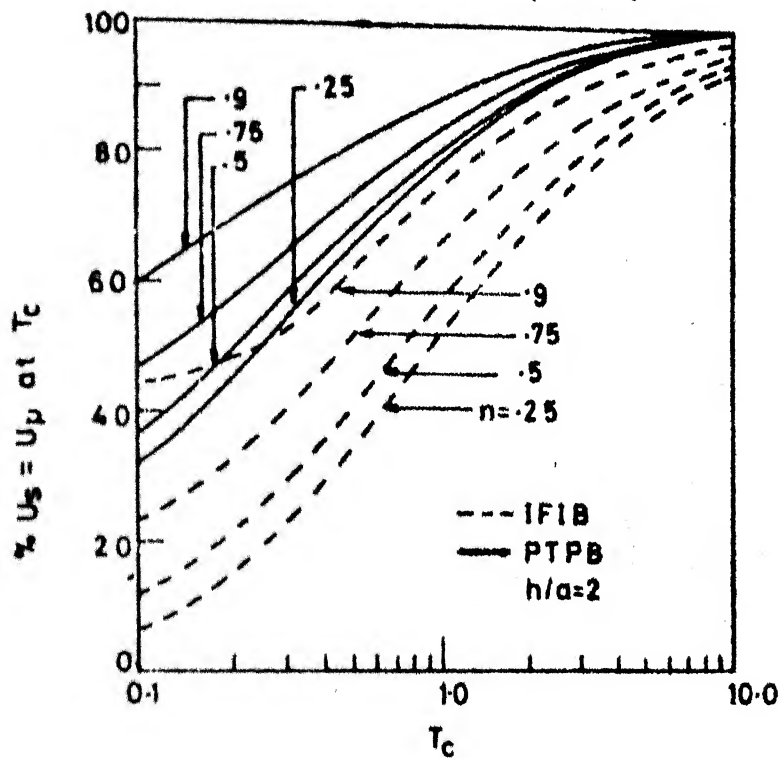


FIG.7.6 FLEXIBLE FOOTING-DEGREE OF CONSOLIDATION AT THE END OF CONSTRUCTION

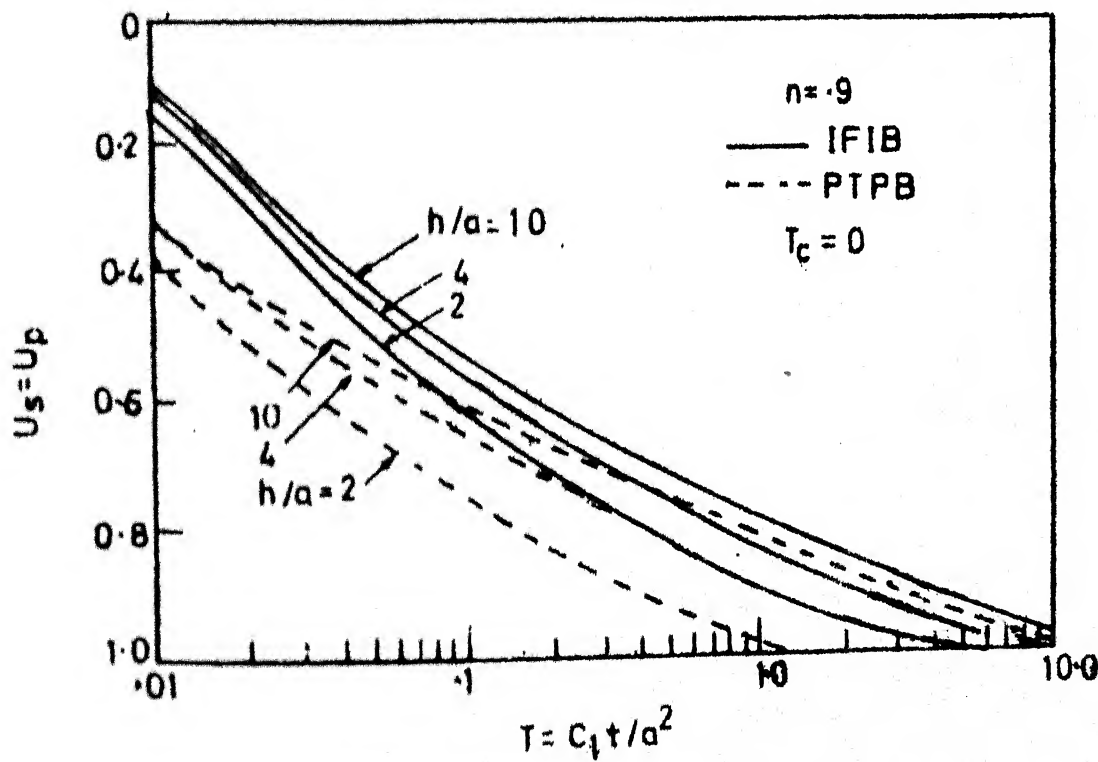
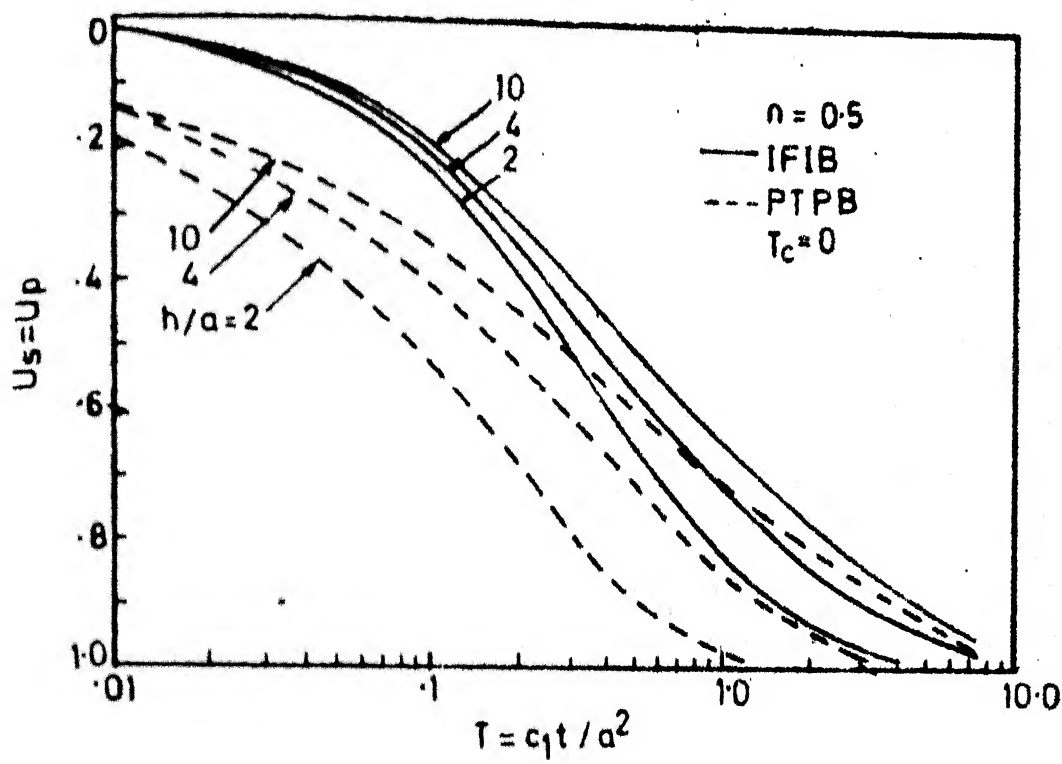


FIG.7.7 EFFECT OF DEPTH OF CONSOLIDATION LAYER

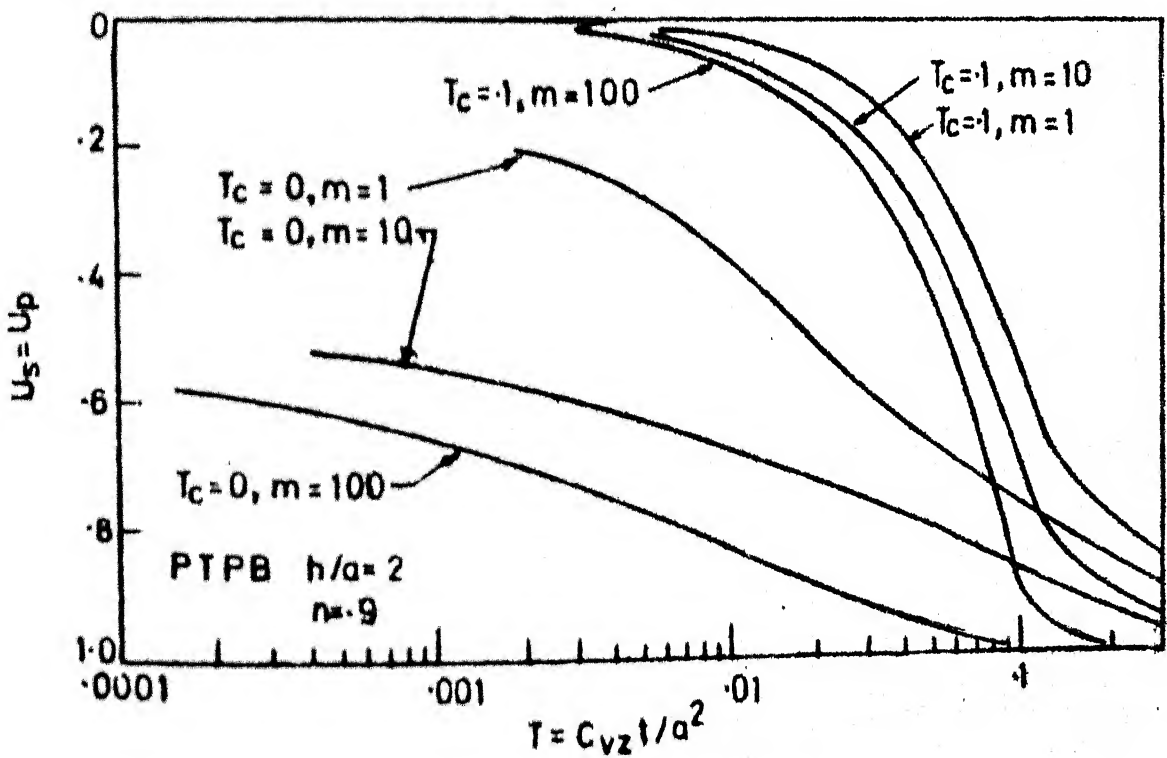
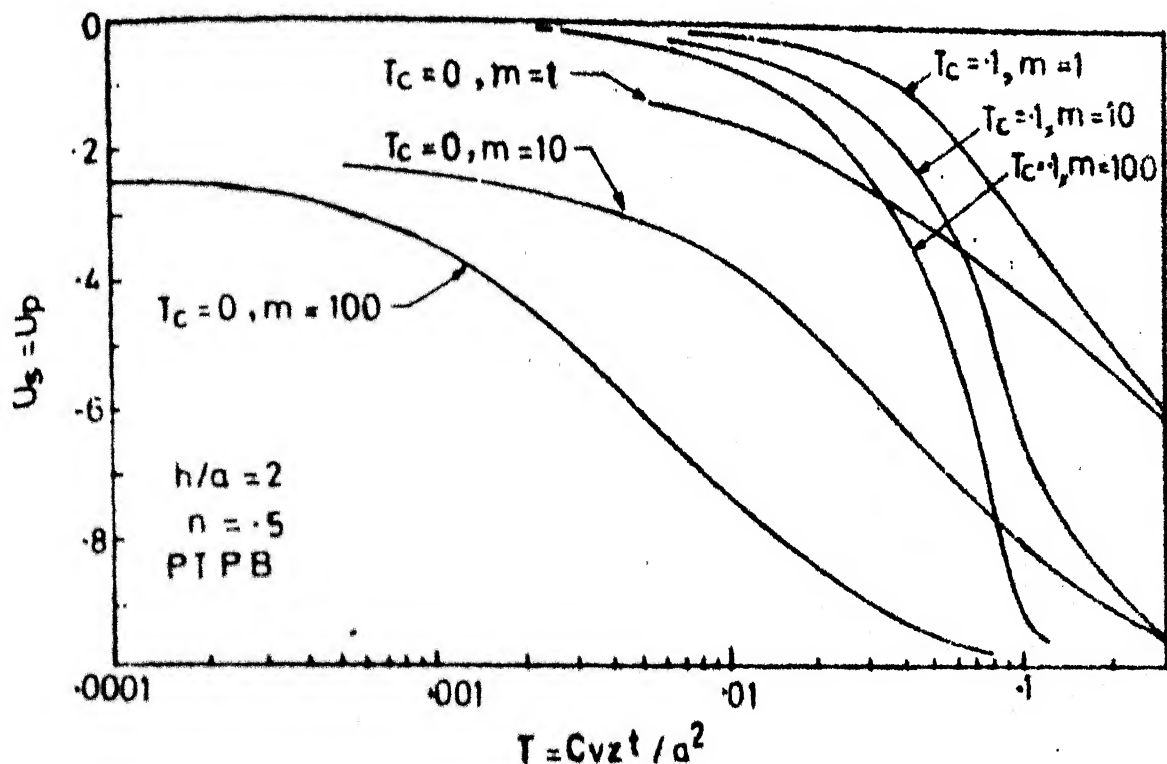


FIG.7.8 FLEXIBLE FOOTING-EFFECT OF ANISOTROPY

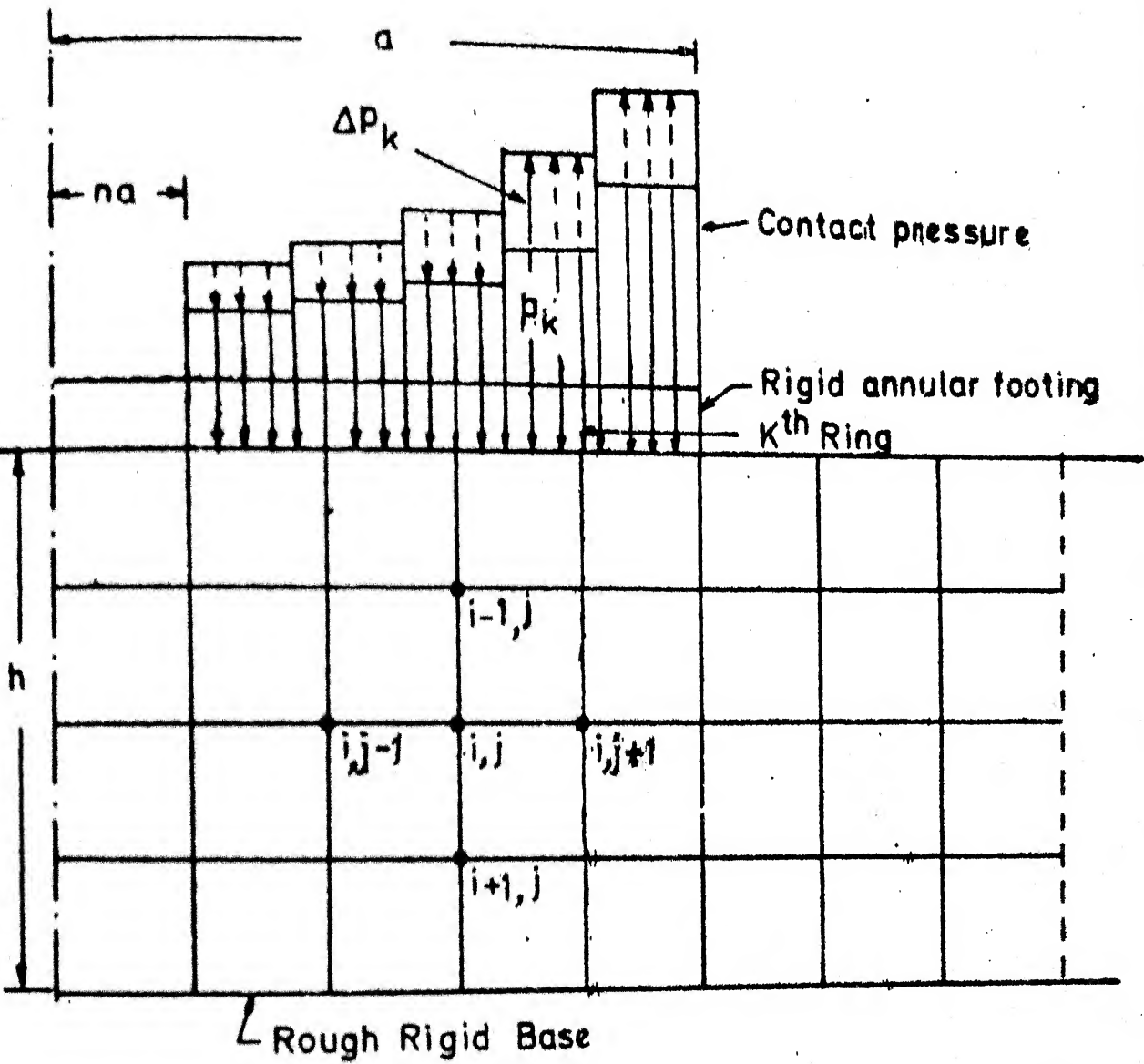


FIG. 7.9 DISCRETISED RIGID RING FOOTING ON FINITE LAYER WITH FINITE DIFFERENCE GRID

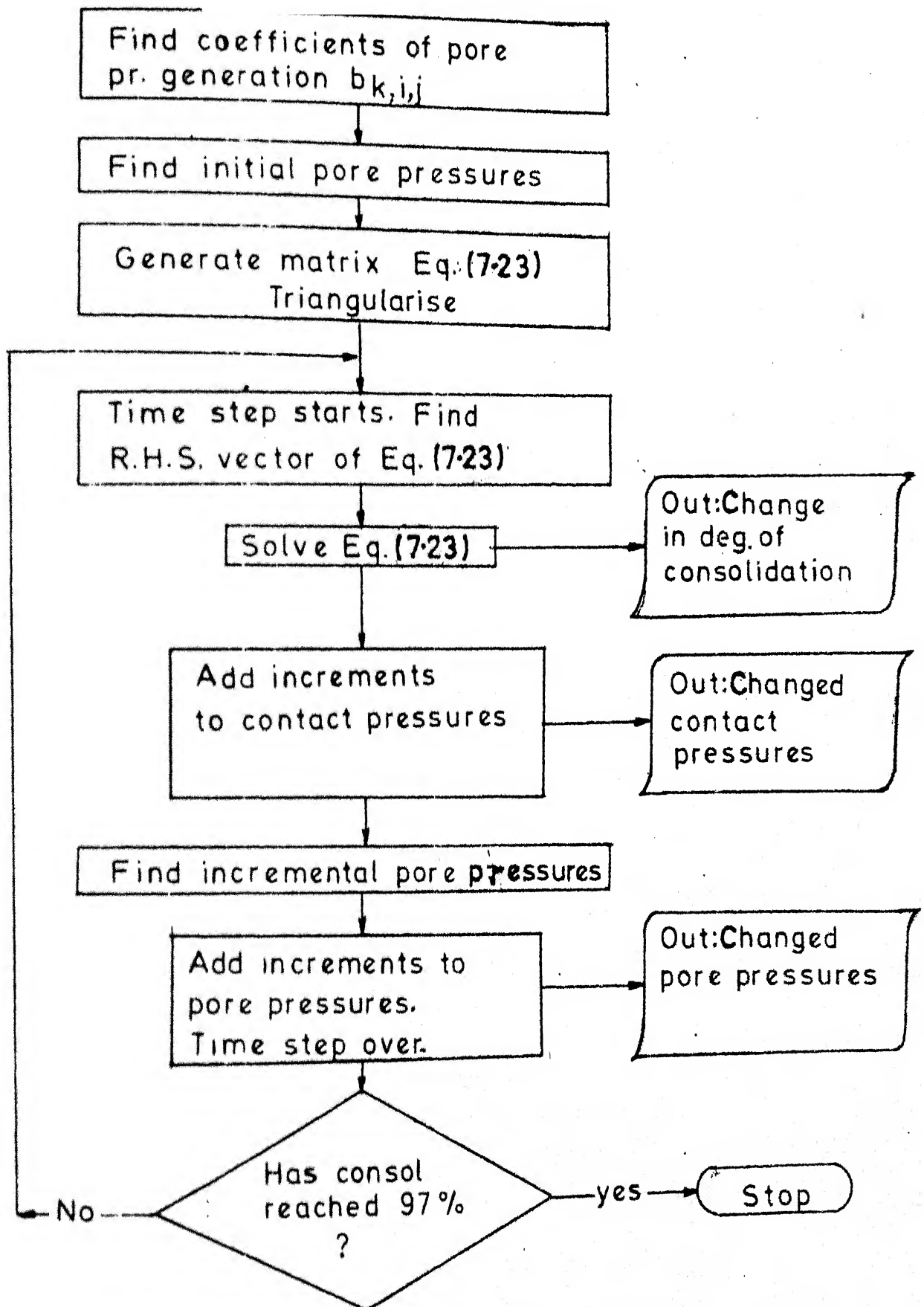


FIG.7.10 OPERATIONAL FLOW CHART (Consolidation under rigid footing)

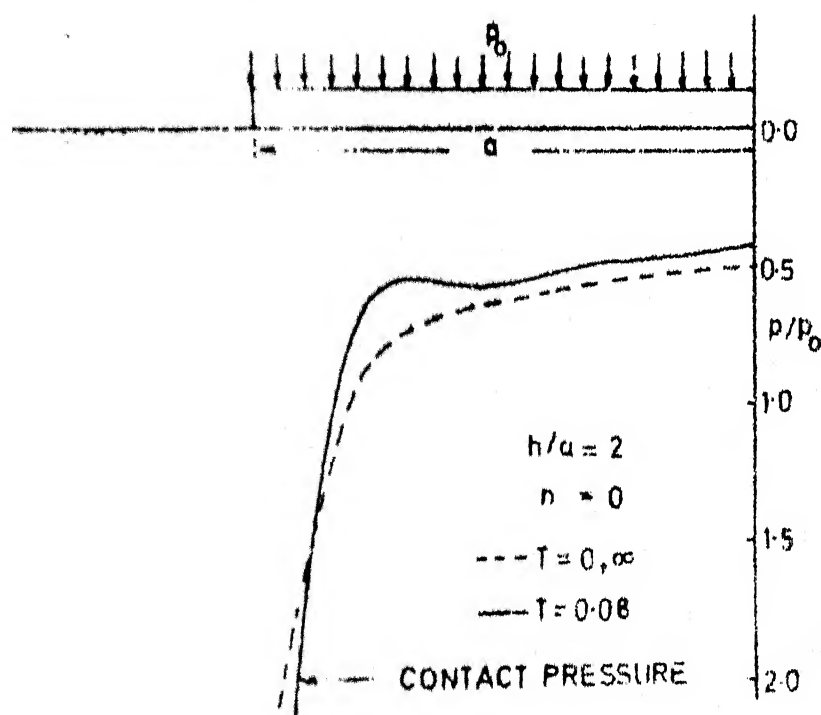
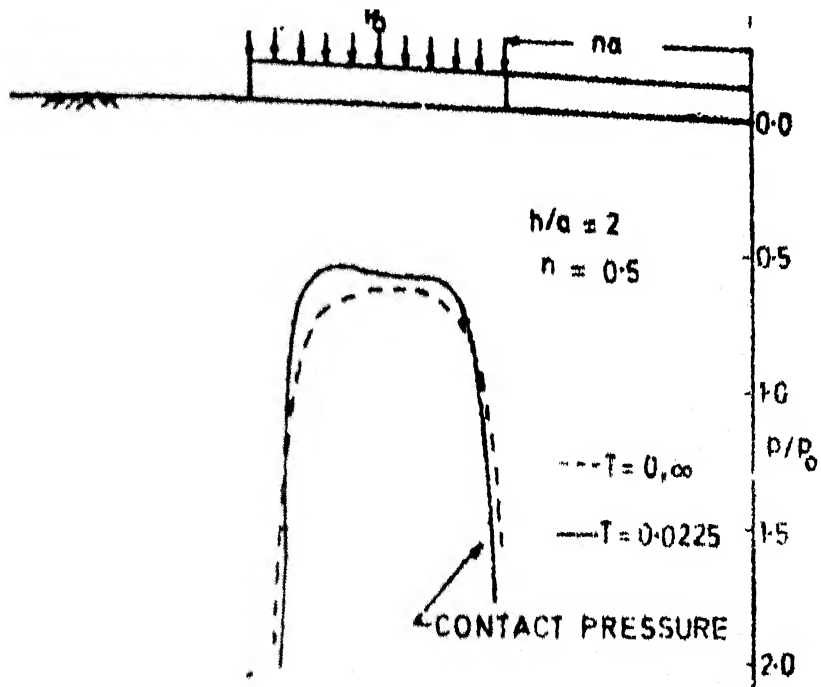
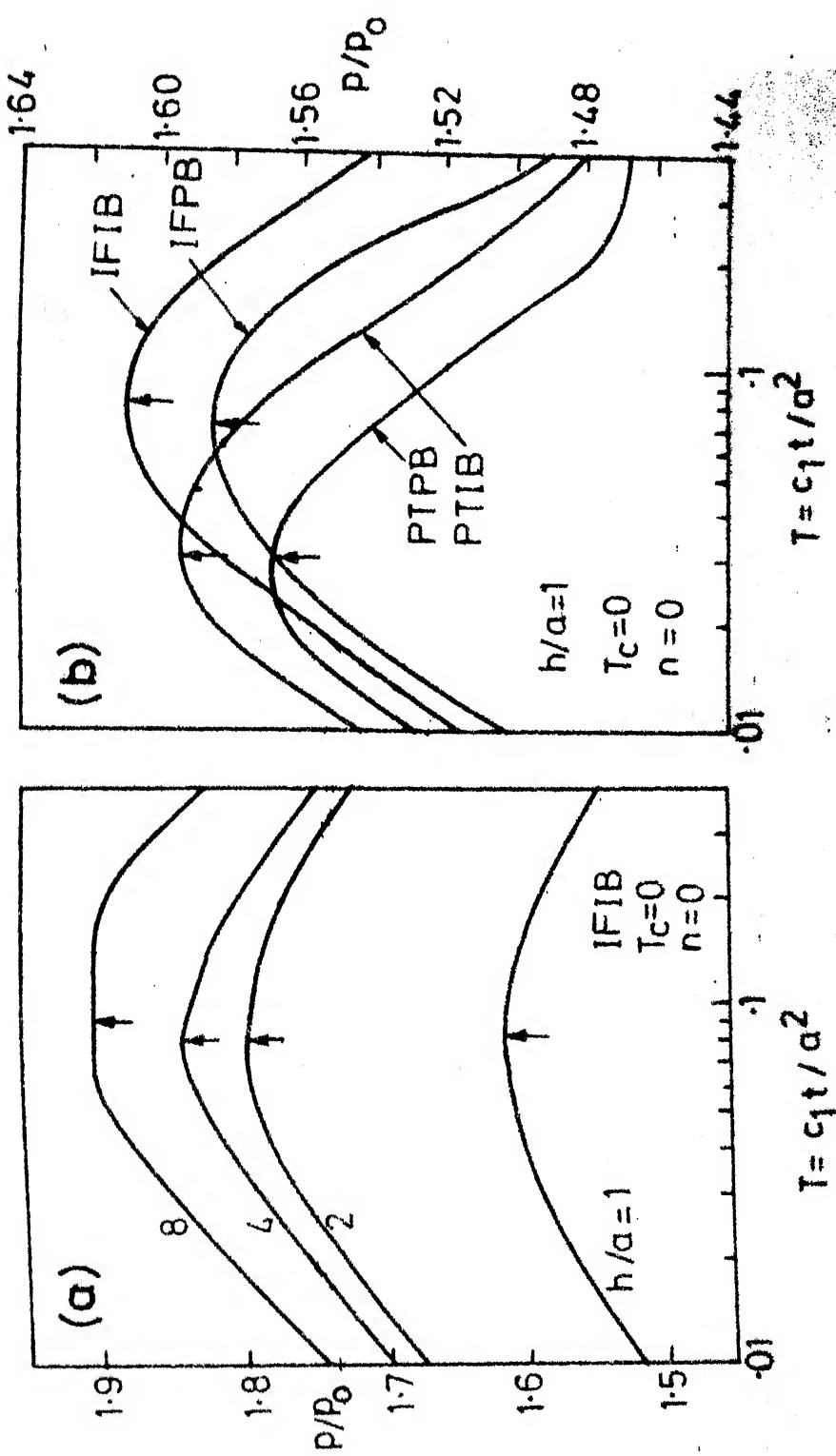


FIG. 7.11 TYPICAL CHANGES IN CONTACT PRESSURE
DURING CONSOLIDATION UNDER A RIGID
RING AND A RIGID CIRCULAR FOOTING

FIG.7.12 EFFECT OF LAYER DEPTH AND DRAINAGE ON PEAKS



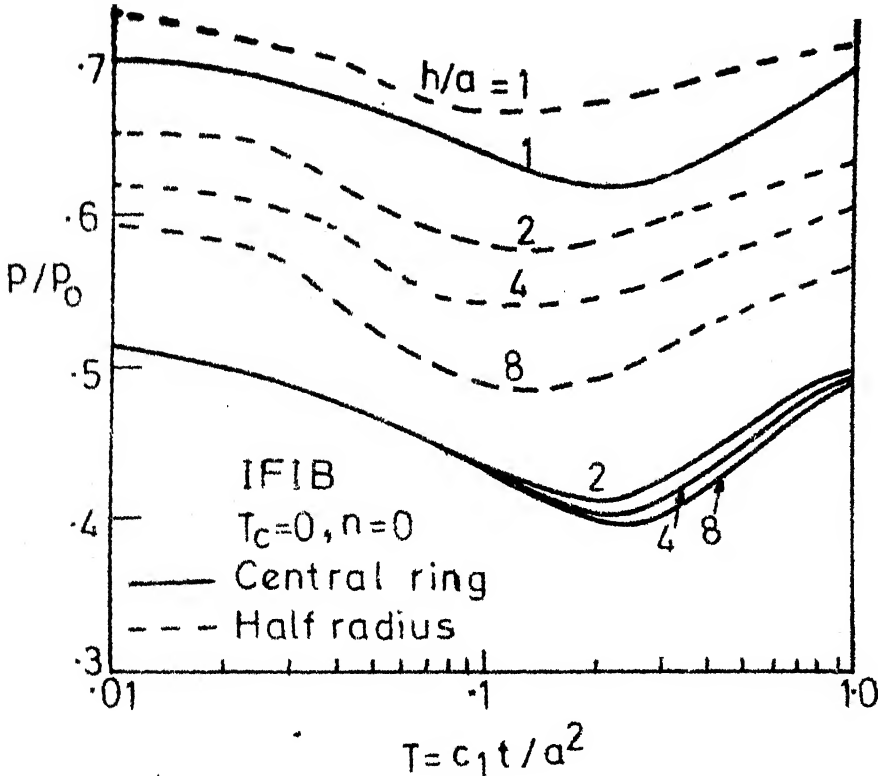


FIG.7.13 CONTACT PRESSURE VARIATION NEAR CENTRE AND HALF RADIUS OF A RIGID CIRCULAR FOOTING

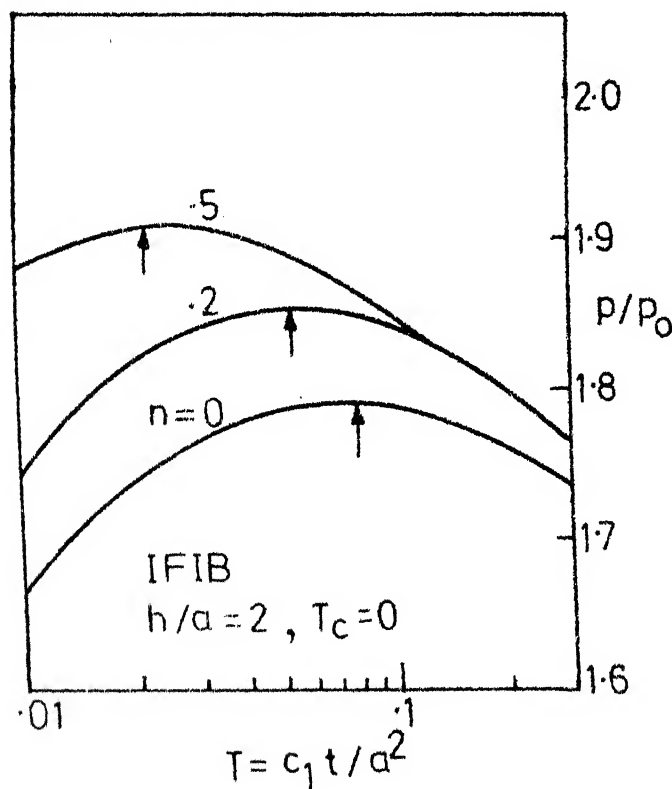


FIG.7.14 EFFECT OF RADIUS RATIO ON

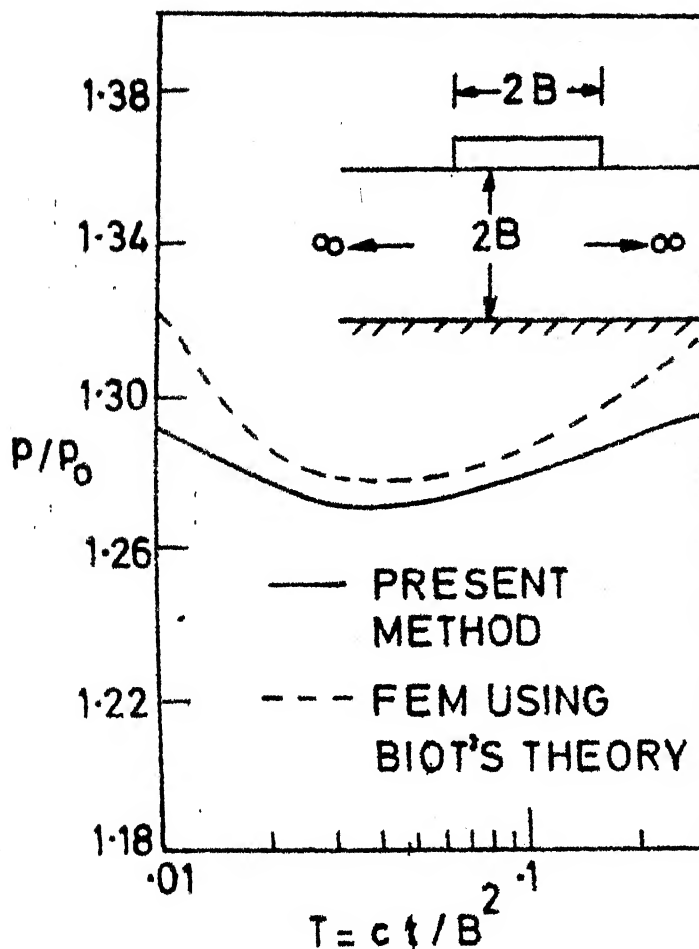


FIG.7.15 COMPARISON OF VARIATION OF EDGE PRESSURE (Average over one tenth width) UNDER RIGID STRIP FOOTING

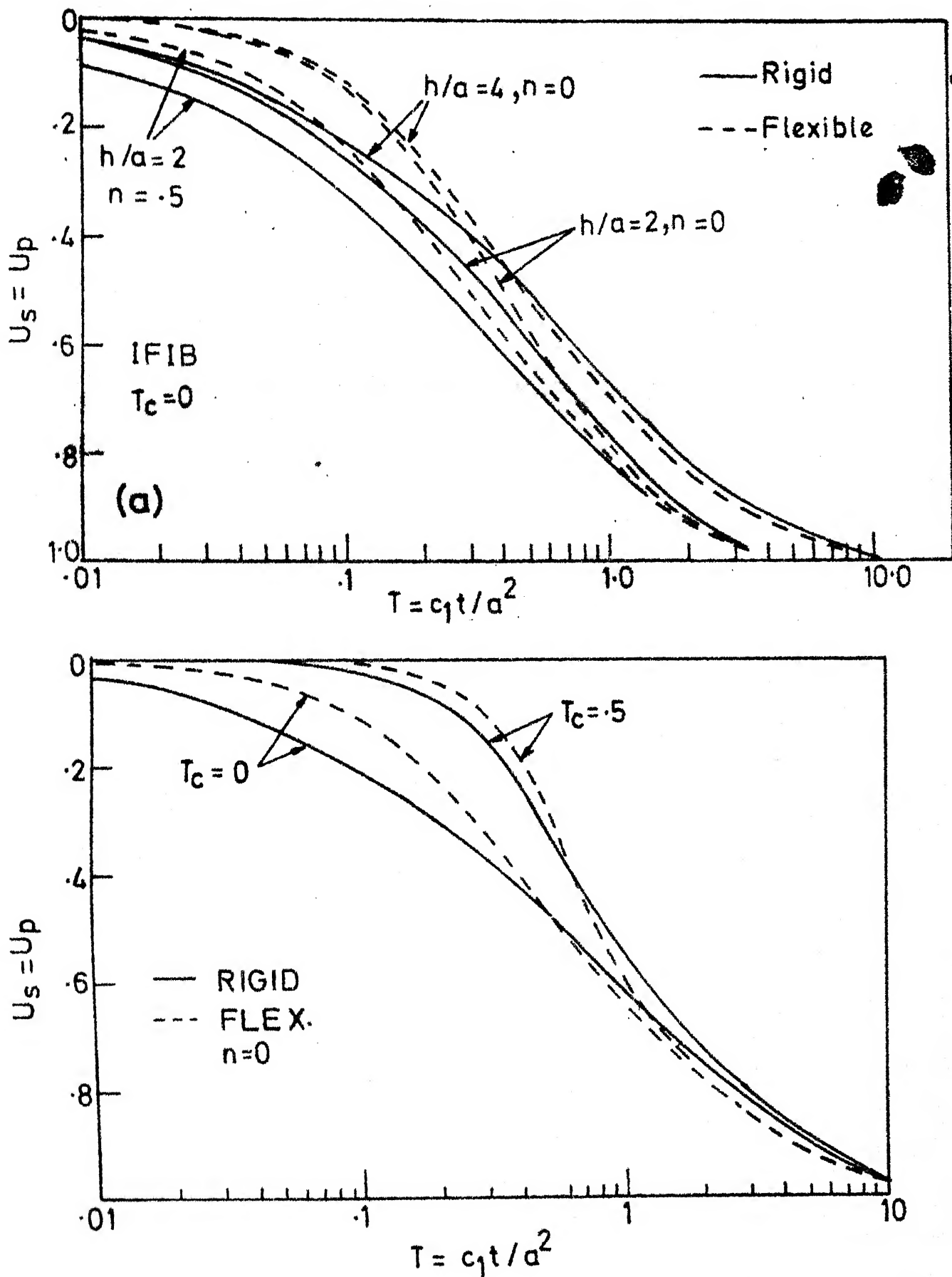


FIG.7.16 COMPARISON OF TIME RATE SETTLEMENT
OF RIGID AND FLEXIBLE FOOTINGS

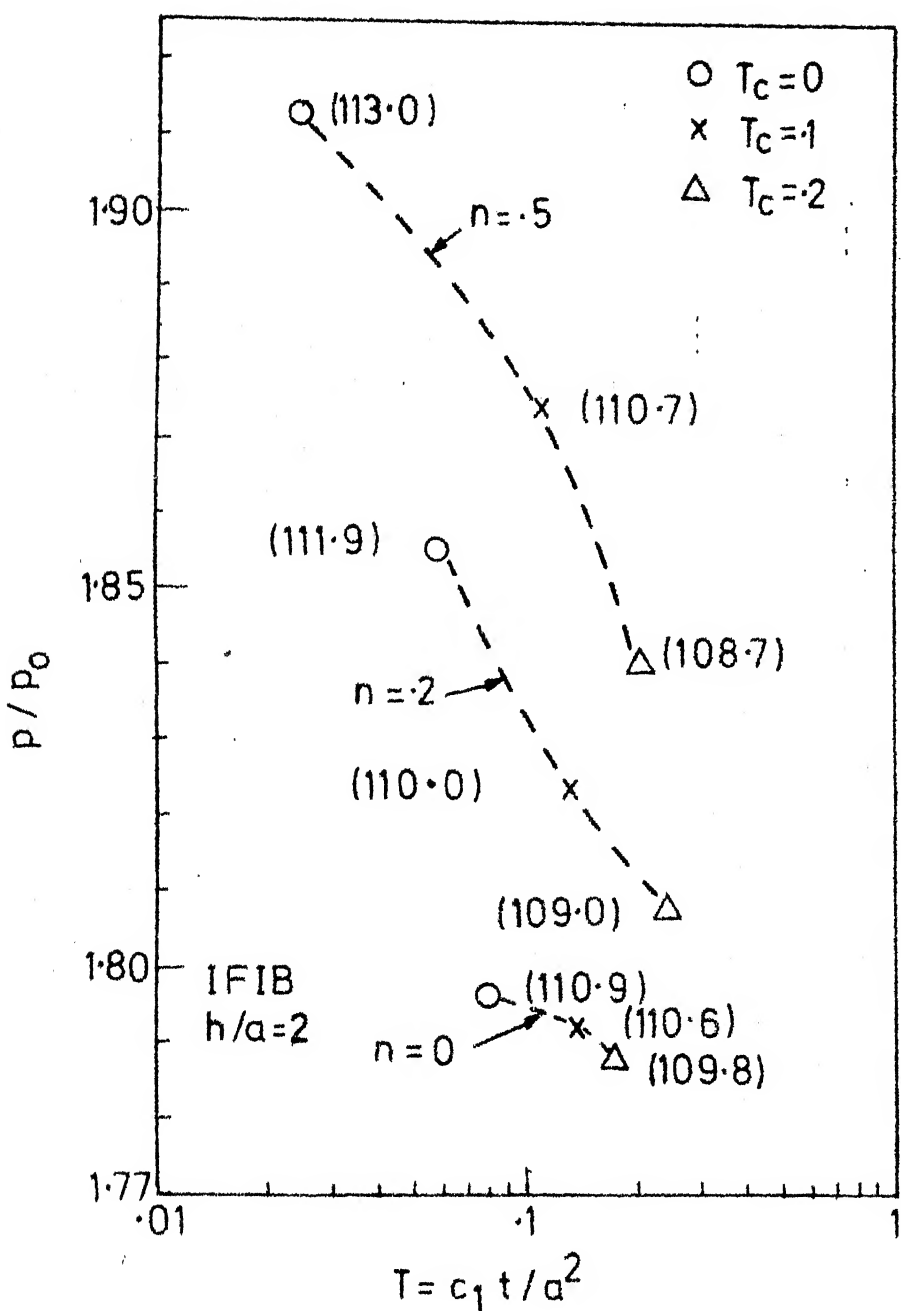


FIG. 7.17 EFFECT OF CONSTRUCTION TIME ON PEAK PRESSURES
 (Figures in brackets indicate % peak edge pressure over initial averaged over one fifth of ring)

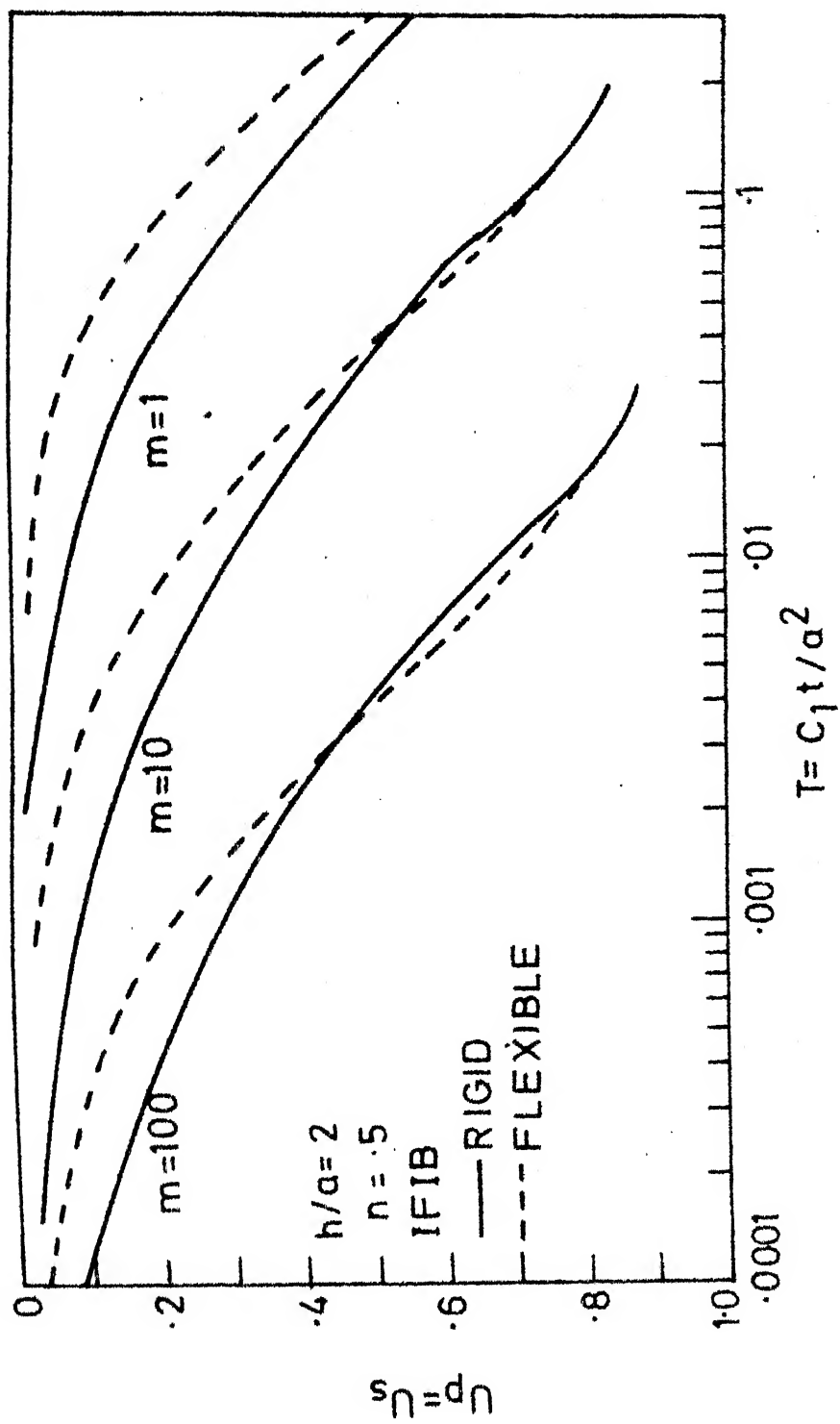


FIG.7.18 COMPARISON OF EFFECT OF ANISOTROPY ON CONSOLIDATION UNDER FLEXIBLE AND RIGID FOOTINGS

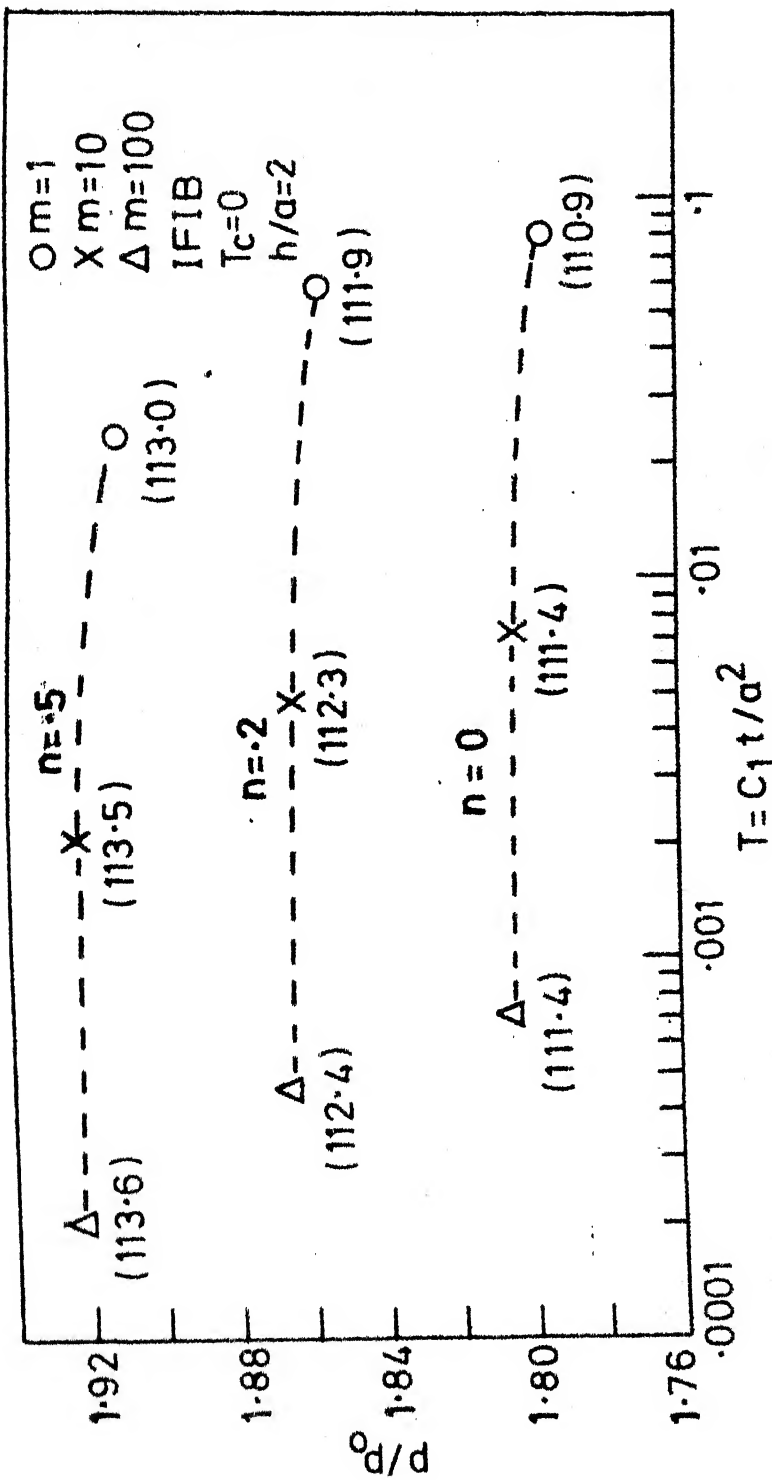


FIG.7.19 EFFECT OF ANISOTROPY ON PEAK PRESSURES
 (Figures in brackets indicate % peak edge pressure over
 initial averaged over one fifth of ring)

CHAPTER 8

SUMMARY AND CONCLUSIONS

8.1 SUMMARY

The aim of this thesis is to make a comprehensive study of the performance of annular footings as foundations, with reference to the load-settlement and time-settlement response. Although annular footings are highly suitable as foundation for structures like water tanks and towers and although millions of such structures are constructed every year all over the world, the potential of the use of annular footings does not seem to have been explored fully, probably because of lack of simpler means of predicting the behaviour at all loads levels and at all times. This thesis is an attempt to provide, for annular footings, a broad parametric study, and some design data for direct use. While circular footing is studied as a particular case of annular footing, a critical comparison between the two types of foundations is included with reference to all the aspects covered in the thesis.

Except for extremely flexible footings, the contact pressures near the edges of an annular (or circular) footing are very high even under small loads, giving rise to plastic

yielding. Plastic yielding can not therefore be neglected in any rational analysis. So also the tension cut-off which occurs especially under eccentric loading, due to the inability of the soil to take tension. These aspects are given utmost importance in the thesis.

The load-settlement response has been studied for the following cases of annular footings (circular footings as a particular case).

- (1) Rigid centrally loaded footings.
- (2) Axisymmetrically loaded footings of finite rigidity with typical loading configurations.
- (3) Rigid centrally loaded footings supplemented by incompressible piles (Piled Ring Foundations).
- (4) Rigid footings eccentrically loaded.

Except for case (3) above, the following types of problems are considered.

- (a) Footing resting on the surface of a semi-infinite soil.
- (b) Footing embedded in the semi-infinite soil.
- (c) Footing resting on the surface of a soil layer of finite depth underlain by rough rigid base.

A piled annular footing is assumed to rest at the surface of a semi-infinite mass of soil.

In all the above cases, the footing and piles are discretized into small elements, the stresses on the elements are assumed to be uniform and idealised to act as point loads wherever appropriate at the centres of elements. The available elastic solutions (such as by Boussinesq, Mindlin) are employed to obtain the influence coefficients of the flexibility matrix connecting the stresses and displacements. Wherever stresses tend to exceed the yield stress value of the soil, they are held at the yield stress value and wherever stresses tend to become negative, they are held at zero value. The influence coefficient matrix is partitioned, the rows corresponding to yielded zone are removed using the limiting values as mentioned and it is modified to represent stress-displacement relations in elastic zone only. Solutions are obtained after incorporating overall equilibrium conditions of the footing. An entire load-settlement response, distribution of contact pressures, and the progress of yield zone under the footing are obtained as solution at all levels of loading and eccentricity if any. In case of eccentric loading, the settlement response is obtained in terms of central settlement and rotation about the centre of the footing.

The effects of embedment and the effect of depth of finite layer are studied and compared with reference

to the condition of semi-infinite soil, in all the cases except piled footings. For piled footings, the effect of length to diameter ratio and number of piles is studied in combination with the footing size. The effect of positioning of piles below the footing in one or more concentric circles is also studied.

The rate of consolidation settlement is studied for fully flexible and fully rigid annular footings resting on a saturated soil layer. Various drainage boundary conditions are included for the purpose of the study. The effect of period of construction, in which the load is assumed to build up linearly, is studied and the amount of degree of consolidation during the construction period is quantified for annular footings. Terzaghi-Rendulic theory is used with time scale correction to formulate a direct finite difference scheme. The same theory is used for rigid footings but using a scheme which becomes implicit because of conditional uniform settlement under the rigid footing and which involves indirect coupling of flow-elastic deformation problems because of generation of pore pressures under changing contact pressures in terms of total stresses elastically induced in the soil mass. Changes of contact pressures with time under the rigid annular footing are also obtained.

In the study of consolidation settlement, the effect of anisotropy resulting from higher permeability in the horizontal direction in comparison to that in the vertical direction is also studied briefly.

8.2 CONCLUSIONS

- (a) With the help of a simplified elasto-plastic analysis, it has been possible to obtain load-settlement response of annular footings over the entire range of loading upto failure. The load-settlement response when compared with some available results from experiments as well as those obtained from FEM, tally well.
- (b) The load-settlement response is non-linear throughout the range of loading. At lower load levels, it is nearly linear and as load approaches the failure load, it is highly non-linear and shows a rapid increase of settlement (and/or rotation in case of eccentric loading).
- (c) For the same load, annular footings indicate less settlement in comparison to circular footings.
- (d) In contrast to circular footing, an annular footing shows a nearly linear load settlement response upto a considerable load level, after which settlement increases rapidly.

(e) The plastic yield of soil starts near the outer edge of a circular footing and advances towards the centre as load increases. In case of annular footing, it starts near the outer as well as inner edges and progresses towards the centre of the width of the footing, this being faster from the outer edge. As load approaches failure load, the contact pressure tends to become uniform.

(f) The settlement of embedded footing is less than that of a surface footing, but the nature of contact pressure distribution and the progress of yield are similar in the two cases. It has been possible to apply corrections to the settlement obtained for surface footing to get the settlement of embedded footing at any load level.

(g) The settlement of a footing resting on finite depth of soil is less than that resting on semi-infinite soil but no direct correlation could be found since the nature of contact pressure distribution itself is different in the two cases. The performance in terms of settlement for the two cases is qualitatively similar. Annular footings are advantageous in this case also in comparison to circular footings from settlement point of view, at all load levels.

(h) For a centrally loaded footing of finite rigidity it is found that whereas the overall load settlement response is not very sensitive to relative rigidity K , the differential settlement, and the bending moments and shear in the footing are sensitive to K . For lower values of K (more flexible footings) the differential settlements are higher and the design moment and shear in the footing are lower. These three quantities and also settlements are lower for embedded footings as well as for surface footings on finite depth of soil in comparison to footings on semi-infinite soil.

(i) For footings of finite rigidity loaded uniformly, it is found that the footings should be designed for values of moment and shear much lower than those given by elastic theory.

(j) For footings of finite rigidity it is found that the worst position of load is near the centre or inner edge, from the points of view of settlements and design moment and shear in the footing. This type of loading may also introduce separation of footing from the soil near the outer edge, if the footing is relatively flexible.

(k) For a loading in the form of an annular ring, it is found that the design moment and shear in a footing of finite rigidity could be calculated on the basis of uniform contact pressure equal to yield stress of soil.

(l) A ring (or circular) footing can be advantageously supplemented by providing a small number of short piles, due to which the settlement of the footing reduces considerably. If the piles do not dominate, the bearing capacity of the annular footing is utilised advantageously. A judicious combination of advantages of a raft and piles can yield a very economic alternative. If a single ring of piles is provided it should be positioned in such a way that it divides the area approximately into equal portions. For ring footings it should be near the centre of the width. This is found to give minimum settlement. It may be found more convenient from the points of view of positioning of the loads on the footing and of structural design of the footing. If more than one row of piles is provided an angularly staggered arrangement is preferable and the response is better.

(m) For eccentrically loaded rigid annular footings, it is found that the rotations are also less for annular

footings, carrying the same load, in comparison to circular footings. It is found that eccentricity also adds to yielding of soil on the compression side and introduces separation or lift-off on the tension side. Separation can occur at eccentricities less than those worked out from elastic theory, because of plastic yielding of the soil.

- (n) Terzaghi-Rendulic theory has been employed, along with time scale corrections to the axisymmetric problems of consolidation under flexible and rigid annular footings. It is found that consolidation settlement of annular footings is faster for higher values of n (narrower footings). The major portion of consolidation settlement in case of annular footings will occur in the earlier stages.
- (o) It is found that considerable amount of consolidation settlement would occur during the period of construction itself. This aspect has been quantified for annular footings.
- (p) It is found that anisotropy with respect to permeability has a marked effect on time rate of settlement of annular footings.
- (q) For consolidation under rigid footings, Terzaghi-Rendulic theory only is used. However the finite difference scheme became implicit because of conditional rigid

settlement. Elastic theory is used to obtain pore pressures due to changes in contact pressure with time due to which an indirect coupling of flow and elastic deformation problems is achieved. The time rate of settlement and contact pressure changes are studied.

- (r) In all the cases, charts are presented which would directly serve as design aids for the range of parameters considered.
- (s) In all the problems, it is found that the computational effort and cost involved is considerably less although an extensive parametric study and generation of considerable amount of design data were involved.

8.3 SUGGESTIONS FOR FURTHER STUDY

- (1) Application of the simplified elasto-plastic settlement analysis used in this thesis to the following cases:
 - (a) Footings of any shape.
 - (b) Surface footings of any shape resting on Gibson soil (using available elastic solutions (Brown and Gibson, 1979)).
 - (c) The case of layered soils using simplified equivalent layer approach (Odemark, 1949) or tabulated elastic solutions(e.g. compilations by Poulos and Davis, 1974).

- (d) Single pile-square raft unit and pile-raft systems of usual configurations.
- (2) Experimental verification through laboratory and field models for annular footings with and without piles.
- (3) Using available elastic solutions for horizontal loading and including the effect of adhesion between the footing and the soil.
- (4) Studying the effect of compressibility of piles and of adhesion coefficient α .
- (5) Study of piled ring footings under eccentric loading.
- (6) Use of the computer programme developed for this thesis for consolidation under multiple strip footings and eccentric loading.
- (7) Study of consolidation under construction loading sequence other than linear.

REFERENCES

Agbezuge, L.K. and Deresiewicz, H. (1975). The Consolidation Settlement of a Circular Footing. Israel J. Tech., Vol. 13, pp. 264-269.

Ahivin, R.G. and Ulery, H.H. (1962). Tabulated Values for Determining the Complete Pattern of Stresses, Strains and Homogeneous Half Space. Highway Research Board, Bulletin. 342, pp. 1-13.

Asproudas, S.A. and Desai, C.S. (1975). Analysis and Application of a Finite Element Procedure for Consolidation. Report, Deptt. Civ. Engrg., Virginia Polytech. Inst. and State Univ., Blacksburg, Virginia, 24061, May 1975.

Babu Shankar, N. (1977) . Stress Distribution Under Embedded Circular Footing. Indian Geotech. J., Vol.7 (1977), No. 2, pp. 178-181.

Banerjee, P.K. (1971). Foundation with a Finite Elastic Layer. Civ. Engrg. Publ. Wks. Rev., Vol.66, pp.1197-1202.

Banerjee, A. and Jankov, Z.D. (1975). Circular Mats Under Arbitrary Loading. J. Struct. Div. Proc. ASCE, Vol.101, No. ST 10, pp. 21-33-2145.

Barden, L. (1966). Contact Pressures Under Circular Slabs. Struct. Engrg. Vol. 43, pp. 153-154.

Bell, R.A. and Iwakiri, J. (1980). Settlement Comparison Used in Tank Failure Study. J. Geotech. Engrg. Div., Proc. ASCE, Vol.106, No. 4T2, pp. 153-165.

Biot M.A. (1941). General Theory of Three-Dimensional Consolidation, J. Appl. Phys. Vol. 12, No.2, pp.155-164.

Bobe, R. and Pietsch, C. (1981). Settlement Calculation by a New Strength Theory. Proc. 10th Int. Conf. SMFE, Stockholm, Vol.1, pp. 53-56.

Boek Madsen, G. and Lagoni, P(1981). Pile Foundation Problems in White Chalk. 10th Int. Conf. SMFE, Stockholm, Vol.1, pp. 31-34.

Booker, J.R. (1973). A Numerical Method for the Solution of Biot's Consolidation Theory. Quart. J. Mech. Appl. Maths., Vol. 26, No.4, pp. 457-470.

Borowicka, H. (1936). Influence of Rigidity of a Circular Foundation Slab on the Distribution of Pressure Over the Contact Surface. Proc. 1st Int. Conf. SMFE, Vol.2, pp. 144-149.

Borowicka, H. (1930). Druckverteilung Unter Elastischen Platten. Ingenieur Archiv, Vol. 10, No.2, pp.113-125.

Borowicka, H. (1943). Über ausmittig belaste starre platten auf elastisch-isotropem Untergrund. Ingenieur-Archiv, Berlin, Vol.1, pp. 1-8.

Boswell, L.F. and Scott, C.R. (1975). A Flexible Circular Plate on a Heterogeneous Elastic Half Space. Influence Coefficients for Contact Stress and Settlements. Geotechnique , Vol.25, No.3, pp. 604-610.

Bozozuk, M. (1972). Foundation Failure of the Vankleek Hill Tower Silo. Performance of Earth and Earth Supported Structures, ASCE Speciality Conf., Vol.1, Pt.2, pp. 885-902.

Boussinesq, M.J. (1885). Application Des Potentiels, a l' Etude de l'Equilibre et du Movvement Des Solides Elastiques. Gauthier-Villars, Paris.

Brinch Hansen, J. (1970). A Revised and Extended Formula for Bearing Capacity. Bulletin No. 28, Danish Geotech. Inst., Copenhagen, pp. 5-11.

Brown, K.F., Poulos, H.G. and Wiesner, T.J. (1975). Piled Raft Foundation Design. Proc. Symp. Raft Foundations, CSIRO, Aust.

Brown, P.T. (1968). The Effect of Local Bearing Failure on Behaviour of Rigid Circular Rafts. Inst. Engrs., Australia, Civil Engrg. Trans., Vol.10, pp. 190-192.

Brown, P.T. (1969). Numerical Analyses of Uniformly Loaded Circular Rafts on Deep Elastic Foundations. Geotechnique, Vol. 19, pp. 399-404.

Brown, P.T. (1965). Numerical Analyses of Uniformly Loaded Circular Rafts on Elastic Layers of Finite Depth. *Geotechnique*, Vol. 19, pp. 301-306.

Brown, P.T. (1969). Raft Foundations. P.G. Course on Analysis of the Settlement of Foundations. School of Civil Engrg., Univ. of Sydney.

Brown, P.T. and Gibson, R.E. (1979). Surface Settlement of a Finite Elastic Layer Whose Modulus Increases Linearly With Depth. Univ. Sydney, School of Civ. Engrg. Res. Rep. No. R 345, 1979.

Buragohain, D.N. and Shah, V.L. (1977). Curved Interface Elements for Interaction Problems. Proc. Int. Symp. Soil Struct. Interaction, Roorkee, 1977, pp. 197-201.

Burland, J.B., Butler, F.G. and Dunican, P. (1966). The Behaviour and Design of Large Diameter Bored Piles in Stiff Clay. Proc. Symp. on Large Bored Piles, Inst. Civ. Engrs., London, pp. 51-71.

Butterfield, R. and Banerjee, P.K. (1971). A Rigid Disc Embedded in an Elastic Half-Space. *Geotech. Engrg.*, Vol. 2, No. 1, pp. 35-52.

Carrier, W.D. and Christian, J.T. (1973). Rigid Circular Plate Resting on a Non-homogeneous Elastic Half space. *Geotechnique*, Vol. 23, No. 1, pp. 67-84.

Chakravorty, A.K. and Ghosh, A. (1975). Finite Difference Solution for Circular Plates on Elastic Foundations. *Int. J. Numer. Mech. Engrg.*, Vol. 9, pp. 73-84.

Chan, S.C. and Cheung, Y.K. (1974). Contact Pressure of Rigid Footings on Elastic Foundations. *Civ. Engrg.*, pp. 51-59.

Chen, W.T. and Engel, P.A. (1972). Impact and Contact Stress Analysis in Multilayer Media. *Int. J. Solids Struct.*, Vol. 8, No. 11, pp. 1257-1281.

Cheung, Y.K. and Nag, D.K. (1968). Plates and Beams on Elastic Foundations- Linear and Non-linear Behaviour. *Geotechnique*, Vol. 18, pp. 250-260.

Chiarella, C. and Booker, J.R. (1975). The Time-Settlement Behaviour of a Rigid Die Resting on a Deep Clay Layer, *Quart. J. Mech. Appl. Math.*, Vol. 28, No. 3, pp. 317-328.

Christian, J.T. and Boehmer, J.W. (1970). Plane Strain Consolidation by Finite Elements. J. SMFE Div., Proc. ASCE, Vol.96, No. SM4, pp. 1435-1457.

Clough, R.W. and Woodward, R.J. (1967). Analysis of Embankment Stresses and Deformations. J. SMFE Div., ASCE, Vol.93, No. SM.4, pp. 529-549.

D'Appolonia, D.J., Lambe, T.W. and Poulos, H.G. (1971). Evaluation of Pore Pressures Beneath an Embankment. J. SMFE Div., ASCE, Vol.97, pp. 881-897.

Das, S.C. and Gangopadhyay, C.R. (1978). Undrained Stresses and Deformations Under Footings. J. Geotech. Engrg. Div. Proc. ASCE, Vol. 104, No. GT1, pp. 11-25.

Dave, P.C. (1977). Soil Pressure on Annular Foundation. J. Inst. Engrs. India, Vol.58, Part CL 2+3, pp. 56-61.

Davis, E.H. (1969). The Analysis of the Settlement of Foundations. P.G. Course on Analysis of the Settlement of Foundations, School of Civil Engrg., Univ. of Sydney.

Davis, E.H. and Poulos, H.G. (1972). Rate of Settlement Under Two- and Three-dimensional Conditions. Geotechnique, Vol.22, No.1, pp. 95-114.

De Jong, G.J. (1957). Application of Stress Functions to Consolidation Problems. Proc. 4th Int. Conf. SMFE, London, 1957, Vol.1, pp. 320-323.

Denvar, H. (1981). A Method of Settlement Calculation. Proc. 10th Int. Conf. SMFE, Stockholm, Sweden, June 1981, Vol.2, pp. 99-102.

Desai, C.S. (1968). Solution of Stress-Deformation Problems in Soil and Rock Mechanics Using the Finite Element Methods. Ph.D. Dissertation, Univ. Texas, Austin.

Desai, C.S. (1972). Nonlinear Analysis Using Spline Functions. J. SMFE Div., ASCE, Vol.98, No. SM9, pp.967-971. Also 1971, Vol.97, SMFE, pp.1461-1480.

Desai, C.S. (1977) in Desai, C.S. and Christian, J.T. (Eds). Numerical Methods in Geotechnical Engineering. McGraw Hill Book Co., New York, 1977.

Desai, C.S. and Abel, J.F. (1972). Introduction to the Finite Element Method. Van Nostrand Reinhold Co., New York.

Desai, C.S. and Christian, J.T. (Eds.) (1977). Numerical Methods in Geomechanical Engineering. McGraw Hill, 1977.

Desai, C.S., Johnson, L.D. and Hargett, C.M. (1974). Analysis of Pile Supported Gravity Lock. J. Geotech. Engrg. Div., ASCE, Vol. 100, No. GT9, pp. 1009-1029.

Desai, C.S. and Reese, L.C. (1970). Stress Analysis of Circular Footings on Layered Soils. J. Soil Mech. and Found. Div., ASCE, Vol. 96, No. SM4, pp. 1289-1310.

Dhaliwal, R.S. (1970). Punch Problem for an Elastic Layer Overlying an Elastic Foundation. Int. J. Engrg. Sci., Vol. 8, No. 4, pp. 273-288.

Dhaliwal, R.S. and Singh, B.M. (1977). Annular Punch on an Elastic Layer Overlying an Elastic Foundation. Int. J. Engrg. Sci., Vol. 15, No. 4, pp. 263-270.

Duncan, J.M. and Chang, C.Y. (1970). Nonlinear Analysis of Stress and Strain in Soils. J. SMFE Div., ASCE, Vol. 96, No. SM5, pp. 1629-1653.

Dunlop, P. and Duncan, J.M. (1970). Development of Failure Around Excavated Slopes. J. SMFE Div. ASCE, Vol. 96, SM2, pp. 471-493.

Egorov, K.E. (1965). Calculation of Bed for Foundation with Ring Footing. Proc. 6th Int. Conf. SMFE, Montreal, 1965, Vol. 2, pp. 41-45.

Egorov, K.E., Barvashov, V.A. and Fedorovsky, V.G. (1973). Some Applications of the Elasticity Theory to Design of Foundations. Proc. 8th Int. Conf. SMFE, Moscow, 1973, Vol. 1, No. 3, pp. 69-74.

Egorov, K.E., Kitaikina, O.V. and Zinovyev, A.V. (1979). Deformation of Ring Foundation Base Proc. 6th Asian Reg. Conf. SMFE, Singapore, 1979, Vol. 1, pp. 281-284.

Egorov, K.E., Konovalov, P.A., Kitaykina, O.V., Salnikov, L.F. and Zinorev, A.V. (1977). Soil Deformations Under Circular Footings. Proc. 9th Int. Conf. SMFE, Tokyo, Japan, July 1977, Vol. 1, pp. 489-492.

Egorov, K.E. and Nichiporovich, A.A. (1961). Research on the Deflexion of Foundations. Proc. 5th Int. Conf. SMFE, Paris, 1961, Vol.1, pp. 861-866.

Egorov, K.E. and Serebrjanyi, R.V. (1963). Determination of Stresses in Rigid Circular Foundation. Proc. 2nd Asian Reg. Conf. SMFE, Japan, 1963, Vol.1, pp. 246-250.

Egorov, K.E., Vronsky, A.V., Finseva, T.V. and Illynykh, V.A. (1980). Study of the Stress and Strain State of a Subgrade Under an Eccentric Load. Proc. 8th Danube-European Conf. SMFE, Varna, Bulgaria, Sept. 1980, Vol. 2, pp. 67-78.

England, A.H. (1962). A Punch Problem for a Transversely Isotropic Layer. Proc. Camb. Phil. Soc., Vol.58, No.3, pp.539-547.

Eringen, A.C. (1962). Nonlinear Theory of Continuous Media. McGraw Hill, New York 1962.

Gazetas, G. (1981). Variational Estimation of the Settlement of a Circular Raft on Anisotropic Soil. Soils and Foundations, Vol.21, No.4, pp. 109-116.

Gazetas, G. (1982). Axisymmetric Parabolic Loading of Anisotropic Half-Space. J. Geotech. Engrg. Div., Proc. ASCE, Vol.108, No. GT4, pp. 654-660.

Gazetas, G. (1982). Stresses and Displacements in Cross-Anisotropic Soil. J. Geotech. Engrg. Div., Proc. ASCE, Vol.108, No. GT4, pp. 532-533.

Germanis, E. and Vallippan, S. (1975). Mining Subsidence at the Graving Dock Site, New Castle. Proc. Symp. Recent Dev. in the Analysis of Soil Behaviour and their Applications to Geotech. Struct., Univ. N.S.W., Australia.

Gerrard C.M. and Harrison, W.J. (1971). Circular Loads Applied To a Cross Anisotropic Half-Space. Tech. Paper No.8, Div. Appl. Geomech., CSIRO, Australia.

Gerrard, C.M. and Wardle, L.J. (1973). Solutions for Point Loads and Generalised Circular Loads Applied to a Cross Anisotropic Half-Space. Tech. Paper No.13, Div. Appl. Geomech., CSIRO, Australia.

Ghaboussi, J. and Wilson, E.L. (1973). Flow of Incompressible Fluid in Porous Elastic Media. Int. J. Numer. Meth. Engrg., Vol.5, pp. 419-442.

Gibson, R.E. and Lumb, P. (1953). Numerical Solution of Some Problems in the Consolidation of Clay. Proc. Instn. Civ. Engrs., Vol. 2, No.1, pp. 182-198.

Gibson, R.E., Schiffman, R.L. and Pu, S.L. (1970). Plane Strain and Axially Symmetric Consolidation of a Clay Layer on a Smooth Impervious Base. Quart. J. Mech. Appl. Math; Vol.23, No.4, pp. 505-520.

Girijavallabhan, C.V. and Reese, L.C. (1968). Finite Element Method Applied to Some Problems in Soil Mechanics. J. SMFE Div. ASCE, Vol.94, No. SM2, pp. 473-496.

Girond , J.P. (1972). Tables Pour le Calcul des Foundations. Dunod, Paris, Vol.1.

Gladwell, G.M. and Iyer, K.R.P. (1974). Unbonded Contact Between a Circular Plate and an Elastic Half-Space. J.E. Elasticity, Vol.4, No.2, pp. 115-130.

Hain, S.J. (1975). A Study of Structure Foundation Interaction. Ph.D. Thesis, Deptt. Civ. Engrg., UNSW, Aust.

Hanuska, A. and Novotny, B. (1978). Rigid Circular Plate on Multilayered Half-Space. Stavebricky Cas. 26 (1978), No. 516, pp. 383-392.

Hara, T., Shibuya, T., Koizumi, T. and Nakahara, I. (1975). An Asymmetric Mixed B.V. Problem of the Thick Elastic Plate: Moment Applied to the Annular Rigid Stamp. Proc. 25th Japan National Conf. for Appl. Mech. 1975, Theoretical and Applied Mechanics, pp. 505-512, Univ. of Tokyo Press.

Harr, M.E. (1966). Foundations of Theoretical Soil Mechanics. McGraw-Hill Book Co., New York.

Hooper, J.A. (1973). Observations on the Behaviour of a Piled Raft Foundation on London Clay. Proc. Inst. Civ. Engrs., pt.2, Vol.55, p. 855.

Hooper, J.A. (1974). Analysis of a Circular Raft in Adhesive Contact with a Thick Elastic Layer. Geotechnique, Vol.24, No.4, pp. 561-580.

Hooper, J.A. (1975). Elastic Settlement of a Circular Raft in Adhesive Contact with a Transversly Isotropic Medium. Geotechnique, Vol.25, No.4, pp. 691-711.

Hooper, J.A. (1976). Parabolic Adhesive Loading of a Flexible Raft Foundation. Geotechnique, Vol.26, No.3, pp. 511-525.

Huang, Y.H. (1969). Finite Element Analysis of Nonlinear Soil Media. Proc. Application of FEM in Civ. Engrg., Vanderbit Univ., pp. 663-690.

Hwang, C.T., Morgenstern, W.R. and Murray, D.W. (1971). On Solutions of Plane Strain Consolidation Problems by FEM. Canad. Geotech. J., Vol.8, No.1, pp. 109-118.

Hwang, C.T., Morgenstern, N.R. and Murray, D.W. (1972). Application of FEM to Consolidation Problems. Proc. Symp. Appl. FEM Geotech. Engrg., Vicksburg, Mississippi, 1972, Vol.2, pp. 739-765.

Ishkova, A.G. (1951). Bending of a Circular Plate on the Elastic Half-Space Under the Action of a Uniform Axisymmetric Load. Uch. Zap. Mosk. Gos. Univ.,3, pp. 152-160.

Keer, L.M. (1967). Mixed Boundary-Value Problems for an Elastic Half-Space . Proc. Camb. Phil. Soc., Vol.63, pp. 1379-1386.

Kodner, R.L. (1963). Hyperbolic Stress-Strain Response: Cohesive Soils. J. SMFE Div., ASCE, Vol.89, No. SM1, pp.115-143.

Komornik, A. and Mazurik, A. (1977). Restrained Settlements of Masonry Buildings. 9th Int. Conf. SMFE, Tokyo, Japan, Proc., Vol.1, pp. 613-618.

Lee, I.K. (Ed.) (1974). Soil Mechanics-New Horizons. Newnes-Butterworths, London.

Leonards, G.A. (1962). Foundation Engineering. McGraw-Hill Book Co. N.Y.

Madhav, M.R. (1980). Settlement and Allowable Pressures for Ring or Annular Footings. Indian Getech. J., Vol.10, No.3, pp. 267-271.

Madhav, M.R. and Vitkar, P.P. (1981). Response of Finite Saturated Layer to Construction Type of Loading. Int. Symp. Mech. Behaviour of Structural Media, Ottawa, Proc. Vol.2, pp. 355-367.

McNamee, J. and Gibson, R.E. (1960). Plane Strain and Axially Symmetric Problems of the Consolidation of a Semi-Infinite Clay Stratum. Quart. J. Mech. Appl. Math., Vol.13, No.2, pp. 210-227.

Mandel, J. (1957). Consolidation des couches d'argiles. Proc. 4th Int. Conf. SMFE, London, 1957, Vol.1, pp. 360-367.

Mandel, J. (1961). Tassements Products par la Consolidation d'une couche d'argile de grande épaisseur. Proc. 5th Int. Conf. SMFE, Paris, 1961, Vol.1, pp.733-736.

Mandel, J. and Salencon, J. (1969). Force Portante d'un sol Sur une assise rigide. Proc. 7th Int. Conf. SMFE, Mexico, Vol.2, pp. 157-164.

Milovic, D.M. (1973). Stresses and Displacements Produced by a Ring Foundation. Prof. 8th Int. Conf. Soil Mech. and Found. Engrg., Moscow, Vol.13, pp. 167-179.

Mindlin, R.D. (1936). Force at a Point in the Interior of a Semi-Infinite Solid. J. Appl. Phys., Vol.7, No.5, pp. 195-202.

Mossakovski, V.I. (1954). The Fundamental General Problem of the Theory of Elasticity for a Half-Space with a Circular Curve Determining Boundary Conditions. Prikl. Mat. Mekh., Vol.18, pp. 187-196 (in Russian).

Murray, R.T. (1978) in Scott, C.R. (Ed). Developments in Soil Mechanics-1. Applied Science Publishers Ltd., London, 1978.

Narasimhan, S.L. (1982). Finite Element Analysis of Piled Foundations. Ph.D. Thesis (under submission), Civ. Engrg. Deptt., I.I.T. Kanpur.

Nishida, Y. (1966). Vertical Stress and Vertical Deformations of Ground Under a Deep Circular Uniform Pressure in the Semi-infinite. Press. 1st Cong. Int. Soc. Rock Mech., Vol.2, pp. 493-498.

Nayak, G.C. and Zienkiewicz, O.C. (1972). Elasto-Plastic Stress Analysis. A Generalization for Various Constitutive Relations Including Strain Softening. Int. J. Numer. Meth. Engrg., Vol.5, pp. 113-135.

Odemark, N. (1949). Investigation as to the Elastic Properties and Soils and Design of Pavements According to the Theory of Elasticity. Statens Vaginstitut, Stockholm.

Oden, J.T. (1972). Finite Element Methods for Nonlinear Continua. McGraw-Hill Book Co., New York.

O'Neill, M.W. and Reese, L.C. (1972). Behaviour of Bored Piles in Beamlout Clay. J. SMFE Div., ASCE, Vol.98, No.SM2, Feb. 1972.

Paria, G. (1957). Axisymmetric Consolidation for a Porous Elastic Material Containing Fluid. J. Maths. Phys., Vol. 36, pp. 338-346.

Parry, R.H.G. (ed.) (1971). Stress-Strain Behaviour of Soils. Proc. Roscoe Mem. Symp. Cambridge Univ., G.T.Foulis and Co. London, 1971.

Patankar, M.V. (1982). Non-linear Analysis of Annular and Circular Foundations by FEM. J. Instn. Engrs. (India), Vol.62, Pt. CI 6, pp. 347-352.

Peck, R.B., Hanson, W.E. and Thornburn, T.H. (1974). Foundation Engineering. Wiley Eastern Ltd., New Delhi, 1980.

Popova, O.V. (1972). Stress and Displacement Distributions in a Homogeneous Half-space Below a Circular Foundation. Soil Mech. Fdn. Engrg., Vol.9, No.2, pp. 86-89.

Poulos, H.G. (1968). The Behaviour of a Rigid Circular Plate Resting on a Finite Elastic Layer. Civ. Engrg. Trans. Instn. Engrs. Australia, CE 10(2), pp. 213-219.

Poulos, H.G. and Davis, E.H. (1974). Elastic Solutions for Soil and Rock Mechanics. Wiley, New York.

Poulos, H.G. and Davis, E.H. (1980). *Pile Foundation Analysis and Design*. John Wiley and Sons, New York, 1980.

Ramberg, W. and Osgood, W.R. (1943). Description of Stress-Strain Curves by Three Parameters. *Natl. Advis. Comm. Aeronaut., Tech., Note 902*, Washington, D.C.

Rauhans, D. (1977). Tables for Calculating Circular Slabs on Elastic Support with Centrally Symmetric Loading. *Bauingenieur 52*, No. 10, pp. 387-392.

Roscoe, K.H. (1970). The Influence of Strains in Soil Mechanics. *Tenth Rankine Lecture. Geotechnique*, Vol. 20, pp. 129-170.

Sandhu, R.S. (1977). Variational Principle for Finite Element Analysis of Consolidation. *Proc. Num. Meth. in Geomech., 2nd Int. Conf. Num. Meth. Virginia*, June 1976.

Sandhu, R.S. and Wilson, E.L. (1969). Finite Element Analysis of Seepage in Elastic Media. *J. Engrg. Mech. Div., Proc. ASCE*, Vol. 95, No. EM3, pp. 641-652.

Santos, J. and Quera, J. (1981). Soil Foundation Interaction With Friction at the Interface. *Proc. 10th Int. Conf. SMFE*, Stockholm, Vol. 2, pp. 253-258.

Schiffman, R.L. and Aggarwala, B.D. (1961). Stresses and Displacements Produced in a Semi-infinite Elastic Solid by a Rigid Elliptical Footing. *Proc. 5th Int. Conf. SMFE*, Paris, 1961, Vol. 1, pp. 795-801.

Schultze, E. (1961). Distribution of Stress Beneath a Rigid Foundation. *Proc. 5th Int. Conf. SMFE*, Vol. 6, pp. 807-813.

Scott, C.R. (Ed.) (1978). *Developments in Soil Mechanics-1*. Applied Science Publishers Ltd., London, 1978.

Scott, R.F. (1963). *Principles of Soil Mechanics*. Addison, Welsey Publ. Co. Inc.

Selvadurai, A.P.S. (1979). *Elastic Analysis of Soil Foundation Interaction*. Elsevier Scientific Publishing Co., Amsterdam, 1979, pp. 223-406.

Selvadurai, A.P.S. (1980). Flexure of a Thick Circular Raft Foundation Resting on an Isotropic Elastic Medium. *Proc. Int. Conf. 'Structural Foundation in Rock'*, Sydney, Australia, May 1980.

Selvadurai, A.P.S. (1980). The Eccentric Loading of a Rigid Circular Foundation Embedded in an Isotropic Elastic Medium. *Int. J. Numer. Analyt. Methods*, Vol.4, No.2, pp. 121-129.

Selvadurai, A.P.S. and Kempthorne, R.H. (1980). Plane Strain-Contact Stress Distribution Beneath a Rigid Footing Resting on a Soft Cohesive Soil. *Canad. Geotech. J.*, Vol.17, No.1, pp. 114-122.

Shelest, L.A. (1975). Distribution of Stresses and Displacements in a Foundation Bed of Finite Thickness Beneath a Circular Rigid Foundation. *Soil Mech. Fdn. Engrg.*, Vol.12, No.6, pp. 404-407.

Shibuya, T., Koizumi, T. and Nakahara, I. (1974). An Elastic Contact Problem for a Half-space Indented by a Flat Annular Rigid Stamp. *Int. J. Engng. Sci.*, Vol.12, No.9, pp. 759-771.

Shibuya, T., Koizumi, T. and Nakahara, I. (1975). An Elastic Contact Problem for a Half-Space Indented by a Flat Annular Rigid Stamp in the Presence of Adhesion. Proc. 25th Japan National Cong. for Appl. Mech. 1975. Theoretical and Applied Mechanics, pp. 497-504, Univ. of Tokyo Press.

Sloan, S.W. and Randolph, M.F. (1982). Numerical Prediction of Collapse Loads Using Finite Element. *Int. J. Numer. Analyt. Meth. Geomech.*, Vol.6, No.1, pp. 45-76.

Smith, I.M. (1970). A Finite Element Approach to Elastic Soil Structure Interaction. *Canad. Geotech. J.* Vol.7, pp. 95-105.

Smith, I.M. and Hobbs, R. (1976). Biot Analysis of Consolidation Beneath Embankments. *Geotechnique*, Vol.26, No.1, pp. 149-171.

Sneddon, I.N. (1946). Boussinesq's Problem for a Flat Ended Cylinder. *Proc. Camb. Phil. Soc.* Vol.42, No.1, pp. 29-39.

Spence, D.A. (1968). Self Similar Solutions to Adhesive Contact Problems with Incremental Loading. *Proc. Roy. Soc. A* 305, pp. 55-80.

Svec, O.J. (1974). The Unbounded Contact Problem of a Plate on the Elastic Half Space. *Computer Meth. in Appl. Mech. Engrg.*, Vol.3, pp. 105-113.

299

Szabo, G. (1970/71). Die Grundlagen einer neuen Festigkeits-theorie. Vol.1 and 2, Bauverlag, Wiesbaden.

Taylor, D.W. (1962). Fundamentals of Soil Mechanics. John Wiley and Sons, New York.

Terzaghi, K. and Peck, R.B. (1948). Soil Mechanics in Engineering Practice. John Wiley and Sons, New York.

Timoshenko, S.P. and Krieger, S.W. (1959). Theory of Plates and Shells. McGraw-Hill Kogakusha Ltd., Tokyo.

Valliappan, S., Hain, S. and Lee, I.K. (Eds.) (1975). Soil Mechanics-Recent Developments. Proc. Gen. Session Symp. Univ. NSW, Australia, July 14-18, 1975.

Valliappan, S. and Lee, I.K. (1975). Consolidation of Non-homogeneous Anisotropic Layered Soil Media. Proc. 2nd Australia-NZ Conf. Geomech., Brisbane, pp. 67-71.

Valov, G.M. (1968). Infinite Elastic Layer and Half-Space Under the Action of a Ring-Shaped Die. J. Appl. Math. Mech., Vol. 32, No. 5, pp. 917-930.

Varadarajan, A. and Arora, K.R. (1982). Interaction of Circular Footing on Sand Bed System. 4th Int. Conf. Numer. Meth. Geomech., Edmonton, Vol. 2, pp. 945-954.

Varma, B.S., Khadilkar, B.S. and Chandrasekaran, V.S. (1977). Circular Footings on Transversely Isotropic Soils. Proc. Int. Symp. Soil Struct. Interaction, Roorkee, 1977, pp. 265-270.

Verruijt, A. (1977) in Finite Elements in Geomechanics. G. Gudehus (Ed.) John Wiley and Sons, London, 1977.

Volterra, E. (1953). Circular Beams on an Elastic Foundation. J. Appl. Mech. Trans. ASME, Vol. 20, No. 2, pp. 227-232.

Wardle, L.J. (1977). A Computer Program for the Analysis of Multiple Complex Circular Loads on Layered Anisotropic Media. User's Manual. CSIRO-Div. Appl. Geomech. Program Circly. Geomech. Computer Program No. 2, 1977.

Whitaker, T. and Cooke, R.W. (1966). An Investigation of Shaft and Base Resistances of Large Bored Piles in London Clay. Proc. Symp. on Large Bored Piles, pp. 7-49.

Wilson, E.L. (1965). Structural Analysis of Axisymmetric Solids. J. Am. Inst. Aero. Astro., Vol.3, No.12, pp. 2269-2274.

Winterkorn, H.F. and Fang, H.Y. (Eds.) (1975). Foundation Engineering Handbook. Van Nostrand Reinhold Co., New York, 1975.

Wong, I.H. (1971). Analysis of Braced Excavations, Sc.D. Thesis, Deptt. Civ. Engrg. MIT, Cambridge.

Wood, L.A. (1977). The Economic Analysis of Raft Foundation. Int. J. Numer. Analyt. Meth. Geomech., Vol.1 (1977), No.4, pp. 397-405.

Yamaguchi, H. (1973). Consolidation and Heaving of a Finite Clay Layer. Proc. 8th Int. Conf. SMFE, Moscow, 1973.

Yegorov, K.E. and Nichiporovich, A.A. (1961) (See Egorov, K.E. and Nichiporovich, A.A. (1961)).

Yokoo, Y., Yamagata, K. and Nagaoka, H. (1971). Finite Element Analysis of Consolidation Following Undrained Deformation. Soils Fdns., Vol.11, No.4, pp.37-58.

Yokoo, Y., Yamagata, K. and Nagaoka, H. (1971). Finite Element Method Applied to Biot's Consolidation Theory. Soils and Fdns. Vol.11, No.1, pp. 29-46.

Yokoo, Y., Yamagata, K. and Nagaoka, H. (1971). Variational Principles for Consolidation, Soils Fdns., Vol.11, No.4, pp. 25-35.

Zbirohowski-Koscia, K.F. and Gunasekera, D.A. (1970). Foundation Settlement and Ground Reaction Calculations Using a Digital Computer.

Zeevaert, L. (1957). Foundation Design and Behaviour of Tower Latino Americana in Mexico City. Geotechnique, Vol.7, No.1, p. 115.

Zeevaert, L. (1972). Foundation Engineering for Difficult Subsoil Conditions. Van Nostrand Reinhold Co.Ltd., New York.

Zienkiewicz, O.C. (1977). The Finite Element Method . Tata McGraw-Hill Publ.Co.Ltd., New Delhi, 1977.

Zienkiewicz, O.C., Valliappan, S. and King, I.P. (1968). Stress Analysis of Rock as a 'No-Tension' Material. Geotechnique, Vol.18, pp. 56-66.

Zinovev, A.N. (1979). Determination of the Deformation of a Base of Finite Thickness Under an Annular Foundation. Translated from Osnovaniya, Fundamenty i Mekhanika Gruntov, No.3, pp. 23-25, May-June, 1979.

50592